

Palladium-Catalyzed Functionalization of C-H Bonds and Alkenes

by

Lopa Vrushank Desai

A dissertation submitted in partial fulfillment
of the requirements for the degree of
Doctor of Philosophy
(Chemistry)
in The University of Michigan
2008

Doctoral Committee:

Associate Professor Melanie S. Sanford, Chair
Professor Edwin Vedejs
Professor Erdogan Gulari
Assistant Professor John P. Wolfe

© Lopa Vrushank Desai

2008

To Dr. Sanford, Dipa
and Smitesh

Acknowledgements

I give my deepest gratitude to all those people who made my graduate experience a memorable and one that I will cherish forever.

I would like to start with the most influential person – Dr. Sanford. I consider myself very fortunate that I got an advisor like you. Your passion, enthusiasm, motivation, dedication, patience and mentorship were paramount in my growth and life. You showed me different ways to approach a problem and guided me when I made mistakes. You taught me how to question, write and present chemistry. Even though you had a lot on your plate; you still devoted endless time to me. You are an amazing mentor because you make your students your priority – you care for us, take time to understand us, go out of your way to build our future and love us for who we are. I thank you for everything you have done for me. I hope that you will continue to be a significant part of my life.

I would like to thank my committee members for their support and feedback in such short notice. Dr. Wolfe, I have learned a lot from you through group meetings and classes. I appreciate all your insightful comments at different stages of my research. Dr. Vedejs, your questions at seminar and in class have always been very thought provoking. Dr. Gulari, thank you for bringing a different perspective to my committee.

Research is not possible without the help of Jim Windak, for mass spectrometry, Eugenio for NMR and Jeff Kampf for all the cystrallography. Thank you to all three of

you for facilitating a productive research environment. I am also grateful to Aiko, Christina and Jerry for addressing my endless administrative questions and problems. The candy from Aiko and Mike Kelly helped me increase my sugar level. I am also grateful to Dr. Matzger for his help with calculations and access to his computers. I want to thank Antek for his support, humor and being himself. I appreciate all the times when you shared and expressed mutual feelings for my ‘arch nemesis’. Thank you for your feedback and solving really hard crystal structures for me. I want to thank Hasnain Malik for working with me on the Oxone project. I am surprised I didn’t scare him away that semester. I have been lucky to have very supportive friends. Josie you are one of them. I am so glad that we did our first rotation together. You are a great person and don’t ever change.

I want to thank my lab mates – the ‘Sanford Mafias’ or ‘Sanfordites’ for being so amazing. I am lucky to have worked with such a talented group of people. What I love the most about my lab mates is no matter what, we are always there for each other. Kami- thank you for all your help, support and feedback these past few years. Camping would be no fun without your tent and blankets. I also appreciate all the ‘goodies’ you have made and shared with me. Salena- your friendship, invaluable suggestions and feedback has taught me a lot. You are a great listener. Smitesh and I will always miss your German Chocolate Cake and ‘Mookies’. Deprez, you are like a big brother with a kind and supportive nature. Thank you for the frosty Nick Ball – it was very thoughtful. Andrew– I enjoyed our ‘random’ lunch conversations. Matt, I appreciate all your probing questions. Joy, thank you for taking care of GC’s while I was working on my dissertation. I am so thrilled to have Dipa, Kara and Tom as my bench-mates. They bring laughter to your

face, even when you feel like there is no hope. They make work place fun, frustrating, crazy, hot, cold and a great homey place. I have enjoyed all the times we have danced, sang, and debated in lab. Hum to aise hai bhaiya. I appreciate Tom's bluntness and Kara's caring and sensitive nature. 'Sorry' Karebear! I loved working with you these past few months. I appreciate you overlooking my occasional burst of irrationality.

Deeps, I wish I could write pages and pages expressing what you mean to me- but I don't want to embarrass you. Bhagwan humse bahut kush hoga isleye usne humko tumhare jesa dost diya. You were like my second mentor, sister, mother and friend. Your incredible work ethic and high standard of research is admirable and inspiring – you truly deserve the best. I am so grateful for your honesty with me – you brought the best out in me. Your meticulous guidance and invaluable suggestions helped me focus and approach problems in different ways. Thank you for carefully reading and commenting on countless versions of anything I have ever written or presented. You have saved me numerous occasions- editing, thinking through problems, and giving me your laptop endlessly. You have been there for me through hard times and good times. I know regardless of my temperamental irrational self–you will always be there for me with your unfaltering friendship and unconditional love.

I want to thank my family – my parents and my brother for their unconditional support and encouragement to pursue my dreams. Thank you for loving me even after dealing with my tantrums and frustrations. Mom, thank you for believing in me and encouraging me to be persistent and reach my highest potential. Tushar you are a great brother and I am lucky to have you. Thank you to my family-in-law (parents, bhai,

bhabhi, and nephews Viraj and Laksh) for their love and support. Mom- you spoilt me these past few months with your cooking.

The last – but not least- person I want to thank is my husband, Smitesh. As corny as this may sound – you complete me. Your constant patience, tolerance of my ‘ups’ and ‘downs’, ‘highs’ and ‘lows’ is a testament in itself of your unyielding love, sacrifice and compromise. Your kindness, love, incredible smartness, zeal to learn, patience, and creativity are the bedrock of my life. Thank you for everything you do to make my life comfortable, full of love, happiness, adventures, emotions and stories. I cannot express how thankful I am of all those times you have come to my rescue – making my posters, designing, formatting my dissertation, generating my table of contents, scheme and figures. Your creativity and aspiration for knowledge is refreshing and inspirational. Thank you for having faith in me and supporting and inspiring my ambitions. You have taught me a lot of values in life and made me a better person. I thank god for making you part of my life and for everything else I have been given. JSK.

Table of Contents

Dedication	ii
Acknowledgements	iii
List of Schemes	x
List of Figures	xviii
List of Tables	xx
Abstract	xxii
Chapter 1	
Introduction	1
1.1 References	6
Chapter 2	
Palladium-Catalyzed Acetoxylation of sp^3 C-H Bonds	7
2.1 Background and Significance	7
2.2 Initial Results	14
2.3 Substrate Scope of Pd-Catalyzed Acetoxylation of 1° sp^3 C-H Bonds	15
2.4 Competition Studies: sp^2 versus sp^3 C-H bonds	25
2.5 Functionalization of Secondary sp^3 C-H bonds	33
2.6 Stereochemical Nature of Reductive Elimination	39
2.7 Deprotection of Directing Groups	45
2.8 Conclusion	47
2.9 Experimental Procedure	47
2.10 References	68

Chapter 3

Oxone and $K_2S_2O_8$ as Alternative Oxidants for C-H Bond Oxygenation	71
3.1 Background and Significance	71
3.2 Initial Screenings of Peroxides	73
3.3 Scope of Acetoxylation of sp^2 C-H Bonds with Oxone and $K_2S_2O_8$	76
3.4 Scope of Acetoxylation of sp^3 C-H Bonds with Oxone and $K_2S_2O_8$	82
3.5 Formation of Methyl Ethers with Oxone and $K_2S_2O_8$	84
3.6 Introduction of Other Nucleophiles at Carbon with Oxone and $K_2S_2O_8$	88
3.7 Conclusions	89
3.8 Experimental Procedure	89
3.9 References	108

Chapter 4

Factors Governing the Dominance of a Directing Group	110
4.1 Background and Significance	110
4.2 Substrate Selection and Optimizations	112
4.3 Competition Studies	116
4.4 Individual Rate Studies	122
4.5 Kinetic Isotope Effect Studies	124
4.6 Order of $PhI(OAc)_2$	125
4.7 Discussion	127
4.8 Application	134
4.9 Conclusions	137
4.10 Experimental Procedure	137
4.11 References	153

Chapter 5

Palladium-Catalyzed 1,2-Difunctionalization of Alkenes	155
5.1 Background and Significance	155
5.2 Initial Investigation	162
5.3: Cyclization of Alcohols	169
5.4 Cyclization of Amines	172
5.5: Cyclization of Acids	174
5.6 Mechanistic Investigations of the Cyclization Reactions	175
5.7 Aminoxygenation Cyclization Reactions with 3-Alken1-ols	178
5.8 Mechanistic Investigations of Amiooxygenation Cyclization	181
5.9 Conclusion	192
5.10 Experimental Procedure	192
5.11 References	219

List of Schemes

Chapter 1

Introduction

Scheme 1.1: Routes for Introducing of Functional Groups into Organic Molecules .	1
Scheme 1.2: Transition Metal Catalyzed Activation/Fucntionalization of C–H Bonds	1
Scheme 1.3: Palladium-Catalyzed Acetoxylation of Chlorobenzene with $\text{PhI}(\text{OAc})_2$	2
Scheme 1.4: Regioselectivity via Cyclopalladation	3
Scheme 1.5: Overall Goal for Direct Transformation of C-H to C-O Bonds	3
Scheme 1.6: Cyclopalladation of Azobenzene	3
Scheme 1.7: Palladium-Catalyzed Directed Acetoxylation of Arene C–H Bonds	4
Scheme 1.8: Proposed Mechanism for $\text{Pd}^{\text{II/IV}}$ Catalyzed Arene Acetoxylation	4
Scheme 1.9: Palladium-Catalyzed Directed Oxidative Functionalization of sp^3 C–H Bonds	5
Scheme 1.10: Use of Peroxides as the Terminal Oxidant in C–H Activation/Oxidation	5
Scheme 1.11: Competition Studies Between Multiple Directing Groups	5
Scheme 1.12: Palladium-Catalyzed 1,2-Aminooxygenation of Alkenes	5

Chapter 2

Palladium-Catalyzed Acetoxylation of sp^3 C-H Bonds

Scheme 2.1: Transition Metal Catalyzed Alkane Functionalization	7
Scheme 2.2: Platinum-Catalyzed Oxidation of Methane	8
Scheme 2.3: Pentane Oxidation with Pt^{II}	8

Scheme 2.4: (bpym)Pt(Cl) ₂ -Catalyzed C–H Activation/Oxidation of Methane	9
Scheme 2.5: Pd-Catalyzed Directed sp ³ C–H Activation/Arylation	10
Scheme 2.6: Platinum Catalyzed Directed sp ³ C–H Activation/C–O Bond Formation	10
Scheme 2.7: Desired Reaction	11
Scheme 2.8: Stoichiometric sp ³ C–H Activation/Oxygenation at Pd ^{II}	11
Scheme 2.9: β-Hydride Elimination Versus Oxidation	13
Scheme 2.10: Potential Applications of the Proposed Reaction	13
Scheme 2.11: Attempted Pd-Catalyzed Acetoxylation of Pinacalone Oxime with PhI(OAc) ₂	14
Scheme 2.12: Proposed Mechanism for Oxidative Deprotection	15
Scheme 2.13: Pd-Catalyzed Acetoxylation of Pinacalone Oxime Methyl Ether with PhI(OAc) ₂	15
Scheme 2.14: Pd-Catalyzed Reaction of Cyclohexanone Methyl Oxime Ether with PhI(OAc) ₂ in AcOH	18
Scheme 2.15: Pd-Catalyzed Reaction of Cyclohexanone Methyl Oxime Ether with PhI(OAc) ₂ in AcOH/Ac ₂ O	18
Scheme 2.16: Palladium-Catalyzed Acetoxylation of Prochiral Methyl Groups with Lauroyl Peroxide	20
Scheme 2.17: Effect of a <i>t</i> -Bu Conformational Lock on the Rate of Pd-Catalyzed C–H Bond Acetoxylation	21
Scheme 2.18: Regioselectivity in sp ³ C–H Bond Acetoxylation	22
Scheme 2.19: Pd-Catalyzed Oxime-Directed Oxidative Ring Opening of Cyclopropanes	23
Scheme 2.20: Proposed Mechanism for Pd-Catalyzed Oxidative Ring Opening of Cyclopropanes	24
Scheme 2.21: Olefin-Assisted Nucleophilic Ring Opening of Cyclopropane	25
Scheme 2.22: Competition Between 91 and 58 in the Same Reaction Vessel	25
Scheme 2.23: Competition Between sp ² and sp ³ C–H bonds within the Same Molecule	26
Scheme 2.24: Equilibration between Oxime Isomers	26

Scheme 2.25: Effect of Sterics on Acetoxylation of 62	32
Scheme 2.26: Competition Between sp^2 and sp^3 C–H Bonds in Oxime Ether Substrate 144	32
Scheme 2.27: Competition between of 2° sp^3 C–H bond and sp^2 bond	33
Scheme 2.28: Studies of Iridium Complexation with 1° and 2° sp^3 C–H bonds	34
Scheme 2.29: Double Chelation Strategy for 2° sp^3 C–H Bond Activation	35
Scheme 2.30: Application of the Double Chelation Strategy	35
Scheme 2.31: Application of Dual Chelation Strategy: Pd-Catalyzed Arylation of a 2° sp^3 C–H Bond	36
Scheme 2.32: Application of Dual Chelation Strategy: Pd-Catalyzed Acetoxylation of a 2° sp^3 C–H Bond	36
Scheme 2.33: Dual Chelation Strategy: Ester and Oxime Ether Directing Groups ...	37
Scheme 2.34: Dual Chelation Strategy: Pyridine and Oxime Ether Directing Groups	37
Scheme 2.35: Dual Chelation Strategy: 8-Amidoquinoline Derivatives	38
Scheme 2.36: Conformational Lock Strategy: <i>trans</i> -Decalone Oxime Ether	38
Scheme 2.37: Conformational Lock Strategy: Pd-Catalyzed Acetoxylation of <i>trans</i> - Decalone Oxime Ether	39
Scheme 2.38: Possible Mechanisms for C–O Bond-Forming Reductive Elimination	40
Scheme 2.39: Reductive Elimination with Inversion of Stereochemistry	40
Scheme 2.40: Reductive Elimination with Retention of Stereochemistry	40
Scheme 2.41: Stoichiometric Cyclopalladation of <i>trans</i> -Decalone Oxime	41
Scheme 2.42: Reaction of Complex 191 with $PhI(OAc)_2$	42
Scheme 2.43: Reaction of Complex 190 with $PhI(OAc)_2$ to Form C–O and C–Cl	43
Scheme 2.44: Oxidation of Complex 191 with $PhICl_2$ and MeI	43
Scheme 2.45: Oxidation of Complex 190 with $PhICl_2$ and MeI	44
Scheme 2.46: Reductive Elimination from $(phpy)_2Pd^{IV}(O_2CAr)_2$ Complexes	45
Scheme 2.47: Formation of β -Amino Acids from Isoxazolines	45
Scheme 2.48: Attempts to Deprotect C–H Activation/Acetoxylation Product 198 with Bronsted Acid	46

Scheme 2.49: Deprotection of C–H Activation/Acetoxylation Product 184 with TiCl ₃	46
---	----

Chapter 3

Oxone and K₂S₂O₈ as Alternative Oxidants for C-H Bond Oxygenation

Scheme 3.1: Proposed Mechanism for C–H Bond Acetoxylation with PhI(OAc) ₂ ...	72
Scheme 3.2: Stoichiometric Oxidation of Pt ^{II} with H ₂ O ₂ in AcOH	73
Scheme 3.3: Palladium-Catalyzed Oxidation of Methane with K ₂ S ₂ O ₈	73
Scheme 3.4: Palladium-Catalyzed Disproportionation of H ₂ O ₂	74
Scheme 3.5: Large Scale Reaction of <i>m</i> -Bromoacetophenone Oxime Ether with Oxone	76
Scheme 3.6: Product Distribution as a Function of Oxidant Stoichiometry	76
Scheme 3.7: Reaction of Substrate 14 with Oxone and PhI(OAc) ₂	79
Scheme 3.8: Palladium-Catalyzed Oxidation of <i>m</i> -Chloroacetanilide	79
Scheme 3.9: Palladium-Catalyzed Reaction of Quinoxaline with Oxone	80
Scheme 3.10: Reaction of Azobenzene Substrate 17 with Oxone	80
Scheme 3.11: Palladium-Catalyzed Reaction of 2-Phenylpyridine with Oxone and PhI(OAc) ₂	81
Scheme 3.12: Reaction of Oxazoline with PhI(OAc) ₂ and Peroxide	81
Scheme 3.13: Acetoxylation of sp ³ C-H Bonds using K ₂ S ₂ O ₈	83
Scheme 3.14: Pd-Catalyzed Oxidation of C–H bonds with Peroxyesters	83
Scheme 3.15: Acetoxylation Reactions of Amino Acid Derivatives	84
Scheme 3.16: Platinum Oxidation in Methanol with H ₂ O ₂	84
Scheme 3.17: Hydrolysis of Electron Rich Oxime Ethers under the Reaction Conditions	87
Scheme 3.18: Catalyst Decomposition Pathway in Alcohol Solvents	87
Scheme 3.19: Reaction of Peroxides in Other Alcohol Solvents	88
Scheme 3.20: Reaction of Substrate 12 with in the Presence of Different Nucleophiles	89

Chapter 4

Factors Governing the Dominance of a Directing Group

Scheme 4.1: Chelate Directed C–H Activation/Functionalization	110
Scheme 4.2: Competition Studies Between Multiple Directing Groups	112
Scheme 4.3: Pyrimidine, Quinoline and Aldehyde Substrates Lacking a Methylene Spacer	116
Scheme 4.4: Representative Competition Experiment	117
Scheme 4.5: Competition Between Benzylpyridine 18 and Oxime Ether 11	117
Scheme 4.6: Competition between Oximes Ethers 13 and 11	118
Scheme 4.7: Electronic Effects with Substituted Benzylpyridine Derivatives	121
Scheme 4.8: Kinetic Isotope Effect in Individual Rate Studies	125
Scheme 4.9: Kinetic Isotope Effect in Competition Studies	125
Scheme 4.10: Reaction Studied for Determining the Order in $\text{PhI}(\text{OAc})_2$	126
Scheme 4.11: Reaction Studied for Determining the Order in $\text{PhI}(\text{OAc})_2$ (Competition)	127
Scheme 4.12: Coordination Studies of Substituted Pyridines with Bimetallic Palladium	129
Scheme 4.13: Hammett Studies with Cyclopalladation of Substituted 3° Benzylamines	129
Scheme 4.14: Directing Group Electronic Effects in the Cyclopalladation of <i>N</i> -Benzyl Triamines	130
Scheme 4.15: TBHP Oxidation of <i>N,N</i> -dimethylbenzylamine Complexes	131
Scheme 4.16: Equilibrium for Substrate Binding Under Competition Conditions	133
Scheme 4.17: Highly Selective Oxime Ether-Directed C–H Acetoxylation of Substrate 63	135
Scheme 4.18: Amide Directed C–H Functionalization of Product 64	135
Scheme 4.19: Intramolecular Competition Between a Pyridine and an Oxime Ether	136
Scheme 4.20: Controlling Direction of C-H activation/functionalization	136

Chapter 5

Palladium-Catalyzed 1,2-Difunctionalization of Alkenes

Scheme 5.1: Osmium-Catalyzed Aminohydroxylation of Alkenes	156
Scheme 5.2: Oxidative Cleavage of Pd-Alkyl Intermediates Formed via Aminopalladation	156
Scheme 5.3: Proposed Mechanism for Enamide 5 Formation	157
Scheme 5.4: Synthesis of Enamide 5 via Aminopalladation/ β -Hydride Elimination ..	157
Scheme 5.5: Stoichiometric Aminoacetoxylation Reaction Reported by Backvall ...	158
Scheme 5.6: Proposed Pd ^{II/IV} Catalyzed Aminoxygenation of Olefin	158
Scheme 5.7: Palladium-Catalyzed Intramolecular Aminochlorination with CuCl ₂ ..	159
Scheme 5.8: Proposed Mechanism for Pd-Catalyzed Intramolecular Aminochlorination	159
Scheme 5.9: Palladium-Catalyzed Intramolecular Aminoacetoxylation with PhI(OAc) ₂	160
Scheme 5.10: Proposed Mechanism for Pd-Catalyzed Intramolecular Aminoacetoxylation	160
Scheme 5.11: Palladium-Catalyzed Intramolecular Diamination Reactions	161
Scheme 5.12: Proposed Mechanism for Diamination Reactions	161
Scheme 5.13: Palladium-Catalyzed Intermolecular Aminoacetoxylation	162
Scheme 5.14: Palladium-Catalyzed Reaction of 1-Octene with Phthalimide and PhI(OAc) ₂	162
Scheme 5.15: Palladium-Catalyzed Reaction of 1-Octene with Tosylamine or Nosylamine and PhI(OAc) ₂	164
Scheme 5.16: Palladium-Catalyzed Reaction of Norbornylene with <i>p</i> -Toluenesulfonamide and PhI(OAc) ₂	165
Scheme 5.17: Palladium-Catalyzed Reaction of Norbornylene with Phthalimide and PhI(OAc) ₂ in CH ₂ Cl ₂	166
Scheme 5.18: Palladium-Catalyzed Reaction of Norbornylene with Phthalimide and PhI(OAc) ₂ in Nitroalkane Solvents	166
Scheme 5.19: Halophenylation of Norbornene	166

Scheme 5.20: Use of Directing Group-Containing Nucleophile 50	167
Scheme 5.21: Use of Directing Group-Containing Substrates 53-56	168
Scheme 5.22: Alcohol Tether Strategy	168
Scheme 5.23: Palladium-Catalyzed Reaction of 3-Butene-1-ol with Phthalimide and PhI(OAc) ₂ to form Tetrahydrofurans	169
Scheme 5.24: Palladium-Catalyzed Cyclization of 3-Buten-1-ol	169
Scheme 5.25: Use of (Mesityl)I(CO ₂ Ph) ₂ as the Oxidant	170
Scheme 5.26: Proposed Lewis Acid Catalyzed Mechanism for Formation of 67 and 68	171
Scheme 5.27: Alcohol Cyclization Reactions	171
Scheme 5.28: Amine Cyclization Reactions	173
Scheme 5.29: Carboxylic Acid Cyclization Reactions	174
Scheme 5.30: 5-Endo-trig Cyclization at Pd ^{II}	176
Scheme 5.31: Lewis Acid Catalyzed Cyclization	176
Scheme 5.32: Literature Precedent for 5-Endo-trig Cyclization at Pd ^{II}	177
Scheme 5.33: Literature Precedent for Bronsted Acid-Catalyzed Cyclization	177
Scheme 5.34: Cyclization Reactions with PhI(OCOCF ₃) ₂	178
Scheme 5.35: Reactions with BF ₃ •Et ₂ O	178
Scheme 5.36: Alkenol Substrates that Exhibited Low Reactivity.....	181
Scheme 5.37: Mechanistic Pathway (i)	182
Scheme 5.38: Mechanistic Pathway (ii)	182
Scheme 5.39: Mechanistic Pathway (iii).....	182
Scheme 5.40: Mechanistic Pathway (iv)	182
Scheme 5.41: Mechanistic Pathway (v)	183
Scheme 5.42: Mechanistic Pathway (vi)	183
Scheme 5.43: Possible S _N 2 Reaction between Phthalimide and THF 65	183
Scheme 5.44: Possible S _N 2 Reaction between Phthalimide and Iodide Product 153 .	184
Scheme 5.45: Attempt to Obtain Aminoxygenation Product 126 with Catalytic BF ₃ •Et ₂ O	184
Scheme 5.46: S _N 2 Reaction of Aminoacetoxylated Intermediate 61	185

Scheme 5.47: Subjection of 4-Phenyl-3-buten-1-ol to Reaction Conditions with O ₂ as the Terminal Oxidant	185
Scheme 5.48: Mechanism iii: Aminopalladation Followed by Oxidatively Induced Cyclization	186
Scheme 5.49: Studies with Deuterium Labelled Substrate 157	187
Scheme 5.50: Aminooxygenation with 4-Phenyl-3-buten-1-ol	187
Scheme 5.51: Rationale for Outcome from β -Hydride Elimination	188
Scheme 5.52: Geometry of Amination Product Under Pd ^{II/0} Reaction Conditions	189
Scheme 5.53: Summary of Proposed Mechanism	190
Scheme 5.54: Probing the Role of the Tethered Alcohol	191

List of Figures

Chapter 2

Palladium-Catalyzed Acetoxylation of sp^3 C-H Bonds

Figure 2.1: Substrates That Did Not Form Isolable Palladacycles	12
Figure 2.2: Substrates Containing Unactivated 2° sp^3 C-H Showing No Reactivity .	34
Figure 2.3: Dual Chelation Strategy: Other Substrates Examined	37
Figure 2.4: Crystal Structure of Deprotected Acetate Product 185	39
Figure 2.5: X-Ray Crystal Structure of Chloro Monomer 190 (pyridine ligand truncated for clarity)	41
Figure 2.6: X-Ray Crystal Structure of Acetate Monomer 191 (pyridine ligand truncated for clarity)	42

Chapter 4

Factors Governing the Dominance of a Directing Group

Figure 4.1: Examples of Biologically Active Molecules Containing a Single Potential Directing Group	111
Figure 4.2: Examples of Biologically Active Molecules Containing Multiple Potential Directing Groups	112
Figure 4.3: Substrates Synthesized to Conduct Dominance Studies	113
Figure 4.4: Elements for Substrate Design	113
Figure 4.5: Relative Reactivity of Directing Groups from Competition Studies in AcOH/Ac ₂ O and Benzene	121
Figure 4.6: Representative Initial Rates Data in AcOH/Ac ₂ O	122
Figure 4.7: Representative Initial Rates Data in Benzene	123

Figure 4.8: Initial Rate Constant as a Function of Oxidant Concentration in AcOH/Ac ₂ O	126
Figure 4.9: Initial Rate Constant as a Function of Oxidant Concentration in Benzene	126
Figure 4.10: Initial Rate Constant of 18 in presence of 52 as a Function of Oxidant Concentration in AcOH/Ac ₂ O	127
Figure 4.11: Initial Rate Constant of 18 in presence of 52 as a Function of Oxidant	127
Figure 4.12: Proposed Catalytic Cycle for Pd-Catalyzed C–H Bond Acetoxylation .	128
Figure 4.13: Proposed Transition States for Cyclopalladation	130

Chapter 5

Palladium-Catalyzed 1,2-Difunctionalization of Alkenes

Figure 5.1: Palladium Catalysts Containing Bi- and Tridentate Ligands	163
Figure 5.2: Additional Amine and Amide Substrates	173
Figure 5.3: Possible Transition States	191

List of Tables

Chapter 2

Palladium-Catalyzed Acetoxylation of sp^3 C-H Bonds

Table 2.1: Substrate Scope for Stoichiometric sp^3 C-H Activation/Oxygenation at Pd ^{II}	12
Table 2.2: Scope of Pd-Catalyzed Directed sp^3 C-H Activation/Acetoxylation: with PhI(OAc) ₂ : Highly Branched Substrates	17
Table 2.3: Scope of Pd-Catalyzed Directed sp^3 C-H Activation/Acetoxylation: with PhI(OAc) ₂ : Substrates with β -Hydrogens	19
Table 2.4: Competition Between Benzylic sp^3 C-H bonds and sp^2 C-H bonds and Function of Directing Group	28
Table 2.5: Effect of Palladacycle Ring Size of Yields of Pd-Catalyzed C-H Activation/Acetoxylation with Isoxazoline Directing Groups I	29
Table 2.6: Effect of Palladacycle Ring Size of Yields of Pd-Catalyzed C-H Activation/Acetoxylation with Oxime Ether and Pyridine Directing Groups	30
Table 2.7: Effect of Palladacycle Ring Size of Yields of Pd-Catalyzed C-H Activation/Acetoxylation with Isoxazoline Directing Groups II	31

Chapter 3

Oxone and K₂S₂O₈ as Alternative Oxidants for C-H Bond Oxygenation

Table 3.1: Screen of Peroxide Oxidants for the Pd-Catalyzed Acetoxylation of <i>m</i> -Bromoacetophenone Oxime Ether	75
Table 3.2: Substrate Scope with Oxone as the terminal Oxidant	77
Table 3.3: Substrate Scope with K ₂ S ₂ O ₈	78

Table 3.4: Substrate Scope for Methoxylation Reactions	86
---	----

Chapter 4

Factors Governing the Dominance of a Directing Group

Table 4.1: Optimization Studies	114
Table 4.2: Scope of Substrates Bearing Different Directing Groups	115
Table 4.3: Competition Ratios in AcOH/Ac ₂ O	119
Table 4.4: Competition ratios in Benzene	120
Table 4.5: Initial Rate Constants for Substrates 11 , 13 , 15-19 , and 21 in AcOH/Ac ₂ O and Benzene	124

Chapter 5

Palladium-Catalyzed 1,2-Difunctionalization of Alkenes

Table 5.1: Substrate Scope for Alcohol Cyclization Reactions	172
Table 5.2: Substrate Scope of Carboxylic Acid Cyclization Reactions	175
Table 5.3: Addition of Additives to the Palladium-Catalyzed Reaction of 3-Butene-1-ol with Phthalamide and PhI(OAc) ₂	179
Table 5.4: Substrate Scope of Aminooxygenation Reactions	180

Abstract

A highly regio- and chemoselective methodology for the ligand-directed palladium-catalyzed C-H activation/acetoxylation of sp^3 C-H bonds was developed. The reaction was found to be general with a variety of directing groups such as oxime ethers, isoxazolines and pyridines. In addition, the reaction exhibited high selectivity for the acetoxylation of 1° sp^3 C-H bonds.

The ligand directed palladium-catalyzed C-H activation/acetoxylation of sp^2 and sp^3 C-H bonds was shown to be effective with alternative oxidants such as Oxone and $K_2S_2O_8$ in place of $PhI(OAc)_2$. The use of these peroxide based oxidants over $PhI(OAc)_2$ is advantageous because they are cheaper and do not release toxic byproducts such as iodobenzene.

A comprehensive investigation to elucidate the factors affecting the C-H activation/acetoxylation by one ligand over another was conducted. It was determined that in the presence of multiple chelating functionalities in a reaction, the substrate bearing the most basic ligand would lead to the predominant product under our reaction conditions. These transformations are believed to proceed via a $Pd^{II/IV}$ catalytic cycle. Mechanistic studies implicate that ligand directed palladium mediated C-H activation is the rate-limiting step in these reactions.

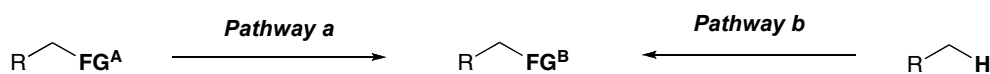
Finally, Pd-alkyl intermediates generated via aminopalladation were intercepted using strong oxidants such as $PhI(OAc)_2$ to afford 1,2-difunctionalized products. Under our optimal conditions, the use of alkenes bearing tethered alcohols, acids, or amines led to the formation of substituted tetrahydrofuran rings, lactones, or pyrrolidines.

Chapter 1

Introduction

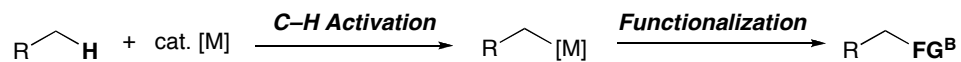
The direct catalytic functionalization of C–H bonds is an important challenge in organic chemistry.¹⁻⁷ Traditionally, the introduction of a functional group in a molecule requires a pre-functionalized starting material (Scheme 1.1, pathway a), which might be challenging to access in the context of complex molecule synthesis. In contrast, C–H bonds are ubiquitous in nature; hence their direct transformation to diverse functional groups would be highly desirable (Scheme 1.1, pathway b).

Scheme 1.1: Routes for Introducing Functional Groups (FG) into Organic Molecules



The direct functionalization of C–H bonds is challenging because C–H bonds are unreactive and robust. Their low reactivity can be attributed to the fact that they are strong, localized, and unpolarized bonds.^{2, 8} Transition metal catalysis can be used to assist in converting C–H bonds to more reactive carbon-metal bonds that can subsequently be functionalized to afford the desired product (Scheme 1.2).

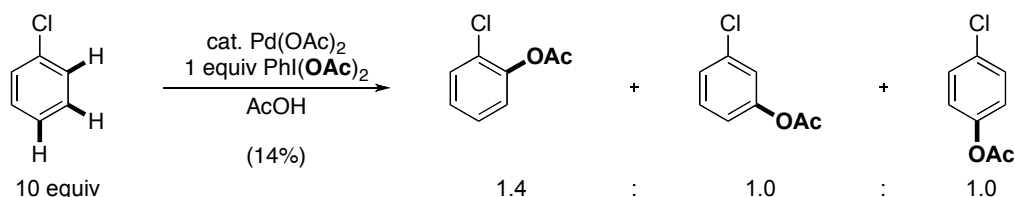
Scheme 1.2: Transition Metal-Catalyzed Activation/Functionalization of C–H Bonds



There were a number of examples of transition metal-catalyzed C–H activation/C–C bond formation prior to our work.⁹ In contrast, C–H activation/carbon–heteroatom bond forming reactions were very limited.¹⁰ Our initial goal was to develop a transition metal-catalyzed mild, regio-, and chemoselective method to convert C–H bonds to C–O bonds. This transformation would be very useful because C–O bonds are widely prevalent in biologically active molecules. Additionally, the petroleum and chemical industries have interest in finding efficient ways to convert inert alkanes into oxygenated hydrocarbons.

Crabtree and coworkers demonstrated the direct transformation of an arene C–H bond to a C–OAc bond.¹¹ In particular, they showed that substrates such as chlorobenzene can be acetoxylation in the presence of catalytic Pd(OAc)₂ and stoichiometric PhI(OAc)₂. As depicted in Scheme 1.3, a mixture of *ortho*, *meta* and *para* regioisomers of the acetoxylation product were obtained. The authors proposed that PhI(OAc)₂ served as the source of the acetate in the final product, and as an oxidant that effects the oxidative functionalization of the carbon-palladium bond resulting from C–H activation. While this report was an important demonstration that C–H bonds can be oxygenated with readily available catalysts under mild conditions, this reaction was limited by its very low yield, the need for large excess of substrate, and the lack of regioselectivity.

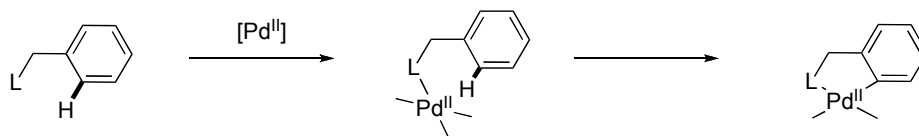
Scheme 1.3: Palladium-Catalyzed Acetoxylation of Chlorobenzene with PhI(OAc)₂



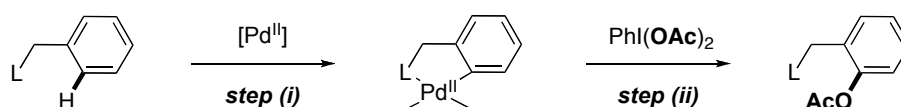
Our group sought to address the challenge of regioselectivity by employing a ligand directed approach for the palladium-catalyzed oxidative functionalization of C–H bonds. This strategy involves the use of substrates bearing coordinating functional groups, such as L in Scheme 1.4, that can chelate to the metal and direct the activation of a proximal C–H bond. We reasoned that the cyclopalladated complex formed upon C–H

activation could then be functionalized using electrophilic reagents such as $\text{PhI}(\text{OAc})_2$ to afford the desired *ortho*-oxygenated product.

Scheme 1.4: Regioselectivity via Cyclopalladation

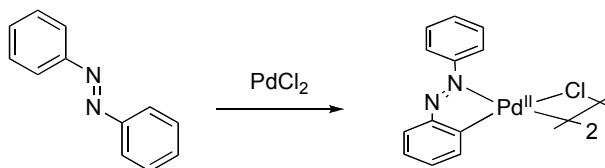


Scheme 1.5: Overall Goal for Direct Transformation of C-H to C-O Bonds



The first step for the proposed reaction, namely ligand-directed C–H activation at Pd^{II} (cyclopalladation), is well documented in literature.¹² One of the earliest reports appeared in 1965 with stoichiometric cyclopalladation of azobenzene (Scheme 1.6).¹³ Since this report, there have been examples illustrating cyclopalladation with a variety of directing groups such as pyridines, amines, amides, and oximes. Additionally, Miura,¹⁴ Sames,¹⁵ Fujiwara¹⁶ and others have effectively employed the ligand-directed approach for palladium metal catalyzed C–H activation/C–C bond forming reactions. The feasibility for the oxygenation step is supported by the palladium-catalyzed arene acetoxylation reaction discussed above (Scheme 1.3).

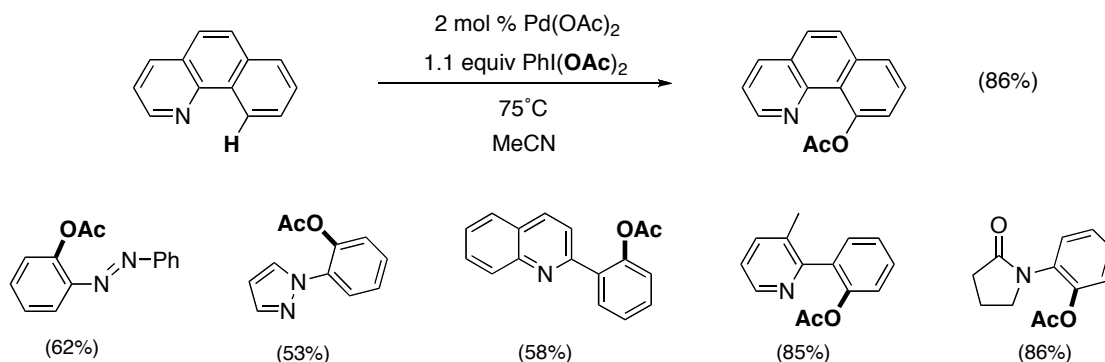
Scheme 1.6: Cyclopalladation of Azobenzene



In 2004, our group reported that the approach shown in Scheme 5 provides an efficient route to the ligand-directed acetoxylation of arene C–H bonds.¹⁷ This methodology was shown to be general with respect to a wide variety of directing groups such as pyridines, pyrazoles, and azo-linkages to afford the acetoxylation products in good

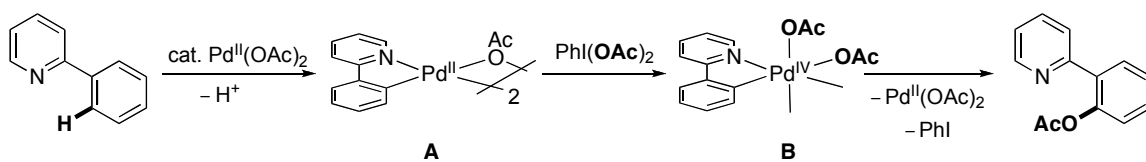
yields (Scheme 1.7).¹⁸ Importantly, these reactions were highly selective for functionalization of the C–H bond adjacent to the chelating group.

Scheme 1.7: Palladium-Catalyzed Directed Acetoxylation of Arene C–H Bonds



This reaction was proposed to proceed through a Pd^{II/IV} catalytic cycle.^{17, 19} As shown in Scheme 1.8, the key steps of the catalytic cycle are proposed to involve: (i) ligand directed C–H activation to afford the cyclopalladated complex **A**, (ii) oxidation of **A** by PhI(OAc)₂ to generate the Pd^{IV} intermediate **B**, and (iii) C–O bond-forming reductive elimination from **B** to release the desired acetoxyated product and regenerate the Pd^{II} catalyst.

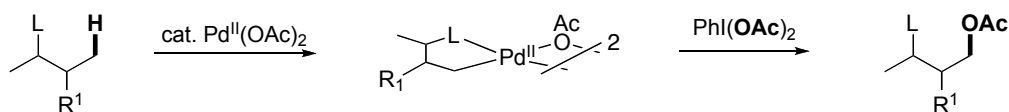
Scheme 1.8: Proposed Mechanism for Pd^{II/IV} Catalyzed Arene Acetoxylation



All of our group's initial work in this area involved functionalization of arene C–H bonds using PhI(OAc)₂ as the terminal oxidant. As such, the goals of my research (as outlined in this thesis) were as follows:

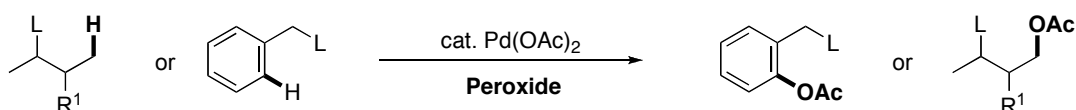
Chapter 2: To extend this methodology to the oxidation of sp³ C–H bonds (Scheme 1.9).

Scheme 1.9: Palladium-Catalyzed Directed Oxidative Functionalization of sp^3 C–H Bonds



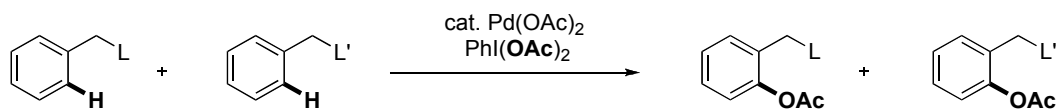
Chapter 3: To explore the use of alternative oxidants (particularly peroxides) in place of $\text{PhI}(\text{OAc})_2$ for Pd-catalyzed directed C–H activation/oxidation reactions (Scheme 1.10).

Scheme 1.10: Use of Peroxides as the Terminal Oxidant in C–H Activation/Oxidation Reactions



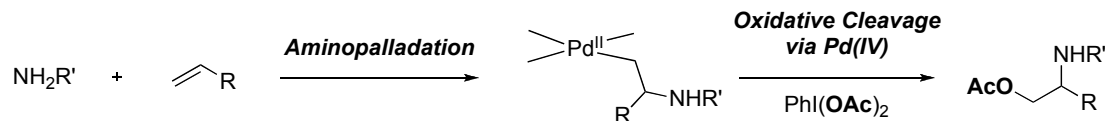
Chapter 4: To determine the factors that control which ligand will direct C–H activation/functionalization when multiple potential chelating functionalities are present in solution (Scheme 11).

Scheme 1.11: Competition Studies Between Multiple Directing Groups



Chapter 5: To oxidatively intercept Pd-alkyl intermediates, generated via aminopalladation of alkenes, to form 1,2-difunctionalized products (Scheme 1.12).

Scheme 1.12: Palladium-Catalyzed 1,2-Aminooxygenation of Alkenes



1.1 References

- (1) Crabtree, R. H. *J. Organomet. Chem.* **2004**, *689*, 4083-4091.
- (2) Labinger, J. A.; Bercaw, J. E. *Nature* **2002**, *417*, 507-514.
- (3) Gretz, E.; Oliver, T. F.; Sen, A. *J. Am. Chem. Soc.* **1987**, *109*, 8109-8111.
- (4) Lafrance, M.; Gorelsky, S. I.; Fagnou, K. *J. Am. Chem. Soc.* **2007**, *129*, 14570-14571.
- (5) Shilov, A. E.; Shul'pin, G. B. *Chem. Rev.* **1997**, *97*, 2879-2932.
- (6) Dick, A. R.; Sanford, M. S. *Tetrahedron* **2006**, *62*, 2439-2463.
- (7) Godula, K.; Sames, D. *Science* **2006**, *312*, 67-72.
- (8) Crabtree, R. H. *Chem. Rev.* **1985**, *85*, 245-269.
- (9) Alberico, D.; Scott, M. E.; Lautens, M. *Chem. Rev.* **2007**, *107*, 174-238.
- (10) Dangel, B. D.; Johnson, J. A.; Sames, D. *J. Am. Chem. Soc.* **2001**, *123*, 8149-8150.
- (11) Yoneyama, T.; Crabtree, R. H. *J. Mol. Catal. A*, **1996**, *108*, 35-40.
- (12) Dunina, V. V.; Zalevskaya, O. A.; Potapov, V. M. *Usp. Khim.* **1988**, *57*, 434-473.
- (13) Cope, A. C.; Siekman, R. W. *J. Am. Chem. Soc.* **1965**, *87*, 3272-3273.
- (14) Wakui, H.; Kawasaki, S.; Satoh, T.; Miura, M.; Nomura, M. *J. Am. Chem. Soc.* **2004**, *126*, 8658-8659.
- (15) Dangel, B. D.; Godula, K.; Youn, S. W.; Sezen, B.; Sames, D. *J. Am. Chem. Soc.* **2002**, *124*, 11856-11857.
- (16) Jia, C.; Kitamura, T.; Fujiwara, Y. *Acc. Chem. Res.* **2001**, *34*, 633-639.
- (17) Dick, A. R.; Hull, K. L.; Sanford, M. S. *J. Am. Chem. Soc.* **2004**, *126*, 2300-2301.
- (18) Kalyani, D.; Sanford, M. S. *Org. Lett.* **2005**, *7*, 4149-4152.
- (19) Dick, A. R.; Kampf, J. W.; Sanford, M. S. *J. Am. Chem. Soc.* **2005**, *127*, 12790-12791.

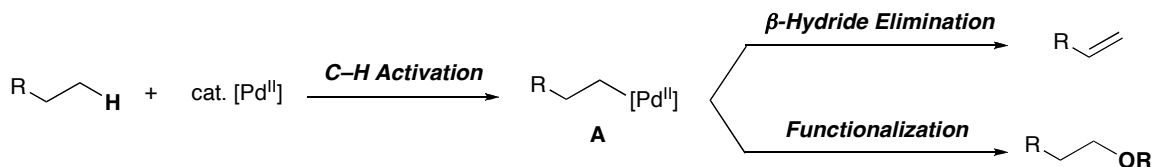
Chapter 2

Palladium-Catalyzed Acetoxylation of sp^3 C-H Bonds

2.1 Background and Significance

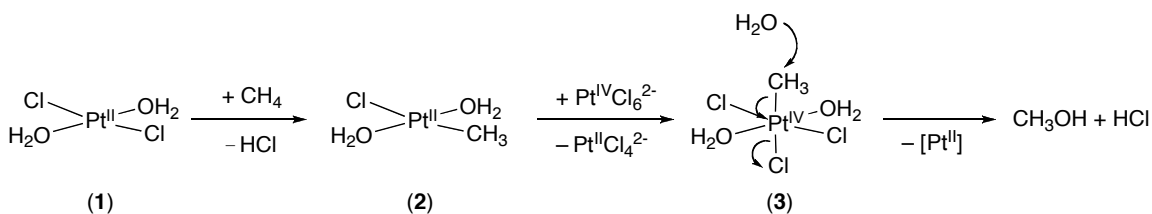
Alkane carbon-hydrogen (C-H) bond activation and functionalization has been a formidable challenge in synthetic organic chemistry. In general, sp^3 C-H bonds are much more difficult to activate than sp^2 C-H bonds. The unreactive nature of alkanes is attributed to (i) the lack of available lone pairs, empty orbitals of low energy, or filled orbitals of high energy, (ii) the low polarity of these substrates, and (iii) the high homolytic and heterolytic strength of C-H bonds (typical bond dissociation energies range from 90-110 kcal mol⁻¹ and pK_a values are greater than 40).^{1, 2} In addition, the metal-alkyl intermediates that are generated upon C-H activation (for example, **A** in Scheme 2.1) are typically susceptible to β -hydride elimination. Alkanes are ubiquitous in nature, and are found in diverse organic compounds, including petroleum, natural gas, organic polymers, natural products, pharmaceuticals, and agrochemicals. Hence, developing a methodology for the direct functionalization C-H bonds in alkanes could have a great practical impact on a variety of different fields.

Scheme 2.1: Transition Palladium-Catalyzed Alkane Functionalization



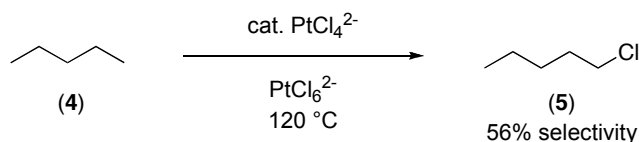
Many research groups have attempted to address the challenge of alkane oxidation.³ One of the most promising approaches to alkane C–H activation/functionalization involves the use of group 10 metal (Pt and Pd) catalysts. Although several promising systems have been developed, most are not suitable for practical use. The most prominent early example comes from the 1970's by Shilov and co-workers.⁴ They demonstrated that sp^3 C–H bonds of simple alkanes such as methane could be functionalized to C–O bonds using catalytic Pt^{II} salts in conjunction with stoichiometric Pt^{IV} -based oxidants (Scheme 2.2).

Scheme 2.2: Platinum-Catalyzed Oxidation of Methane



While the mild conditions and simplicity of the catalysts in these reactions are remarkable, the utility of this transformation is limited by (i) the requirement of stoichiometric amounts of Pt^{IV} and (ii) low selectivity. For instance, pentane is converted to pentyl chloride with only 56% terminal selectivity (Scheme 2.3).⁵ Chlorination at other positions on the alkyl chain was also observed. Despite its limitations, this platinum system shows potentially useful features and would be rendered more practical if the Pt^{IV} could be replaced with another strong oxidant.

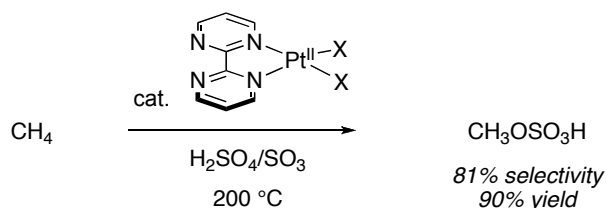
Scheme 2.3: Pentane Oxidation with Pt^{II}



An important recent advancement in Pt-catalyzed alkane oxidation was reported by Periana in 1998.⁶ This report demonstrated the oxidation of methane to methylbisulfate using a Pt^{II} catalyst (bpym)Pt(Cl)₂ (bpym = bipyrimidine) in fuming

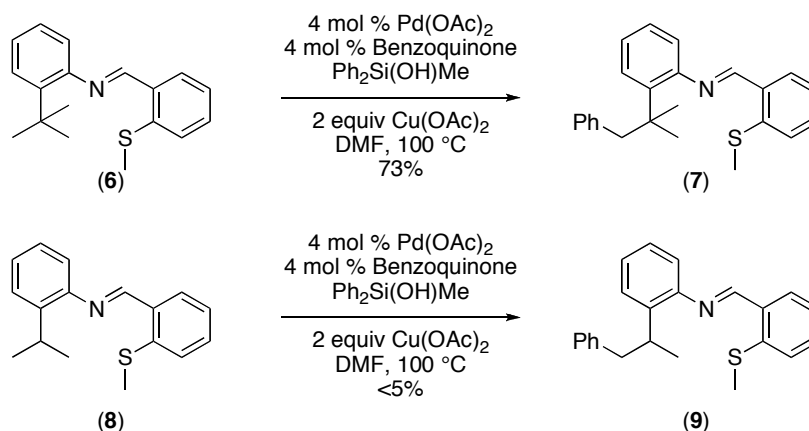
sulfuric acid with SO₃ as the terminal oxidant (Scheme 2.4). The mechanism of this reaction is proposed to involve: (i) electrophilic C–H activation to afford a platinum alkyl complex, (ii) oxidation by SO₃ to afford a Pt^{IV} species, and finally (iii) reductive elimination from this Pt^{IV} intermediate to provide methyl bisulfate. This reaction is attractive due to its high yield (90%) and selectivity (81%). Installation of an electron withdrawing sulfonic acid group protects the product from further oxidation. However, the utility of this reaction is limited by the requirement of fuming sulfuric acid and high temperatures (200 °C). Other hydrocarbon substrates, under these harsh conditions, result in low turnover numbers and low levels of regio- and chemoselectivity.

Scheme 2.4: (bpym)Pt(Cl)₂-Catalyzed C–H Activation/Oxidation of Methane



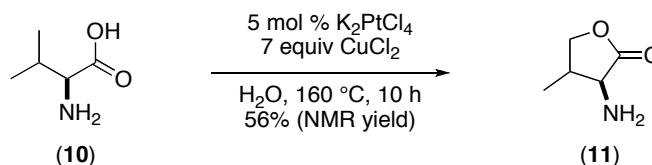
Sames has reported some of the earliest examples of group 10 metal catalyzed alkane C–H functionalization, addressing regioselectivity by using a directing functional group.^{7, 8} As shown in Scheme 2.5, directed arylation of *ortho-tert*-butylaniline with phenylvinylsilanol was achieved in the presence of catalytic Pd(OAc)₂ using Cu(OAc)₂ as a terminal oxidant. A mechanism involving dual coordination of the imine and the thioether to Pd was proposed to lead to the high selectivity for the 1° C–H bond. Though catalytic, the reaction is limited by its modest substrate scope. For example, replacing the *tert*-butyl in **6** with an *iso*-propyl moiety resulted in only trace amounts of the desired product **9** (Scheme 2.5).

Scheme 2.5: Pd-Catalyzed Directed sp^3 C–H Activation/Arylation



Sames has also reported one of the first examples of heteroatom-directed oxygenation of sp^3 C–H bonds involving the Pt^{II}-catalyzed selective functionalization of α -amino acids in water.⁹ As shown in Scheme 2.6, this report demonstrated that subsection of valine to 5 mol % K₂PtCl₄ and 7 equiv CuCl₂ in water at 160 °C resulted in 56% NMR yield of lactone **11**. The reaction was proposed to proceed via chelate-directed electrophilic C–H activation by Pt^{II} followed by oxidative functionalization to form the C–O bond. Although this reaction is an important advancement in directed functionalization of alkyl groups in complex substrates, its utility is limited by the moderate yields and the harsh reaction conditions (particularly the high temperatures and the requirement for large excesses of oxidant). Importantly, there were no examples of palladium-catalyzed directed sp^3 C–H activation/C–O bond formation when we started this project.

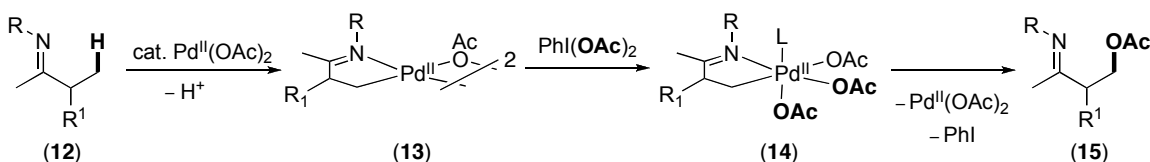
Scheme 2.6: Platinum Catalyzed Directed sp^3 C–H Activation/C–O Bond Formation



We aimed to address the challenge of C–H activation/functionalization of sp^3 C–H bonds by employing the Pd^{II/IV} catalyzed methodology developed for functionalization of sp^2 C–H bonds (Chapter 1, Scheme 1.7). The key step in the sp^2 C–H bond

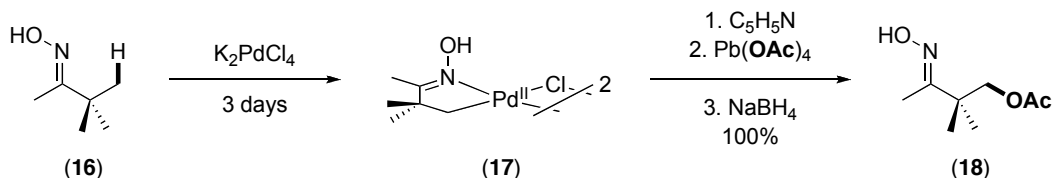
functionalization reaction is the oxidative interception of a palladium-aryl intermediate, generated upon C–H activation, with $\text{PhI}(\text{OAc})_2$ (Scheme 1.8, Chapter 1).¹⁰ Our goal was to generate an analogous palladium-alkyl intermediate **13** via ligand-directed sp^3 C–H bond activation (Scheme 2.7). Oxidative cleavage of the Pd–C bond in **13** with $\text{PhI}(\text{OAc})_2$, would then allow us to install an OAc group at the sp^3 carbon center via the Pd^{IV} intermediate **14**.

Scheme 2.7: Desired Reaction



While Pd-catalyzed directed sp^3 C–H activation/oxygenation reactions were unprecedented prior to our work, several previous reports had described stoichiometric versions of this transformation.^{11–13} For example, Baldwin and co-workers illustrated that the reaction of pinacolone oxime **16** with stoichiometric K_2PdCl_4 leads to the formation of palladacycle **17** via ligand directed activation of a terminal C–H bond of the *tert*-butyl group. Subsequent oxidation of **17** with $\text{Pb}(\text{OAc})_4$ was then shown to form the acetoxyated product **18** (Scheme 2.8).¹¹

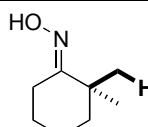
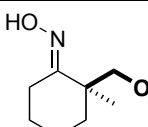
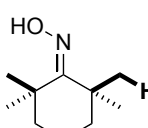
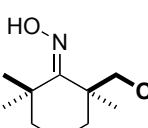
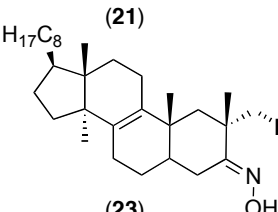
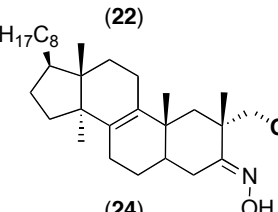
Scheme 2.8: Stoichiometric sp^3 C–H Activation/Oxygenation at Pd^{II}



Although this reaction demonstrates the viability of directed sp^3 C–H bond activation, it is impractical for several reasons. First of all, it is stoichiometric in both an expensive Pd^{II} salt and a highly toxic Pb^{IV} salt. Second, it has a very limited substrate scope. As shown in Table 2.1, methylated cyclohexanone oximes **19** and **21** and the steroid derivative **23** were the only substrates that were successfully acetoxyated by

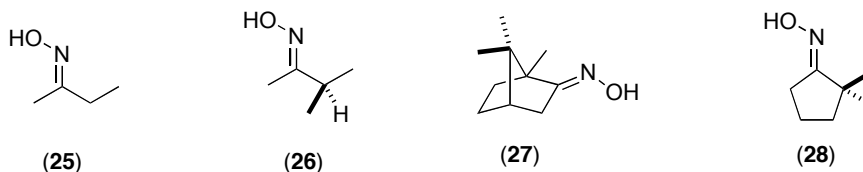
Baldwin using this method. In contrast, isolable palladacycles could not be obtained for substrates that lacked α -branching (for example, **25** in Figure 2.1), for substrates in which the C–H bond and the directing group were not coplanar (for example, **27** and **28** in Figure 2.1), and for substrates that were susceptible to β -hydride elimination upon C–H activation (for example, **25** and **26** in Figure 2.1).

Table 2.1: Substrate Scope for Stoichiometric sp^3 C–H Activation/Oxygenation at Pd^{II}

Entry	Substrate	Product	Yield
1	 (19)	 (20)	96%
2	 (21)	 (22)	76%
3	 (23)	 (24)	76%

Conditions: (i) Na_2PdCl_4 , (ii) pyridine (iii) $Pb(OAc)_4$ and (iv) $NaBH_4$

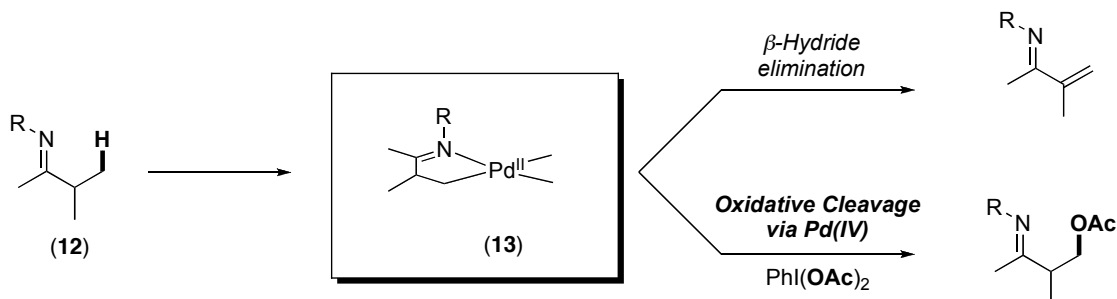
Figure 2.1: Substrates That Did Not Form Isolable Palladacycles



Based on this early report, we aimed to develop an efficient palladium-catalyzed method to acetoxylation sp^3 C–H bonds that was directed by ketone or aldehyde-derived directing groups. We wanted to use a terminal oxidant that was less toxic and more practical than $Pb(OAc)_4$. Additionally, in order to make this reaction general for a wide variety of substrates, we hoped to develop reaction conditions under which the relative

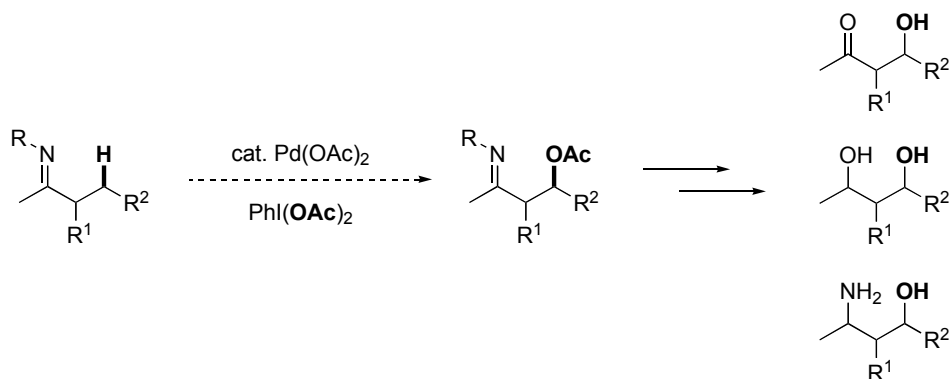
rate of oxidative cleavage of the Pd–C bond in **13** was faster than the undesired β -hydride elimination reaction (Scheme 2.9).

Scheme 2.9: β -Hydride Elimination Versus Oxidation



Importantly, the proposed methodology could potentially allow access to β -amino alcohols, β -hydroxy ketones, and functionalized β -amino acids (Scheme 2.10). It could also provide a tool for the synthesis and functionalization of alkaloids and polyketides as well as other classes of natural products. The ability to selectively functionalize a variety of C–H bonds to C–O bonds could also allow for the efficient synthesis of drug molecules to be tested in structure-activity relationship (SAR) studies. Finally, the insights gained from this palladium-catalyzed ligand-directed oxygenation of sp^3 C–H bonds could then potentially be applied towards functionalization of alkane C–H bonds without the use of directing groups. This would then allow us to address an important challenge of methane oxidation to methanol.

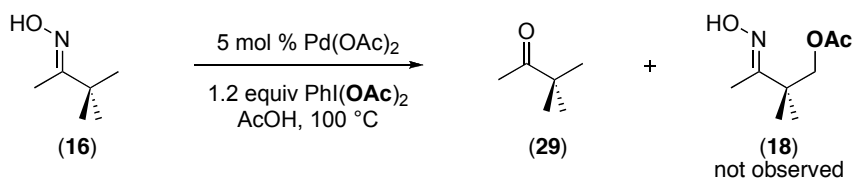
Scheme 2.10: Potential Applications of the Proposed Reaction



2.2 Initial Results

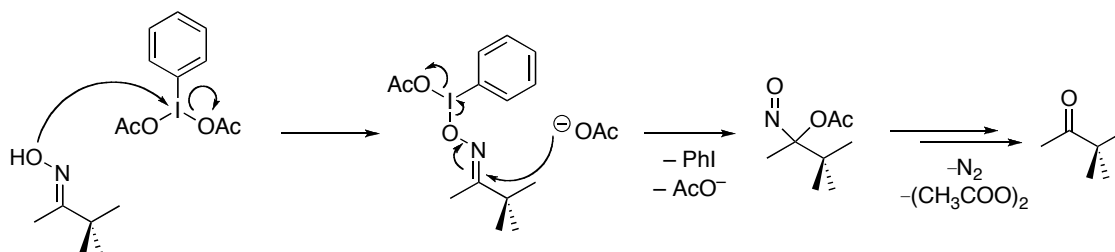
Our studies began with using pinacolone oxime **16** as the substrate. This choice was based on Baldwin's results, which demonstrated the successful oxygenation of the β -C–H bond of **16** using stoichiometric K_2PdCl_4 and $\text{Pb}(\text{OAc})_4$ (Scheme 2.8).¹² We first subjected **16** to the reaction conditions developed in our lab for sp^2 C–H acetoxylation (5 mol % $\text{Pd}(\text{OAc})_2$, 1.5 equiv $\text{PhI}(\text{OAc})_2$ in AcOH at 100 °C). However, under these conditions we obtained none of the desired oxygenated product **18** and instead recovered the deprotected ketone **29** (Scheme 2.11). This indicates that the relative rate of deprotection of the oxime was faster than the rate of oxime-directed C–H activation at Pd^{II} . The ketone product of this deprotection is then expected to be a poor ligand for palladium, and hence unable to direct the functionalization.

Scheme 2.11: Attempted Pd-Catalyzed Acetoxylation of Pinacolone Oxime with $\text{PhI}(\text{OAc})_2$



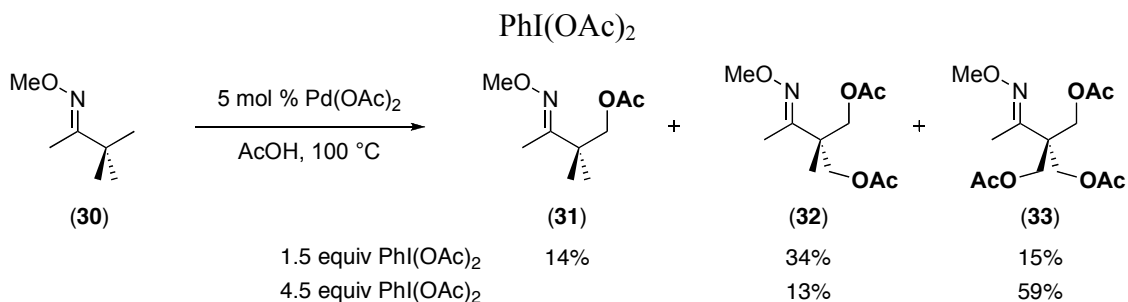
This result suggested that in order to achieve the desired catalytic oxygenation reaction, we would need to prevent deprotection of the oxime. As depicted in Scheme 2.12, a key step in the proposed mechanism for this deprotection involves nucleophilic attack of the oxime hydroxyl group on the iodine.¹⁴ Based on this mechanism we hypothesized that replacing the hydroxyl group with an alkyl ether might attenuate the oxidative deprotection while still maintaining the ligand's coordinating ability to palladium.

Scheme 2.12: Proposed Mechanism for Oxidative Deprotection



Based on this analysis, the oxime ether substrate **30** was synthesized and subjected to the catalytic reaction conditions (5 mol % Pd(OAc)₂, 1.5 equiv PhI(OAc)₂ in AcOH at 100 °C). Gratifyingly, the desired mono-oxygenated product **31** was obtained in 14% isolated yield along with the corresponding di- (34%) and tri-acetoxyated compounds (15%) (Scheme 2.13). Notably, the use of an excess of PhI(OAc)₂ (4.5 equiv) increased the yield of the tri-oxygenated product **33** to 59%.

Scheme 2.13: Pd-Catalyzed Acetoxylation of Pinacalone Oxime Methyl Ether with



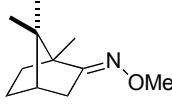
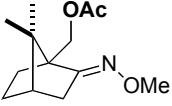
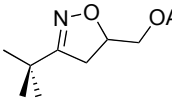
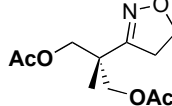
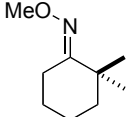
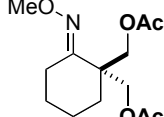
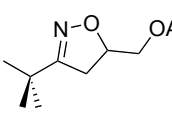
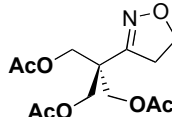
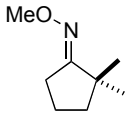
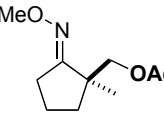
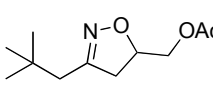
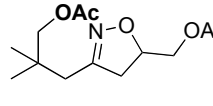
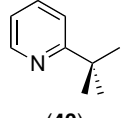
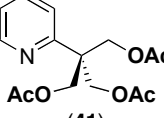
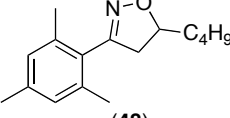
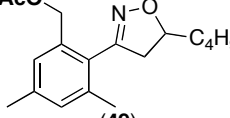
2.3 Substrate Scope of Pd-Catalyzed Acetoxylation of 1° sp³ C-H Bonds

Highly Branched Substrates. We were pleased to find that ligand-directed Pd-catalyzed C–H bond activation/acetoxylation was general with respect to a variety of directing groups (Table 2.2).¹⁵ My colleague Kami Hull demonstrated the use of pyridine directing groups in these reactions, while my work showed that oxime ethers (**34–38**) and isoxazolines (**42–48**) are also effective in mediating the desired acetoxylation reaction. Furthermore, acetoxylation was achieved in systems that proceeded via either a five-

membered (entries 1-6) or a six-membered palladacyclic intermediate (entry 8). Unlike substrate **48**, the six-membered cyclopalladation is not facile with unactivated C-H bonds such as in substrate **46**. Selectivity between mono-, di- or tri-acetoxyated products could be tuned by changing the stoichiometry of the oxidant. For example, the di- and tri-acetoxyated products **43** and **45** were formed in 45% and 55% isolated yields using either two or three equivalents of $\text{PhI}(\text{OAc})_2$, respectively. Importantly, control reactions (in the absence of Pd catalyst) were run for each substrate, and generally showed no reaction under our standard conditions.

Interestingly, the C-H bond in camphor methyl oxime ether **34** was successfully acetoxyated (entry 1). This is particularly notable because Baldwin was unable to obtain an isolable palladacycle with this substrate. We believe that **34** affords the product under our reaction conditions because, unlike in stoichiometric experiments, a catalytic reaction does not require that the palladacycle have an appreciable lifetime. Instead, it just needs to be generated transiently and then can be intercepted by the oxidant to afford the desired product.

Table 2.2: Scope of Pd-Catalyzed Directed sp^3 C–H Activation/Acetoxylation with $\text{PhI}(\text{OAc})_2$: Highly Branched Substrates

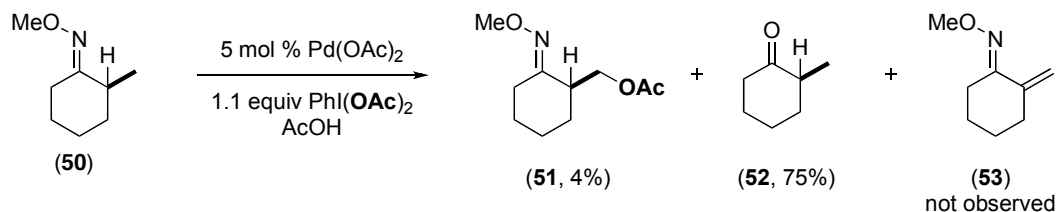
Entry	Substrate	Product	Yield ^a	Entry	Substrate	Product	Yield ^a
1			75%	5			45% ^b
2			51% ^b	6			55% ^c
3			61%	7			0%
4			63% ^c	8			60%

^a Conditions: 5 mol % $\text{Pd}(\text{OAc})_2$, 1.5 equiv $\text{PhI}(\text{OAc})_2$, AcOH , $100\text{ }^\circ\text{C}$; ^b 2.0 equiv $\text{PhI}(\text{OAc})_2$ were used
^c 3.0 equiv of $\text{PhI}(\text{OAc})_2$ were used

Substrates Containing β -Hydrogens. The substrates presented in Table 2.2 do not bear hydrogens α to the carbon being functionalized. Hence, β -hydride elimination from the palladacyclic intermediate is not a potential competing reaction in these systems. As such, we next turned our attention towards substrates that could undergo β -hydride elimination following C–H activation. We wanted to explore whether the relative rate of oxidative cleavage of intermediate **13** would be faster than the undesired β -hydride elimination under our reaction conditions (Scheme 2.9).

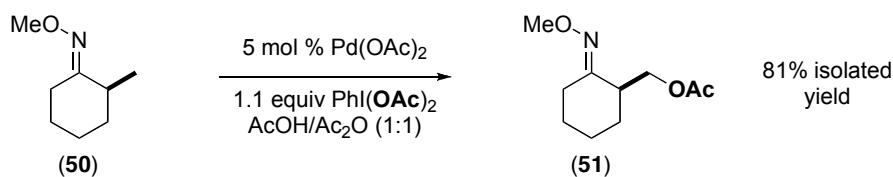
We first synthesized the oxime ether of methyl cyclohexanone. We were pleased to find that subjection of this substrate to our reaction conditions did not afford any of the β -hydride elimination product **53**. Furthermore, the desired acetoxylation product **51** was obtained from this reaction, albeit in a modest yield of 4% (Scheme 2.14). This low yield was due to competitive formation of the corresponding ketone **52**.

Scheme 2.14: Pd-Catalyzed Reaction of Cyclohexanone Methyl Oxime Ether with $\text{PhI}(\text{OAc})_2$ in AcOH



The ketone **52** was not formed via oxidative deprotection of the directing group, since substrate **50** also reacted to generate **52** in AcOH in the absence of $\text{PhI}(\text{OAc})_2$. Instead, we theorized that since **50** is less sterically hindered than the previously studied substrates, it was simply undergoing hydrolysis in the reaction medium. This result suggested that the addition of acetic anhydride (Ac_2O) might be used to sequester the water in the reaction mixture and hence prevent this competing hydrolysis. In order to probe this hypothesis, we subjected substrate **50** to the catalytic reaction conditions using 50% AcOH/50% Ac_2O as the solvent in place of pure AcOH. We were delighted to find that these conditions afforded the acetoxyated product **51** in 81% yield.

Scheme 2.15: Pd-Catalyzed Reaction of Cyclohexanone Methyl Oxime Ether with $\text{PhI}(\text{OAc})_2$ in AcOH/ Ac_2O



These optimal reaction conditions were general for a variety of other substrates containing β -hydrogens (Table 2.3).¹⁵ Importantly, products resulting from β -hydride elimination were not observed for any of these substrates, indicating that the oxidative cleavage of the palladacyclic intermediate out-competes β -hydride elimination in these systems. Interestingly, substrates that did not afford isolable palladacycles in the Baldwin system were successfully functionalized under our catalytic conditions (entries 1 and 3).¹¹ Additionally, substrates lacking branching at the α -position (**54**) were also acetoxyated.

Such systems were challenging to functionalize under the reaction conditions developed by both Baldwin and Sames.

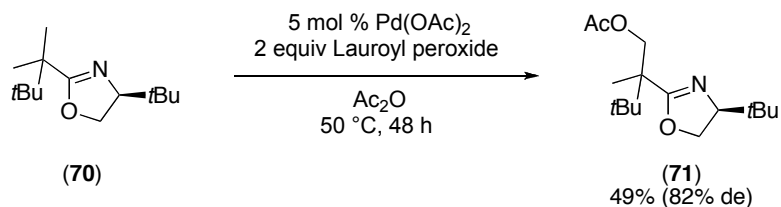
Table 2.3: Scope of Pd-Catalyzed Directed sp^3 C–H Activation/Acetoxylation with $\text{PhI}(\text{OAc})_2$: Substrates with β -Hydrogens

Entry	Substrate	Product	Yield ^a	Entry	Substrate	Product	Yield ^a
1			39%	5			30%
2			37%	6			0%
3			74%	7			47% (1:1 dr)
4			86%	8			25% (1:1 dr)

^a Conditions: 5 mol % $\text{Pd}(\text{OAc})_2$, 1.2 equiv $\text{PhI}(\text{OAc})_2$, $\text{AcOH}/\text{Ac}_2\text{O}$, 100 °C

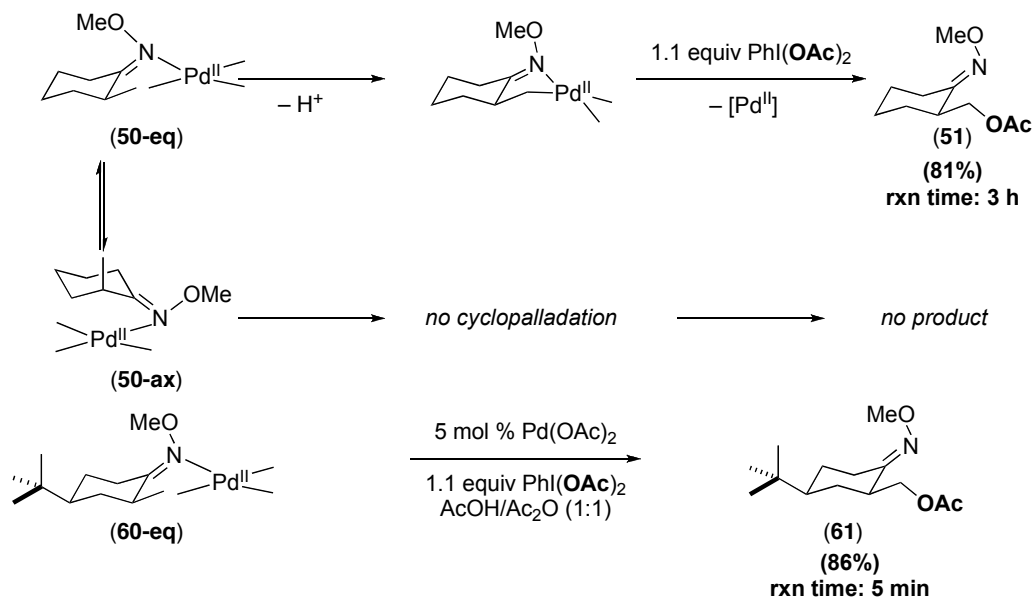
In the isoxazoline substrates containing a stereocenter, the functionalization of diastereotopic methyl groups proceeded with no selectivity. However, after our initial findings, Yu reported 82% de in the Pd-catalyzed acetoxylation of prochiral methyl groups in oxazoline substrate **70**.¹⁶ Notably, substrates in which the *tert*-butyl group on the tertiary carbon was replaced with other alkyl groups or ethers exhibited lower dr values ranging between 18% and 60%. Based on these results, it appears that both the location of the stereocenter within the substrate as well as the steric nature of the stereocenter and the substrate are key to attaining diastereoselectivity in these C–H activation reactions.

Scheme 2.16: Palladium-Catalyzed Acetoxylation of Prochiral Methyl Groups with
Lauroyl Peroxide



Conformational Effects on Reactivity. While conducting these studies we made an interesting observation regarding the reactivity differences between substrates **50** and **60**. Both these substrates lead to similar yields of the corresponding products **51** and **61**. However, while reaction of substrate **50** took 3 h to reach completion, reaction of **60** was finished in only 5 min. This dramatic difference can be rationalized based on the relative amounts of the reactive conformers of **50-eq** and **50-ax** in solution (Scheme 2.17). Methyl cyclohexanone **50** exists in two conformers of similar energy that are at rapid equilibrium – one in which the methyl group is in the equatorial position (**50-eq**) and one in which the methyl group is in the axial position (**50-ax**). However, only conformer **50-eq** has the C–H bond of the methyl group co-planar with the oxime, the geometry required for cyclopalladation. In contrast, substrate **60**, possessing a *tert*-butyl group on the cyclohexane ring, essentially exists only as the more reactive conformer **60-eq** with the β-C–H bond coplanar with the oxime ether.

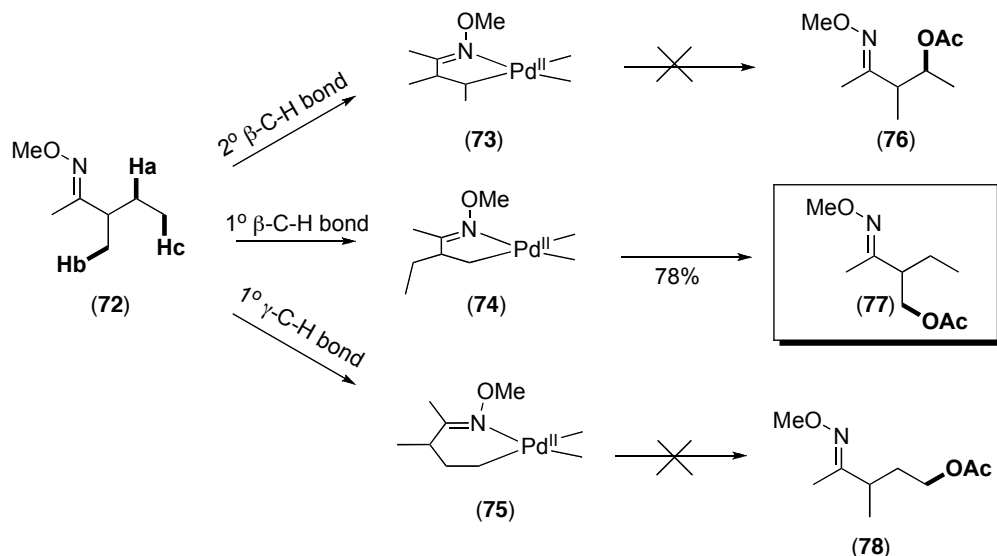
Scheme 2.17: Effect of a *t*-Bu Conformational Lock on the Rate of Pd-Catalyzed C–H Bond Acetoxylation



Regioselectivity. We were next interested in exploring the relative preference for functionalization of 1° relative to 2° sp³ C–H bonds under our reaction conditions. In addition, we wanted to compare the selectivity for the functionalization of sp³ C–H bonds that are four versus five bonds away from the chelating group. Substrate **72** was synthesized in order to investigate both issues. This substrate possesses three potential sites for C–H activation: (i) a 2° β-C–H bond (H_a), whose activation would lead to the formation of a five-membered palladacycle intermediate **73**, (ii) a primary β-C–H bond (H_b), whose activation would also afford a five-membered palladacycle **74**, and (iii) a 1° γ C–H bond (H_c), whose activation would afford the six-membered palladacycle **75** (Scheme 2.18). When **72** was subjected to our reaction conditions, we were pleased to see that C–H activation/acetoxylation proceeded with very high selectivity. This reaction afforded 78% isolated yield of a single product (**77**), in which a 1° β-C–H bond was acetoxyated. This result indicates that directed C–H activation at Pd(OAc)₂ shows a high preference for 1° over 2° C–H bonds. Notably, the observed selectivity is much higher than that in the Pt-catalyzed Shilov system.⁴ This selectivity is complementary to that obtained using other C–H functionalization methods that proceed by radical or cationic mechanisms.^{1, 17, 18} In addition, the results in Scheme 2.18 show that there is a preference

for the formation of five-membered palladacycles over six-membered palladacycles. This preference is further exemplified by the lack of reactivity of substrates such as **64** (Table 2.3) and **46** (Table 2.2). Notably, although formation of both 5- and 6-membered palladacycles is reported in literature,¹⁹ generally a preference for 5-membered metallacycles has been noted. It has been reasoned that this could be due to the requirement of a square-planar coordination environment at the metal. Six membered palladacycles have been achieved when (i) C-H bonds that can form five-membered metallacycle are absent and (ii) steric features of the substrate influence metallacycle formation.¹⁹

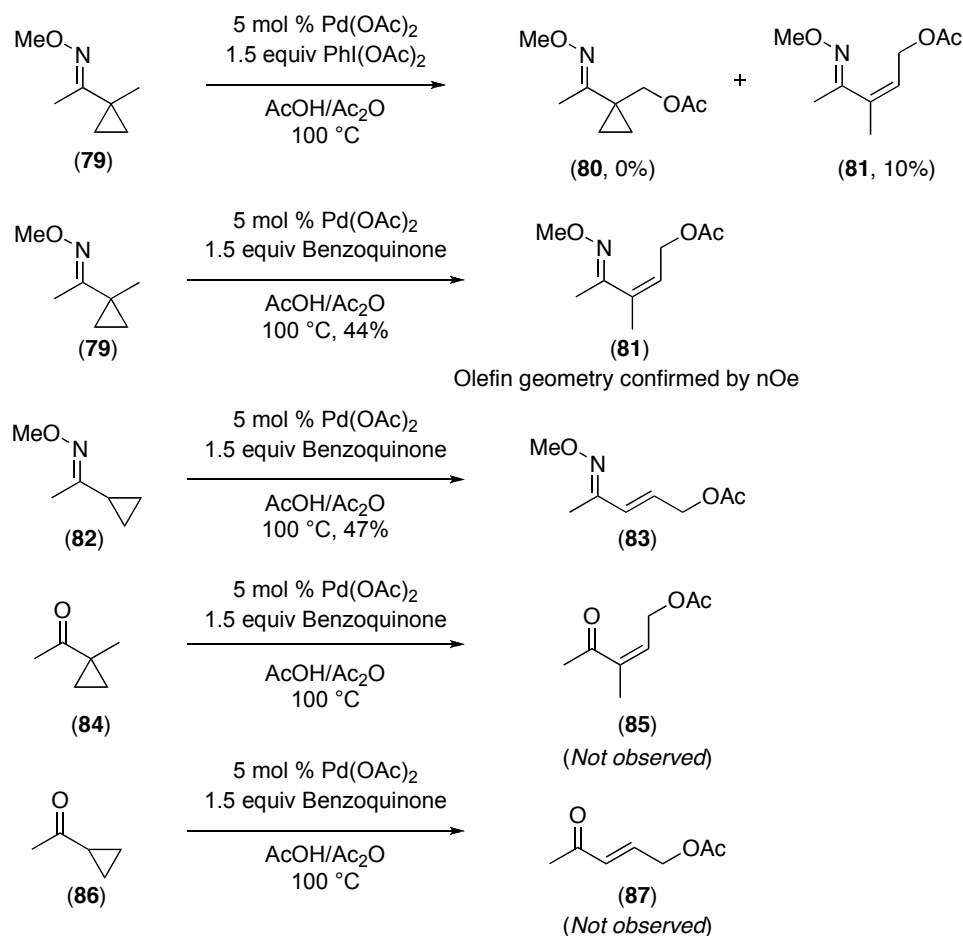
Scheme 2.18: Regioselectivity in sp^3 C-H Bond Acetoxylation



Cyclopropane Substrates. During efforts aimed at expanding the scope of this methodology, an interesting reaction was observed with the cyclopropyl methyl oxime ether substrate **79**. Subjection of **79** to the standard reaction conditions (5 mol % Pd(OAc)₂, 1.2 equiv PhI(OAc)₂ in a 1:1 mixture of AcOH/Ac₂O at 100 °C) resulted in the formation of a ring opened product **81**, rather than the expected acetoxyated product **80** (Scheme 2.19). Importantly, control experiments in the absence of Pd(OAc)₂ showed none of product **81**, indicating that this reaction is palladium-catalyzed. Interestingly, product **81** was also obtained when the reaction was carried out in the presence of benzoquinone, a weaker oxidant than PhI(OAc)₂ that is traditionally used in Pd^{0/II}

catalyzed reactions. This result indicates that the acetate in the product is derived from the solvent and further that the reaction does not involve Pd^{IV} intermediates.

Scheme 2.19: Pd-Catalyzed Oxime-Directed Oxidative Ring Opening of Cyclopropanes



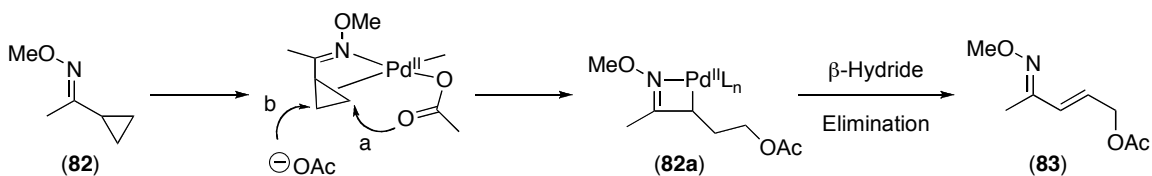
Substrate **82** also yielded the ring-opened product in 83% yield when subjected to catalytic conditions (5 mol % Pd(OAc)₂, 1.5 equiv benzoquinone, 100 °C in AcOH/Ac₂O) (Scheme 2.19). However, interestingly, the analogous reaction with ketones **84** and **86** did not afford ring opened products (Scheme 2.19). Instead, unreacted starting material was recovered. This indicates that the oxime ether directs ring opening in the reaction.

Notably, Yu and co-workers observe C-H activation/iodination of the cyclopropane C-H bond, resulting in products similar to **80**, instead of ring-opened products such as **81**, using oxazoline directing groups.²⁰ These transformations occur in

CH₂Cl₂ at room temperature with 10 mol% Pd(OAc)₂, I₂ in conjunction with PhI(OAc)₂. These results are in sharp contrast to the cyclopropane ring-opening observed in our reactions.

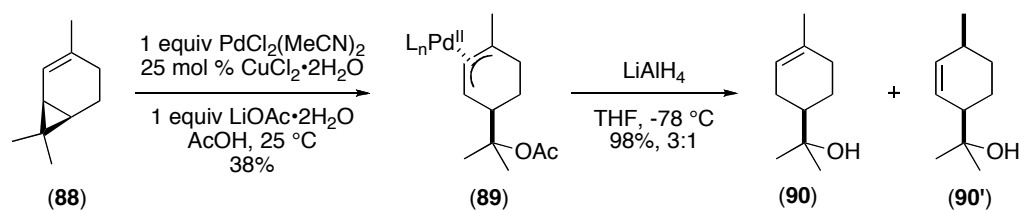
A proposed mechanism for this reaction involves the Pd^{0/II} pathway shown in Scheme 2.20. Simultaneous coordination of the palladium to the oxime ether and cyclopropane could facilitate either intramolecular (path a) or intermolecular (path b) acetate attack on the 3-membered ring to afford intermediate **82a** (Scheme 2.20). Subsequent β -hydride elimination from intermediate **82a** would then afford product **83**.

Scheme 2.20: Proposed Mechanism for Pd-Catalyzed Oxidative Ring Opening of Cyclopropanes



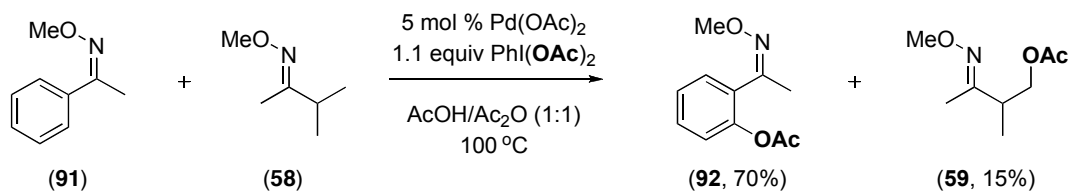
Even though we have not conducted detailed mechanistic studies, the above mechanism can be surmised based on preliminary data and on literature precedence. First, the lack of reactivity with ketones **84** and **86**, implicates the necessity of a directing group and its possible role in assisting the metal to activate the cyclopropane ring. Second, control reactions of substrates **79** and **82**, in the absence of palladium, did not afford even traces of **81** and **83**. This result and the fact that benzoquinone is necessary for turnover, together indicate the possibility of a Pd^{II/0} catalytic cycle.

There are a few literature reports of nucleophilic directed ring opening of cyclopropanes at Pd^{II}. For example, Backvall has shown the nucleophilic ring opening of the cyclopropane in substrates such as 2-carene using stoichiometric Pd(Cl)₂(MeCN)₂ (Scheme 2.21).²¹ He speculates that the palladium binds to the olefin, which assists the metal in activating the cyclopropane for nucleophilic attack by the solvent, acetic acid. The ring-opened palladium complex **89** is then reduced to two isomeric allyl and homoallyl alcohols.

Scheme 2.21: Olefin-Assisted Nucleophilic Ring Opening of Cyclopropane 88**2.4 Competition Studies: sp² versus sp³ C–H bonds**

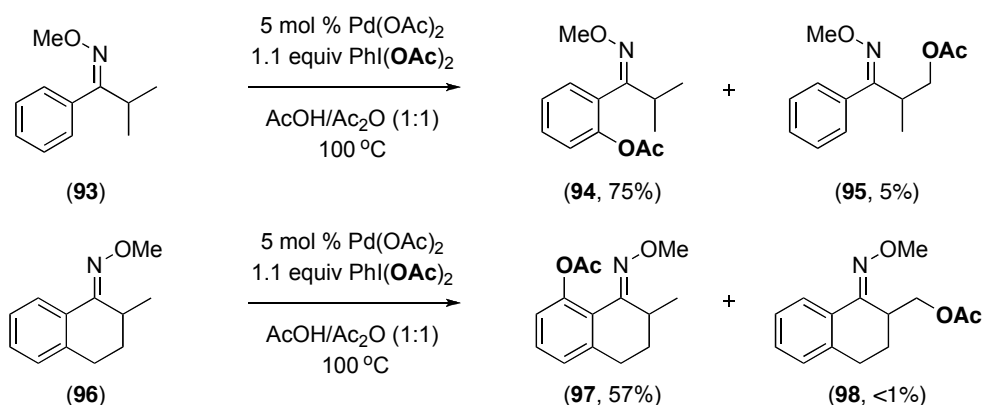
We next desired to investigate the relative rates of functionalization of sp² and sp³ C–H bonds. It has been widely reported that cyclometallation of sp³ C–H bonds is much more difficult at transition metal centers than their sp² counterparts.^{22, 23} Several reports have studied the competition between sp² and sp³ C–H bonds in stoichiometric cyclopalladation reactions.²⁴⁻²⁷ However, the effects of directing group and of chelate ring size on the relative rate of sp² versus sp³ C–H bond functionalization has not been systematically investigated in Pd-catalyzed reactions.

We began our investigations by carrying out a competition experiment between oxime ether substrates **91** and **58**, bearing sp² and sp³ C–H bonds, respectively. When **91** and **58** were subjected to the catalytic reaction conditions in the same reaction vessel, a 4.7 : 1 ratio of products **92** : **59** was obtained. After statistical correction for the number of C–H bonds available in each case, we obtain a relative reactivity of 15.6 : 1 for the sp² and sp³ C–H bond, respectively. However, this is not a completely fair comparison, as oxime ether coordination is likely to be favored for the less-sterically hindered substrate **91**, thereby further favoring formation of product **92**.

Scheme 2.22: Competition Between 91 and 58 in the Same Reaction Vessel

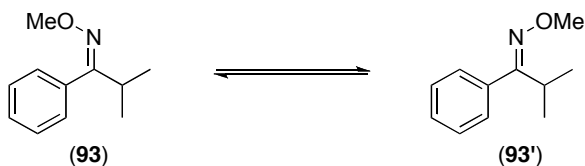
In order to exclude the possibility of varying coordinating abilities of the oxime ether in two different substrates, we designed substrates **93** and **96**, which contain both sp^3 and sp^2 C–H bonds to be functionalized in the same molecule. The Pd-catalyzed acetoxylation of these molecules resulted in preferential functionalization of the sp^2 C–H bond (Scheme 2.23). With substrate **96**, product **97** was formed exclusively and none of the corresponding sp^3 C–H acetoxylation product was observed.

Scheme 2.23: Competition Between sp^2 and sp^3 C–H bonds within the Same Molecule



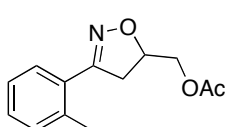
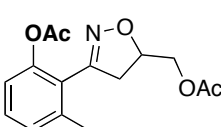
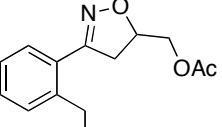
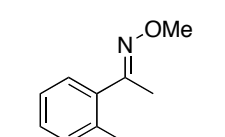
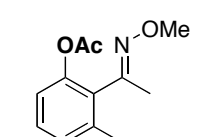
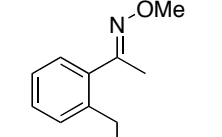
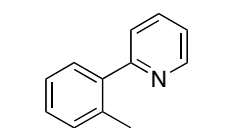
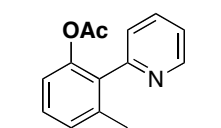
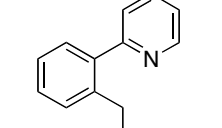
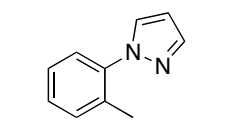
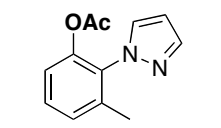
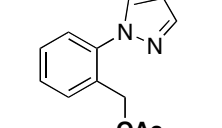
The formation of **94** as the major product might be due to the greater propensity of arene C–H bonds to undergo C–H activation. Alternatively, this preference of sp^2 C–H bond acetoxylation could result from the biases in the oxime isomer conformers. As illustrated in Scheme 2.24, substrate **93** can exist in two different oxime isomer conformations that equilibrate under our reaction conditions. Oxime isomer conformation **93'** favors cyclopalladation of the sp^2 C–H bond while **93** would lead to C–H activation at an sp^3 site.

Scheme 2.24: Equilibration between Oxime Isomers



We next carried out a systematic study of the effects of different directing groups on the relative rates of acetoxylation of sp^2 and sp^3 C–H bonds. We began with studying the competition between sp^2 C–H bonds and benzylic C–H bonds. Substrates bearing four different directing groups were synthesized – oxime ether (**102**), isoxazoline (**99**), pyridine (**105**) and pyrazole (**108**). In these systems, functionalization of the benzylic position would require formation of a six membered palladacyclic intermediate while activation of the arene site would proceed via a 5-membered palladacycle (Table 2.4). As shown in Table 2.4, the pyridine and pyrazole directing groups led to products **106** and **109**, resulting from exclusive functionalization of an arene C–H bond (entries 3 and 4). Substrate **102** bearing the oxime ether directing group exhibited somewhat decreased selectivity for acetoxylation of the sp^2 C–H bond and produced **103** and **104** in a 12 : 1 ratio (entry 2). Interestingly, the isoxazoline substrate **99** presented only modest preference for sp^2 over sp^3 C–H bonds, affording a mixture of products **100** and **101** in a 0.8 : 1 ratio. Notably, after correcting for statistics (the number of C–H bonds available), the ratio of sp^2 to sp^3 for substrate **99** becomes 2 : 1. Hence, the sp^2 center is still slightly favored, even here.

Table 2.4: Competition Between Benzylic sp^3 C–H Bonds and sp^2 C–H Bonds as a Function of Directing Group

Entry	Substrate	Product A	Product B	Ratio A:B
1	 (99)	 (100 , 27%)	 (101 , 34%)	0.8 : 1
2	 (102)	 (103 , 58%)	 (104 , 5%)	12 : 1
3	 (105)	 (106 , 65%)	 (107 , 0%)	1 : 0
4	 (108)	 (109 , 90%)	 (110 , 0%)	1 : 0

As mentioned above, the ring sizes of the palladacyclic intermediates formed with sp^2 and sp^3 C–H bonds in substrates **99-108** were different. Therefore, we wondered if the selectivity would be reversed if the two ring sizes were switched. However, before answering this question, we sought to determine the largest size palladacycle that could be formed and functionalized under our reaction conditions. Three different directing groups – isoxazoline, pyridine and methyl oxime ether – were selected for this study, and the chain length between the directing group and an appended phenyl ring was systematically varied. As shown in Table 2.5, isoxazoline substrates **113** and **114**, which

react via 6- and 7-membered palladacycles, respectively, afforded the acetoxyated products in high yields (entries 2 and 3). However, substrates **117-121**, which require formation of 8-, 10-, and 12-membered palladacyclic intermediates, did not form appreciable amounts of the desired acetoxyated products (entries 4, 5, and 6, respectively).

Table 2.5: Effect of Palladacycle Ring Size on Yields of Pd-Catalyzed C–H Activation/Acetoxylation with Isoxazoline Directing Groups I

Entry	Substrate	Major Product	Yield
1			30%
2			72%
3			75%
4			<5%
5			0%
6			0%

Unlike the isoxazolines, the oxime ether and pyridine directing groups only afforded C–H activation/acetoxylation products via the formation of 5- or 6-membered palladacycles (Table 2.6). The oxime ether substrate **127** provided low (17%) yield of the acetoxyated product **128** generated via a seven-membered palladacycle (entry 3), while the corresponding pyridine substrate **133** showed essentially no reaction (entry 6).

Table 2.6: Effect of Palladacycle Ring Size on Yields in Pd-Catalyzed C–H Activation/Acetoxylation with Oxime Ether and Pyridine Directing Groups

Entry	Substrate	Major Product	Yield
1			73%
2			89%
3			17%
4			83%
5			44%
6			0%

With this data in hand, we predicted that an sp^3 C–H bond that was five bonds away from the chelating group might be functionalized selectively over an sp^2 C–H bond that was further removed. To test this hypothesis, we synthesized isoxazoline substrates **135-141**, which all contain an sp^3 C–H bond 5 bonds from the directing group and an sp^2 C–H bond 5, 6, or 7 bonds away from the chelating nitrogen atom (Table 2.7). However, surprisingly, reaction of substrates **135** and **138** afforded predominantly sp^2 C–H functionalization products **136** and **139**, along with only traces of **137** and **140**. Even when the sp^2 C–H bond was too far to undergo efficient functionalization, such as in substrate **141**, the sp^3 C–H bond did not react.

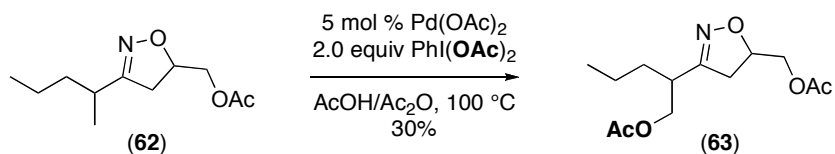
Table 2.7: Effect of Palladacycle Ring Size on Yields in Pd-Catalyzed C–H Activation/Acetoxylation with Isoxazoline Directing Groups II

Entry	Substrate	Product A	Product B
1	 (135)	 (136, 56%)	 (137, <2%)
2	 (138)	 (139, 60%)	 (140, <2%)
3	 (141)	 (142, 10%)	 (143, <2%)

We thought that this lack of reactivity might be due to a steric or conformational effect of the alkyl chain in these systems. In order to test this proposal, we replaced the phenyl group with a propyl chain (substrate **62**). As shown in Scheme 2.25, even this

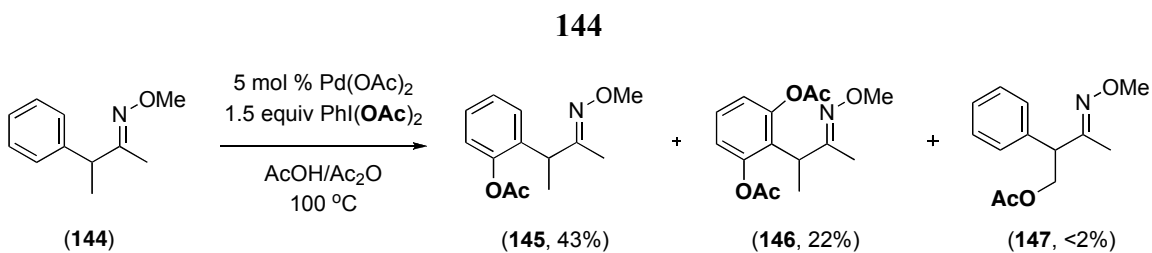
substrate afforded only modest 30% yield of the acetoxyated product (compared to 47% for the corresponding *i*-Pr substituted derivative **66**), confirming that this class of substrates exhibits inherently low reactivity.

Scheme 2.25: Effect of Sterics on Acetoxylation of **62**



We wondered if the effect discussed above was specific to isoxazoline directing groups. Consequently, we repeated the above experiment with oxime ether substrate **144**, which could undergo sp^2 C–H activation to form a 6-membered palladacycle or sp^3 C–H activation to generate a 5-membered palladacycle (Scheme 2.26). Subjection of **144** to the catalytic reaction conditions afforded similar results as the isoxazoline, and only products **145** and **146**, resulting from mono- and di-functionalization of the arene, were observed.

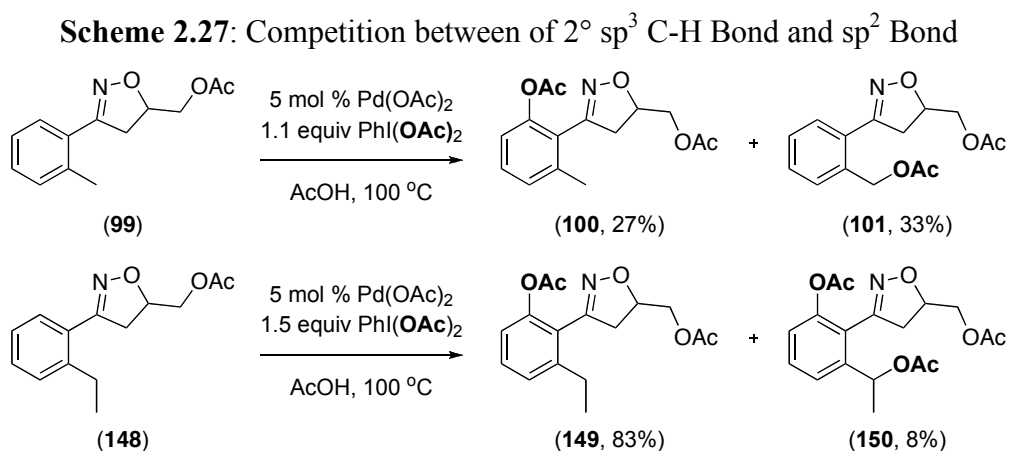
Scheme 2.26: Competition Between sp^2 and sp^3 C–H Bonds in Oxime Ether Substrate



In all, these results indicate that in general, regardless of the nature of the directing group or the size of the palladacyclic intermediates, the relative rate of functionalization of an arene C–H bond appears to be faster than that of an sp^3 C–H bond. However, these studies also emphasize how difficult it is to design systems that really give a fair comparison.

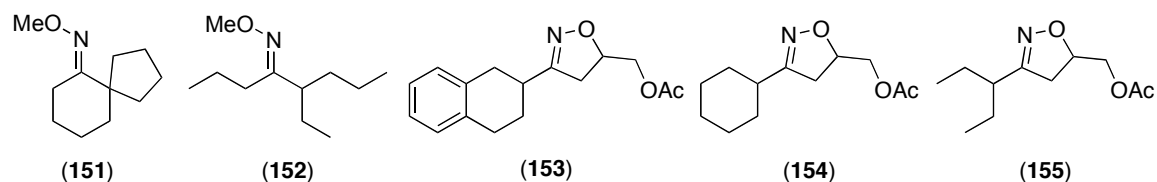
2.5 Functionalization of Secondary sp^3 C-H bonds

As discussed above, the activation of 2° sp^3 C-H bonds is even more challenging than that of the corresponding 1° substrates. For example, substrate **99**, which bears a 1° C-H bond and a sp^2 C-H bond proximal to the directing group, reacted to form a 2 : 1 (after statistical correction) mixture of the two possible mono-acetoxylation products (Scheme 2.27). However the analogous substrate **148**, where the methyl group is replaced by an ethyl group, afforded only 8% of the 2° sp^3 C-H bond functionalized product **150** (Scheme 2.27). Furthermore, this functionalization took place after the sp^2 C-H bond was already acetoxyated (*ie*, when no other sites were available for directed C-H activation). In addition, substrate **148** contains an “activated” benzylic 2° sp^3 C-H bond. These results emphasize that unactivated 2° C-H bonds are expected to be even more unreactive.



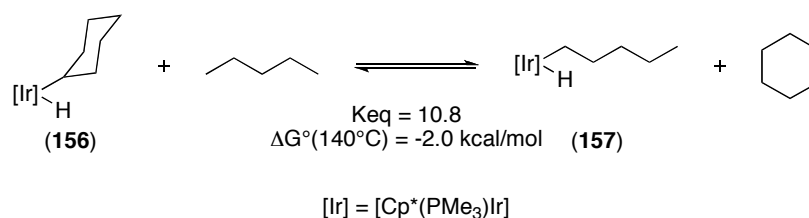
Several different features were explored in an attempt to promote Pd-catalyzed C-H activation/acetoxylation of unactivated 2° sp^3 C-H bonds. These include: (i) increasing branching α to the directing group (substrates **152** and **155** in Figure 2.2), (ii) the use of substrates that would form 5- or 6-membered palladacycles (**151**, **153-155** and **152**, respectively), and (iii) the use of different directing groups. However, none of these substrates afford any of the desired acetoxyated products under our standard conditions (5 mol % Pd(OAc)₂, 1.5 equiv PhI(OAc)₂ in AcOH or AcOH/Ac₂O at 100 °C).

Figure 2.2: Substrates Containing Unactivated 2° sp³ C–H Bonds Showing No Reactivity



We believe that the functionalization of 2° sp³ C–H bonds is challenging for two reasons. First, literature studies show that activation of 2° sp³ C–H bond at transition metal centers is less thermodynamically favourable. Bergman illustrated this concept through studies of the reaction of Ir complexes with cyclohexane and *n*-pentane.²⁸ As shown in Scheme 2.28, a K_{eq} of 10.8 was obtained, indicating that the 1° Ir alkyl complex **157** was more stable than the 2° alkyl species **156**.

Scheme 2.28: Studies of Iridium Complexation with 1° and 2° sp³ C–H Bonds

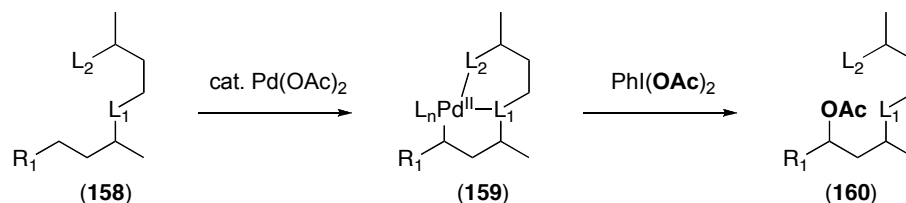


Another reason 2° sp³ C–H bonds are hard to functionalize is due to conformational restriction. It can be challenging to achieve co-planarity between the directing group and the C–H bond, which is known to facilitate C–H activation. As such, we thought we could promote activation of 2° sp³ C–H bonds, by taking advantage of the double chelation effect and the conformational effects observed earlier (Scheme 2.17).

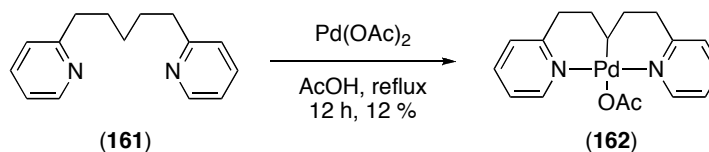
Double Chelation Effect. The strategy behind ‘double chelation’ is to employ substrates consisting of two different potential directing groups rather than just one. In these systems, the simultaneous coordination of both the ligands to the metal center is expected to lock the Pd proximal to the desired C–H bond (for example, intermediate **159** in Scheme 2.29 where L₁ and L₂ are two different chelating ligands for palladium), hence leading to more facile activation of the 2° C–H bond. This concept has been demonstrated in the cyclometalation literature. For example, Canty has shown that the cyclopalladation

of substrate **161** proceeds in 12% yield (Scheme 2.30). In contrast, 2-butyropyridine is unreactive under identical conditions.²⁹

Scheme 2.29: Double Chelation Strategy for 2° sp³ C–H Bond Activation

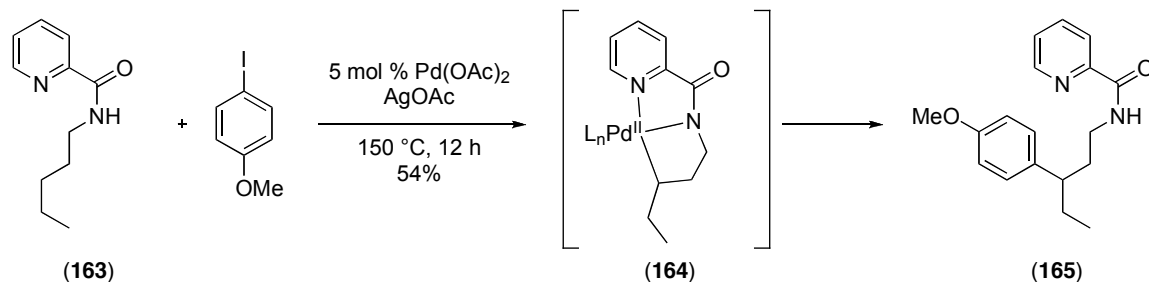


Scheme 2.30: Application of the Double Chelation Strategy

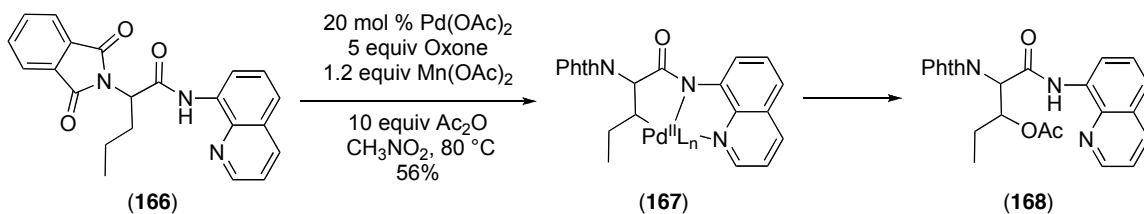


After the introduction of our chemistry in 2004, several other groups described related Pd-catalyzed reactions involving directed functionalization of sp³ C–H bonds. Several of these reports, including work by Daugulis and by Corey, described the use of the double chelation strategy for the functionalization of 2° sp³ C–H bonds. In one example, Daugulis demonstrated the arylation of a 2° sp³ C–H bond in substrate **163**, and proposed a mechanism involving simultaneous coordination of the quinoline and amide directing groups to the Pd^{II} center (Scheme 2.31).³⁰ Similarly, Corey successfully transformed a 2° sp³ C–H bond in 8-aminoquinoline derivative **166** into a C–OAc bond.³¹ Again, dual chelation of the amide and quinoline functionalities was proposed to be critical for the success of this reaction (Scheme 2.32).

Scheme 2.31: Application of Dual Chelation Strategy: Pd-Catalyzed Arylation of a 2° sp³ C–H Bond

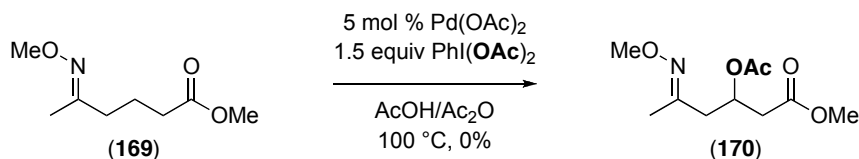


Scheme 2.32: Application of Dual Chelation Strategy: Pd-Catalyzed Acetoxylation of a 2° sp³ C–H Bond



We had similarly reasoned that a dual chelation strategy might be applied in our C–H activation/acetoxylation reactions. In order to investigate this possibility, we synthesized a number of different substrates containing multiple functionalities with the ability to coordinate to the palladium. Substrate **169**, containing an oxime ether and an ester functionality, displayed no reactivity under the reaction conditions (5 mol % Pd(OAc)₂, 1.5 equiv PhI(OAc)₂ at 100 °C in AcOH/Ac₂O) (Scheme 2.33). Reaction of substrate **171**, containing pyridine and oxime ether directing groups, under our standard conditions afforded only product **172**, where pyridine-directed functionalization occurred at the 1° sp³ C–H bond α to the oxime (Scheme 2.34). Oxime ether derived substrates **174–177** (Figure 2.3), which contain amide and pyridine functionalities as the two directing groups, did not afford an appreciable amount of acetoxyated products under the standard reaction conditions. Optimization studies involving different solvents, temperatures, and catalysts with substrates **174–177**, either led to decomposition (substrates **174** and **177**) or recovered starting material (substrates **175** and **176**). The application of Corey’s conditions with these substrates also produced similar results.³¹

Scheme 2.33: Dual Chelation Strategy: Ester and Oxime Ether Directing Groups



Scheme 2.34: Dual Chelation Strategy: Pyridine and Oxime Ether Directing Groups

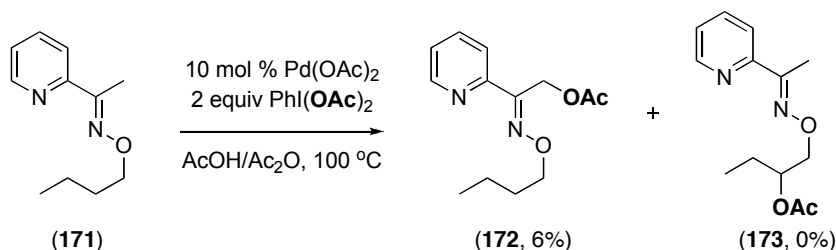
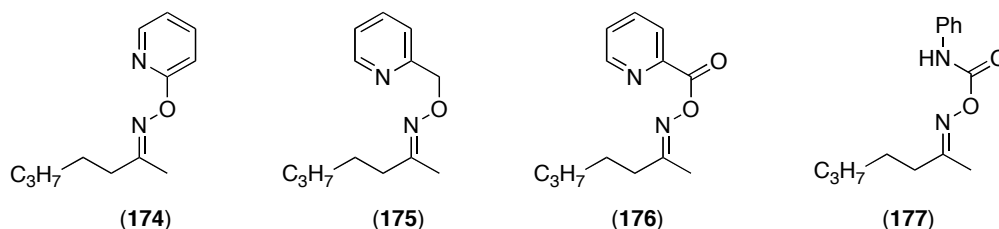
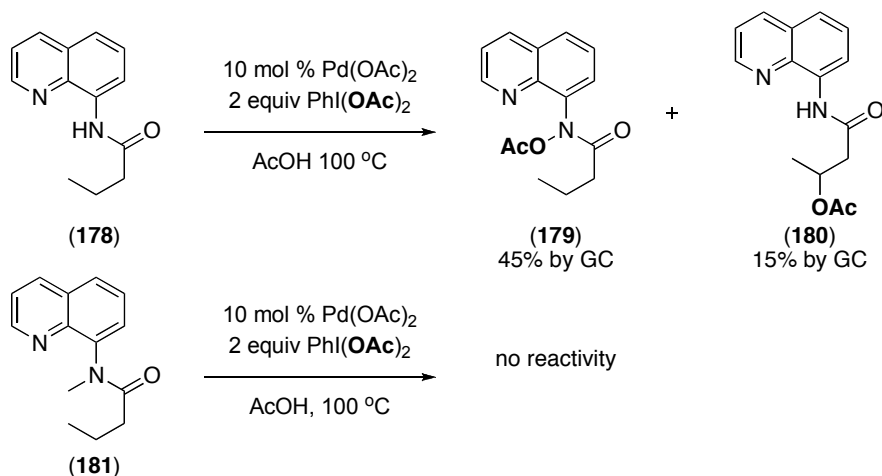


Figure 2.3: Dual Chelation Strategy: Other Substrates Examined



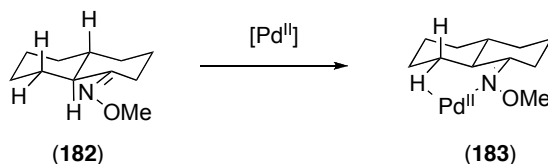
Since substrates **169-177** did not afford any acetoxylation at the 2° positions, we next examined substrates more similar to Corey's compound **166** under our reaction conditions.³¹ Hence, substrate **178**, containing an amide and a quinoline as potential directing groups, was synthesized and subjected to 10 mol % Pd(OAc)₂, 2 equiv PhI(OAc)₂ in AcOH at 100 °C (Scheme 2.35). Gratifyingly, product **180**, in which a 2° C–H bond was acetylated, was obtained, albeit in low (15%) yield. This low yield appears to be due to competitive *N*-acetoxylation to form product **179**. To address this side reaction, we next examined the analogous *N*-methylated substrate **181**. However, as shown in Scheme 2.35, **181** displayed no reactivity, implicating that the free amide is involved in binding to the palladium and directing C–H activation in substrate **178**.

Scheme 2.35: Dual Chelation Strategy: 8-Amidoquinoline Derivatives



Conformational Lock Effect. We next sought to explore the application of conformational effects to facilitate 2° sp³ C–H bond functionalization. We reasoned that C–H activation would be facilitated in substrates with the 2° sp³ C–H bond locked in the same plane as the directing group. To test this hypothesis, we synthesized the methyl oxime ether of *trans*-decalone (**182**.) In this substrate there are two β 2° C–H bonds, one in the axial position and the other in the equatorial position. As shown in Scheme 2.36, the C–H bond in the equatorial position is locked in the same plane as the directing group.

Scheme 2.36: Conformational Lock Strategy: *trans*-Decalone Oxime Ether



We were pleased to find that the *trans*-decalone oxime ether underwent clean C–H bond acetoxylation under our standard conditions (5 mol % Pd(OAc)₂, 1.1 equiv PhI(OAc)₂ in AcOH/Ac₂O at 100 °C) to provide **184** in 81% yield as a single diastereomer (Scheme 2.37). Importantly, both NMR coupling constant analysis and x-ray crystallography revealed that this diastereomer contained the acetate in the equatorial position, *cis* to the proton at the junction of the fused rings. The coupling constant

between H_a and H_b was 10.9 Hz, indicating a *trans* relationship. Since oxime ether **182** was an oil, the crystal structure of the deprotected ketone product **185** was obtained (Figure 2.4), and, again, this confirmed the proposed stereochemistry.

Scheme 2.37: Conformational Lock Strategy: Pd-Catalyzed Acetoxylation of *trans*-Decalone Oxime Ether

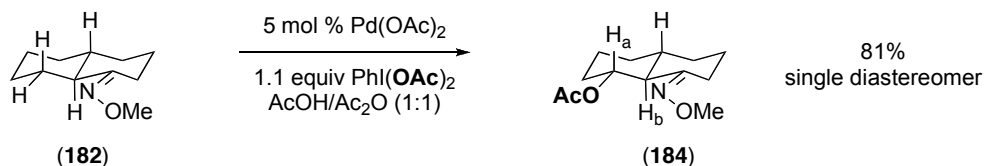
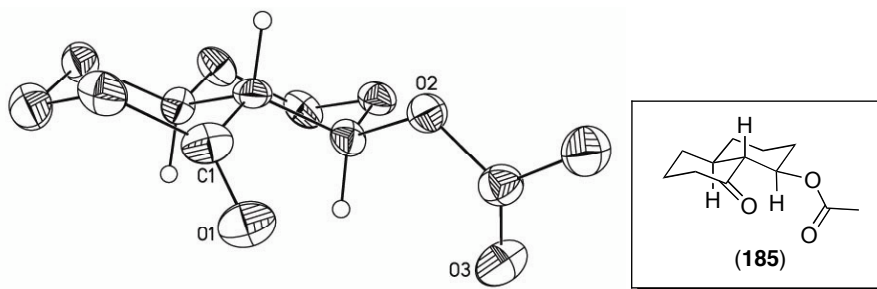


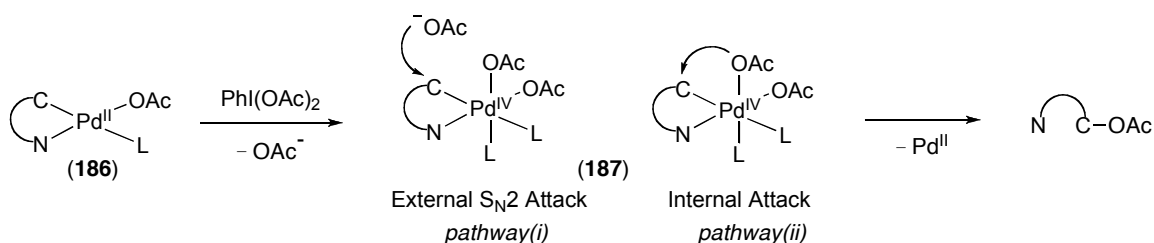
Figure 2.4: Crystal Structure of Deprotected Acetate Product **185**



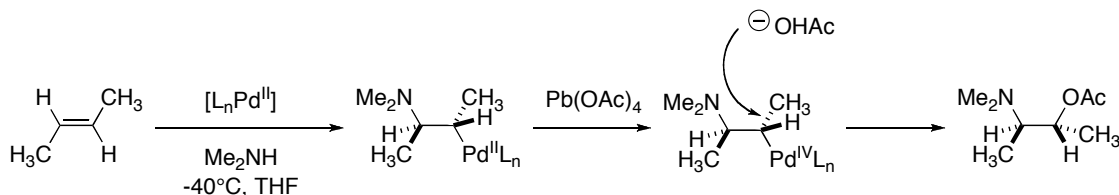
2.6 Stereochemical Nature of Reductive Elimination

The high diastereoselectivity of the reaction in Scheme 2.37 indicates that C–H activation and functionalization occur with high stereochemical fidelity in this system. This substrate also serves as a probe for the stereochemical nature of the reductive elimination step. As shown in Scheme 2.38, after oxidation of the cyclopalladated complex **186** to Pd^{IV}, there are two potential pathways through which reductive elimination can take place. These are: (i) external acetate attack via an S_N2-type mechanism leading to inversion of stereochemistry at carbon or (ii) direct reductive elimination of coordinated acetate leading to retention of stereochemistry at carbon. There is precedent for the oxidative functionalization of Pd-alkyl intermediates with both inversion (Scheme 2.39)³² and retention (Scheme 2.40)³³ in the literature.

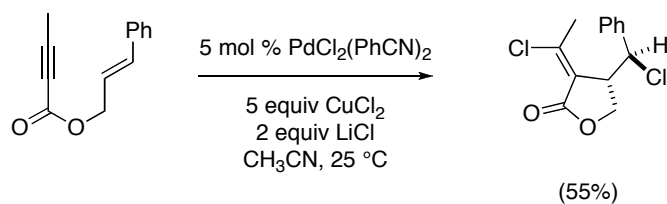
Scheme 2.38: Possible Mechanisms for C–O Bond-Forming Reductive Elimination



Scheme 2.39: Reductive Elimination with Inversion of Stereochemistry



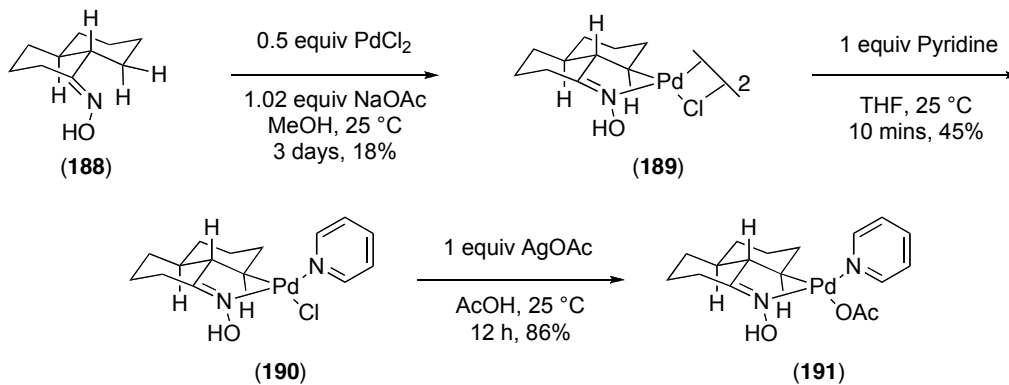
Scheme 2.40: Reductive Elimination with Retention of Stereochemistry



In order to confirm which mechanism is operating in this system, we studied the stoichiometric conversion of a cyclopalladated *trans*-decalone oxime complex to the mono-acetoxyated organic product **184**. Initial attempts to synthesize a palladacycle of the oxime ether **182** yielded complex mixtures of products that could not be separated. However, literature precedent suggested that palladacycle formation is much more facile for oximes.¹¹ Hence, we synthesized the chloride-bridged palladacycle dimer of *trans*-decalone oxime (**189**), by stirring **188** in MeOH with stoichiometric Na_2PdCl_4 and NaOAc at room temperature for 3 days (Scheme 2.41). Reaction of the dimer with pyridine in THF, then afforded the desired chloride-monomer along with $Pd(py)_2(Cl)_2$ (py = pyridine) as an impurity (Scheme 2.41). The reaction time was critical in dictating the amount of impurity formed, and 10 min was found to be optimal, leading to a $Pd(py)_2(Cl)_2$: **190** ratio of 1.5 : 1. Multiple purifications by column chromatography and crystallization afforded the desired complex in 93% purity. The chloride monomer was

also transformed to the acetate monomer **191** by reaction with AgOAc in AcOH (Scheme 2.41).

Scheme 2.41: Stoichiometric Cyclopalladation of *trans*-Decalone Oxime



The structures of the chloride and acetate monomers **190** and **191** were confirmed by X-ray crystallography. The crystal structures of these complexes are shown in Figures 2.5 and 2.6. As predicted in Scheme 2.41 above, the palladacycles formed via activation of the equatorial β C–H bond.

Figure 2.5: X-Ray Crystal Structure of Chloro Monomer **190** (pyridine ligand truncated for clarity)

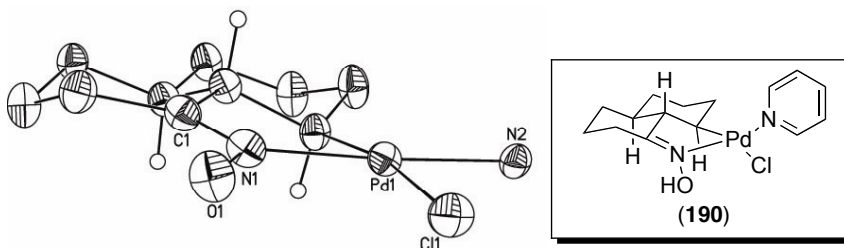
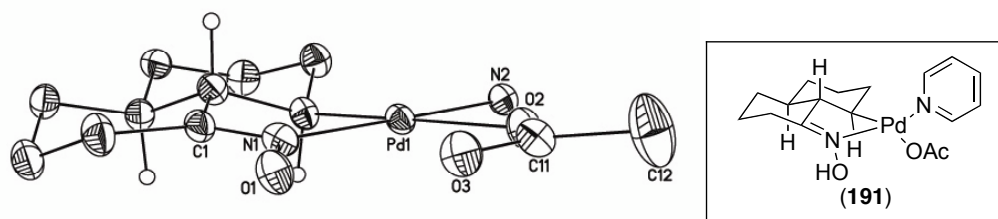
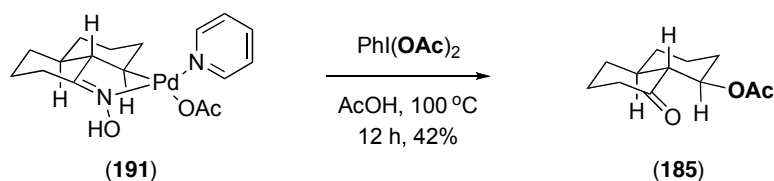


Figure 2.6: X-Ray Crystal Structure of Acetate Monomer **191** (pyridine ligand truncated for clarity)



We next studied the oxidation of **190** and **191** with $\text{PhI}(\text{OAc})_2$. Reaction of the acetate monomer **191** with $\text{PhI}(\text{OAc})_2$ at 100 °C in AcOH, provided the acetoxy ketone product **185** as a single diastereomer. As shown in Scheme 2.12 above, the ketone was presumably formed via deprotection of the oxime in the presence of the hypervalent iodine oxidant. The crystal structure of product **185** is shown in Figure 2.4 and clearly confirms that the OAc group is in the equatorial position. This data definitively demonstrates that the C–O bond-forming reaction proceeds with retention of stereochemistry at the carbon center, which implicates pathway ii in Scheme 2.38.

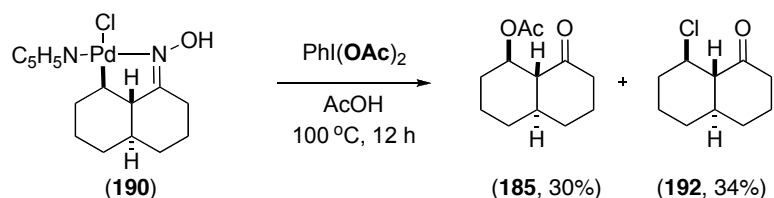
Scheme 2.42: Reaction of Complex **191** with $\text{PhI}(\text{OAc})_2$



Interestingly, the reaction of the chloride monomer with $\text{PhI}(\text{OAc})_2$ yielded two organic products – the expected acetate compound **185** and the chloride-containing product **192**. Importantly, both had the new functional group in the equatorial position, again demonstrating retention of stereochemistry at carbon in this reaction. The stereochemistry of the chloride product **192** was determined via coupling constant analysis (the coupling constant was 10.8 Hz, indicating a *trans* relationship between the ring junction hydrogen and the hydrogen on the carbon bearing the acetate). The

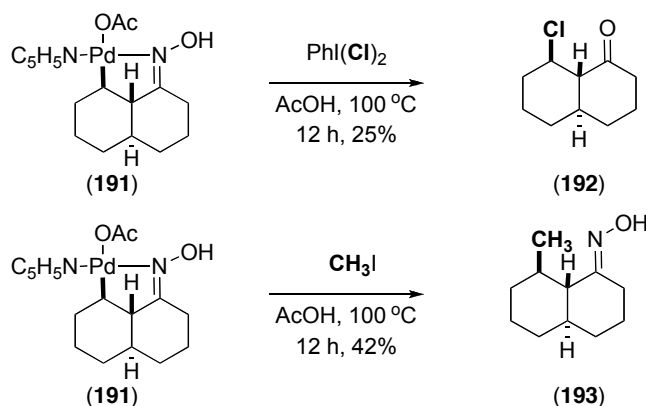
formation of **185** and **192** in an approximately 1 : 1 ratio implies that C–O and C–Cl bond-forming reductive elimination from Pd^{IV} are competitive under these conditions.

Scheme 2.43: Reaction of Complex **190** with PhI(OAc)₂ to Form C–O and C–Cl Functionalized Products



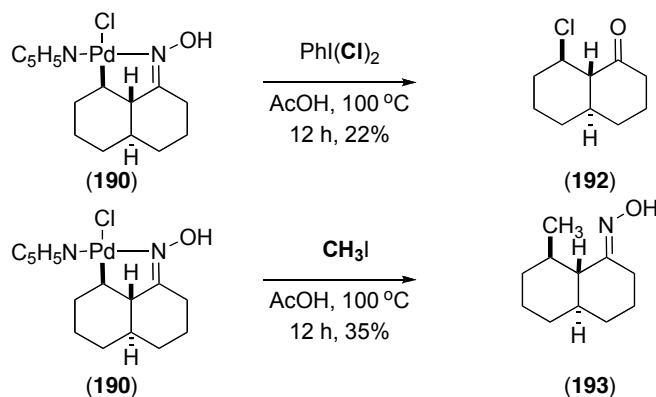
The next question we hoped to address was the relative rates of reductive elimination of different functional groups from Pd. In order to probe this, we carried out the reactions of chloro and acetate complexes **190** and **191** with two additional oxidants – PhICl₂ and MeI. Interestingly, the reaction of acetate monomer **191** with PhICl₂ afforded the chloride product **192** exclusively (Scheme 2.44), suggesting that despite the acetate ligand initially on the metal, only C–Cl bond-forming reductive elimination took place. Similarly, when MeI was used as the oxidant in the reaction of **191**, methylated compound **193** was the sole organic product obtained (Scheme 2.44). Again, the Me group was in the equatorial position (verified by x-ray crystal structure), indicating that reductive elimination occurred with retention.

Scheme 2.44: Oxidation of Complex **191** with PhICl₂ and MeI



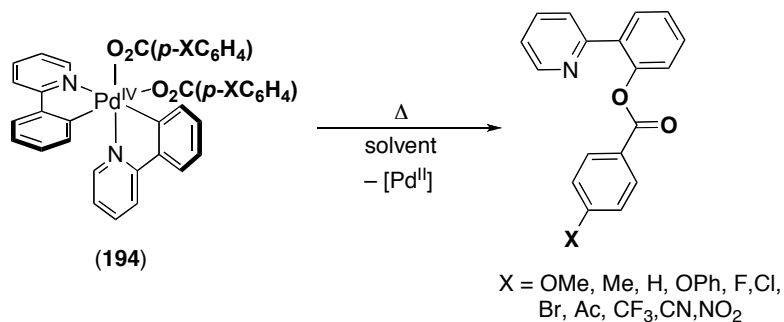
As shown in Scheme 2.45, reaction of the chloride monomer **190** with MeI formed solely the methylated product **193**, indicating preferential C–Me bond forming reductive elimination. As expected substitution of the chloride monomer **190** to PhICl₂ afforded the chloride product **192** (Scheme 2.45).

Scheme 2.45: Oxidation of Complex **190** with PhI(Cl)₂ and MeI



The data discussed above suggests that the order of preference for reductive elimination from Pd^{IV} is Me > Cl > OAc. Notably, we do realize that the *cis* versus *trans* geometry of the ligands in the transient Pd^{IV} intermediate can also influence the reductive elimination product distribution, since the X ligand must be *cis* to the carbon center for bond formation to take place. Nonetheless, the results thus far suggest a higher preference for reductive elimination of the most nucleophilic ligand. Importantly, the trend observed in the stoichiometric oxidation studies above is consistent with what has been observed in the benzoate Pd^{IV} complexes studied previously in our lab. Reductive elimination reactions from complexes such as **194** proceeded fastest with more electron donating substituents X on the benzoate ligand (Scheme 2.46).³⁴

Scheme 2.46: Reductive Elimination from (phpy)₂Pd^{IV}(O₂CAr)₂ Complexes

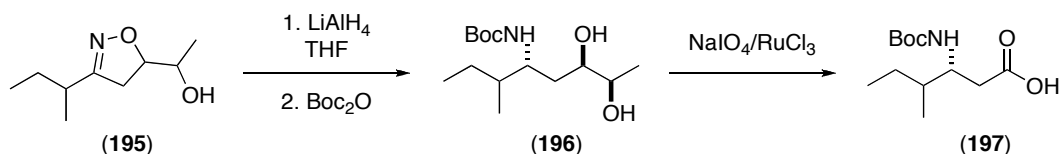


Notably, we have not yet been able to observe any appreciable amount of chlorinated or methylated products in catalytic reactions where PhI(OAc)₂ was substituted with PhICl₂ and MeI. With PhICl₂ we observed substrate decomposition and/or unselective chlorination. Reactions with MeI were hampered by the lack of catalytic turnover, and we typically recovered unreacted starting material.

2.7 Deprotection of Directing Groups

As mentioned in the introduction, the advantage of employing oxime ethers and isoxazolines as directing groups for C–H bond acetoxylation is that the products are useful synthons. Through functional group manipulations, we can access β -amino acids, β -hydroxy ketones, β -amino alcohols, and 1,3-diols. Several groups have studied the synthetic applications of isoxazolines. For example, Mapp and co-workers have developed an attractive method to transform isoxazolines into β -amino acids (Scheme 2.47).³⁵

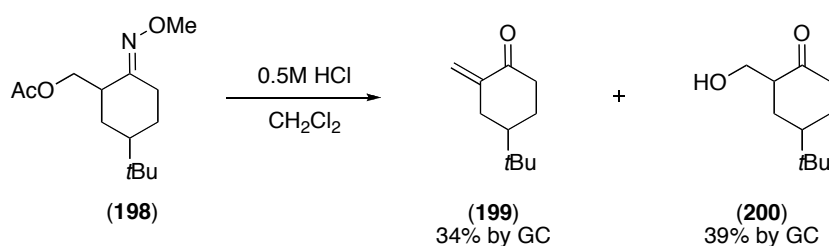
Scheme 2.47: Formation of β -Amino Acids from Isoxazolines



Methyl oxime ethers are robust protecting groups, and hence there are relatively limited literature examples of their deprotection.³⁶ In some cases, we have found that

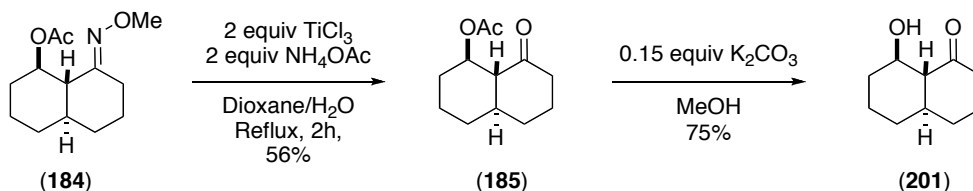
oxime ethers can be deprotected under acidic conditions. However, under those conditions, we also observe competitive elimination and/or hydrolysis of the acetate group. For example, subsection of substrate **198** to 0.5 M HCl in CH₂Cl₂ afforded the hydrolyzed product **200** along with alkene **199** (Scheme 2.48). A similar distribution of undesired products was obtained when the reaction of substrate **198** was conducted in refluxing 1 M AcOH.³⁶

Scheme 2.48: Attempts to Deprotect C–H Activation/Acetoxylation Product **198** with Bronsted Acids



These side reactions could be avoided using a procedure developed by Corey in the synthesis of prostaglandins.³⁷ Subsection of substrate **184** to Corey's conditions (2 equiv TiCl₃ and 2 equiv of NH₄OAc, in a refluxing mixture of 1:10 H₂O : dioxane) afforded deprotected β-keto-acetate product like **185** (Scheme 2.49) in 56% yield. This product could then be readily converted to the corresponding β-hydroxy ketone in 75% yield by reaction with 0.1 equiv K₂CO₃ in MeOH (Scheme 2.49).

Scheme 2.49: Deprotection of C–H Activation/Acetoxylation Product **184** with TiCl₃



2.8 Conclusion

In summary, Pd-catalyzed selective oxidation of 1° sp³ C–H bonds was achieved using directing groups such as oxime ethers and isoxazolines. Importantly, this reaction was applied to diverse substrates, and competitive β-hydride elimination was not observed. Competition studies between sp² and sp³ C–H bonds indicated a high preference for sp² C–H activation/functionalization. The functionalization of an unactivated 2° sp³ C–H bond was achieved by taking advantage of conformational effects in *trans*-decalone. This reaction proceeded with high diastereoselectivity, and allowed determination that C–O, C–Cl, and C–Me bond-forming reductive elimination from Pd^{IV} all proceed with retention of stereochemistry in this system. These studies also revealed a high preference for the reductive elimination of more nucleophilic ligands, with Me > Cl > OAc. Finally, products from these C–H activation/acetoxylation reactions have been converted to useful synthons via functional group interconversion reactions.

2.9 Experimental Procedure

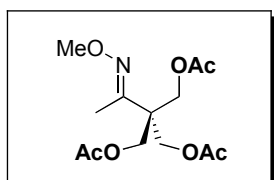
General Procedures: NMR spectra were obtained on a Varian Inova 500 (499.90 MHz for ¹H; 125.70 MHz for ¹³C) or a Varian Inova 400 (399.96 MHz for ¹H; 100.57 MHz for ¹³C) spectrometer. ¹H NMR chemical shifts are reported in parts per million (ppm) relative to TMS, with the residual solvent peak used as an internal reference. Multiplicities are reported as follows: singlet (s), doublet (d), doublet of doublets (dd), doublet of triplets (dt), triplet (t), quartet (q), multiplet (m), and broad resonance (br).

Materials and Methods: Oxime ether substrates were prepared by reaction of the analogous ketones with MeONH₂•HCl/pyridine.³⁸ Oximes were obtained as mixtures of E/Z isomers when the α-position was mono or disubstituted. The parent ketones of substrates **8** and **15** were prepared by alkylation of the analogous hydrazones followed by hydrolysis with 1 M HCl. Substrate **56** was prepared following a procedure by Chan.³⁹

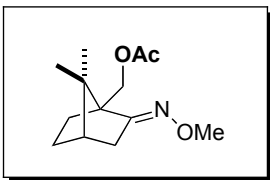
Isoxazolines were prepared by following a literature protocol.³⁵ Substrates that were commercially available were obtained from Acros, Lancaster, Aldrich or TCI America and used as received. $\text{PhI}(\text{OAc})_2$ and $\text{Pd}(\text{OAc})_2$ were obtained from Acros and Pressure Chemical, respectively, and were used as received. Solvents were obtained from Fisher Chemical and used without further purification. Flash chromatography was performed on EM Science silica gel 60 (0.040–0.063 mm particle size, 230–400 mesh) and thin layer chromatography was performed on Merck TLC plates pre-coated with silica gel 60 F₂₅₄.

General Procedure for Palladium-Catalyzed Acetoxylation of sp^3 C-H bonds:

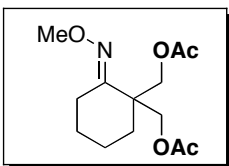
3-Methyl-2-butanone *O*-methyl oxime (200 mg, 1.74 mmol, 1 equiv), $\text{PhI}(\text{OAc})_2$ (621 mg, 1.91 mmol, 1.1 equiv), and $\text{Pd}(\text{OAc})_2$ (19 mg, 0.087 mmol, 0.05 equiv) were combined in AcOH (7 mL) and Ac_2O (7 mL) in a 20 mL vial. The vial was sealed with a Teflon lined cap, and the reaction was heated at 100°C for 3 h. The resulting mixture was filtered through a plug of glass wool and diluted with pentane (20 mL), and the pentane layer was washed with H_2O (2 x 20 mL), saturated NaHCO_3 (2 x 20 mL) and brine (2 x 20 mL). The organic layer was dried over MgSO_4 , filtered, and concentrated to afford a yellow oil, which was purified by chromatography on silica gel ($R_f = 0.3$ in 90% hexanes/10% ethyl acetate). The product **9** was obtained as pale yellow oil (222 mg, 74% yield), which was a 6:1 mixture of the oxime E/Z isomers. Each substrate was optimized was optimized for reaction time, equiv of oxidant as indicated below.



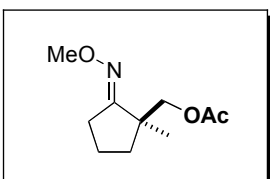
The reaction was run with 4.5 equiv of $\text{PhI}(\text{AcO})_2$ for 3.5 h in AcOH. Product **33** was isolated as a off-white solid ($R_f = 0.28$ in 70% hexanes/30% ethyl acetate, 62% yield). ^1H NMR (CDCl_3): δ 4.25 (s, 6H), 3.84 (s, 3H), 2.05 (s, 9H), 1.83 (s, 3H), $^{13}\text{C}\{^1\text{H}\}$ NMR (CDCl_3): δ 170.69, 154.34, 62.41, 62.01, 47.50, 20.95, 11.12. Anal. Calcd for $\text{C}_{13}\text{H}_{21}\text{NO}_3$: C, 51.48, H, 6.98, N, 4.62; Found: C, 51.16, H, 7.07, N, 4.80



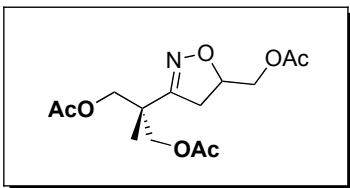
The reaction was run with 2.0 equiv of $\text{PhI}(\text{OAc})_2$ in AcOH. Product **35** was obtained as a viscous oil (75%, $R_f = 0.3$ in 90% hexanes/10% ethyl acetate). ^1H NMR (CDCl_3): δ 4.32 (d, $J = 12$ Hz, 1H), 4.19 (d, $J = 12$ Hz, 1H), 3.74 (s, 3H), 2.44 (m, 1H), 1.99 (s, 3H), 1.95-1.78 (multiple peaks, 4H), 1.40 (m, 1H), 1.20 (m, 1H), 0.95 (s, 3H), 0.84 (s, 3H). $^{13}\text{C}\{^1\text{H}\}$ NMR (CDCl_3): δ 171.18, 165.94, 61.87, 61.59, 54.17, 48.51, 44.82, 33.49, 28.42, 27.04, 21.12, 20.17, 19.95. Anal. Calcd for $\text{C}_{13}\text{H}_{21}\text{NO}_3$: C, 65.25, H, 8.84, N, 5.85; Found: C, 65.00, H, 8.83, N, 5.87.



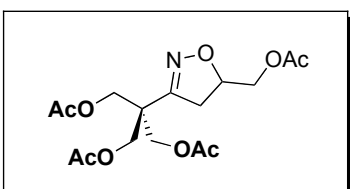
The reaction was run with 2.8 equiv of $\text{PhI}(\text{OAc})_2$ in AcOH. Product **37** was obtained as a viscous oil (51% yield). ^1H NMR (CDCl_3): δ 4.46 (d, $J = 11.7$ Hz, 2H), 4.07 (d, $J = 11.5$ Hz, 2H), 3.79 (s, 3H), 2.50 (m, 2H), 2.05 (s, 3H), 1.68-1.59 (multiple peaks, 6H), 1.53 (m, 1H), 1.13 (s, 3H).



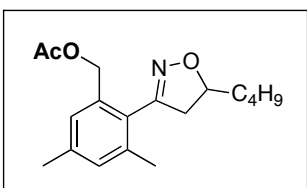
The reaction was run with 1.1 equiv of $\text{PhI}(\text{OAc})_2$ in AcOH. Product **39** was obtained as a viscous oil (61% yield). Unreacted starting material (28 mg, 28% recovered) was also isolated. ^1H NMR (CDCl_3): δ 4.02 (d, $J = 11$ Hz, 1H), 3.97 (d, $J = 11$ Hz, 1H), 3.78 (s, 3H), 2.42 (m, 2H), 2.02 (s, 3H), 1.80-1.64 (multiple peaks, 3H), 1.53 (m, 1H), 1.13 (s, 3H). $^{13}\text{C}\{^1\text{H}\}$ NMR (CDCl_3): δ 171.06, 167.11, 69.32, 61.51, 45.37, 36.16, 27.52, 22.48, 20.99, 20.90. Anal. Calcd for $\text{C}_{10}\text{H}_{17}\text{NO}_3$: C, 60.28, H, 8.60, N, 7.03; Found: C, 60.57, H, 8.69, N, 6.90.



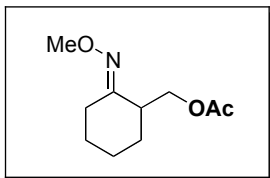
The reaction was run with 2.0 equiv of $\text{PhI}(\text{OAc})_2$ in AcOH. Product **43** was obtained as a viscous oil (45% yield). ^1H NMR (CDCl_3): δ 4.78 (m, 1H), 4.19 (s, 4H), 4.09 (m, 2H), 3.08 (dd, $J = 16.5, 10.5$ Hz, 1H), 2.77 (dd, $J = 16.5, 7.0$ Hz, 1H), 2.07 (s, 6H), 2.06 (s, 3H). $^{13}\text{C}\{^1\text{H}\}$ NMR (CDCl_3): δ 170.62, 170.48, 170.46, 159.30, 77.32, 40.52, 36.99, 20.70, 18.50.



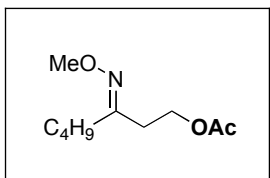
The reaction was run with 2.0 equiv of $\text{PhI}(\text{OAc})_2$ in AcOH. Product **45** was obtained as a viscous oil (55% yield). ^1H NMR (CDCl_3): δ 7.09 (s, 1H), 7.04 (s, 1H), 5.05 (s, 2H), 4.73 (m, 1H), 3.27 (dd, $J = 17.0, 10.5$, 1H), 2.87 (dd, $J = 17.0, 8.5$ Hz, 1H), 2.33 (s, 3H), 2.27 (s, 3H), 2.07 (s, 6H), 1.84 (m, 1H), 1.64 (m, 1H), 1.50 (m, 1H), 1.43-1.37 (multiple peaks, 3H), 0.94 (t, $J = 7.0$ Hz, 3H). $^{13}\text{C}\{^1\text{H}\}$ NMR (CDCl_3): δ 170.56, 170.22, 156.71, 64.38, 61.95, 44.41, 37.25, 20.66, 20.63. HRMS (ESI, m/z): $[\text{M} + \text{Na}]^+$ calcd for $\text{C}_{16}\text{H}_{23}\text{NO}_9$, 304.1913; found, 304.1901.



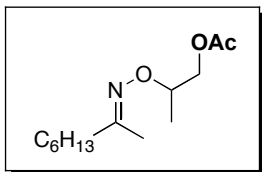
The reaction was run with 2.0 equiv of $\text{PhI}(\text{OAc})_2$ in AcOH. Product **49** was obtained as a viscous oil (60% yield). ^1H NMR (CDCl_3): δ 4.79 (m, 1H), 4.27 (s, 6H), 4.08 (m, 2H), 3.10 (dd, $J = 17.0, 10.5$ Hz, 1H), 2.79 (dd, $J = 17.0, 7.5$ Hz, 1H), 2.05 (s, 9H). $^{13}\text{C}\{^1\text{H}\}$ NMR (CDCl_3): δ 170.51, 156.32, 139.08, 136.93, 134.58, 131.15, 127.86, 126.88, 81.04, 64.28, 44.43, 35.00, 27.84, 22.51, 21.09, 21.02, 19.59, 13.96. HRMS (ESI, m/z): $[\text{M} + \text{Na}]^+$ calcd for $\text{C}_{16}\text{H}_{23}\text{NO}_9$, 396.1271; found, 396.1263.



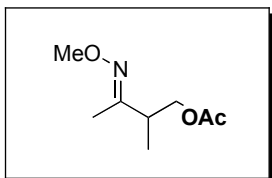
The reaction was run with 1.1 equiv $\text{PhI}(\text{OAc})_2$ in $\text{AcOH}/\text{Ac}_2\text{O}$. The product **51** was obtained as a clear oil. The two isomers were isolated as pale yellow oils (major isomer: 173 mg, 61% yield; minor isomer: 57 mg, 20% yield). Each of the pure isomers was re-subjected to the reaction conditions and the equilibrium mixture (~3:1) was rapidly reestablished in each case. **Major Isomer:** ^1H NMR (CDCl_3): δ 4.39 (dd, $J = 11.2, 5.9$ Hz, 1H), 3.99 (dd, $J = 11.2, 8.1$ Hz, 1H), 3.74 (s, 3H), 2.76 (m, 1H), 2.46 (m, 1H), 1.96 (m, 2H), 1.99 (s, 3H), 1.67 (m, 2H), 1.40 (multiple peaks, 3H). $^{13}\text{C}\{^1\text{H}\}$ NMR (CDCl_3): δ 171.24, 158.86, 64.92, 61.39, 41.21, 30.40, 25.98, 24.30, 24.08, 21.13. **Minor Isomer:** ^1H NMR (CDCl_3): δ 4.17 (dd, $J = 10.8, 7.8$ Hz, 1H), 4.06 (dd, $J = 10.8, 6.4$ Hz, 1H), 3.76 (s, 3H), 3.65 (m, 1H), 2.28 (m, 1H), 2.12 (m, 1H), 1.99 (s, 3H), 1.86 (m, 1H), 1.75 (m, 1H), 1.57-1.33 (multiple peaks, 4H). Anal. Calcd for $\text{C}_{10}\text{H}_{17}\text{NO}_3$ (mixture of E/Z isomers): C, 60.28, H, 8.60, N, 7.03; Found: C, 59.90, H, 8.91, N, 6.81.



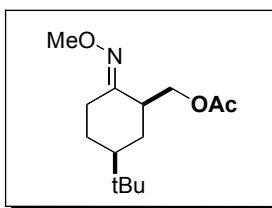
The reaction was run with 1.1 equiv of $\text{PhI}(\text{OAc})_2$ in $\text{AcOH}/\text{Ac}_2\text{O}$. The two isomers of **55** were isolated as pale yellow oils (isomer a: 137 mg, 19.5%; isomer b: 137 mg, 19.5%). Each of the pure isomers was re-subjected to the reaction conditions and the equilibrium mixture (~1:1) was reestablished rapidly in each case (as determined by gas chromatography). **Isomer a:** ^1H NMR (CDCl_3): δ 4.20 (t, $J = 7.0$ Hz, 2H), 3.74 (s, 3H), 2.42 (t, $J = 7.0$ Hz, 2H), 2.24, (m, 2H), 1.99 (s, 3H), 1.38 (m, 2H), 1.28 (m, 2H), 0.85 (t, $J = 7.3$ Hz, 3H). $^{13}\text{C}\{^1\text{H}\}$ NMR (CDCl_3): δ 171.12, 157.84, 61.62, 61.43, 33.27, 28.23, 27.98, 23.01, 21.10, 13.97. **Isomer b:** ^1H NMR (CDCl_3): δ 4.26 (t, $J = 6.6$ Hz, 2H), 3.76 (s, 3H), 2.56 (t, $J = 6.6$ Hz, 2H), 2.13, (m, 2H), 1.99 (s, 3H), 1.38 (m, 2H), 1.28 (m, 2H), 0.83 (t, $J = 7.3$ Hz, 3H). Anal. Calcd for $\text{C}_{10}\text{H}_{19}\text{NO}_3$ (mixture of E/Z isomers): C, 59.68, H, 9.52, N, 6.96; Found: C, 59.75, H, 9.25, N, 7.26.



The reaction was run with 2.0 equiv of $\text{PhI}(\text{OAc})_2$ in AcOH . Product **49** was obtained as a viscous oil (60% yield). ^1H NMR (CDCl_3): δ 4.35 (m, 1H), 4.19-4.09 (multiple peaks, 2H), 2.29 (m, 1H), 2.16-2.12 (multiple peaks, 2H), 2.07 (s, 3H), 1.81 (s, 3H), 1.48 (m, 2H), 1.35-1.27 (multiple peaks, 4H), 1.25 (d, $J = 7.2$ Hz, 3H), 0.88 (t, $J = 7.5$ Hz, 3H). $^{13}\text{C}\{^1\text{H}\}$ NMR (CDCl_3): δ 171.02, 158.36, 75.73, 75.69, 66.45, 66.40, 35.84, 31.68, 31.37, 29.26, 26.12, 25.21, 22.39, 22.35, 20.93, 19.98, 16.58, 14.04, 13.98, 13.92.

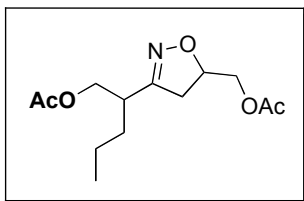


The reaction was run with 1.1 equiv of $\text{PhI}(\text{AcO})_2$ for 3 h in $\text{AcOH}/\text{Ac}_2\text{O}$. The product **57** was isolated as a pale yellow oil ($R_f = 0.3$ in 90% hexanes/10% ethyl acetate, 222 mg, 74% yield), which was a 6:1 mixture of the oxime E/Z isomers. Major Isomer: ^1H NMR (CDCl_3): δ 4.10 (dd, $J = 10.9, 7.3$ Hz, 1H), 3.99 (dd, $J = 10.9, 6.9$ Hz, 1H), 3.77 (s, 3H), 2.62 (m, 1H), 1.99 (s, 3H), 1.74 (s, 3H), 1.05 (d, $J = 7.2$ Hz, 3H). $^{13}\text{C}\{^1\text{H}\}$ NMR (CDCl_3): δ 171.10, 157.94, 66.24, 61.45, 39.13, 21.05, 14.95, 11.77. Anal. Calcd for $\text{C}_8\text{H}_{15}\text{NO}_3$: C, 55.47, H, 8.73, N, 8.09; Found: C, 55.55, H, 8.57, N, 7.81.

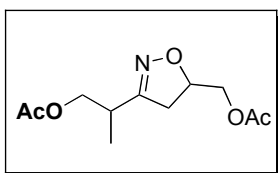


The reaction was run with 1.1 equiv $\text{PhI}(\text{OAc})_2$ in $\text{AcOH}/\text{Ac}_2\text{O}$. The product **61** was obtained as pale yellow oil (202 mg, 78% yield). ^1H NMR (CDCl_3): δ 4.50 (dd, $J = 11.0, 4.4$ Hz, 1H), 3.97 (dd, $J = 11.0, 8.1$ Hz, 1H), 3.75 (s, 3H), 3.27 (m, 1H), 2.39 (m, 1H), 2.08 (m, 1H), 2.02 (s, 3H), 1.86 (m, 1H), 1.55 (m, 1H), 1.24 (m, 1H), 1.09 (m, 1H), 0.94 (m, 1H), 0.83 (s, 9H). $^{13}\text{C}\{^1\text{H}\}$ NMR (CDCl_3): δ 174.09, 158.82, 65.20, 61.45, 47.04,

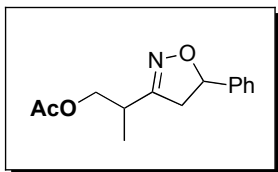
41.63, 32.22, 27.74, 26.98, 24.91, 21.22. Anal. Calcd for C₁₄H₂₅NO₃: C, 65.85, H, 9.87, N, 5.49; Found: C, 65.58, H, 10.10, N, 5.48



The reaction was run with 2.0 equiv of PhI(OAc)₂ in AcOH. Product **63** was obtained as a viscous oil (30% yield, 1:1). ¹H NMR (CDCl₃): δ 4.79 (m, 2H), 4.19-4.06 (multiple peaks, 8H), 3.06-2.94 (multiple peaks, 4H), 2.73 (m, 2H), 2.08 (s, 3H), 2.05 (s, 3H), 1.51 (m, 4H), 1.35 (m, 4H), 0.92 (m, 6H). ¹³C{¹H} NMR (CDCl₃): δ 170.75, 64.97, 64.87, 64.65, 37.71, 31.02, 30.95, 20.82, 20.75, 20.08, 13.87, 13.83. HRMS (ESI, m/z): [M + Na]⁺ calcd for C₁₃H₂₁NO₅, 294.1317; found, 294.1305.

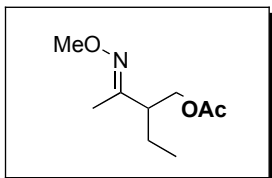


The reaction was run with 1.5 equiv of PhI(OAc)₂ in AcOH. Product **67** was obtained as a viscous oil (47% yield, 1:1). ¹H NMR (CDCl₃): δ 4.76 (m, 2H), 4.16-4.07 (multiple peaks, 8H), 3.04 (dd, J = 17.0, 10.5 Hz, 2H), 2.75-2.70 (multiple peaks, 4H), 2.08 (s, 12H), 1.18 (d, J = 6.5 Hz, 6H). ¹³C{¹H} NMR (CDCl₃): δ 186.65, 170.83, 65.17, 49.66, 37.21, 27.77, 20.80, 20.02.

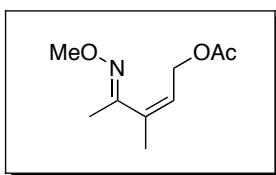


The reaction was run with 1.5 equiv of PhI(OAc)₂ in AcOH. Product **69** was obtained as a viscous oil (25% yield, 1:1). **Isomer 1**: ¹H NMR (CDCl₃): δ 7.38-7.29 (multiple peaks, 5H), 5.55 (dd, J = 11.0, 8.0 Hz, 1H), 4.21 (dd, J = 11.0, 7.0 Hz, 1H), 4.14 (dd, J = 12.0, 6.0 Hz, 1H), 3.40 (dd, J = 17.0, 11.0, 1H), 3.02 (quin, J = 7.0 Hz, 1H), 2.92 (dd, J = 17.0, 8.0 Hz, 1H), 2.04 (s, 3H), 1.23 (d, J = 7.0 Hz, 3H). ¹³C{¹H} NMR (CDCl₃): δ 170.81, 159.32, 141.01, 128.68, 128.09, 125.68, 81.46, 65.95, 43.39, 32.83, 20.81, 14.78. **Isomer 1'**: ¹H NMR (CDCl₃): δ 7.37-7.30 (multiple peaks, 5H), 5.55 (dd, J = 11.0, 7.5 Hz, 1H),

4.20-4.11 (multiple peaks, 2H), 3.40 (dd, $J = 17.0, 11.0$, 1H), 3.03 (quin, $J = 6.5$ Hz, 1H), 2.91 (dd, $J = 17.0, 7.5$ Hz, 1H), 2.01 (s, 3H), 1.23 (d, $J = 7.5$ Hz, 3H). $^{13}\text{C}\{^1\text{H}\}$ NMR (CDCl_3): δ 170.73, 159.27, 141.11, 128.67, 128.08, 125.65, 81.39, 65.91, 43.16, 32.71, 20.76, 14.74. HRMS electrospray (m/z): $[\text{M} + \text{Na}]^+$ calcd for $\text{C}_{14}\text{H}_{17}\text{NO}_3$, 270.1106 found, 270.1099.

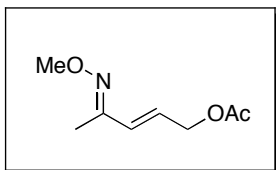


The reaction was run with 1.1 equiv $\text{PhI}(\text{OAc})_2$ in $\text{AcOH}/\text{Ac}_2\text{O}$. The product **72** was obtained as a mixture of the two isomers, as pale yellow oils (major isomer: 189 mg, 65% yield; minor isomer: 38 mg, 13% yield). Each of the pure isomers was re-subjected to the reaction conditions and the equilibrium mixture ($\sim 5:1$) was reestablished rapidly in each case (as determined by gas chromatography). **Major Isomer:** ^1H NMR (CDCl_3): δ 4.07 (pseudo q, $J = 13.9, 7.8, 6.4$ Hz, 2H), 3.79 (s, 3H), 2.45 (m, 1H), 1.99 (s, 3H), 1.72 (s, 3H), 1.45 (m, 2H), 0.84 (t, $J = 7.4$ Hz, 3H). $^{13}\text{C}\{^1\text{H}\}$ NMR (CDCl_3): δ 171.09, 157.09, 65.00, 61.46, 46.03, 22.01, 21.07, 11.48, 11.43. **Minor Isomer:** ^1H NMR (CDCl_3): 4.16 (dd, $J = 10.9, 5.6$ Hz, 1H), 4.04 (dd, $J = 10.9, 8.3$ Hz, 1H), 3.80, (s, 3H), 3.45 (m, 1H), 2.03, (s, 3H), 1.80 (s, 3H), 1.49 (m, 2H), 0.90 (t, $J = 7.5$ Hz, 3H). Anal. Calcd for $\text{C}_9\text{H}_{17}\text{NO}_3$ (major isomer): C, 57.73, H, 9.15, N, 7.48; Found: C, 57.71, H, 9.40, N, 7.22.

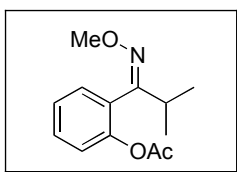


Cyclopropane **79** was reacted with 2.0 equiv Benzoquinone and 5 mol % $\text{Pd}(\text{OAc})_2$ in $\text{AcOH}/\text{Ac}_2\text{O}$ (1:1, 0.12M) in a 20 mL scintillation vial at 100 °C for 12 h. The resulting mixture was filtered through a plug of glass wool and diluted with pentane (20 mL), and the pentane layer was washed with H_2O (2 x 20 mL), saturated NaHCO_3 (2 x 20 mL) and brine (2 x 20 mL). The organic layer was dried over MgSO_4 , filtered, and concentrated to afford a yellow oil, which was purified by chromatography on silica gel ($R_f = 0.3$ in 90% hexanes/10% ethyl acetate). The product **81** was obtained as a mixture of the two oxime isomers, as pale yellow oils (44%, 3:1). **Major Isomer:** ^1H NMR (CDCl_3): δ 5.89

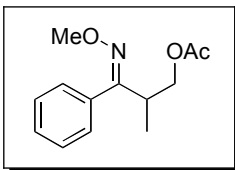
(td, $J = 6.4, 1.5$ Hz, 1H), 4.76 (d, $J = 6.4$ Hz, 2H), 3.91 (s, 3H), 2.08 (s, 3H), 1.96 (s, 3H), 1.90 (br s, 3H). $^{13}\text{C}\{^1\text{H}\}$ NMR (CDCl_3): δ 170.87, 155.57, 137.09, 124.58, 61.78, 61.33, 20.90, 12.80, 10.49. HRMS electrospray (m/z): $[\text{M} + \text{Na}]^+$ calcd for $\text{C}_9\text{H}_9\text{NO}_3$, 208.0950 found, 208.0941.



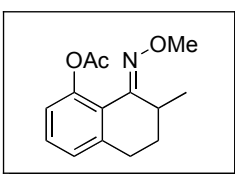
Cyclpropane **82** was reacted with 2.0 equiv Benzoquinone and 5 mol % $\text{Pd}(\text{OAc})_2$ in $\text{AcOH}/\text{Ac}_2\text{O}$ (1:1, 0.12M) in a 20 mL scintillation vial at 100 °C for 12 h. The resulting mixture was filtered through a plug of glass wool and diluted with pentane (20 mL), and the pentane layer was washed with H_2O (2 x 20 mL), saturated NaHCO_3 (2 x 20 mL) and brine (2 x 20 mL). The organic layer was dried over MgSO_4 , filtered, and concentrated to afford a yellow oil, which was purified by chromatography on silica gel ($R_f = 0.3$ in 90% hexanes/10% ethyl acetate). The product **83** was obtained as a mixture of the two oxime isomers, as pale yellow oils (47%, 3:1). **Major Isomer:** ^1H NMR (CDCl_3): δ 6.32 (td, $J = 16.0, 1.2$ Hz, 1H), 6.06 (dt, $J = 16.0, 6.0$ Hz, 1H), 4.67 (dd, $J = 6.0, 1.2$ Hz, 2H), 3.90 (s, 3H), 2.08 (s, 3H), 1.94 (s, 3H). $^{13}\text{C}\{^1\text{H}\}$ NMR (CDCl_3): δ 170.41, 154.28, 130.65, 127.72, 64.08, 61.72, 20.72, 9.96. Anal. Calcd for $\text{C}_8\text{H}_7\text{NO}_3$ (mixture of E/Z isomers): C, 56.13, H, 7.65, N, 8.18; Found: C, 56.02, H, 7.68, N, 8.13.



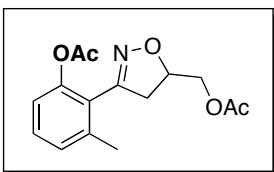
The reaction was run with 1.1 equiv $\text{PhI}(\text{OAc})_2$ in $\text{AcOH}/\text{Ac}_2\text{O}$. The product **94** was obtained as a pale yellow oil (75%). ^1H NMR (CDCl_3): δ 7.37 (m, 1H), 7.28-7.23 (multiple peaks, 2H), 7.14 (d, $J = 8.4$ Hz, 1H), 3.91 (s, 3H), 3.94 (septet, $J = 6.4$ Hz, 1H), 2.26 (s, 3H), 1.09 (d, $J = 6.4$ Hz, 6H).



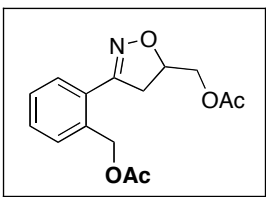
The reaction was run with 1.1 equiv $\text{PhI}(\text{OAc})_2$ in $\text{AcOH}/\text{Ac}_2\text{O}$. The product **95** was obtained as a pale yellow oil (5%). ^1H NMR (CDCl_3): δ 7.34-7.29 (multiple peaks, 2H), 7.23-7.15 (multiple peaks, 2H), 7.09 (d, $J = 8.4$ Hz, 1H), 4.16 (dd, $J = 11.2, 7.6$ Hz, 1H), 4.04 (dd, $J = 11.2, 7.6$ Hz, 1H) 3.75 (s, 3H), 2.99 (m, 1H), 1.98 (s, 3H), 1.11 (d, $J = 6.4$ Hz, 3H).



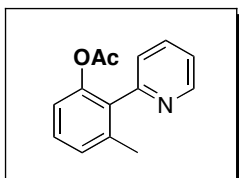
The reaction was run with 1.1 equiv $\text{PhI}(\text{OAc})_2$ in $\text{AcOH}/\text{Ac}_2\text{O}$. The product **97** was obtained as a pale yellow oil (57%). ^1H NMR (CDCl_3): δ 7.18 (t, $J = 7.6$ Hz, 1H), 7.00 (d, $J = 7.2$ Hz, 1H), 6.86 (d, $J = 8.0$ Hz, 1H), 3.91 (s, 3H), 3.45 (sextet, $J = 6.8$ Hz, 1H) 2.82 (m, 1H), 2.58 (m, 1H), 2.25 (s, 3H), 1.97 (m, 1H), 1.45 (m, 1H), 1.12 (d, $J = 6.8$ Hz, 3H).



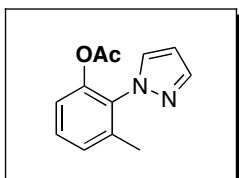
The reaction was run with 1.02 equiv of $\text{PhI}(\text{OAc})_2$ in AcOH . Product **100** was obtained as a viscous oil (27% yield). ^1H NMR (CDCl_3): δ 7.32 (t, $J = 8.0$ Hz, 1H), 7.13 (d, $J = 8.0$ Hz, 1H), 7.00 (d, $J = 8.0$ Hz, 1H), 4.95 (m, 1H), 4.26-4.18 (multiple peaks, 2H), 3.33 (dd, $J = 17.5, 10.5$ Hz, 1H), 3.00 (dd, $J = 17.5, 7.5$ Hz, 1H), 2.36 (s, 3H), 2.28 (s, 3H), 2.11 (s, 3H). $^{13}\text{C}\{^1\text{H}\}$ NMR (CDCl_3): δ 170.72, 169.13, 153.61, 148.89, 138.74, 130.07, 128.04, 122.41, 120.14, 77.62, 64.72, 40.37, 20.95, 20.78, 20.09. HRMS (ESI, m/z): $[\text{M} + \text{Na}]^+$ calcd for $\text{C}_{15}\text{H}_{17}\text{NO}_5$, 314.1004 found, 314.1006.



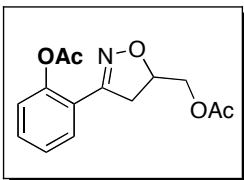
The reaction was run with 1.02 equiv of $\text{PhI}(\text{OAc})_2$ in AcOH. Product **101** was obtained as a viscous oil (34% yield). ^1H NMR (CDCl_3): δ 7.51 (d, $J = 8.0$ Hz, 1H), 7.43 (m, 1H), 7.38-7.37 (multiple peaks, 2H), 5.42 (s, 2H), 4.95 (m, 1H), 4.28 (dd, $J = 12.0, 4.0$ Hz, 1H), 4.21 (dd, $J = 12.0, 5.5$, 1H), 3.53 (dd, $J = 17.0, 11.0$ Hz, 1H), 3.20 (dd, $J = 17.0, 7.0$ Hz, 1H), 2.14 (s, 3H), 2.10 (s, 3H). $^{13}\text{C}\{^1\text{H}\}$ NMR (CDCl_3): δ 170.82, 170.54, 156.10, 135.79, 129.80, 128.79, 128.35, 127.84, 127.33, 64.88, 64.85, 39.36, 20.79. HRMS (ESI, m/z): $[\text{M} + \text{Na}]^+$ calcd for $\text{C}_{15}\text{H}_{17}\text{NO}_5$, 314.1004 found, 314.1007.



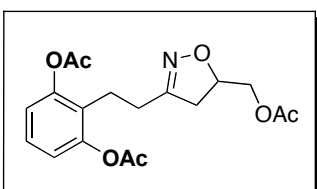
The reaction was run with 1.02 equiv of $\text{PhI}(\text{OAc})_2$ in AcOH. Product **106** was obtained as a viscous oil (65% yield). ^1H NMR (CDCl_3): δ 8.71 (m, 1H), 7.74 (td, $J = 7.5, 2.0$ Hz, 1H), 7.33-7.25 (multiple peaks, 3H), 7.17 (d, $J = 8.0$ Hz, 1H), 6.98 (d, $J = 8.0$ Hz, 1H), 2.15 (s, 3H), 1.94 (s, 3H). $^{13}\text{C}\{^1\text{H}\}$ NMR (CDCl_3): δ 169.21, 155.56, 149.26, 148.18, 137.92, 135.86, 133.34, 128.63, 127.76, 124.53, 121.92, 119.76, 20.30, 19.67. HRMS (ESI, m/z): $[\text{M} + \text{Na}]^+$ calcd for $\text{C}_{14}\text{H}_{13}\text{NO}_2$, 250.0844 found, 250.0847.



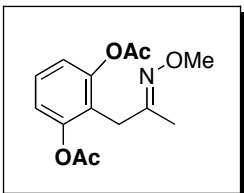
The reaction was run with 1.02 equiv of $\text{PhI}(\text{OAc})_2$ in AcOH. Product **109** was obtained as a viscous oil (90% yield). ^1H NMR (CDCl_3): δ 7.73 (d, $J = 2.0$ Hz, 1H), 7.46 (d, $J = 2.0$ Hz, 1H), 7.36 (t, $J = 8.0$ Hz, 1H), 7.21 (d, $J = 7.5$ Hz, 1H), 7.04 (d, $J = 7.5$ Hz, 1H), 6.42 (t, $J = 2.0$ Hz, 1H), 2.11 (s, 3H), 2.02 (s, 3H). $^{13}\text{C}\{^1\text{H}\}$ NMR (CDCl_3): δ 169.21, 146.87, 140.54, 137.88, 132.80, 131.42, 129.56, 128.33, 120.72, 105.96, 20.38, 17.34. HRMS (ESI, m/z): $[\text{M} + \text{Na}]^+$ calcd for $\text{C}_{12}\text{H}_{12}\text{N}_2\text{O}_2$, 239.0796 found, 239.0787.



The reaction was run with 1.02 equiv of $\text{PhI}(\text{OAc})_2$ in AcOH. Product **112** was obtained as a viscous oil (30% yield). ^1H NMR (CDCl_3): δ 7.50 (dd, $J = 8.0, 1.5$ Hz, 1H), 7.46 (td, $J = 8.0, 2.0$ Hz, 1H), 7.32 (td, $J = 8.0, 1.5$ Hz, 1H), 7.15 (d, $J = 8.0$ Hz), 4.91 (m, 1H), 4.27 (dd, $J = 12.0, 4.0$ Hz, 1H), 4.18 (dd, $J = 12.0, 6.0$ Hz, 1H), 3.47 (dd, $J = 16.5, 10.5$, 1H), 3.16 (dd, $J = 16.5, 7.0$ Hz, 1H), 2.32 (s, 3H), 2.10 (s, 3H). $^{13}\text{C}\{^1\text{H}\}$ NMR (CDCl_3): δ 170.70, 169.51, 153.55, 148.32, 130.88, 129.36, 126.17, 123.76, 77.46, 64.69, 38.53, 21.14, 20.67. HRMS (ESI, m/z): $[\text{M} + \text{Na}]^+$ calcd for $\text{C}_{14}\text{H}_{15}\text{NO}_5$, 300.0848 found, 300.0857.

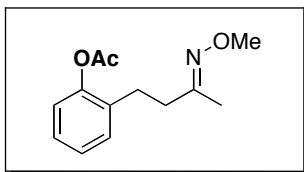


The reaction was run with 2.1 equiv of $\text{PhI}(\text{OAc})_2$ in AcOH. Product **116** was obtained as a viscous oil (75% yield). ^1H NMR (CDCl_3): δ 7.25 (t, $J = 8.0$ Hz, 1H), 6.97 (d, $J = 8.0$ Hz, 2H), 4.74 (m, 1H), 4.10 (t, $J = 4.4$ Hz, 2H), 2.93 (dd, $J = 17.2, 10.8$ Hz, 1H), 2.76 (t, $J = 7.6$ Hz, 2H), 2.63 (dd, $J = 17.2, 6.8$ Hz, 1H), 2.48 (t, $J = 7.2$, 2H), 2.31 (s, 6H), 2.06 (s, 3H). $^{13}\text{C}\{^1\text{H}\}$ NMR (CDCl_3): δ 170.68, 169.11, 157.64, 149.70, 127.41, 125.58, 120.23, 77.32, 64.87, 39.74, 26.88, 21.87, 20.83, 20.68. HRMS (ESI, m/z): $[\text{M} + \text{Na}]^+$ calcd for $\text{C}_{18}\text{H}_{21}\text{NO}_7$, 386.1216 found, 386.1207.

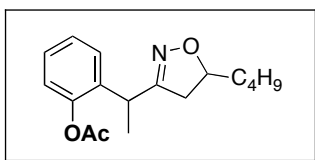


The reaction was run with 2.1 equiv of $\text{PhI}(\text{OAc})_2$ in AcOH. Product **126** was obtained as a viscous oil (89% yield). ^1H NMR (CDCl_3): δ 7.30 (t, $J = 8.0$ Hz, 1H), 6.98 (d, $J = 8.0$ Hz, 2H), 3.83 (s, 3H), 3.39 (s, 2H), 2.31 (s, 6H), 1.64 (s, 3H). $^{13}\text{C}\{^1\text{H}\}$ NMR (CDCl_3): δ

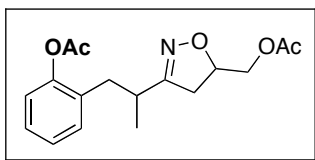
154.98, 150.24, 127.87, 122.08, 120.43, 61.15, 31.04, 20.87, 12.89. HRMS (ESI, m/z): $[M + Na]^+$ calcd for $C_{14}H_{17}NO_5$, 302.1004 found, 302.0999.



The reaction was run with 2.1 equiv of $PhI(OAc)_2$ in AcOH. Product **128** was obtained as a viscous oil (17% yield). 1H NMR ($CDCl_3$): δ 7.27-7.22 (multiple peaks, 2H), 7.18 (t, $J = 7.5$ Hz, 1H), 7.03 (d, $J = 7.5$ Hz, 1H), 3.84 (s, 3H), 2.73 (t, $J = 8.0$ Hz, 2H), 2.42 (t, $J = 8.0$ Hz, 2H), 2.34 (s, 3H), 1.84 (s, 3H). $^{13}C\{^1H\}$ NMR ($CDCl_3$): (mixture of oxime isomers) δ 169.39, 157.15, 156.47, 148.88, 148.82, 132.94, 132.91, 130.11, 130.06, 127.37, 127.30, 126.15, 122.28, 61.09, 61.05, 36.17, 29.84, 27.30, 26.27, 20.86, 20.80, 20.23, 14.15. HRMS (ESI, m/z): $[M + Na]^+$ calcd for $C_{13}H_{17}NO_3$, 258.1106 found, 258.1105.

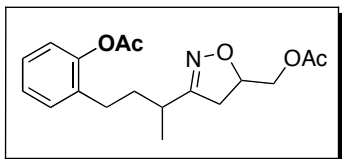


The reaction was run with 1.1 equiv of $PhI(OAc)_2$ in AcOH. Product **136** was obtained as a viscous oil (56% yield). 1H NMR ($CDCl_3$): δ 7.32-7.23 (multiple peaks, 3H), 7.05 (m, 1H), 4.47 (m, 1H), 3.93 (q, $J = 7.0$ Hz, 1H), 2.67 (dd, $J = 17.0, 10.0$ Hz, 1H), 2.37-2.32 (multiple peaks, 4H), 1.63 (m, 1H), 1.51 (d, $J = 6.5$, 3H), 1.44 (m, 1H), 1.34-1.22 (multiple peaks, 4H), 0.87 (t, $J = 7.0$ Hz, 3H). $^{13}C\{^1H\}$ NMR ($CDCl_3$): δ 169.66, 160.54, 148.60, 133.35, 128.13, 128.00, 126.51, 122.97, 80.63, 40.50, 34.71, 33.54, 27.56, 22.42, 20.86, 17.73, 13.87. HRMS (ESI, m/z): $[M + Na]^+$ calcd for $C_{17}H_{23}NO_3$, 290.1756 found, 290.1742.

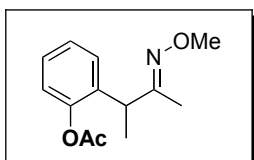


The reaction was run with 1.1 equiv of $PhI(OAc)_2$ in AcOH. Product **139** was obtained as a viscous oil (60% yield). 1H NMR ($CDCl_3$): δ 7.28-7.17 (multiple peaks, 3H), 7.04 (d, $J = 8.4$ Hz, 1H), 4.73 (m, 1H), 4.13-4.04 (multiple peaks, 2H), 3.98 (dd, $J = 12.0, 6.0$ Hz,

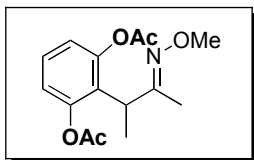
1H), 3.02-2.84 (multiple peaks, 3H), 2.70-2.59 (multiple peaks, 2H), 2.33 (s, 3H), 2.06 (s, 3H), 1.16 (d, $J = 8.0$, 3H). $^{13}\text{C}\{^1\text{H}\}$ NMR (CDCl_3): δ 170.77, 169.37, 161.72, 149.09, 131.02, 130.86, 127.78, 126.14, 122.58, 122.55, 76.83, 65.02, 64.95, 37.46, 37.53, 35.13, 35.10, 33.31, 21.01, 20.77, 17.97. HRMS (ESI, m/z): $[\text{M} + \text{Na}]^+$ calcd for $\text{C}_{17}\text{H}_{21}\text{NO}_5$, 342.1311 found, 342.1311.



The reaction was run with 1.1 equiv of $\text{PhI}(\text{OAc})_2$ in AcOH. Product **142** was obtained as a viscous oil (10% yield, 1:1). **Isomer 1**: ^1H NMR (CDCl_3): δ 7.26-7.12 (multiple peaks, 4H), 4.72 (m, 1H), 4.17-4.00 (multiple peaks, 2H), 2.90 (m, 1H), 2.73-2.49 (multiple peaks, 2H), 2.04 (s, 3H), 2.02 (s, 3H), 1.86-1.64 (multiple peaks, 2H), 1.51 (m, 3H).

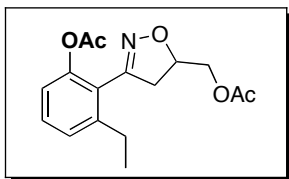


The reaction was run with 1.5 equiv of $\text{PhI}(\text{OAc})_2$ in AcOH. Product **145** was obtained as a viscous oil (43% yield, Oxime Isomers 1:1). **Oxime Isomer 1**: ^1H NMR (CDCl_3): δ 7.31-7.21 (multiple peaks, 3H), 7.01 (d, $J = 8.0$ Hz, 1H), 3.88 (s, 3H), 3.79 (q, $J = 7.0$ Hz, 1H), 2.32 (s, 3H), 1.59 (s, 3H), 1.40 (d, $J = 7.0$ Hz, 3H). $^{13}\text{C}\{^1\text{H}\}$ NMR (CDCl_3): δ 169.41, 158.49, 148.94, 133.97, 128.17, 127.74, 126.22, 122.77, 61.33, 61.14, 39.61, 20.87, 17.25, 12.27. HRMS electrospray (m/z): $[\text{M} + \text{Na}]^+$ calcd for $\text{C}_{13}\text{H}_{17}\text{NO}_3$, 258.1106 found, 258.1096. **Oxime Isomer 2**: ^1H NMR (CDCl_3): δ 7.34 (dd, $J = 7.0$, 1.5 Hz, 1H), 7.29-7.23 (multiple peaks, 2H), 7.01 (dd, $J = 7.5$, 2.0 Hz, 1H), 4.71 (q, $J = 7.5$ Hz, 1H), 3.86 (s, 3H), 2.26 (s, 3H), 1.50 (s, 3H), 1.36 (d, $J = 7.5$ Hz, 3H). HRMS (ESI, m/z): $[\text{M} + \text{Na}]^+$ calcd for $\text{C}_{13}\text{H}_{17}\text{NO}_3$, 258.1106 found, 258.1095.

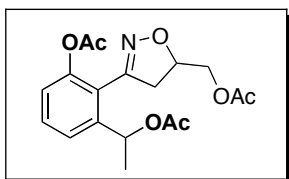


The reaction was run with 1.5 equiv of $\text{PhI}(\text{OAc})_2$ in AcOH. Product **146** was obtained as a viscous oil (22% yield). ^1H NMR (CDCl_3): δ 7.28 (t, $J = 8.5$ Hz, 1H), 6.95 (d, $J = 8.5$

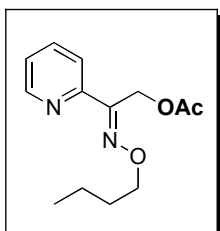
Hz, 2H), 3.88 (s, 3H), 3.68 (q, $J = 7.0$ Hz, 1H), 2.29 (s, 6H), 1.61 (s, 3H), 1.38 (d, $J = 7.0$ Hz, 3H). $^{13}\text{C}\{^1\text{H}\}$ NMR (CDCl_3): δ 169.12, 157.44, 149.74, 127.60, 127.48, 120.94, 61.19, 37.66, 20.75, 15.35, 14.03. HRMS (ESI, m/z): $[\text{M} + \text{Na}]^+$ calcd for $\text{C}_{15}\text{H}_{19}\text{NO}_5$, 316.1161 found, 316.1173.



The reaction was run with 1.5 equiv of $\text{PhI}(\text{OAc})_2$ in AcOH. Product **149** was obtained as a viscous oil (83% yield). ^1H NMR (CDCl_3): δ 7.37 (d, $J = 7.6$ Hz, 1H), 7.18 (d, $J = 7.6$ Hz, 1H), 7.00 (d, $J = 8.4$ Hz, 1H), 4.96 (m, 1H), 4.27-4.18 (multiple peaks, 2H), 3.32 (dd, $J = 17.2, 10.8$ Hz, 1H), 3.01 (dd, $J = 17.2, 6.8$ Hz, 1H), 2.66 (q, $J = 7.6$ Hz, 1H), 2.28 (s, 3H), 2.12 (s, 3H), 1.23 (t, $J = 7.6$ Hz, 3H). $^{13}\text{C}\{^1\text{H}\}$ NMR (CDCl_3): δ 170.74, 169.07, 153.51, 148.83, 144.96, 130.28, 126.37, 121.81, 120.11, 77.65, 64.73, 41.04, 26.51, 20.98, 20.78, 15.68. HRMS (ESI, m/z): $[\text{M} + \text{Na}]^+$ calcd for $\text{C}_{15}\text{H}_{19}\text{NO}_3$, 328.1161 found, 328.1151.

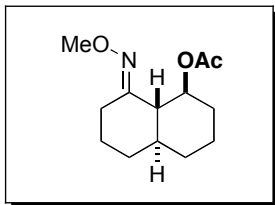


The reaction was run with 1.5 equiv of $\text{PhI}(\text{OAc})_2$ in AcOH. Product **150** was obtained as a viscous oil (8% yield, 1:1). *Isomer 1*: ^1H NMR (CDCl_3): δ 7.44 (d, $J = 7.6$ Hz, 1H), 7.38 (d, $J = 7.6$ Hz, 1H), 7.12 (m, 1H), 5.79 (quin, $J = 6.4$ Hz, 1H), 5.00 (m, 1H), 4.26-4.21 (multiple peaks, 2H), 3.50 (dd, $J = 17.2, 11.2$ Hz, 1H), 3.09 (dd, $J = 17.2, 7.2$ Hz, 1H), 2.30 (s, 3H), 2.11 (s, 3H), 2.01 (s, 3H), 1.53 (d, $J = 6.4$ Hz, 3H).



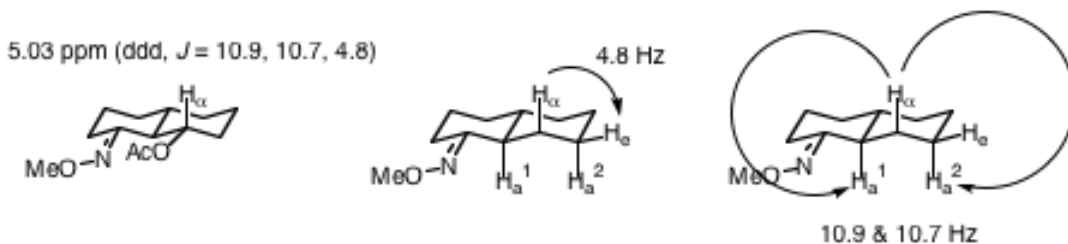
The reaction was run with 1.5 equiv of $\text{PhI}(\text{OAc})_2$ in AcOH. Product **172** was obtained as a viscous oil (6% yield). ^1H NMR (CDCl_3): δ 8.59 (d, $J = 5.5$ Hz, 1H), 7.86 (d, $J = 8.0$ Hz, 1H), 7.67 (td, $J = 9.0, 1.5$ Hz, 1H), 7.25 (m, 1H), 5.35 (s, 2H), 4.26 (t, $J = 6.0$ Hz,

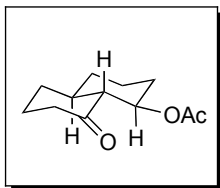
2H), 2.01 (s, 3H), 1.70 (m, 2H), 1.41 (m, 2H), 0.93 (t, $J = 7.5$ Hz, 3H). $^{13}\text{C}\{^1\text{H}\}$ NMR (CDCl_3): δ 170.58, 152.66, 152.58, 148.92, 136.29, 123.63, 120.93, 75.12, 54.84, 31.16, 20.72, 19.02, 13.84.



Decalone *O*-methyl oxime (200 mg, 1.11 mmol, 1 equiv), $\text{PhI}(\text{OAc})_2$ (539 mg, 1.66 mmol, 1.5 equiv), and $\text{Pd}(\text{OAc})_2$ (12 mg, 0.055 mmol, 0.05 equiv) were combined in AcOH (5 mL) and Ac_2O (5 mL) in a 20 mL vial. The vial was sealed with a Teflon lined cap, and the reaction was stirred at 80°C for 5 h. The reaction mixture was evaporated to dryness and then taken up in 3 mL of pyridine. The pyridine suspension was filtered through a short plug of silica, and the silica was washed with copious ethyl acetate to remove all of the organic products. The resulting solution was concentrated under vacuum to afford a reddish oil, which was purified by chromatography on silica gel ($R_f = 0.3$ in 90% hexanes/10% ethyl acetate). The product **184** was obtained as pale yellow crystals (210 mg, 81% yield). ^1H NMR (CDCl_3): δ 5.03 (ddd, $J = 10.9, 10.7, 4.8$ Hz, 1H), 3.69 (s, 3H), 3.24 (br d, $J = 13.1$, 1H), 2.0 (m, 1H), 1.93 (s, 3H), 1.91 (d, $J = 10.9$, 1H), 1.81-0.96 (multiple peaks, 12H). $^{13}\text{C}\{^1\text{H}\}$ NMR (CDCl_3): δ 170.18, 157.54, 70.42, 61.06, 51.70, 43.31, 33.32, 32.97, 31.60, 25.59, 25.38, 23.12, 21.09. Anal. Calcd for $\text{C}_{13}\text{H}_{21}\text{NO}_3$: C, 65.25, H, 8.84, N, 5.85; Found: C, 65.51, H, 8.79, N, 5.77.

The equatorial stereochemistry of the OAc group of 31 was assigned based on standard analysis of the coupling constants of H_a as shown below:





Product **184** was reacted with 2 equiv TiCl_3 and 2 equiv NH_4OAc in refluxing degassed $\text{AcOH}:\text{Dioxane}:\text{H}_2\text{O}$ for 2 h. The reaction was extracted with ether. The ethereal layer was dried over MgSO_4 , filtered and concentrated. The resulting oil was purified by chromatography on silica gel ($R_f = 0.3$ in 90% hexanes/10% ethyl acetate). Product **185** was obtained as white crystalline solid. ^1H NMR (CDCl_3): δ 5.00 (td, $J = 11.2, 5.2$ Hz, 1H), 2.38-2.26 (multiple peaks, 2H), 2.19-2.04 (multiple peaks, 2H), 1.98 (s, 3H), 1.87-1.66 (multiple peaks, 4H), 1.52-1.48 (multiple peaks, 2H), 1.35-1.11 (multiple peaks, 4H).

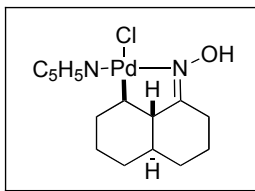
Structure Determination.

Colorless needles of **185** were grown from an ether solution at -10 deg. C. A crystal of dimensions $0.50 \times 0.10 \times 0.04$ mm was mounted on a standard Bruker SMART CCD-based X-ray diffractometer equipped with a LT-2 low temperature device and normal focus Mo-target X-ray tube ($\lambda = 0.71073$ Å) operated at 2000 W power (50 kV, 40 mA). The X-ray intensities were measured at 123(2) K; the detector was placed at a distance 4.980 cm from the crystal. A total of 2338 frames were collected with a scan width of 0.3° in ω and ϕ with an exposure time of 60 s/frame. The integration of the data yielded a total of 17004 reflections to a maximum 2θ value of 46.76° of which 1704 were independent and 1325 were greater than $2\theta(I)$. The final cell constants (Table 1) were based on the xyz centroids of 3514 reflections above $10\sigma(I)$. Analysis of the data showed negligible decay during data collection; the data were processed with SADABS. No correction for absorption was necessary. The structure was solved and refined with the Bruker SHELXTL (version 6.12) software package, using the space group $\text{Pca}2(1)$ with $Z = 8$ for the formula $\text{C}_{12}\text{H}_{18}\text{O}_3$. All non-hydrogen atoms were refined anisotropically with the hydrogen atoms placed in idealized positions. Full matrix least-squares refinement based on F^2 converged at $R1 = 0.0538$ and $wR2 = 0.1379$ [based on $I > 2\sigma(I)$], $R1 = 0.0769$ and $wR2 = 0.1585$ for all data.

Sheldrick, G.M. SHELXTL, v. 6.12; Bruker Analytical X-ray, Madison, WI, 2001.

Sheldrick, G.M. SADABS, v. 2.10. Program for Empirical Absorption Correction of Area Detector Data, University of Gottingen: Gottingen, Germany, 2003.

Saint Plus, v. 7.01, Bruker Analytical X-ray, Madison, WI, 2003.



Decalone oxime was reacted with 1.0 equiv Na_2PdCl_4 and 1.12 equiv NaOAc in MeOH at rt for 3 days.⁴⁰ The crude reaction was concentrated in vacuum. The crude red brown solid was dissolved in CH_2Cl_2 and filtered through celite. The resulting solution is concentrated and dissolved in hot methanol. The crude solid is collected and reacted with 1.0 equiv pyridine in THF for 10 minutes. The crude reaction is concentrated and purified by chromatography on silica gel (50% hexanes/50% ethyl acetate to 35% hexanes/65% ethyl acetate). Product **190** was obtained as yellow solid (93% pure). ^1H NMR (CDCl_3): δ 9.85 (s, 1H), 8.75 (d, 7.6 Hz, 2H), 7.75 (t, $J = 7.6$ Hz, 1H), 7.33 (dd, $J = 7.6, 6.8$ Hz, 2H), 3.07-3.00 (multiple peaks, 2H), 2.07 (m, 1H), 1.97-1.83 (multiple peaks, 2H), 1.68 (m, 1H), 1.57-1.52 (multiple peaks, 2H), 1.43-1.32 (multiple peaks, 4H), 1.14-1.02 (multiple peaks, 3H). $^{13}\text{C}\{^1\text{H}\}$ NMR (CDCl_3): δ 169.15, 152.79, 137.49, 125.10, 60.72, 47.14, 44.06, 33.99, 33.96, 31.18, 28.21, 27.17, 25.34, 23.03, 22.53.

Structure Determination.

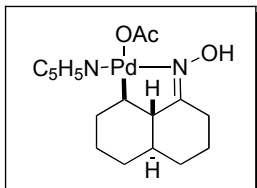
Pale yellow needles of **190** were grown from a dichloromethane/pentane solution at 22 deg. C. A crystal of dimensions 0.60 x 0.34 x 0.10 mm was mounted on a standard Bruker SMART CCD-based X-ray diffractometer equipped with a LT-2 low temperature device and normal focus Mo-target X-ray tube ($\lambda = 0.71073$ Å) operated at 2000 W power (50 kV, 40 mA). The X-ray intensities were measured at 123(2) K; the detector was placed at a distance 4.980 cm from the crystal. A total of 3040 frames were collected with a scan width of 0.2° in ω and ϕ with an exposure time of 10 s/frame. The integration of the data yielded a total of 17473 reflections to a maximum 2θ value of 56.64° of which 3703 were independent and 3525 were greater than $2\sigma(I)$. The final cell constants (Table 1) were based on the xyz centroids of 6708 reflections above $10\sigma(I)$. Analysis of the data showed negligible decay during data collection; the data were processed with SADABS and corrected for absorption. The structure was solved and refined with the Bruker SHELXTL (version 6.12) software package, using the space group $P2(1)/c$ with $Z = 4$ for the formula $\text{C}_{15}\text{H}_{21}\text{N}_2\text{OPd}$. All non-hydrogen atoms were refined anisotropically with the hydrogen atoms placed in idealized positions with the exception of the oxime hydrogen which was

located on a difference Fourier map. Full matrix least-squares refinement based on F^2 converged at $R1 = 0.0210$ and $wR2 = 0.0568$ [based on $I > 2\sigma(I)$], $R1 = 0.0223$ and $wR2 = 0.0576$ for all data.

Sheldrick, G.M. SHELXTL, v. 6.12; Bruker Analytical X-ray, Madison, WI, 2001.

Sheldrick, G.M. SADABS, v. 2.10. Program for Empirical Absorption Correction of Area Detector Data, University of Gottingen: Gottingen, Germany, 2003.

Saint Plus, v. 7.01, Bruker Analytical X-ray, Madison, WI, 2003.



Product **190** was reacted with AgOAc in AcOH at 25°C for 12 h. The reaction was filtered through celite and concentrated. Recrystallization of product **191** with CH_2Cl_2 and hexanes afforded a yellow solid (93% pure). ^1H NMR (CDCl_3): δ 8.66 (d, 5.2 Hz, 2H), 7.75 (t, $J = 6.8$ Hz, 1H), 7.31 (dd, $J = 6.0$ Hz, 2H), 3.13 (dd, $J = 17.2, 9.2$, 1H), 2.80 (t, $J = 9.2$ Hz, 1H), 2.00 (t, $J = 10.0$ Hz, 1H), 1.91-1.76 (multiple peaks, 4H), 1.61-1.44 (multiple peaks, 3H), 1.34-1.18 (multiple peaks, 4H), 1.05-0.90 (multiple peaks, 3H).

Structure Determination.

Colorless blocks of **191** were grown from a dichloromethane solution at 22 deg. C. A crystal of dimensions $0.34 \times 0.22 \times 0.14$ mm was mounted on a standard Bruker SMART CCD-based X-ray diffractometer equipped with a LT-2 low temperature device and normal focus Mo-target X-ray tube ($\lambda = 0.71073$ Å) operated at 2000 W power (50 kV, 40 mA). The X-ray intensities were measured at $123(2)$ K; the detector was placed at a distance 4.980 cm from the crystal. A total of 4545 frames were collected with a scan width of 0.2° in ω and ϕ with an exposure time of 10 s/frame. The integration of the data yielded a total of 58517 reflections to a maximum 2θ value of 56.80° of which 4660 were independent and 4297 were greater than $2\sigma(I)$. The final cell constants (Table 1) were based on the xyz centroids of 9446 reflections above $10\sigma(I)$. Analysis of the data showed negligible decay during data collection; the data were processed with SADABS and corrected for absorption. The structure was solved and refined with the Bruker SHELXTL (version 6.12) software package, using the space group $I4(1)/a$ with $Z = 16$ for the formula $\text{C}_{17}\text{H}_{24}\text{N}_2\text{O}_3\text{Pd}$. All non-hydrogen atoms were refined anisotropically with the hydrogen atoms placed in both idealized and refined positions. Full matrix least-squares refinement

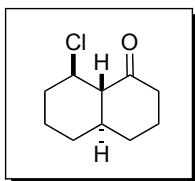
based on F^2 converged at $R1 = 0.0365$ and $wR2 = 0.0878$ [based on $I > 2\sigma(I)$], $R1 = 0.0390$ and $wR2 = 0.0887$ for all data.

Sheldrick, G.M. SHELXTL, v. 6.12; Bruker Analytical X-ray, Madison, WI, 2001.

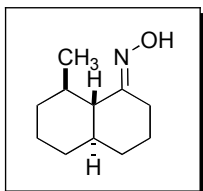
Sheldrick, G.M. SADABS, v. 2.10. Program for Empirical Absorption Correction of Area Detector Data, University of Gottingen: Gottingen, Germany, 2003.

Saint Plus, v. 7.01, Bruker Analytical X-ray, Madison, WI, 2003.

General Procedure for Stoichiometric Reactions of Palladacycle Monomers with Oxidants ($PhI(OAc)_2$, $PhICl_2$, MeI): Monomers **190** and **191** were reacted with 1.0 equiv of the Oxidant in AcOH at 100 °C for 12 h. The reaction was concentrated and their crude NMR's taken to determine the ratio and yields of products obtained.



Product **192**: 1H NMR ($CDCl_3$): δ 4.08 (dt, $J = 10.8, 4.0$ 1H), 2.52-2.41 (multiple peaks, 3H), 2.30-2.26 (multiple peaks, 2H), 2.13-2.09 (multiple peaks, 2H), 1.84-1.49 (multiple peaks, 5H), 1.30-1.19 (multiple peaks, 2H).



Structure Determination.

Colorless plates of **193** were grown from an ether solution at 22 deg. C. A crystal of dimensions 0.28 x 0.20 x 0.05 mm was mounted on a standard Bruker SMART CCD-based X-ray diffractometer equipped with a LT-2 low temperature device and normal focus Mo-target X-ray tube ($\lambda = 0.71073$ Å) operated at 2000 W power (50 kV, 40 mA). The X-ray intensities were measured at 123(2) K; the detector was placed at a distance 4.980 cm from the crystal. A total of 3698 frames were collected with a scan width of 0.2° in ω and ϕ with an exposure time of 30 s/frame. The integration of the data yielded a total of 11491 reflections to a maximum 2θ value of 56.68° of which 2558 were independent and 1864 were greater than $2\sigma(I)$. The final cell constants (Table 1) were based on the xyz centroids of 3409 reflections above $10\sigma(I)$. Analysis of the data showed negligible decay during data

collection; the data were processed with SADABS, no correction for absorption was necessary. The structure was solved and refined with the Bruker SHELXTL (version 6.12) software package, using the space group P2(1)/n with Z = 4 for the formula C₁₁H₁₉NO. All non-hydrogen atoms were refined anisotropically with the hydrogen atoms placed in idealized positions. Full matrix least-squares refinement based on F² converged at R1 = 0.0459 and wR2 = 0.1178 [based on I > 2sigma(I)], R1 = 0.0709 and wR2 = 0.1307 for all data.

Sheldrick, G.M. SHELXTL, v. 6.12; Bruker Analytical X-ray, Madison, WI, 2001.

Sheldrick, G.M. SADABS, v. 2.10. Program for Empirical Absorption Correction of Area Detector Data, University of Gottingen: Gottingen, Germany, 2003.

Saint Plus, v. 7.01, Bruker Analytical X-ray, Madison, WI, 2003.

2.10 References

- (1) Crabtree, R. H. *J. Organomet. Chem.* **2004**, *689*, 4083-4091.
- (2) Labinger, J. A.; Bercaw, J. E. *Nature* **2002**, *417*, 507-514.
- (3) Crabtree, R. H. *J. Chem. Soc. Dalton Trans.* **2001**, 2437-2450.
- (4) Shilov, A. E.; Shul'pin, G. B. *Chem. Rev.* **1997**, *97*, 2879-2932.
- (5) Shilov, A. E.; Shteinman, A. A. *Coord. Chem. Rev.* **1977**, *24*, 97-143.
- (6) Periana, R. A.; Taube, D. J.; Gamble, S.; Taube, H.; Satoh, T.; Fujii, H. *Science* **1998**, *280*, 560-564.
- (7) Dangel, B. D.; Godula, K.; Youn, S. W.; Sezen, B.; Sames, D. *J. Am. Chem. Soc.* **2002**, *124*, 11856-11857.
- (8) Sezen, B.; Franz, R.; Sames, D. *J. Am. Chem. Soc.* **2002**, *124*, 13372-13373.
- (9) Dangel, B. D.; Johnson, J. A.; Sames, D. *J. Am. Chem. Soc.* **2001**, *123*, 8149-8150.
- (10) Dick, A. R.; Hull, K. L.; Sanford, M. S. *J. Am. Chem. Soc.* **2004**, *126*, 2300-2301.
- (11) Baldwin, J. E.; Jones, R. H.; Najera, C.; Yus, M. *Tetrahedron* **1985**, *41*, 699-711.
- (12) Baldwin, J. E.; Najera, C.; Yus, M. *J. Chem. Soc., Chem. Comm.* **1985**, 126-127.
- (13) Carr, K.; Saxton, H. M.; Sutherland, J. K. *J. Chem. Soc., Perkin Trans. 1* **1988**, 1599-1601.
- (14) Moriarty, R. M.; Prakash, O.; Vavilikolanu, P. R. *Syn. Commun.* **1986**, *16*, 1247-1253.
- (15) Desai, L. V.; Hull, K. L.; Sanford, M. S. *J. Am. Chem. Soc.* **2004**, *126*, 9542-9543.
- (16) Giri, R.; Liang, J.; Lei, J.; Li, J.; Wang, D.; Chen, X.; Naggar, I. C.; Guo, C.; Foxman, B. M.; Yu, J. *Angew. Chem., Int. Ed.* **2005**, *44*, 7420-7424.
- (17) Dick, A. R.; Sanford, M. S. *Tetrahedron* **2006**, *62*, 2439-2463.
- (18) Fokin, A. A.; Schreiner, P. R. *Chem. Rev.* **2002**, *102*, 1551-1594.
- (19) Dunina, V. V.; Zalevskaya, O. A.; Potapov, V. M. *Usp. Khim.* **1988**, *57*, 434-473.
- (20) Giri, R.; Chen, X.; Yu, J. Q. *Angew. Chem., Int. Ed.* **2005**, *44*, 2112-2115.

- (21) Wilhelm, D.; Baeckvall, J. E.; Nordberg, R. E.; Norin, T. *Organometallics* **1985**, *4*, 1296-1302.
- (22) Stoccoro, S.; Soro, B.; Minghetti, G.; Zucca, A.; Cinellu, M. A. *J. Organomet. Chem.* **2003**, *679*, 1-9.
- (23) Zucca, A.; Cinellu, M. A.; Pinna, M. V.; Stoccoro, S.; Minghetti, G.; Manassero, M.; Sansoni, M. *Organometallics* **2000**, *19*, 4295-4304.
- (24) Albert, J.; Ceder, R. M.; Gomez, M.; Granell, J.; Sales, J. *Organometallics* **1992**, *11*, 1536-1541.
- (25) Dunina, V. V.; Gorunova, O. N.; Averina, E. B.; Grishin, Y. K.; Kuz'mina, L. G.; Howard, J. A. K. *J. Organomet. Chem.* **2000**, *603*, 138-151.
- (26) Mawo, R. Y.; Mustakim, S.; Young, V. G.; Hoffmann, M. R.; Smoliakova, I. P. *Organometallics* **2007**, *26*, 1801-1810.
- (27) Tamaru, Y.; Kagotani, M.; Yoshida, Z. *Angew. Chem., Int. Ed. Engl.* **1981**, *20*, 980-981.
- (28) Buchanan, J. M.; Stryker, J. M.; Bergman, R. G. *J. Am. Chem. Soc.* **1986**, *108*, 1537-1550.
- (29) Canty, A. J.; Patel, J.; Skelton, B. W.; White, A. H. *J. Organomet. Chem.* **2000**, *607*, 194-202.
- (30) Zaitsev, V. G.; Shabashov, D.; Daugulis, O. *J. Am. Chem. Soc.* **2005**, *127*, 13154-13155.
- (31) Reddy, B. V. S.; Reddy, L. R.; Corey, E. J. *Org. Lett.* **2006**, *8*, 3391-3394.
- (32) Baeckvall, J. E. *Acc. Chem. Res.* **1983**, *16*, 335-342.
- (33) Zhu, G. X.; Ma, S. M.; Lu, X. Y.; Huang, Q. C. *J. Chem. Soc., Chem. Commun.* **1995**, 271-273.
- (34) Dick, A. R.; Kampf, J. W.; Sanford, M. S. *J. Am. Chem. Soc.* **2005**, *127*, 12790-12791.
- (35) Minter, A. R.; Fuller, A. A.; Mapp, A. K. *J. Am. Chem. Soc.* **2003**, *125*, 6846-6847.
- (36) Greene, T. W.; Wuts, P. G. M. *In Protection for the Carbonyl Group; Protective Groups in Organic Synthesis* (Third Edition), **2002**, 293-368.
- (37) Corey, E. J.; Niimura, K.; Konishi, Y.; Hashimoto, S.; Hamada, Y. *Tetrahedron Lett.* **1986**, *27*, 2199-2202.

- (38) Booth, S. E.; Jenkins, P. R.; Swain, C. J.; Sweeney, J. B. *J. Chem. Soc., Perkin Trans. 1* **1994**, 3499-3508.
- (39) Li, C. B.; Zhang, H.; Cui, Y.; Zhang, S. M.; Zhao, Z. Y.; Choi, M. C. K.; Chan, A. S. *C. Syn. Commun.* **2003**, 33, 543-546.
- (40) Constable, A. G.; McDonald, W. S.; Sawkins, L. C.; Shaw, B. L. *J. Chem. Soc., Dalton Trans.* **1980**, 1992-2000.

Chapter 3

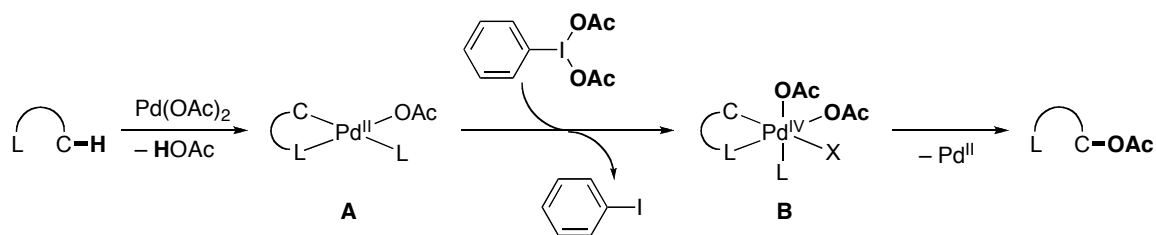
Oxone and $\text{K}_2\text{S}_2\text{O}_8$ as Alternative Oxidants for C-H Bond Oxygenation

3.1 Background and Significance

Significant current efforts in the literature are focused on the development of “green” catalytic reactions that are safe, scalable, environmentally friendly, and cost effective. In particular, such studies have explored the application of practical green oxidants, such as organic and inorganic peroxides, in transition metal catalyzed transformations. Peroxides are considered practical and green oxidants due to their low toxicity and expense. Two of these oxidants – H_2O_2 and Oxone ($2\text{KHSO}_5 \cdot \text{KHSO}_4 \cdot \text{K}_2\text{SO}_4$) – have been especially widely used in the metal catalyzed oxidation of alkenes,^{1, 2} sulfides³ and alcohols.^{4, 5} We envisioned that we could apply these peroxide oxidants in our palladium-catalyzed C–H bond oxygenation reactions.

Our group has shown that $\text{Pd}(\text{OAc})_2$ in conjunction with $\text{PhI}(\text{OAc})_2$ serves as an efficient catalyst to transform sp^2 and sp^3 C–H bonds to C–OAc bonds, affording acetoxyated products in excellent yield and extremely high selectivity.⁶⁻⁸ As summarized in Scheme 3.1, the mechanism of these reactions is proposed to involve initial ligand-directed C–H activation to provide cyclometalated Pd^{II} complex **A**. Complex **A** is then believed to undergo oxidation by $\text{PhI}(\text{OAc})_2$ to afford a Pd^{IV} intermediate **B**. Both of the acetates from the oxidant are transferred to the metal in this step, and iodobenzene is released as a byproduct. Carbon-oxygen bond forming reductive elimination then affords the final acetoxyated product.

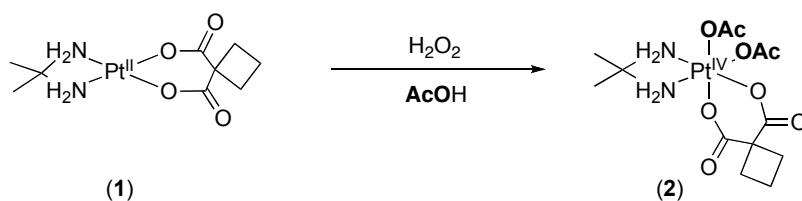
Scheme 3.1: Proposed Mechanism for C–H Bond Acetoxylation with $\text{PhI}(\text{OAc})_2$



Even though $\text{PhI}(\text{OAc})_2$ serves as an effective oxidant to oxygenate a wide range of substrates, there are some disadvantages associated with its use. The byproduct from these reactions, iodobenzene, is toxic, and, therefore further purification processes are required for its usage. As the equivalents of oxidant increase, the accumulation of this byproduct increases, which reduces the overall atom economy of the system. Additionally, $\text{PhI}(\text{OAc})_2$ is relatively expensive, at approximately \$1/gram. Based on these disadvantages, we desired to replace $\text{PhI}(\text{OAc})_2$ with greener and less costly oxidants such as peroxides.

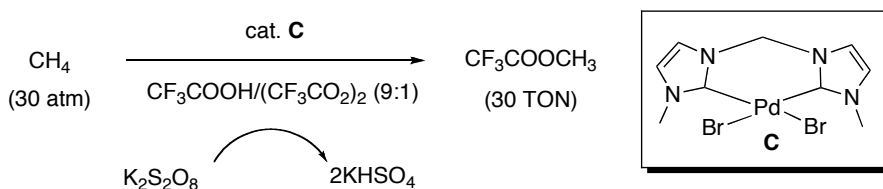
The key intermediate in Pd-catalyzed C–H bond oxygenation transformations is the Pd^{IV} complex **B** (Scheme 3.1). We wondered if it would be possible to generate this complex using alternative oxidants. While Pd^{IV} complexes are plausible intermediates, they are typically not easily observed because of their high reactivity. As a result, Pt^{IV} complexes are often used as models for putative Pd^{IV} intermediates, since platinum is in the same group as palladium in the periodic table. It is well known in the literature that Pt^{II} complexes react with oxidants in a very similar fashion to Pd^{II} complexes, but the resulting products are more stable.⁹⁻¹² As shown in Scheme 3.2, Jung and coworkers have shown that it is possible to oxidize Pt^{II} to Pt^{IV} , using H_2O_2 as the oxidant and AcOH as the solvent.¹³ In this reaction, H_2O_2 serves to oxidize Pt^{II} to Pt^{IV} and AcOH serves as the source of acetate in the final product. If platinum is a true model for palladium, then this result suggests that peroxides in AcOH could potentially be used as stoichiometric oxidants in place of $\text{PhI}(\text{OAc})_2$ to generate catalytic intermediate **B**.

Scheme 3.2: Stoichiometric Oxidation of Pt^{II} Complex with H₂O₂ in AcOH



Herrmann and coworkers have reported a rare example where an inorganic peroxide – K₂S₂O₈ – was used as the stoichiometric oxidant in a Pd-catalyzed C–H bond oxygenation reaction.¹⁴ Subjecting a suspension of K₂S₂O₈ in CF₃CO₂H/(CF₃CO)₂O to 20 bar CH₄ in the presence of a catalytic amount of Pd^{II} catalyst **C** led to the formation of CH₃O₂CCF₃ (Scheme 3.3).

Scheme 3.3: Palladium-Catalyzed Oxidation of Methane with K₂S₂O₈



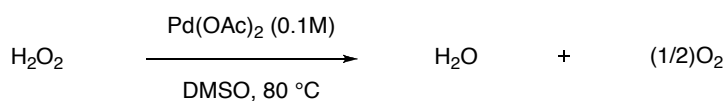
Although the authors do not speculate on the mechanism, we believe that the reaction likely proceeds via a high oxidation state Pd^{IV} intermediate analogous to **2** above. Similar to the Jung system, the trifluoroacetic acid is expected to serve as a source of trifluoroacetate groups on the metal, which upon reductive elimination form the product CH₃O₂CCF₃. Although this reaction is a promising initial lead, the requirement of 100 equiv of K₂S₂O₈ as well as the high pressure of methane limits its practical utility.

3.2 Initial Screenings of Peroxides

Initial studies focused on applying peroxides as stoichiometric oxidants in the Pd-catalyzed directed acetoxylation of *m*-bromoacetophenone oxime ether. Based on Jung's report, we chose to employ acetic acid as the reaction media and the source of acetate in the final product. A variety of peroxides were screened under our previously determined

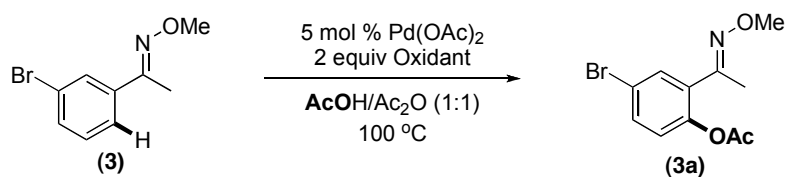
reaction conditions for $\text{PhI}(\text{OAc})_2$ -mediated acetoxylation reactions (5 mol % $\text{Pd}(\text{OAc})_2$, 2 equiv of oxidant in AcOH at 100 °C) (Table 3.1). Interestingly, the use of H_2O_2 in this Pd -catalyzed reaction resulted in only 11% of our desired product (entry 1), despite the fact that it was a highly effective stoichiometric oxidant for Pt^{II} (Scheme 3.2). We rationalize this result based on reports that Pd^{II} rapidly catalyzes the disproportionation of H_2O_2 to H_2O and O_2 (Scheme 3.4), and O_2 is not capable of oxidizing Pd^{II} to Pd^{IV} in these systems.¹⁵

Scheme 3.4: Palladium-Catalyzed Disproportionation of H_2O_2



Other peroxides such as *m*-chloroperoxybenzoic acid (*m*-CPBA) and peracetic acid provided slightly higher yields than H_2O_2 (14% and 34%, respectively – entries 3 and 4); however, despite attempts to further optimize these reactions, they never afforded synthetically useful quantities of the product. The most promising results were obtained using the inorganic peroxides Oxone and $\text{K}_2\text{S}_2\text{O}_8$ as terminal oxidants. These reagents afforded the acetoxyated product in comparable yield as $\text{PhI}(\text{OAc})_2$ (Table 3.1, entries 7 and 8). Notably, use of the tetrabutylammounium salt of Oxone substantially lowered the yield of the acetoxyated product (entry 5), suggesting that increasing the solubility of the oxidant was unfavorable. Importantly, control reactions of substrate **3** with Oxone and $\text{K}_2\text{S}_2\text{O}_8$, in the absence of $\text{Pd}(\text{OAc})_2$, did not afford any of the desired acetoxyated product **3a**. Instead about 25% decomposition of the starting material to a complex mixture of unidentified products was observed.

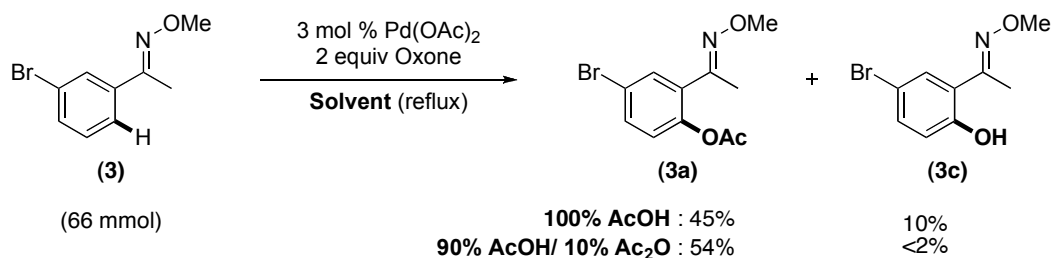
Table 3.1: Screen of Peroxide Oxidants for the Pd-Catalyzed Acetoxylation of *m*-Bromoacetophenone Oxime Ether



Entry	Oxidant	Isolated Yield
1	H ₂ O ₂	11%
2	Urea•H ₂ O ₂	10%
3	<i>m</i> -CPBA	14%
4	(CH ₃) ₃ CO ₃ H	18%
5	(Bu ₄ N) ₅ 2HSO ₅ •HSO ₄ •SO ₄ ²⁻	21%
6	CH ₃ CO ₃ H	34%
7	Oxone (2KHSO ₅ •KHSO ₄ •K ₂ SO ₄)	68%
8	K ₂ S ₂ O ₈	76%
9	PhI(OAc) ₂	81%

Palladium-catalyzed C–H bond acetoxylation with Oxone is an exciting result, because this oxidant is environmentally benign, safe (not explosive like many other peroxides), and inexpensive. These features make Oxone attractive for large-scale applications. We have conducted the reaction of substrate **3** with Oxone effectively at scales ranging from 1 mmol to 66 mmol. When we initially executed the 66 mmol scale reaction in AcOH, we obtained the desired product, via Kugelrohr distillation, in modest 45% yield (in contrast, the yield on 1 mmol scale was 68%). This reduction in yield was due to competitive formation of the hydrolyzed product **3c** (Scheme 3.5). The hydrolysis was addressed by addition of 10% acetic anhydride to the reaction mixture, which improved the yield of product **3a** to 54% on a 66 mmol scale. Importantly, these large scale reactions were optimized with 3 mol % of Pd(OAc)₂. Further reduction in the amount of catalyst was possible; however, longer reaction times were required.

Scheme 3.5: Large Scale Reaction of *m*-Bromoacetophenone Oxime Ether with Oxone



3.3 Scope of Acetoxylation of sp² C–H Bonds with Oxone and K₂S₂O₈

We next desired to explore the scope of the acetoxylation of substrates with Oxone and K₂S₂O₈ in AcOH. This reaction was applied to substrates containing a variety of directing groups, including oxime ethers of ketones and aldehydes, amides, and isoxazolines (Table 3.2 and 3.3).¹⁶ We were delighted to see that substrates that required the formation of five (substrates **5-11**) and six (substrates **12-13**) membered palladacyclic intermediates upon C–H activation were all effectively functionalized by Oxone and K₂S₂O₈. Both electron rich and poor arenes as well as oxidizable functionalities such as benzylic C–H bonds were well tolerated. Notably, substrates **9-13** afforded better yields of the desired acetoxyated products with K₂S₂O₈ than Oxone (Table 3.3). Tuning the stoichiometry of the oxidant allowed for the formation of mono or diacetoxyated products as desired (Scheme 3.6, products **4a** and **4b**). Acetic anhydride was used in conjunction with AcOH in the reaction for some substrates (particularly electron rich oxime ethers and oxime ethers derived from aldehydes) to attenuate hydrolysis.

Scheme 3.6: Product Distribution as a Function of Oxidant Stoichiometry

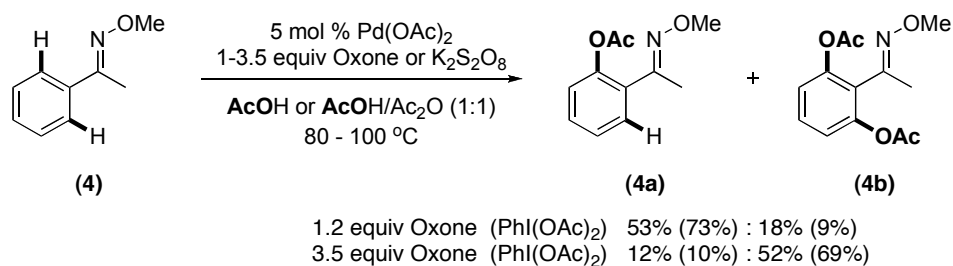
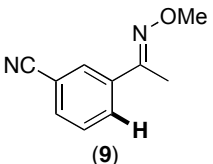
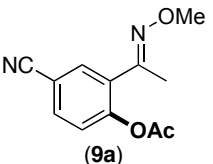
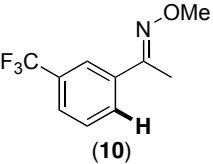
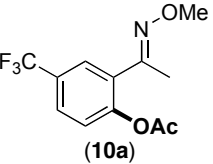
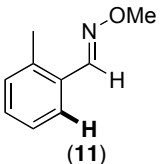
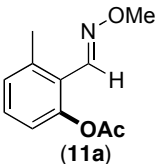
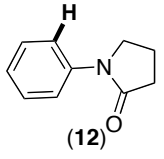
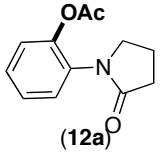
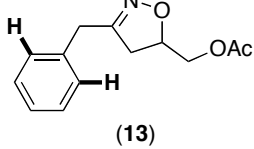
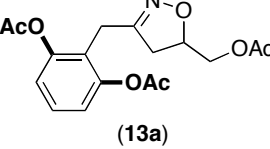


Table 3.2: Substrate Scope with Oxone as the Terminal Oxidant

Entry	Substrate	Product	Yield with Oxone ^a	Yield with PhI(OAc) ₂ ^a
1	 (5)	 (5a)	71%	72%
2	 (6)	 (6a)	69%	78%
3	 (7)	 (7a)	63%	57%
4	 (8)	 (8a)	53%	40%

^aConditions: 5 mol % Pd(OAc)₂, 1.0-2.0 equiv Oxidant, AcOH or AcOH/Ac₂O at 100 °C

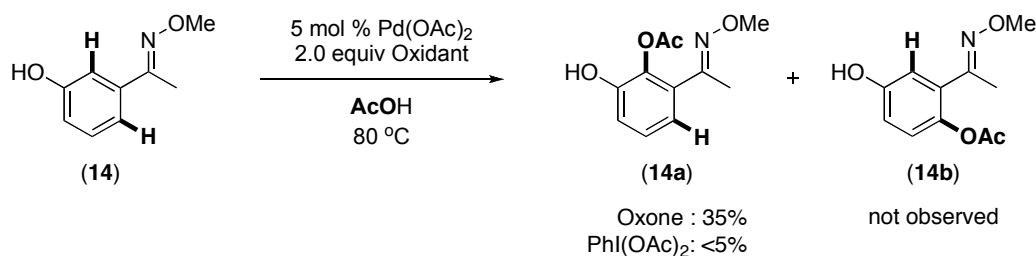
Table 3.3: Substrate Scope with $K_2S_2O_8$

Entry	Substrate	Product	Yield with $K_2S_2O_8^a$	Yield with $PhI(OAc)_2^a$
1	 (9)	 (9a)	57%	66%
2	 (10)	 (10a)	75%	95%
3	 (11)	 (11a)	53%	69%
4	 (12)	 (12a)	75%	77%
5	 (13)	 (13a)	53%	72%

^aConditions: 5 mol % $Pd(OAc)_2$, 1.0-2.0 equiv Oxidant, AcOH or AcOH/Ac₂O at 100 °C

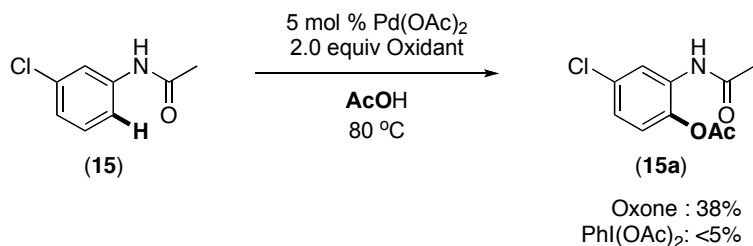
In substrates containing substituents *meta* to the directing group (for example, **5-10**), two different *ortho*-C–H bonds could potentially be functionalized. In most of these reactions, the sterically less hindered C–H bond was acetoxyated selectively (Table 3.1 and 2, entries 1-4 and 1-2 respectively).⁸ On the contrary, in the *meta*-hydroxy substrate **14**, the sterically more hindered C–H bond was acetoxyated (Scheme 3.7). We believe that the alcohol and the oxime ether functionalities may chelate to the palladium and thereby afford this reversal of selectivity. Importantly, the selectivity of this reaction was confirmed by synthesizing authentic samples of products **14a** and **14b**.

Scheme 3.7: Reaction of Substrate **14** with Oxone and $\text{PhI}(\text{OAc})_2$



My colleague Hasnain Malik obtained the corresponding yields of products **3a-13a** from reactions with $\text{PhI}(\text{OAc})_2$. In general, yields with Oxone and $\text{K}_2\text{S}_2\text{O}_8$ were comparable to those with $\text{PhI}(\text{OAc})_2$. However, two notable exceptions were substrates **14** and **15**. Subjection of substrate **14** under our catalytic conditions using $\text{PhI}(\text{OAc})_2$ resulted in less than 5% of the desired product, presumably due to undesired oxidation of **14** to the corresponding quinone.¹⁷ In contrast, reaction of substrate **14** with Oxone afforded 35% of the desired product (Scheme 3.7). The low yield here is due to decomposition of the starting material to unidentified products. Similarly, reaction of amide **15** with $\text{PhI}(\text{OAc})_2$ resulted in decomposition of the starting material, presumably via uncatalyzed reaction between the hypervalent iodine oxidant and the amide functionality. $\text{PhI}(\text{OAc})_2$ has been shown to react with amides to form rearranged products via a $\text{RCONHI}(\text{Ph})\text{OAc}$ intermediate.^{18, 19} However, reaction of **15** with Oxone afforded 38% of the acetoxyated product **15a** (Scheme 3.8). In this case, the balance of material was accounted for as unreacted substrate **15**.

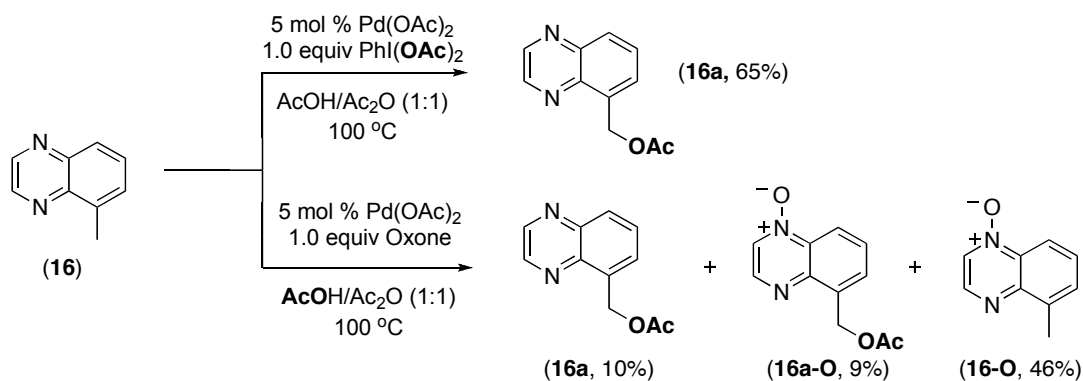
Scheme 3.8: Palladium-Catalyzed Oxidation of *m*-Chloroacetanilide



There are some limitations associated with the use of Oxone and $\text{K}_2\text{S}_2\text{O}_8$ as oxidants in place of $\text{PhI}(\text{OAc})_2$. For example, substrates **16-18** resulted in low yields and/or reactivity with these peroxides in comparison with $\text{PhI}(\text{OAc})_2$. With substrates **16**

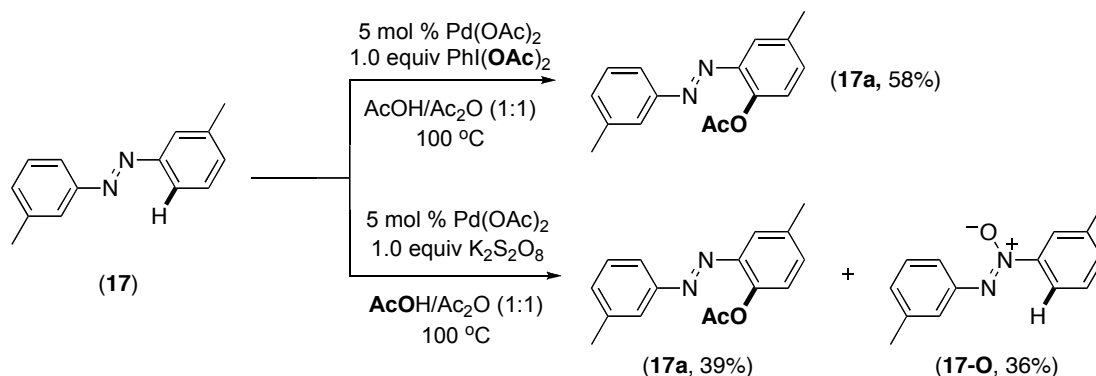
and **17**, we believe that these limitations are due to competitive *N*-oxide formation. For example, subjection of quinoxaline **16** to the catalytic reaction conditions with $\text{PhI}(\text{OAc})_2$ resulted in a single acetoxyated product **16a** in 65% yield. In contrast, subjection of **16** to catalytic conditions with Oxone afforded three products – acetoxyated compound **16a**, the *N*-oxide of the acetoxyated product (**16a-O**), and the *N*-oxide of the starting material (**16-O**). The assignment of the regioselectivity of *N*-oxidation was made based on comparison of the NMR of **16a** to **16a-O** following a similar approach taken in literature.²⁰

Scheme 3.9: Palladium-Catalyzed Reaction of Quinoxaline with Oxone

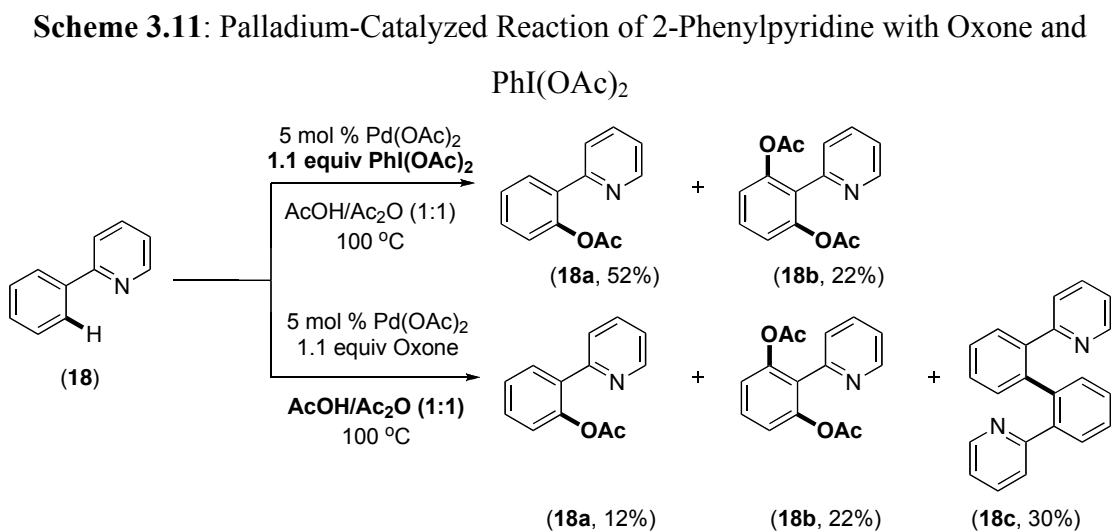


Similarly, subjection of azobenzene substrate **17** under catalytic conditions with $\text{PhI}(\text{OAc})_2$ afforded the desired acetoxyated product **17a** in 58% yield. On the other hand, reaction of azobenzene with Oxone yielded significant quantities of the corresponding *N*-oxide (**17-O**) along with the acetoxyated product **17a**.

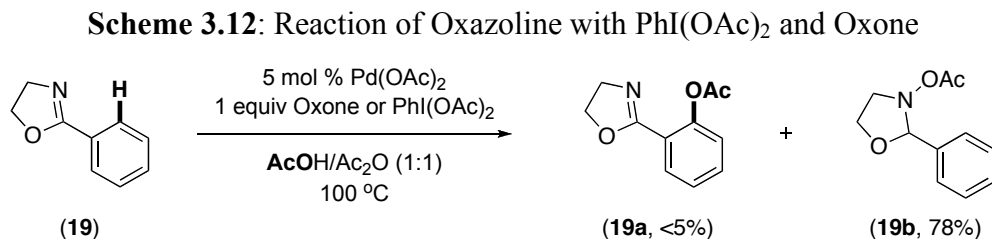
Scheme 3.10: Reaction of Azobenzene Substrate **17** with Oxone



The yield of the desired acetoxyated product in reactions of substrates bearing pyridine directing groups appears to be hampered by another palladium-catalyzed side reaction. For example, reaction of 2-phenylpyridine with Oxone resulted in the formation of the desired acetoxyated product **18a**, diacetoxyated product **18b**, and a new compound. As shown in Scheme 3.11, this new compound was identified as the homodimer **18c** by Kami Hull.²¹ In contrast, reaction of **18** with $\text{PhI}(\text{OAc})_2$ afforded the acetoxyated product **18a** (52% yield) and the diacetoxyated product **18b** (22% yield), and *none* of product **18c** was observed.

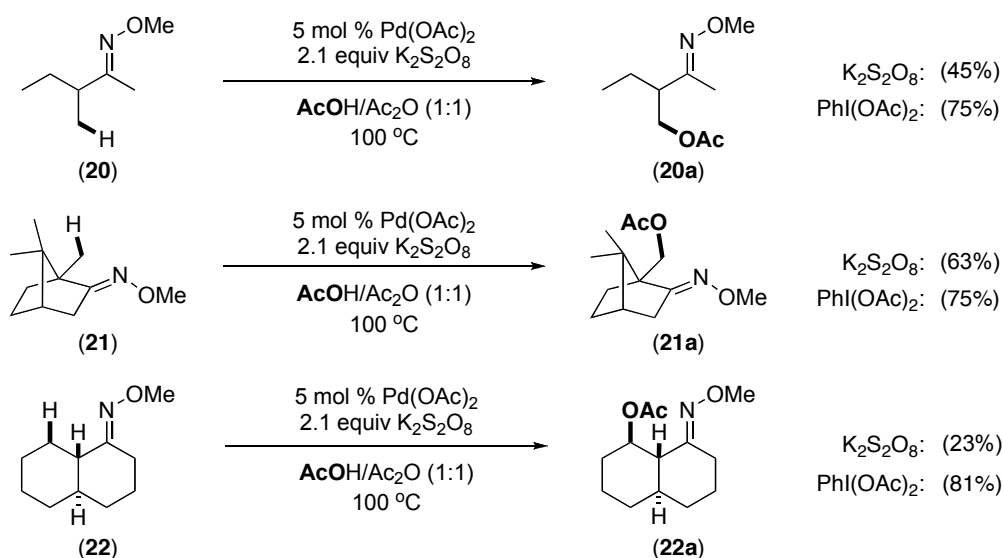


There were also directing groups that resulted in low yields of the desired acetoxyated product with both Oxone and $\text{PhI}(\text{OAc})_2$ due to uncatalyzed side reactions of the substrate with the oxidant. For example, reaction of oxazoline **19** with both $\text{PhI}(\text{OAc})_2$ and Oxone afforded <5% of acetoxyated product **19a**. This low yield is due to uncatalyzed addition of HOAc across the imine.

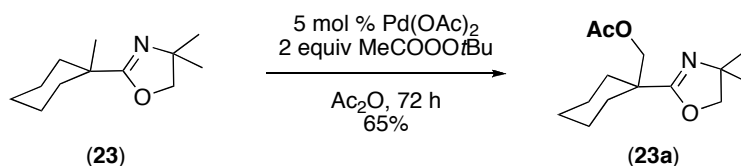


3.4 Scope of Acetoxylation of sp^3 C–H Bonds with Oxone and $K_2S_2O_8$

Excitingly, sp^3 C–H bonds were also effectively functionalized to afford acetoxyated products with Oxone and $K_2S_2O_8$. Reaction of substrate **20** with Oxone is particular notable (Scheme 3.13). Even though there are multiple different 1° C–H bonds as well as weaker 2° C–H bonds that could undergo oxidation, high selectivity was observed for the 1° β -C–H bond. This high selectivity for 1° C–H bonds with Oxone suggests strongly against the possibility of radical reaction pathways (common for peroxide reagents with weak O–O bonds) and instead is indicative of a ligand-directed C–H activation at palladium. Notably, the yield of product **20a** with Oxone was low in comparison to that with $PhI(OAc)_2$, (45% versus 75%, respectively), and the balance of the material was decomposition of the starting material. Similarly, Pd-catalyzed reaction of Oxone with camphor substrate **21** also afforded the desired acetoxyated product (Scheme 3.13). Finally, the reaction of *trans*-decalone substrate **22** with Oxone afforded a single diastereomeric product (**22a**) in 23% yield. The same diastereoselectivity was observed with $PhI(OAc)_2$ (although the product was obtained in significantly higher 81% yield in this case). This result implies that reductive elimination from Pd^{IV} under both the Oxone and the $PhI(OAc)_2$ proceeds via a similar mechanism – with retention of stereochemistry at carbon. The low yields of the desired products with substrates **20-22** were due to decomposition of the starting material under the oxidative conditions. Subjection of the substrate and product individually to the reaction conditions, in the absence of palladium, only led to 60% recovery due to the formation of unidentified decomposition products.

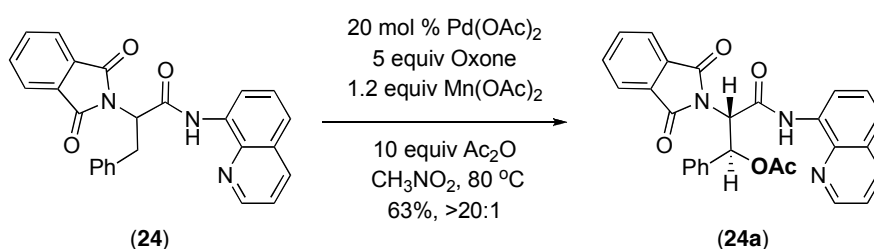
Scheme 3.13: Acetoxylation of sp^3 C-H Bonds using $K_2S_2O_8$ 

Concurrent to the work described herein, Yu and coworkers reported the use of peroxyesters in Ac_2O for the Pd-catalyzed oxazoline-directed acetoxylation of sp^3 C-H bonds (Scheme 3.14).²² They proposed that this reaction proceeds via a $Pd^{II/IV}$ catalytic cycle, where $MeCOOOtBu$ serves to oxidize Pd^{II} to Pd^{IV} . The authors also proposed that acetic anhydride is essential for catalytic turnover, and state that it is required both to introduce acetate ligands at Pd^{IV} and to regenerate $Pd(OAc)_2$ by acetylating the Pd-OR complex formed at the end of the catalytic cycle. Notably, this is in sharp contrast to what is observed in our peroxide-mediated C-H bond acetoxylation reaction. First, Ac_2O is clearly not required to introduce the OAc group into the products, since high yields of acetoxyated products are observed in the absence of this reagent. Second, Ac_2O is not needed for catalytic turnover in our reactions, since we obtain >10 turnovers without any added Ac_2O .

Scheme 3.14: Pd-Catalyzed Oxidation of C-H bonds with Peroxyesters

In addition, subsequent to the results described herein, Corey reported the use of Oxone for the Pd-catalyzed oxidation of C–H bonds in amino acid derivatives.²³ This report described the installation acetates at 2° positions in 8-aminoquinoline derivatives using 20 mol % Pd(OAc)₂, 5 equiv Oxone, 1.2 equiv Mn(OAc)₂, and 10 equiv Ac₂O in nitromethane at 80 °C (Scheme 3.15). Importantly, the products from this reaction were obtained with high levels of diastereoselectivity and could allow access to β-hydroxy amino acids.

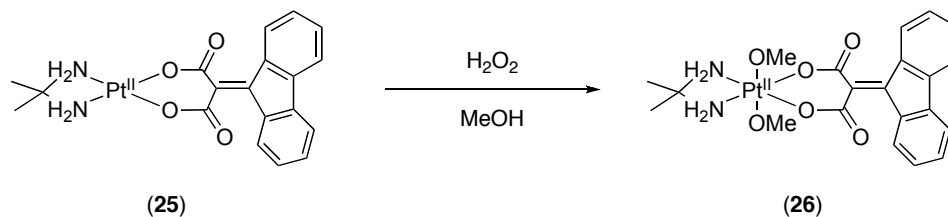
Scheme 3.15: Acetoxylation Reactions of Amino Acid Derivatives



3.5 Formation of Methyl Ethers with Oxone and K₂S₂O₈

We were next interested in using a similar approach for the conversion of C–H bonds to C–OR bonds of ethers, which are also very important and prevalent in biologically active molecules.²⁴ A literature search revealed that Pt^{IV} alkoxides could be generated by oxidizing Pt^{II} with H₂O₂ in methanol.²⁵ These products were analogous to those obtained when the same oxidation was carried out in AcOH (Scheme 3.16)

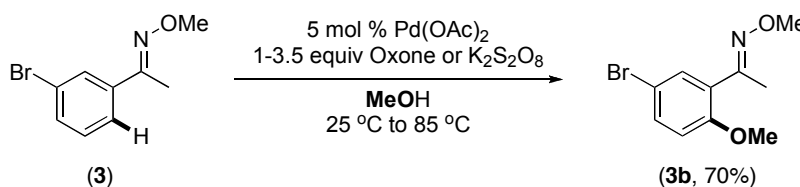
Scheme 3.16: Platinum Oxidation in Methanol with H₂O₂

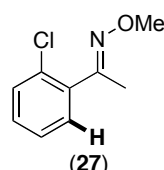
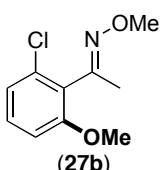
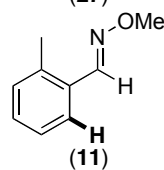
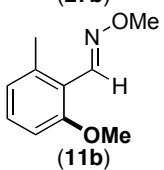
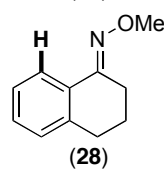
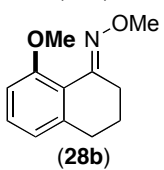
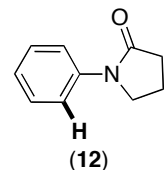
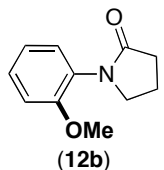
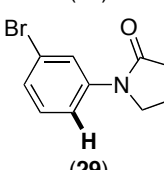
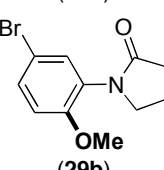
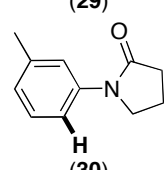
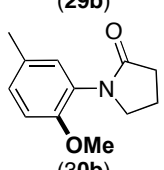


Based on this result, we reasoned that by changing the solvent of our reactions with Oxone or K₂S₂O₈ to methanol we might be able to install methyl ethers in the final

products. We were pleased to find that, using Pd(OAc)₂ as the catalyst and Oxone or K₂S₂O₈ as oxidants in methanol, we were able to obtain a variety of methoxylated products in good yields (Table 3.4).¹⁶ The methoxylation reactions also exhibited excellent tolerance to benzylic C–H bonds (entries 2, 3 and 6), aryl halides (entries 1 and 5), and aldehyde oxime ethers (entry 2). Similar to the acetoxylation reactions, higher yields of the methoxylated products were obtained when K₂S₂O₈ was used as the oxidant for substrates **12**, **29** and **30**. On the contrary, substrates **3**, **27**, **11** and **28** showed better reactivity with Oxone.

Table 3.4: Substrate Scope for Methoxylation Reactions

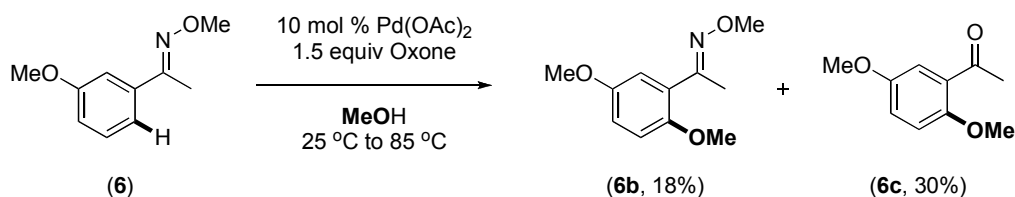


Entry	Substrate	Product	Yield with Peroxide
1	 (27)	 (27b)	60%
2	 (11)	 (11b)	59%
3	 (28)	 (28b)	33%
4	 (12)	 (12b)	72%
5	 (29)	 (29b)	61%
6	 (30)	 (30b)	57%

In the methoxylation reactions with electron rich oxime ethers, we observed competing deprotection of the oxime ether. For example, subjection of substrate **6** to Oxone in MeOH afforded 18% of the desired product **6b** along with 30% of the ketone **6c** (Scheme 3.17). Unlike the AcOH reactions, neither addition of acetic anhydride nor the use anhydrous methanol suppressed the hydrolysis. We believe the hydrolysis reaction

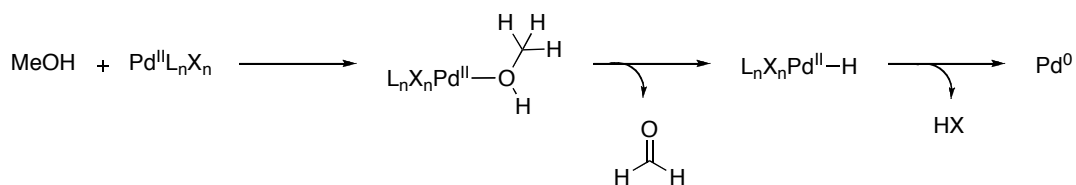
also increases the rate of catalyst decomposition. This was determined when subjection of the corresponding ketone **6c** to the reaction conditions in MeOH resulted in precipitation of Pd black within 5 minutes. This may be due to the poor ligand abilities of the ketone relative to the oxime ether. Without stabilization by coordination of the substrate, the Pd is more likely to undergo decomposition.

Scheme 3.17: Hydrolysis of Electron Rich Oxime Ethers under the Reaction Conditions



Unlike the acetoxylation reactions with Oxone and K₂S₂O₈, these methoxylation reactions were very sensitive to temperature and reaction time. Each substrate required a slow ramp of the temperature from room temperature to 45 °C. After stirring the reaction at 45 °C for 5 h, the temperature was then slowly ramped to 60 °C. After another 15 min, the temperature was then ramped slowly to 80 °C. This rigorous care with temperature was necessary to limit competing catalyst decomposition. Palladium(II) species are well known to react with methanol to form palladium hydrides and formaldehyde.²⁶ These Pd^{II} hydrides can then undergo reductive elimination of HX to generate Pd⁰ (Scheme 3.18). Catalyst decomposition occurs as Pd⁰ plates out of the reaction rather than getting oxidized to Pd^{II}, which is required to initiate the desired Pd^{II/IV} catalytic cycle to form acetoxyated compounds.

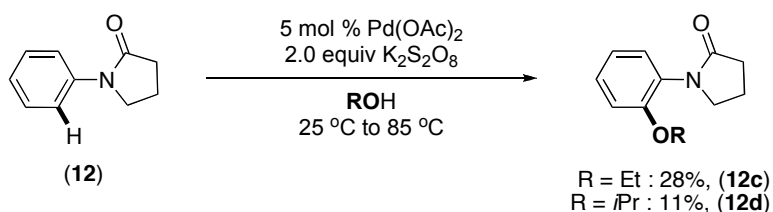
Scheme 3.18: Potential Catalyst Decomposition Pathway in Alcohol Solvents



Due to the increased rate of catalyst decomposition with alcoholic solvents, we have thus far been unable to achieve high yielding etherification reactions in other

alcohols like isopropanol or ethanol. We believe that as the size of the alcohol increases, the rate of etherification slows down and the rate of catalyst decomposition increases. Notably, the solvent polarity also changes from MeOH (dielectric constant = 32.6) to isopropanol (dielectric constant = 18.3), which could also play a role in the observed reactivity differences. Subjection of amide substrate **12** in ethanol with $K_2S_2O_8$ afforded the ethoxy product **12c** in modest 28% yield. When the alcohol was changed to isopropanol, the yield of the desired isopropoxy product **12d** was even lower at 11% (Scheme 3.19).

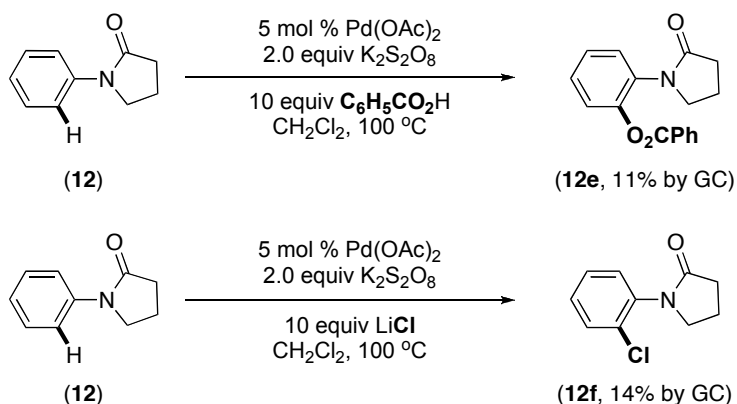
Scheme 3.19: Reaction of Peroxides in Other Alcohol Solvents



3.6 Introduction of Other Nucleophiles at Carbon with Oxone and $K_2S_2O_8$

As discussed above, we have successfully achieved the Pd-catalyzed conversion of C–H bonds to C–OAc and C–OR bonds using Oxone and $K_2S_2O_8$ as the oxidants in the corresponding nucleophilic solvent. Based on these results, we speculated that other functionalities could potentially be introduced by using the appropriate nucleophile in an inert solvent. Encouragingly, the Pd-catalyzed reaction of **12** with $K_2S_2O_8$ in CH_2Cl_2 in the presence of 10 equiv of benzoic acid afforded benzoate product **12e** in modest 11% yield (Scheme 3.20). Similarly, Pd-catalyzed reaction of **12** with $K_2S_2O_8$ and LiCl in CH_2Cl_2 afforded the chlorinated product **12f**, along with three undesired regioisomeric chlorinated products. These preliminary results are promising, and we anticipate that after further optimization these reactions will prove highly general and effective for converting C–H bonds to C–O, C–N, and C–halogen bonds

Scheme 3.20: Reaction of Substrate **12** in the Presence of Different Nucleophiles



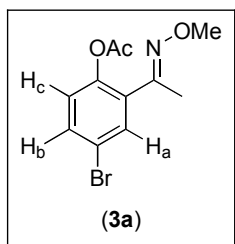
3.7 Conclusions

In summary, this chapter demonstrates the functionalization of sp² and sp³ C–H bonds to C–O bonds using cost effective and environmentally benign oxidants such as Oxone and K₂S₂O₈. With AcOH as the reaction medium, acetate functionality can be installed at carbon. Changing the reaction medium to MeOH allows formation of methyl ether functionalities. These reactions are general across a variety of substrates and tolerate most common functional groups. Furthermore, for the most part, yields obtained with Oxone and K₂S₂O₈ are comparable to those obtained with PhI(OAc)₂.

3.8 Experimental Procedure

General Procedures: NMR spectra were obtained on a Varian Inova 500 (499.90 MHz for ¹H; 125.70 MHz for ¹³C) unless otherwise noted. ¹H NMR chemical shifts are reported in parts per million (ppm) relative to TMS, with the residual solvent peak used as an internal reference. Multiplicities are reported as follows: singlet (s), doublet (d), doublet of doublets (dd), doublet of doublets of doublets (ddd), doublet of triplets (dt), triplet (t), quartet (q), quintet (quin), multiplet (m), and broad resonance (br). IR spectra were obtained on a Perkin-Elmer Spectrum BX FT-IR spectrometer.

Materials and Methods: Oxime substrates **3-11**, **14**, **20-22**, and **27-28** were prepared following the procedure described previously.²⁷ The isoxazoline **13** was prepared following a procedure by Mapp and coworkers.²⁸ The amide substrates **29-30** were prepared by palladium-catalyzed arylation of the corresponding lactone.⁸ Substrate **17** was prepared following a procedure by Gokel et al.²⁹ Pd(OAc)₂ was obtained from Pressure Chemical and used as received, and PhI(OAc)₂ was obtained from Merck Research Laboratories and used as received. Oxone was obtained from Acros and used as received, and K₂S₂O₈ was obtained from Fisher Chemical and used as received. Solvents were obtained from Fisher Chemical and used without further purification. Flash chromatography was performed on EM Science silica gel 60 (0.040–0.063 mm particle size, 230–400 mesh) and thin layer chromatography was performed on Merck TLC plates pre-coated with silica gel 60 F²⁵⁴. Control reactions (in the absence of Pd catalyst) were run for each substrate, and generally showed no reaction. The regioselectivity of acetoxylation and etherification was determined based on coupling constant analysis and assignment of each aromatic proton of the products as detailed below.



General Procedure for Table 3.1. Peroxide (1.75 mmol, 2.0 equiv) and Pd(OAc)₂ (9.81 mg, 0.044 mmol, 0.05 equiv) were combined in AcOH (3.7 mL) and Ac₂O (3.7 mL) in a 20 mL vial. Substrate **3** (200 mg, 0.88 mmol, 1.0 equiv) was then added to the mixture. The vial was sealed with a Teflon lined cap, and the reaction was heated at 100 °C for 12 h. The reaction mixture was diluted with ethyl acetate, and the vial was washed with copious diethyl ether. A 10% aqueous solution of Na₂SO₃ (450 mL) was added to the reaction, and the resulting mixture was stirred at 25 °C for 15 min. The organic and the aqueous layers were separated and the organic layer was extracted with water (2 x 50 mL), NaHCO₃ (1 x 50 mL), and brine (1 x 50 mL). The organic layer was dried over MgSO₄, filtered, and concentrated. The resulting oil was purified by

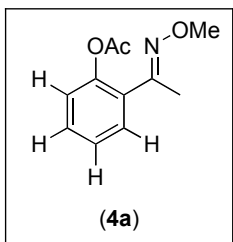
chromatography on silica gel to afford two oxime (E/Z) isomers (major oxime isomer: $R_f = 0.25$ in 88% hexanes/12% ethyl acetate; minor oxime isomer: $R_f = 0.23$ in 88% hexanes/12% ethyl acetate). The two oxime isomers were isolated as yellow oils in a ratio of 5:1. The ratio of regioisomers was >20:1.

Procedure for 66 mmol scale reaction. Oxone (80.79 g, 131.41 mmol, 2.0 equiv) and Pd(OAc)₂ (441 mg, 1.97 mmol, 0.03 equiv) were combined in AcOH (493 mL) and Ac₂O (55 mL) in a 1000 mL round bottom flask. Substrate **3** (15 g, 65.7 mmol, 1.0 equiv) was then added to the mixture. The reaction was refluxed for 18 h. The reaction mixture was diluted with ethyl acetate (500 mL) and filtered through a pad of celite and washed with ethyl acetate (1 L). The ethyl acetate, AcOH and Ac₂O were removed under reduced pressure. The product was obtained as a yellow oil through Kugelrohr distillation (10.15 g, 54% yield).

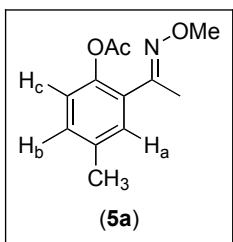
Major Oxime Isomer: ¹H NMR (CDCl₃): δ 7.56 (d, $J = 2.4$ Hz, 1H_a), 7.47 (dd, $J = 8.6, 2.4$ Hz, 1H_b), 6.98 (d, $J = 8.6$ Hz, 1H_c), 3.97 (s, 3H), 2.27 (s, 3H), 2.13 (s, 3H). ¹³C{¹H} NMR (CDCl₃): δ 168.82, 152.23, 147.02, 132.49, 132.23, 132.09, 124.87, 119.07, 62.07, 20.96, 14.89. **Minor Oxime Isomer:** ¹H NMR (CDCl₃): δ 7.48 (dd, $J = 8.7, 2.4$ Hz, 1H_b), 7.32 (d, $J = 2.4$ Hz, 1H_a), 7.03 (d, $J = 8.7$ Hz, 1H_c), 3.79 (s, 3H), 2.25 (s, 3H), 2.12 (s, 3H). IR (thin film): 2937, 1768 cm⁻¹. HRMS (ESI, m/z): [M⁺] calcd for C₁₁H₁₂BrNO₃, 285.0000; found, 285.0005. GC analysis (RESTEK Rtx[®]-5, FID detector): 99% integration. Anal. Calcd. for C₁₁H₁₂BrNO₂ (mixture of oxime isomers): C, 46.18, H, 4.23, N, 4.90; Found: C, 46.20, H, 4.19, N, 4.90.

General Method for Directed C-H Bond Acetoxylation with Oxone: Oxone (783 mg, 1.27 mmol, 0.95 equiv) and Pd(OAc)₂ (15 mg, 0.07 mmol, 0.05 equiv) were combined in AcOH (11.2 mL) in a 20 mL vial. Substrate **3** (200 mg, 1.34 mmol, 1.0 equiv) was then added to the mixture. The vial was sealed with a Teflon lined cap, and the reaction was heated at 100°C for 12 h. The reaction mixture was diluted with ethyl acetate (25 mL), and the vial was washed with copious diethyl ether. A 10% aqueous solution of Na₂SO₃ (450 mL) was added to the reaction, and the resulting mixture was stirred at 25 °C for 15 min. The organic and the aqueous layers were separated, and the

organic layer was extracted with water (2 x 50 mL), NaHCO₃ (1 x 50 mL), and brine (1 x 50 mL). The organic layer was dried over MgSO₄, filtered, and concentrated. The resulting oil was purified by chromatography on silica gel. Each substrate was optimized for reaction time, solvent (AcOH versus AcOH/Ac₂O) and equiv of the oxidant, as indicated below.

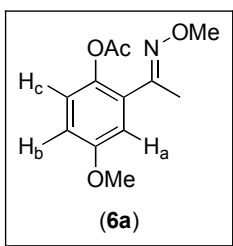


The reaction was run for 12 h with 0.95 equiv of Oxone in AcOH. Product **4a** was obtained as two oxime E/Z isomers (major oxime isomer: R_f = 0.26 in 89% hexanes/11% ethyl acetate; minor oxime isomer: R_f = 0.25 in 89% hexanes/11% ethyl acetate). The two isomers were isolated as yellow oils (147 mg total, 53% yield, ratio of oxime isomers = 5:1). **Major Oxime Isomer:** ¹H NMR (CDCl₃): δ 7.43 (dd, *J* = 7.7, 1.7 Hz, 1H), 7.37 (td, *J* = 7.8, 1.7 Hz, 1H), 7.25 (td, *J* = 7.5, 1.2 Hz, 1H), 7.10 (dd, *J* = 8.1, 1.2 Hz, 1H), 3.97 (s, 3H), 2.29 (s, 3H), 2.16 (s, 3H). ¹³C{¹H} NMR (CDCl₃): δ 169.25, 153.44, 147.95, 130.30, 129.72, 129.45, 126.10, 123.21, 61.94, 21.08, 15.09. **Minor Oxime Isomer:** ¹H NMR (CDCl₃): δ 7.37 (dd, *J* = 7.4, 1.8 Hz, 1H), 7.29 (m, 1H), 7.21 (dd, *J* = 7.6, 1.8 Hz, 1H), 7.14 (dd, *J* = 8.1, 1.5 Hz, 1H), 3.79 (s, 3H), 2.26 (s, 3H), 2.14 (s, 3H). IR (thin film): 2938, 1764 cm⁻¹. Anal. Calcd. for C₁₁H₁₃NO₃ (mixture of oxime isomers): C, 63.76, H, 6.32, N, 6.76; Found: C, 63.88, H, 6.08, N, 6.81.



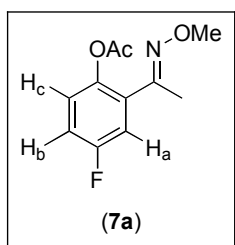
The reaction was run for 12 h with 1.0 equiv of Oxone in AcOH. Under the reaction conditions the OAc of **5a** partially hydrolyzed to the corresponding alcohol. The reaction mixture was concentrated under vacuum and Ac₂O (2.4 mL) and pyridine (0.46 mL) was added and the reaction stirred for 18 h. The reaction was stirred in water (5 mL) for 30

minutes and then extracted with ether. The ethereal layer was washed with water (2 x 50 mL), and NaHCO₃ (1 x 50 mL). The organic layer was dried over MgSO₄, filtered, and concentrated. The resulting oil was purified by chromatography on silica gel to afford the product as a 2:1 mixture of oxime isomers (major oxime isomer: R_f = 0.25 in 89% hexanes/11% ethyl acetate; minor oxime isomer: R_f = 0.20 in 89% hexanes/11% ethyl acetate). The two oxime isomers were isolated as yellow oils (192 mg total, 71% yield, ratio of oxime isomers = 2:1). The ratio of regioisomers was 11:1. **Major Oxime Isomer/Major Regioisomer:** ¹H NMR (CDCl₃): δ 7.23 (d, *J* = 2.2 Hz, 1H_a), 7.16 (dd, *J* = 8.2, 2.2 Hz, 1H_b), 6.98 (d, *J* = 8.2 Hz, 1H_c), 3.97 (s, 3H), 2.34 (s, 3H), 2.26 (s, 3H), 2.15 (s, 3H). ¹³C{¹H} NMR (CDCl₃): δ 169.32, 153.53, 145.66, 135.68, 131.33, 130.22, 129.75, 122.79, 61.80, 20.95, 20.65, 15.04. **Minor Oxime Isomer/Major Regioisomer:** ¹H NMR (CDCl₃): δ 7.17 (d, *J* = 8.3, 2.2 Hz, 1H_b), 7.02 (dd, *J* = 8.3 Hz, 1H_c), 6.99 (d, *J* = 2.2 Hz, 1H_a), 3.79 (s, 3H), 2.35 (s, 3H), 2.24 (s, 3H), 2.12 (s, 3H). **Major Oxime Isomer/Minor Regioisomer:** ¹H NMR (CDCl₃): δ 7.23 (m, 2H), 7.17 (d, *J* = 7.6 Hz, 1H), 3.96 (s, 3H), 2.30 (s, 3H), 2.19 (s, 3H), 2.15 (s, 3H). IR (thin film): 2937, 1765 cm⁻¹. HRMS (ESI, *m/z*): [M⁺] calcd for C₁₂H₁₅NO₃, 221.1047; found, 221.1052. GC analysis (RESTEK Rtx[®]-5, FID detector): 100% integration.



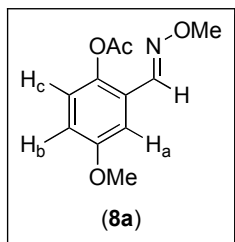
The reaction was run for 12 h with 1.1 equiv of Oxone in AcOH. Under the reaction conditions the OAc of **6a** partially hydrolyzed to the corresponding alcohol. The reaction mixture was concentrated under vacuum and Ac₂O (2.2 mL) and pyridine (0.43 mL) was added and the reaction stirred for 18 h. The reaction was stirred in water (5 mL) for 30 minutes and then extracted with ether. The ethereal layer was washed with water (2 x 50 mL), and NaHCO₃ (1 x 50 mL). The organic layer was dried over MgSO₄, filtered, and concentrated. The resulting oil was purified by chromatography on silica gel to afford the product as a 3:1 mixture of oxime isomers (major oxime isomer: R_f = 0.23 in 85% hexanes/15% ethyl acetate; minor oxime isomer: R_f = 0.18 in 85% hexanes/15% ethyl

acetate). The two oxime isomers were isolated as yellow oils (180 mg total, 69% yield, ratio of oxime isomers = 9:1). The ratio of regioisomers was 18:1. **Major Oxime Isomer:** ^1H NMR (acetone- d_6) (399.97 Hz): δ 7.05 (d, $J = 8.7$ Hz, 1H_c), 6.99 (d, $J = 3.0$ Hz, 1H_a), 6.95 (dd, $J = 8.7, 3.0$ Hz, 1H_b), 3.90 (s, 3H), 3.81 (s, 3H), 2.22 (s, 3H), 2.11 (s, 3H). $^{13}\text{C}\{^1\text{H}\}$ NMR (acetone- d_6) (100.57 Hz): δ 169.87, 158.12, 153.83, 142.69, 132.13, 125.17, 115.58, 115.06, 62.14, 56.03, 20.99, 15.12. **Minor Oxime Isomer:** ^1H NMR (CDCl₃): δ 7.05 (d, $J = 8.9$ Hz, 1H_c), 6.88 (dd, $J = 8.9, 3.0$ Hz, 1H_b), 6.70 (d, $J = 3.0$ Hz, 1H_a), 3.80 (s, 3H), 3.80 (s, 3H), 2.24 (s, 3H), 2.12 (s, 3H). IR (thin film): 2939, 1764 cm⁻¹. Anal. Calcd. for C₁₂H₁₅NO₄ (mixture of oxime isomers): C, 60.75, H, 6.37, N, 5.90; Found: C, 60.97, H, 6.23, N, 6.09



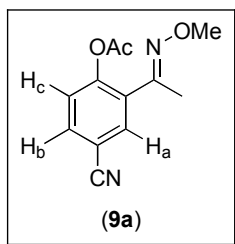
The reaction was run for 12 h with 1.0 equiv of Oxone in AcOH/Ac₂O. Product **7a** was obtained as an inseparable mixture of four products ($R_f = 0.27-0.24$) – 2 regioisomers and 2 oxime isomers of each regioisomer – as a clear oil (170 mg total, 63% yield). The identity of the major regioisomer and its oxime isomers was confirmed by independent synthesis, and the NMR spectra reported below are for this independently synthesized product. Gas chromatographic analysis showed that the reaction afforded a 1.6:1 mixture of regioisomers and that each of the regioisomers was a 6:1 mixture of oxime isomers. **Major Oxime Isomer/Major Regioisomer:** ^1H NMR (C₆D₆): δ 7.02 (dd, 9.0, 3.0 Hz, 1H), 6.71 (dd, 8.9, 5.0 Hz, 1H), 6.60 (m, 1H), 3.76 (s, 3H), 1.95 (s, 3H), 1.74 (s, 3H). $^{13}\text{C}\{^1\text{H}\}$ NMR (CDCl₃): δ 169.09, 159.87 ($^1J_{\text{CF}} = 245$ Hz), 152.29 ($^4J_{\text{CF}} = 1.7$ Hz), 143.74 ($^4J_{\text{CF}} = 2.9$ Hz), 131.66 ($^3J_{\text{CF}} = 8.0$ Hz), 124.56 ($^3J_{\text{CF}} = 8.7$ Hz), 116.16 ($^2J_{\text{CF}} = 23$ Hz), 115.93 ($^2J_{\text{CF}} = 24$ Hz), 61.93, 20.80, 14.67. ^{19}F NMR (CDCl₃): δ -116.3 - -116.36 (m). **Minor Oxime Isomer/Major Regioisomer:** ^1H NMR (C₆D₆): δ 6.77 (dd, $J = 8.9, 5.0$ Hz, 1H), 6.62 (dd, $J = 9.0, 3.0$ Hz, 1H), 6.61-6.56 (overlapping peaks), 3.64 (s, 3H), 1.90 (s, 3H), 1.50 (s, 3H). IR (thin film): 2939, 1770 cm⁻¹. HRMS (ESI, m/z): [M⁺] calcd for

C₁₁H₁₂FNO₃, 225.0801; found, 225.0797. GC analysis (RESTEK Rtx[®]-5, FID detector): 99% integration.

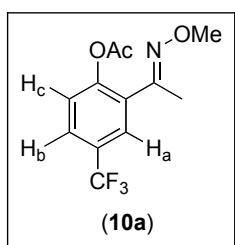


The reaction was run for 12 h with 2.0 equiv of K₂S₂O₈ in AcOH. The product was obtained as a yellow oil (143 mg, 53% yield). The ratio of oxime isomers 17:1 and regioisomers was >20:1 (R_f = 0.28 in 90% hexanes/10% ethyl acetate). ¹H NMR (CDCl₃): δ 8.07 (s, 1H), 7.28 (d, *J* = 3.0 Hz, 1H_a), 7.01 (d, *J* = 8.9 Hz, 1H_c), 6.93 (dd, *J* = 8.9, 3.0 Hz, 1H_b), 3.99 (s, 3H), 3.82 (s, 3H), 2.31 (s, 3H). ¹³C{¹H} NMR (CDCl₃): δ 169.69, 157.46, 143.95, 142.54, 125.21, 123.95, 117.37, 110.97, 62.30, 55.79, 20.98. IR (thin film): 2938, 1763 cm⁻¹. HRMS (ESI, *m/z*): [M +] calcd for C₁₁H₁₃NO₄, 223.0845; found, 223.0842. GC analysis (RESTEK Rtx[®]-5, FID detector): 100% integration.

General Method for Directed C-H Bond Acetoxylation with K₂S₂O₈: K₂S₂O₈ (373 mg, 1.38 mmol, 2.0 equiv) and Pd(OAc)₂ (7.7 mg, 0.03 mmol, 0.05 equiv) were combined in AcOH (2.88 mL) and Ac₂O (2.88 mL) in a 20 mL vial. Substrate **10** (150 mg, 0.69 mmol, 1.0 equiv) was then added to the mixture. The vial was sealed with a Teflon lined cap, and the reaction was heated at 100°C for 12 h. The reaction mixture was diluted with ethyl acetate, and the vial was washed with copious diethyl ether. A 10% aqueous solution of Na₂SO₃ (50 mL) was added to the filtrate, and the resulting mixture was stirred at 25 °C for 15 min. The organic and the aqueous layers were separated and the organic layer was extracted with water (2 x 50 mL), NaHCO₃ (1 x 50 mL), and brine (1 x 50 mL). The organic layer was dried over MgSO₄, filtered, and concentrated. The resulting oil was purified by chromatography on silica gel. Each substrate was optimized for reaction time, solvent (AcOH versus AcOH/Ac₂O) and equiv of the oxidant, as indicated below.

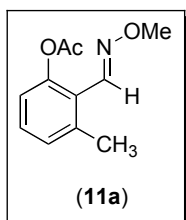


The reaction was run for 12 h with 1.0 equiv of $K_2S_2O_8$ in AcOH/Ac₂O. The product was obtained as a mixture of two oxime E/Z isomers (major oxime isomer: $R_f = 0.27$ in 78% hexanes/22% ethyl acetate; minor oxime isomer: $R_f = 0.25$ in 78% hexanes/22% ethyl acetate). The two oxime isomers were isolated as a pale yellow solid (115 mg total, 57% yield, ratio of oxime isomers = 6:1). The ratio of regioisomers was 6:1. **Major Oxime Isomer/Major Regioisomer:** ¹H NMR (CDCl₃): δ 7.78 (d, $J = 2.1$ Hz, 1H_a), 7.68 (dd, $J = 8.4, 2.1$ Hz, 1H_b), 7.27 (d, $J = 8.4$ Hz, 1H_c), 4.01 (s, 3H), 2.33 (s, 3H), 2.17 (s, 3H). ¹³C{¹H} NMR (CDCl₃): δ 168.26, 151.68, 151.31, 133.65, 133.18, 131.78, 124.51, 117.80, 110.19, 62.24, 20.98, 14.87. **Minor Oxime Isomer/Major Regioisomer:** ¹H NMR (CDCl₃): δ 7.66 (dd, $J = 8.4, 2.0$ Hz, 1H_b), 7.52 (d, $J = 2.0$ Hz, 1H_a), 7.29 (d, $J = 8.5$ Hz, 1H_c), 3.79 (s, 3H), 2.89 (s, 3H), 2.14 (s, 3H). **Major Oxime Isomer/Minor Regioisomer:** ¹H NMR (CDCl₃): δ 7.67 (t, $J = 8.8, 7.8$ Hz, 2H), 7.37 (t, $J = 7.8$ Hz, 1H), 3.98 (s, 3H), 2.38 (s, 3H), 2.16 (s, 3H). IR (thin film): 2230, 1770 cm⁻¹. HRMS (ESI, m/z): [M⁺] calcd for C₁₂H₁₂N₂O₃, 232.0848; found, 232.0848. GC analysis (RESTEK Rtx[®]-5, FID detector): 100% integration.

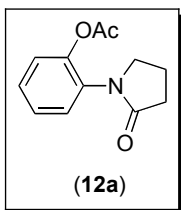


The reaction was run for 12 h with 2.0 equiv of $K_2S_2O_8$ in AcOH/Ac₂O. The product was obtained as a mixture of two oxime (E/Z) isomers (major oxime isomer: $R_f = 0.27$ in 87% hexanes/13% ethyl acetate; minor oxime isomer: $R_f = 0.25$ in 87% hexanes/13% ethyl acetate). The two oxime isomers were isolated as yellow oils (142 mg total, 75% yield, ratio of oxime isomers = 5:1). The ratio of regioisomers was >20:1. **Major Oxime Isomer:** ¹H NMR (CDCl₃): δ 7.71 (d, $J = 2.3$ Hz, 1H_a), 7.63 (dd, $J = 8.5, 2.3$ Hz, 1H_b),

7.24 (d, $J = 8.5$ Hz, 1H_c), 3.99 (s, 3H), 2.31 (s, 3H), 2.17 (s, 3H). $^{13}\text{C}\{^1\text{H}\}$ NMR (CDCl₃): δ 168.62, 152.30, 150.49, 131.07, 128.38 ($^2J_{\text{CF}} = 33$ Hz), 126.85 ($^3J_{\text{CF}} = 3.8$ Hz), 126.62 ($^3J_{\text{CF}} = 3.6$ Hz), 123.60 ($^1J_{\text{CF}} = 272$ Hz), 123.91, 62.14, 20.96, 14.93. ^{19}F NMR (CDCl₃): δ -62.37 (s). **Minor Oxime Isomer:** ^1H NMR (CDCl₃): δ 7.60 (m, 1H_b), 7.43 (d, $J = 2.7$ Hz, 1H_a), 7.20 (d, $J = 8.5$ Hz, 1H_c), 3.76 (s, 3H), 2.25 (s, 3H), 2.12 (s, 3H). IR (thin film): 2942, 1770 cm⁻¹. HRMS (ESI, m/z): [M⁺] calcd for C₁₂H₁₂F₃NO₃, 275.0769; found, 275.0775. GC analysis (RESTEK Rtx[®]-5, FID detector): 100% integration.

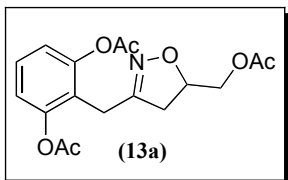


The reaction was run for 12 h with 2.0 equiv of K₂S₂O₈ in AcOH. The product was obtained as a mixture of two oxime (E/Z) isomers (major oxime isomer: R_f = 0.24 in 92% hexanes/8% ethyl acetate; minor oxime isomer: R_f = 0.24 in 92% hexanes/8% ethyl acetate). The product was isolated as a yellow oil (106 mg total, 53% yield, ratio of oxime isomers = 5:1). **Major Oxime Isomer:** ^1H NMR (CDCl₃): δ 8.25 (s, 1H), 7.27 (t, $J = 8.0, 7.5$ Hz, 1H), 7.12 (d, $J = 7.5$ Hz, 1H), 6.95 (d, $J = 8.0$ Hz, 1H), 3.99 (s, 3H), 2.47 (s, 3H), 2.33 (s, 3H). $^{13}\text{C}\{^1\text{H}\}$ NMR (CDCl₃): δ 169.69, 149.12, 144.60, 139.47, 129.93, 128.84, 123.32, 120.97, 62.19, 21.26, 21.13. **Minor Oxime Isomer:** ^1H NMR (CDCl₃): δ 7.39 (s, 1H), 7.29 (t, $J = 7.9$ Hz, 1H), 7.10 (d, $J = 7.7$ Hz, 1H), 6.96 (d, $J = 8.1$ Hz, 1H), 3.90 (s, 3H), 2.29 (s, 3H), 2.27 (s, 3H). IR (thin film): 2969, 1769 cm⁻¹. HRMS (ESI, m/z): [M⁺] calcd for C₁₁H₁₃NO₃, 207.0895; found, 207.0892. GC analysis (RESTEK Rtx[®]-5, FID detector): 99% integration.

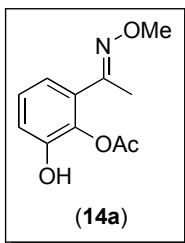


The reaction was run for 12 h with 1.5 equiv of K₂S₂O₈ in AcOH. The product was obtained as a yellow oil (272 mg, 75% yield). (R_f = 0.26 in 15% hexanes/85% ethyl acetate). ^1H NMR (CDCl₃): δ 7.29-7.21 (multiple peaks, 3H), 7.15 (d, $J = 7.6$ Hz, 1H),

3.70 (t, $J = 6.9$ Hz, 2H), 2.49 (t, $J = 8.0$ Hz, 2H), 2.24 (s, 3H), 2.13 (quin, $J = 7.2$ Hz, 2H). $^{13}\text{C}\{^1\text{H}\}$ NMR (CDCl_3): δ 173.88, 168.53, 145.64, 130.80, 127.86, 126.89, 126.25, 123.41, 49.82, 30.94, 20.71, 19.02. IR (thin film): 1766, 1702 cm^{-1} . HRMS (ESI, m/z): $[\text{M}^+]$ calcd for $\text{C}_{12}\text{H}_{13}\text{NO}_3$, 219.0895; found, 219.0894. GC analysis (RESTEK Rtx[®]-5, FID detector): 100% integration.

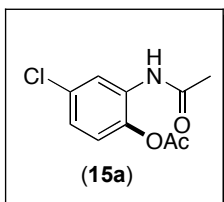


The reaction was run for 12 h with 3.0 equiv of $\text{K}_2\text{S}_2\text{O}_8$ in AcOH. The product was obtained as a pale yellow viscous oil (79.0 mg, 53% yield) ($R_f = 0.26$ in 55% hexanes/45% ethyl acetate). ^1H NMR (CDCl_3): δ 7.33 (t, $J = 8.1$ Hz, 1H), 6.99 (d, $J = 8.2$ Hz, 2H), 4.70-4.66 (m, 1H), 4.06-4.05 (multiple peaks, 2H), 3.59 (d, $J = 3.3$ Hz, 2H), 2.78 (dd, $J = 17.4, 10.8$ Hz, 1H), 2.44 (dd, $J = 17.4, 7.8$ Hz, 1H), 2.32 (s, 6H), 2.04 (s, 3H). $^{13}\text{C}\{^1\text{H}\}$ NMR (CDCl_3): δ 170.72, 169.22, 155.92, 150.10, 128.48, 120.89, 120.64, 77.76, 64.92, 38.22, 23.23, 20.78, 20.69. IR (thin film): 2939, 1769, 1742 cm^{-1} . HRMS (ESI, m/z): $[\text{M}^+]$ calcd for $\text{C}_{17}\text{H}_{19}\text{NO}_7$, 349.1162; found, 349.1160. GC analysis (RESTEK Rtx[®]-5, FID detector): 99% integration.

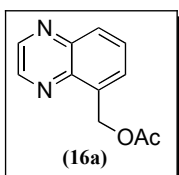


The reaction was run for 12 h with 2.0 equiv of Oxone[®] in AcOH. The product was obtained as a mixture of two products ($R_f = 0.25$ in 90% hexanes/10% ethyl acetate). Under the chromatography conditions the OAc underwent partial hydrolysis to the corresponding alcohol. The product was isolated as a pale yellow solid (100 mg total, 37% yield, ratio of OAc to free OH, 2:1); mp = 67–72 $^{\circ}\text{C}$. The ratio of oxime isomers and regioisomers was $>20:1$. ^1H NMR of **14a** (CDCl_3): δ 11.65 (s, 1H), 7.31 (dd, $J = 8.1, 1.5$ Hz, 1H), 7.06 (dd, $J = 7.9, 1.5$ Hz, 1H), 6.88 (t, $J = 8.0$ Hz, 1H), 3.99 (s, 3H), 2.35 (s, 3H), 2.30 (s, 3H). $^{13}\text{C}\{^1\text{H}\}$ NMR (CDCl_3): δ 169.08, 158.17, 149.79, 139.25, 125.09,

123.98, 119.81, 118.49, 62.54, 20.65, 11.61. IR (KBr): 2943, 1760 cm^{-1} . HRMS (ESI, m/z): $[M^+]$ calcd for $\text{C}_{11}\text{H}_{13}\text{NO}_4$, 223.0844; found, 223.0843. GC analysis (RESTEK Rtx[®]-5, FID detector): 100% integration. Hydrolyzed (OH) product: ^1H NMR (CDCl_3): δ 6.96 (t, $J = 7.5$ Hz, 2H), 6.81 (t, $J = 7.9$ Hz, 1H), 5.71 (s, 1H), 4.02 (s, 3H), 2.30 (s, 3H).

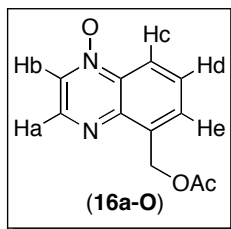


The reaction was run for 12 h with 1.5 equiv of $\text{K}_2\text{S}_2\text{O}_8$ in AcOH. The product was obtained as a pale yellow viscous oil (38% yield) ($R_f = 0.26$ in 55% hexanes/45% ethyl acetate). ^1H NMR (C_6D_6): δ 8.29 (br s, 1H), 7.21 (br s, 1H), 7.07 (br s, 2H), 2.36 (s, 3H), 2.18 (s, 3H).

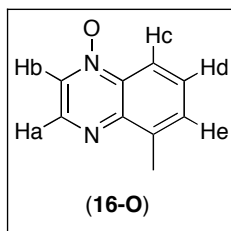


Oxone (853 mg, 1.39 mmol, 1.0 equiv) and $\text{Pd}(\text{OAc})_2$ (16 mg, 0.07 mmol, 0.05 equiv) were combined in AcOH (11.6 mL) in a 20 mL vial. Substrate **16** (200 mg, 1.39 mmol, 1.0 equiv) was then added to the mixture. The vial was sealed with a Teflon lined cap, and the reaction was heated at 100 $^\circ\text{C}$ for 12 h. The reaction mixture was diluted with chloroform and extracted with water (2 x 50 mL), NaHCO_3 (1 x 50 mL), and brine (1 x 50 mL). The organic layer was dried over MgSO_4 , filtered, and concentrated. The resulting oil was purified by chromatography on silica gel ($R_f = 0.18$ in 80% hexanes/20% ethyl acetate). The product was obtained as a yellow solid (28 mg, 10% yield). mp = 86-88 $^\circ\text{C}$. ^1H NMR (399.96 Hz) (CDCl_3): δ 8.87 (s, 2H), 8.09 (d, $J = 8.3$ Hz, 1H), 7.84-7.75 (multiple peaks, 2H), 5.80 (s, 2H), 2.10 (s, 3H). $^{13}\text{C}\{^1\text{H}\}$ NMR (100.57 Hz) (CDCl_3): δ 170.85, 145.03, 144.32, 142.83, 141.12, 134.71, 129.71, 129.70, 129.40, 61.85, 21.03. IR (KBr): 2927, 1739 cm^{-1} . HRMS (ESI, m/z): $[M + \text{Na}]$ calcd for $\text{C}_{11}\text{H}_{10}\text{N}_2\text{O}_2$, 202.0742; found, 202.0738. GC analysis (RESTEK Rtx[®]-5, FID detector): 99% integration. Along with the product **16a**, the *N*-oxide of the starting material (101 mg, 46% yield), ($R_f = 0.15$ in 70% hexanes/30% ethyl acetate) and the *N*-oxide of **16a**

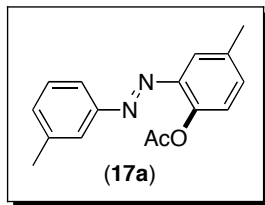
(27.0 mg, 9% yield), ($R_f = 0.1$ in 70% hexanes/30% ethyl acetate) were obtained, whose spectroscopic data are described below.



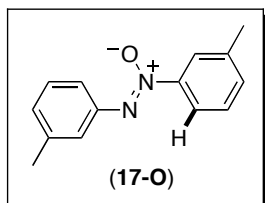
^1H NMR (CDCl_3): δ 8.70 (d, $J = 3.5$ Hz, 1H_a), 8.57 (d, $J = 8.7$ Hz, 1H_c), 8.38 (d, $J = 3.5$ Hz, 1H_b), 7.88 (d, $J = 7.2$ Hz, 1H_e), 7.75 (t, $J = 7.3$ Hz, 1H_d), 5.78 (s, 2H), 2.17 (s, 3H). ^{13}C NMR (CDCl_3): δ 170.71, 145.31, 144.05, 137.59, 135.73, 130.83, 129.80, 129.35, 118.94, 61.78, 20.98. IR (KBr): 1735, 1242 cm^{-1} . mp = 112-113 $^\circ\text{C}$. HRMS (ESI, m/z): $[\text{M} + \text{Na}]$ calcd for $\text{C}_{11}\text{H}_{10}\text{N}_2\text{O}_3$, 218.0691; found, 218.0689. GC analysis (RESTEK Rtx[®]-5, FID detector): 99% integration. The assignment of the regioselectivity of *N*-oxidation was made based on comparison of the NMR of **16a-O** to **16a** as detailed in reference 4.



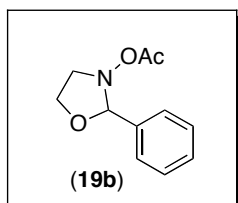
^1H NMR (CDCl_3): δ 8.62 (d, $J = 3.45$ Hz, 1H_a), 8.37 (d, $J = 8.2$ Hz, 1H_c), 8.31 (d, $J = 3.46$ Hz, 1H_b), 7.61-7.55 (multiple peaks, 2H_{d, e}), 2.73 (s, 3H). $^{13}\text{C}\{^1\text{H}\}$ NMR (CDCl_3): δ 145.04, 144.38, 138.65, 137.59, 131.72, 129.77, 128.87, 116.56, 17.66. mp = 132-133 $^\circ\text{C}$. IR (KBr): 1501, 1309 cm^{-1} . HRMS (ESI, m/z): $[\text{M} + \text{Na}]$ calcd for $\text{C}_9\text{H}_8\text{N}_2\text{O}$, 160.0637; found, 160.0634. GC analysis (RESTEK Rtx[®]-5, FID detector): 99% integration.



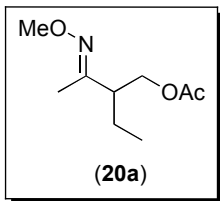
The reaction was run at rt for 12 h with 1.5 equiv of $K_2S_2O_8$ in AcOH. The product was obtained as a pale yellow oil ($R_f = 0.26$ in 55% hexanes/45% ethyl acetate) (39% yield). 1H NMR (C_6D_6): δ 7.66-7.56 (multiple peaks, 3H), 7.38 (t, $J = 7.6$ Hz, 1H), 7.31-7.28 (multiple peaks, 2H), 7.12 (d, $J = 8.4$ Hz, 1H), 2.45 (s, 3H), 2.41 (s, 3H), 2.39 (s, 3H). HRMS (ESI, m/z): $[M^+]$ calcd for $C_{10}H_{12}ClNO_2$, 268.1209; found, 268.1209. Along with the product **17a**, the *N*-oxide of the starting material (36% yield), ($R_f = 0.15$ in 70% hexanes/30% ethyl acetate) was obtained, whose spectroscopic data is described below.



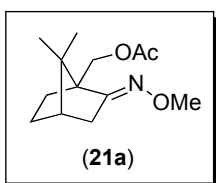
1H NMR (C_6D_6): δ 7.75-7.66 (multiple peaks, 4H), 7.41 (t, $J = 8.0$ Hz, 1H), 7.29 (d, $J = 7.6$ Hz, 1H), 7.16 (dd, $J = 8.0, 1.6$ Hz, 1H), 6.93 (d, $J = 8.4$ Hz, 1H), 2.46 (s, 3H), 2.39 (s, 3H).



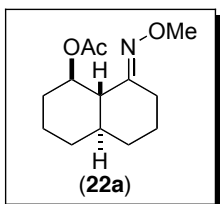
The reaction was run at rt for 12 h with 1.5 equiv of $K_2S_2O_8$ or Oxone or $PhI(OAc)_2$ in AcOH. The product was obtained as a yellow oil (78% yield, $R_f = 0.15$ in 70% hexanes/30% ethyl acetate). 1H NMR (C_6D_6): δ 7.78 (d, $J = 7.0$ Hz, 2H), 7.51 (t, $J = 7.5$ Hz, 1H), 7.45 (m, 2H), 6.59 (br s, 1H), 4.29 (t, $J = 5.0$ Hz, 2H), 3.73 (q, $J = 5.0$ Hz, 2H), 2.09 (s, 3H). $^{13}C\{^1H\}$ NMR ($CDCl_3$): δ 171.47, 167.55, 134.18, 131.61, 128.60, 126.91, 63.34, 39.55, 20.92. IR (KBr): 1734 cm^{-1} .



The reaction was run for 12 h with 2.0 equiv of $K_2S_2O_8$ in AcOH. The product was obtained as two oxime (E/Z) isomers (major oxime isomer: $R_f = 0.3$ in 90% hexanes/10% ethyl acetate; minor oxime isomer: $R_f = 0.21$ in 90% hexanes/10% ethyl acetate). The two oxime isomers were isolated as yellow oils (45% yield, ratio of oxime isomers = 5:1). The NMR data was identical to that reported previously for this compound.⁷



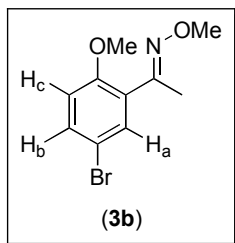
The reaction was run for 12 h with 2.0 equiv of $K_2S_2O_8$ in AcOH. The product was isolated as a clear oil ($R_f = 0.28$ in 90% hexanes/10% ethyl acetate), (63% yield). The NMR data was identical to that reported previously for this compound.⁷



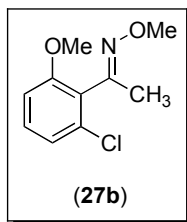
The reaction was run for 12 h with 2.0 equiv of $K_2S_2O_8$ in AcOH. The product was isolated as a clear oil ($R_f = 0.28$ in 90% hexanes/10% ethyl acetate), (23% yield). The NMR data was identical to that reported previously for this compound.⁷

General Method for Directed C-H Bond Methoxylation with Oxone: Oxone® (808 mg, 1.31 mmol, 2.0 equiv) and $Pd(OAc)_2$ (15 mg, 0.07 mmol, 0.1 equiv) were combined in MeOH (5.48 mL) in a 20 mL vial. Substrate **3** (150 mg, 0.66 mmol, 1.0 equiv) was then added to the mixture. The vial was sealed with a Teflon lined cap, and the reaction was stirred at rt for 12 h and then stirred at 80 °C for another 12 h. The reaction mixture was diluted with ethyl acetate, and extracted with water (2 x 50 mL), $NaHCO_3$ (1 x 50 mL), and brine (1 x 50 mL). The organic layer was dried over $MgSO_4$,

filtered, and concentrated. The resulting oil was purified by chromatography on silica gel. Each substrate was optimized for reaction time and equiv of the oxidant, as indicated below.

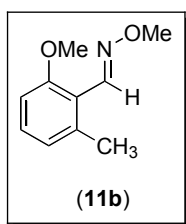


The reaction was run was stirred at rt for 12 h and then stirred at 80 °C for another 12 h, with 2.0 equiv of Oxone®. Product **3b** was obtained as two oxime (E/Z) isomers (major oxime isomer: 0.28 R_f = 90% in hexanes/10% ethyl acetate; minor oxime isomer: R_f = 0.26 in 90% hexanes/10% ethyl acetate). The two isomers were isolated as yellow oils. Under the reaction conditions oxime **3b** underwent partial hydrolysis to the corresponding ketone. Isolated product (119 mg total, 70% yield, ratio of oxime isomers = 5:1, ratio of oxime to ketone = 4:1). The ratio of regioisomers was >20:1. **Major Oxime Isomer of 3b:** ¹H NMR (acetone-*d*₆): δ 7.51 (dd, *J* = 8.8, 2.6 Hz, 1H_b), 7.38 (d, *J* = 2.6 Hz, 1H_a), 7.03 (d, *J* = 8.8 Hz, 1H_c), 3.90 (s, 3H), 3.87 (s, 3H), 2.10 (s, 3H). ¹³C{¹H} NMR (CDCl₃): δ 156.64, 155.28, 132.64, 132.16, 128.78, 112.84, 112.69, 61.86, 55.72, 15.77. IR (thin film): 2932, 1606, 1486 cm⁻¹. HRMS (ESI, *m/z*): [M⁺] calcd for C₁₀H₁₂BrNO₂, 257.0051; found, 257.0045. GC analysis (RESTEK Rtx®-5, FID detector): 100% integration. **Ketone:** ¹H NMR (CDCl₃): δ 7.49 (d, *J* = 2.4 Hz, 1H), 7.32 (dd, *J* = 8.7, 2.8 Hz, 1H), 6.86 (d, *J* = 8.7 Hz, 1H), 4.01 (s, 3H), 2.28 (s, 3H).

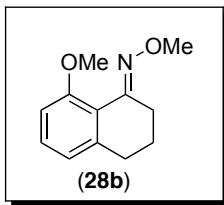


The reaction was run at rt for 12 h and then stirred at 80 °C for another 12 h with 2.0 equiv of Oxone®. The two oxime isomers were isolated as clear oils. (E/Z) isomers (major oxime isomer: R_f = 0.26 in 97% hexanes/3% ethyl acetate; minor oxime isomer: R_f = 0.26 in 97% hexanes/3% ethyl acetate). Under the reaction conditions, oxime **27b**

underwent partial hydrolysis to the corresponding ketone (102 mg total, 60% yield, ratio of oxime isomers = 3:1, Ratio of oxime : ketone = 7:1). **Major Oxime Isomer:** ^1H NMR (CDCl_3): δ 7.22 (t, $J = 8.2$ Hz, 1H), 7.02 (dd, $J = 8.1, 0.9$ Hz, 1H), 6.82 (dd, $J = 8.4, 0.9$ Hz, 1H), 4.00 (s, 3H), 3.82 (s, 3H), 2.12 (s, 3H). $^{13}\text{C}\{^1\text{H}\}$ NMR (CDCl_3): δ 158.39, 152.81, 133.83, 129.89, 125.97, 121.64, 109.28, 61.80, 55.98, 15.75. **Minor Oxime Isomer:** ^1H NMR (CDCl_3): δ 7.22 (t, $J = 8.2$ Hz, 1H), 7.01 (dd, $J = 8.1, 0.9$ Hz, 1H), 6.82 (dd, $J = 8.1$ Hz, 0.9 Hz, 1H), 4.02 (s, 3H), 3.82 (s, 3H), 2.32 (s, 3H). IR of **27b** (KBr): 2936, 1590, 1573 cm^{-1} . HRMS (ESI, m/z): $[\text{M}^+]$ calcd for $\text{C}_{10}\text{H}_{12}\text{ClNO}_2$, 213.0557; found, 213.0554. GC analysis (RESTEK Rtx[®]-5, FID detector): 99% integration. **Ketone:** ^1H NMR (CDCl_3): δ 7.13 (t, $J = 8.1$ Hz, 1H), 6.95 (dd, $J = 8.0, 1.1$ Hz, 1H), 6.89 (dd, $J = 8.3, 1.1$ Hz, 1H), 3.82 (s, 3H), 2.13 (s, 3H).

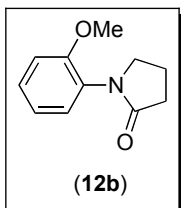


The reaction was run at rt for 12 h and then the temperature was slowly ramped to 80 °C over 20 minutes for another 12 h with 2.0 equiv of Oxone in MeOH. The product was obtained as two oxime (E/Z) isomers (major oxime isomer: $R_f = 0.25$ in 95% hexanes/5% ethyl acetate; minor oxime isomer: $R_f = 0.24$ in 95% hexanes/5% ethyl acetate). The two oxime isomers were isolated as yellow oils (106 mg total, 59% yield, ratio of oxime isomers = 3:1). **Major Oxime Isomer:** ^1H NMR (CDCl_3): δ 8.51 (s, 1H), 7.21 (t, $J = 8$ Hz, 1H), 6.83 (d, $J = 8$ Hz, 1H), 6.74 (d, $J = 8.5$ Hz, 1H), 3.99 (s, 3H), 3.83 (s, 3H), 2.52 (s, 3H). $^{13}\text{C}\{^1\text{H}\}$ NMR (CDCl_3): δ 158.48, 146.23, 139.09, 129.73, 123.55, 119.42, 108.13, 61.89, 55.65, 22.123. **Minor Oxime Isomer:** ^1H NMR (CDCl_3): δ 7.52 (s, 1H), 7.23 (t, $J = 7.8$ Hz, 1H), 6.84 (d, $J = 7.8$, 1H), 6.74 (d, $J = 8.3$ Hz, 1H), 3.93 (s, 3H), 3.80 (s, 3H), 2.25 (s, 3H). IR (thin film): 2935, 1595 cm^{-1} . HRMS (ESI, m/z): $[\text{M}^+]$ calcd for $\text{C}_{10}\text{H}_{13}\text{NO}_2$, 179.0946; found, 179.0940. GC analysis (RESTEK Rtx[®]-5, FID detector): 99% integration.



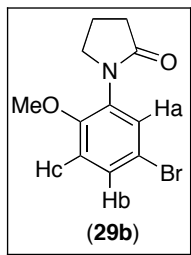
The reaction was run at rt for 12 h and then stirred at 80 °C for another 12 h with 2.0 equiv of Oxone in MeOH. The product was obtained as a pale yellow oil ($R_f = 0.26$ in 97% hexanes/3% ethyl acetate). ^1H NMR (C_6D_6): δ 6.80-6.73 (multiple peaks, 3H), 3.89 (s, 3H), 3.67 (s, 3H), 2.69 (t, $J = 7.5$ Hz, 2H), 2.36 (t, $J = 7.5$ Hz, 2H), 1.97 (quin, $J = 7.5$ Hz, 2H). $^{13}\text{C}\{^1\text{H}\}$ NMR (CDCl_3): δ 174.42, 146.55, 143.78, 127.36, 122.60, 119.47, 108.74, 56.16, 51.68, 33.71, 29.16, 25.08.

General Method for Directed C-H Bond Methoxylation with $\text{K}_2\text{S}_2\text{O}_8$: $\text{K}_2\text{S}_2\text{O}_8$ (309 mg, 1.14 mmol, 2.0 equiv) and $\text{Pd}(\text{OAc})_2$ (12.8 mg, 0.11 mmol, 0.1 equiv) were combined in MeOH (4.76 mL) in a 20 mL vial. Substrate **30** (100 mg, 0.57 mmol, 1.0 equiv) was then added to the mixture. The vial was sealed with a Teflon lined cap, and the reaction was stirred at rt for 12 h and then stirred at 40 °C for another 12 h. The reaction mixture was diluted with ethyl acetate, and extracted with water (2 x 50 mL), NaHCO_3 (1 x 50 mL), and brine (1 x 50 mL). The organic layer was dried over MgSO_4 , filtered, and concentrated. Each substrate was optimized for reaction time and equiv of the oxidant, as indicated below.

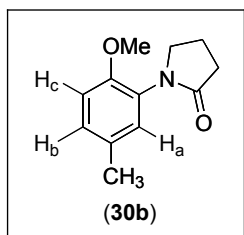


The reaction was run at rt for 12 h and then at 40 °C for 12 h with 2.0 equiv of $\text{K}_2\text{S}_2\text{O}_8$ in MeOH. The product was obtained as a yellow oil (85 mg, 72% yield). ($R_f = 0.26$ in 25% hexanes/75% ethyl acetate). ^1H NMR (CDCl_3): δ 7.29-7.25 (multiple peaks, 2H), 7.01-6.96 (multiple peaks, 2H), 3.84 (s, 3H), 3.76 (t, $J = 7.0$ Hz, 2H), 2.56 (t, $J = 7.9$ Hz, 2H), 2.19 (quin, $J = 7.2$ Hz, 2H). $^{13}\text{C}\{^1\text{H}\}$ NMR (CDCl_3): δ 175.12, 154.80, 128.60, 128.59, 127.20, 120.85, 111.99, 55.57, 49.90, 31.18, 18.92. IR (thin film): 2945, 1696 cm^{-1} .

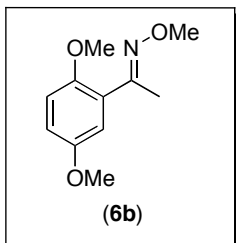
HRMS (ESI, m/z): [M^+] calcd for $C_{11}H_{13}NO_2$, 191.0946; found, 191.0943. GC analysis (RESTEK Rtx[®]-5, FID detector): 100% integration.



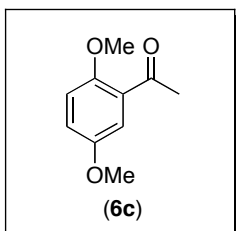
The reaction was run at rt for 12 h and then stirred at 40 °C for another 12 h with 3.0 equiv of $K_2S_2O_8$ in MeOH. The product was obtained as a brown solid as a single regioisomer ($R_f = 0.25$ in 25% hexanes/75% ethyl acetate) (67 mg, 61% yield); mp = 95–110 °C. 1H NMR ($CDCl_3$): δ 7.40 (d, $J = 2.5$ Hz, 1H_a), 7.37 (dd, $J = 9.0, 2.5$ Hz, 1H_b), 6.84 (d, $J = 8.5$ Hz, 1H_c), 3.83 (s, 3H), 3.74 (t, $J = 7.0$ Hz, 2H), 2.55 (t, $J = 7.9$ Hz, 2H), 2.19 (q, $J = 7.7$ Hz, 2H). $^{13}C\{^1H\}$ NMR ($CDCl_3$): δ 175.07, 154.08, 131.460, 131.27, 128.55, 113.47, 112.35, 55.86, 49.79, 31.04, 18.96. IR (KBr): 2924, 1674 cm^{-1} . HRMS (ESI, m/z): [M^+] calcd for $C_{11}H_{12}BrNO_2$, 269.0051; found, 269.0046. GC analysis (RESTEK Rtx[®]-5, FID detector): 100% integration.



The reaction was run at rt for 12 h and then stirred at 40 °C for another 12 h with 2.0 equiv of $K_2S_2O_8$ in MeOH. The product was obtained as single regioisomer as a viscous pale yellow oil (67.0 mg, 57% yield, $R_f = 0.22$ in 25% hexanes/75% ethyl acetate). 1H NMR (C_6D_6): δ 7.18 (s, 1H_a), 6.85 (d, $J = 8.3$ Hz, 1H_b), 6.50 (d, $J = 8.3$ Hz, 1H_c), 3.39–3.35 (multiple peaks, 2H), 3.28 (s, 3H), 2.17 (t, $J = 7.7$ Hz, 2H), 2.10 (s, 3H), 1.47 (quin, $J = 7.8$ Hz, 2H). $^{13}C\{^1H\}$ NMR ($CDCl_3$): δ 175.19, 152.69, 130.34, 129.14, 129.06, 126.86, 112.02, 55.75, 50.00, 31.25, 20.39, 18.96. IR (KBr): 2932, 1694 cm^{-1} . HRMS (ESI, m/z): [M^+] calcd for $C_{12}H_{15}NO_2$, 205.1103; found, 205.1094. GC analysis (RESTEK Rtx[®]-5, FID detector): 99% integration.



The reaction was run at rt for 12 h and then stirred at 80 °C for another 12 h with 2.0 equiv of Oxone in MeOH. The product was obtained as a pale yellow oil, mixture of two oxime (E/Z) isomers (major oxime isomer: $R_f = 0.26$ in 97% hexanes/3% ethyl acetate; minor oxime isomer: $R_f = 0.26$ in 97% hexanes/3% ethyl acetate). Under the reaction conditions, oxime **6b** underwent partial hydrolysis to the corresponding ketone (**6c** mg total, 48% yield, ratio of oxime isomers = 3:1, Ratio of oxime : ketone = 1:1.7). **Major Oxime Isomer:** $^1\text{H NMR}$ (C_6D_6): δ 7.55 (d, $J = 8.5$ Hz, 1H), 7.50 (m, 1H), 7.13 (dd, $J = 8.5, 3.0$ Hz, 1H), 3.88 (s, 3H), 3.80 (s, 3H), 3.79 (s, 3H), 2.62 (s, 3H). Ketone NMR data is shown below.



$^1\text{H NMR}$ (C_6D_6): δ 6.94-6.90 (multiple peaks, 2H), 6.87 (dd, $J = 9, 2.5$ Hz, 1H), 4.00 (s, 3H), 3.78 (s, 3H), 2.29 (s, 3H).

3.9 References

- (1) Yang, D. *Acc. Chem. Res.* **2004**, *37*, 497-505.
- (2) Murphy, A.; Pace, A.; Stack, T. D. P. *Org. Lett.* **2004**, *6*, 3119-3122.
- (3) Karimi, B.; Ghoreishi-Nezhad, M.; Clark, J. H. *Org. Lett.* **2005**, *7*, 625-628.
- (4) Travis, B. R.; Sivakumar, M.; Hollist, G. O.; Borhan, B. *Org. Lett.* **2003**, *5*, 1031-1034.
- (5) Plietker, B. *Org. Lett.* **2004**, *6*, 289-291.
- (6) Dick, A. R.; Hull, K. L.; Sanford, M. S. *J. Am. Chem. Soc.* **2004**, *126*, 2300-2301.
- (7) Desai, L. V.; Hull, K. L.; Sanford, M. S. *J. Am. Chem. Soc.* **2004**, *126*, 9542-9543.
- (8) Kalyani, D.; Sanford, M. S. *Org. Lett.* **2005**, *7*, 4149-4152.
- (9) Canty, A. J.; Denney, M. C.; van Koten, G.; Skelton, B. W.; White, A. H. *Organometallics* **2004**, *23*, 5432-5439.
- (10) Dick, A. R.; Kampf, J. W.; Sanford, M. S. *Organometallics* **2005**, *24*, 482-485.
- (11) Huang, T. M.; Chen, J. T.; Lee, G. H.; Wang, Y. *Organometallics* **1991**, *10*, 175-179.
- (12) Wolowska, J.; Eastham, G. R.; Heaton, B. T.; Iggo, J. A.; Jacob, C.; Whyman, R. *Chem. Commun.* **2002**, 2784-2785.
- (13) Lee, Y.; Yoo, K. H.; Jung, O. *Bull. Chem. Soc. Jpn.* **2003**, *76*, 107-110.
- (14) Muehlhofer, M.; Strassner, T.; Herrmann, W. A. *Angew. Chem., Int. Ed.* **2002**, *41*, 1745-+.
- (15) Steinhoff, B. A.; Fix, S. R.; Stahl, S. S. *J. Am. Chem. Soc.* **2002**, *124*, 766-767.
- (16) Desai, L. V.; Malik, H. A.; Sanford, M. S. *Org. Lett.* **2006**, *8*, 1141-1144.
- (17) Uno, H.; Murakami, S.; Fujimoto, A.; Yamaoka, Y. *Tetrahedron Lett.* **2005**, *46*, 3997-4000.
- (18) Beckwith, A.; Dyllal, L. *Aust. J. Chem.* **1990**, *43*, 451-461.
- (19) Radhakrishna, A. S.; Parham, M. E.; Riggs, R. M.; Loudon, G. M. *J. Org. Chem.* **1979**, *44*, 1746-1747.

- (20) Barbieri, G.; Benassi, R.; Lazzeretti, P.; Schenetti, L.; Taddei, F. *Org. Magn. Reson.* **1975**, *7*, 451-454.
- (21) Hull, K. L.; Lanni, E. L.; Sanford, M. S. *J. Am. Chem. Soc.* **2006**, *128*, 14047-14049.
- (22) Giri, R.; Liang, J.; Lei, J.; Li, J.; Wang, D.; Chen, X.; Naggar, I. C.; Guo, C.; Foxman, B. M.; Yu, J. *Angew. Chem., Int. Ed.* **2005**, *44*, 7420-7424.
- (23) Reddy, B. V. S.; Reddy, L. R.; Corey, E. J. *Org. Lett.* **2006**, *8*, 3391-3394.
- (24) Khan, K. M.; Maharvi, G. M.; Perveen, S.; Khan, M. T. H.; Abdel-Jalil, R. J.; Shah, S. T. A.; Fecker, M.; Choudhary, M. I.; Atta-ur-Rahman; Voelter, W. *Chem. Biodivers.* **2005**, *2*, 470-476.
- (25) Lee, Y.; Jung, O. *Bull. Chem. Soc. Jpn.* **2002**, *75*, 1533-1537.
- (26) Belov, A. P.; Moiseev, I. I.; Satsko, N. G.; Syrkin, Y. K. *Russ. Chem. Bull.* **1971**, *20*, 209-211.
- (27) Booth, S. E.; Jenkins, P. R.; Swain, C. J.; Sweeney, J. B. *J. Chem. Soc., Perkin Trans. 1* **1994**, 3499-3508.
- (28) Minter, A. R.; Fuller, A. A.; Mapp, A. K. *J. Am. Chem. Soc.* **2003**, *125*, 6846-6847.
- (29) Kaifer, A.; Gustowski, D. A.; Echevoyen, L.; Gatto, V. J.; Schultz, R. A.; Cleary, T. P.; Morgan, C. R.; Goli, D. M.; Rios, A. M.; Gokel, G. W. *J. Am. Chem. Soc.* **1985**, *107*, 1958-1965.

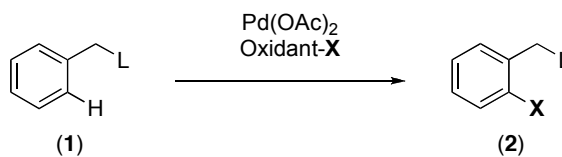
Chapter 4

Factors Governing the Dominance of a Directing Group

4.1 Background and Significance

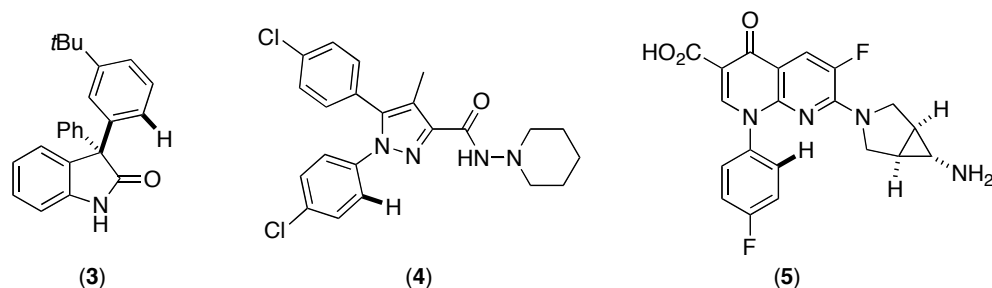
Palladium-catalyzed ligand directed C–H activation/functionalization has emerged as a powerful method for the regioselective conversion of C–H bonds to C–X bonds (X = C, O, Cl, Br, I and F).¹⁻¹⁰ The ligand directed approach allows for the site selective functionalization of the C–H bond proximal to a directing group in molecules containing an appropriate chelating functionality (Scheme 4.1).

Scheme 4.1: Chelate Directed C–H Activation/Functionalization



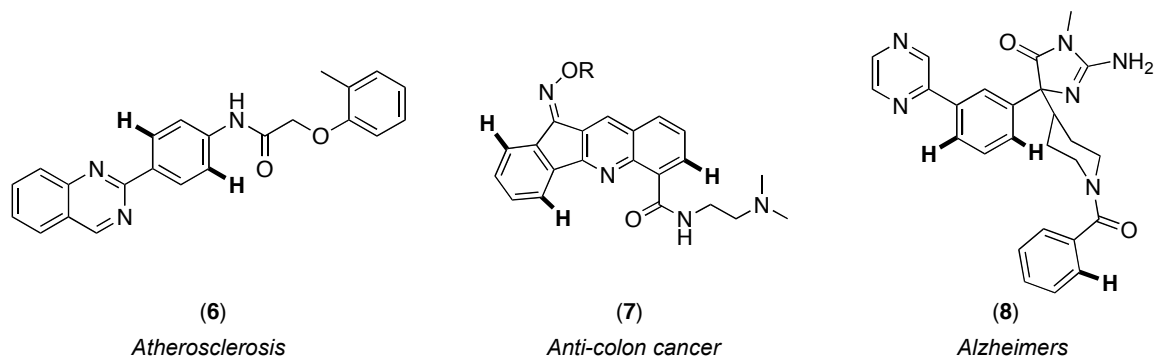
Recently, we and others have shown that this methodology is general with respect to a wide variety of directing groups such as pyridines, oxime ethers, isoxazolines, amides, quinolines, and oxazolines.¹⁻⁹ Importantly, these functionalities are widely prevalent in biologically active molecules.^{11, 12} Hence, this methodology could potentially be used for functionalization of C–H bonds adjacent to chelating groups to generate libraries of synthetic analogues of important pharmaceutical targets.

Figure 4.1: Examples of Biologically Active Molecules Containing a Single Potential Directing Group



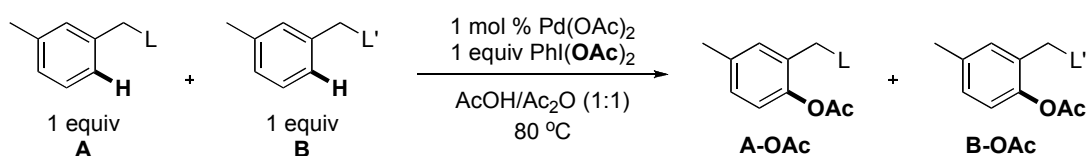
The palladium-catalyzed chelate directed functionalization reactions have thus far been demonstrated in molecules bearing a single chelating functionality. Hence, they could be applicable to molecules such as **3**, **4** and **5** that contain only one potential ligand (Figure 4.1).¹³⁻¹⁵ However, the vast majority of biologically active molecules contain multiple chelating functionalities (for example, **6**, **7**, and **8** in Figure 4.2).^{11, 12} Subjection of these molecules to C–H activation/functionalization reactions could possibly lead to mixtures of products resulting from functionalization adjacent to the different directing groups present in these compounds. In order to enhance the applicability of these ligand-directed transformations, an understanding of the factors that control functionalization adjacent to one chelating moiety over another is essential. Despite the potential synthetic utility of this chemistry, to date there has been no systematic study to address this important issue. This chapter describes a comprehensive investigation of the factors that govern the dominance of a directing group in palladium-catalyzed activation/functionalization of C–H bonds to C–OAc bonds. The insights gained from this study could ultimately be applied towards transformation of C–H bonds to other C–X bonds (X = Cl, Br, I, F, C, and N) as well.

Figure 4.2. Examples of Biologically Active Molecules Containing Multiple Potential Directing Groups



Strategy: Our approach towards elucidating the dominance of a directing group involved systematically studying how different directing groups affect the distribution of products in Pd-catalyzed C–H bond functionalization with $\text{PhI}(\text{OAc})_2$. As shown in Scheme 4.2, we designed a series of experiments to compete two directing groups against one another in the same reaction flask (mimicking situations where two potential ligands are present within the same molecule). In these systems, 1 equiv of substrate **A** and 1 equiv of substrate **B** were subjected to Pd-catalyzed reaction with 1 equiv of $\text{PhI}(\text{OAc})_2$. The ratio of acetoxyated products (**A-OAc/B-OAc**) was then determined, and this value was taken to represent the relative reaction rates of the two directing groups (k_A/k_B) under a given set of conditions (Scheme 4.2).

Scheme 4.2: Competition Studies Between Multiple Directing Groups



4.2 Substrate Selection and Optimizations

Our studies began with the synthesis of substrates bearing a variety of different directing groups (Figure 4.3). Importantly, the key design elements for these substrates include (i) selection of directing groups shown to be effective ligands for palladium and

present in biologically active molecules, (ii) installation of a methylene unit between the directing ligand and the aryl ring to limit electronic communication between the directing group and the arene being functionalized, and (iii) introduction of an electronically neutral methyl substituent at the *meta*-position of the aryl ring being functionalized in order to promote selective mono-acetoxylation of the sterically less hindered C-H bond (Figure 4.4).⁴

Figure 4.3. Substrates Synthesized to Conduct Dominance Studies

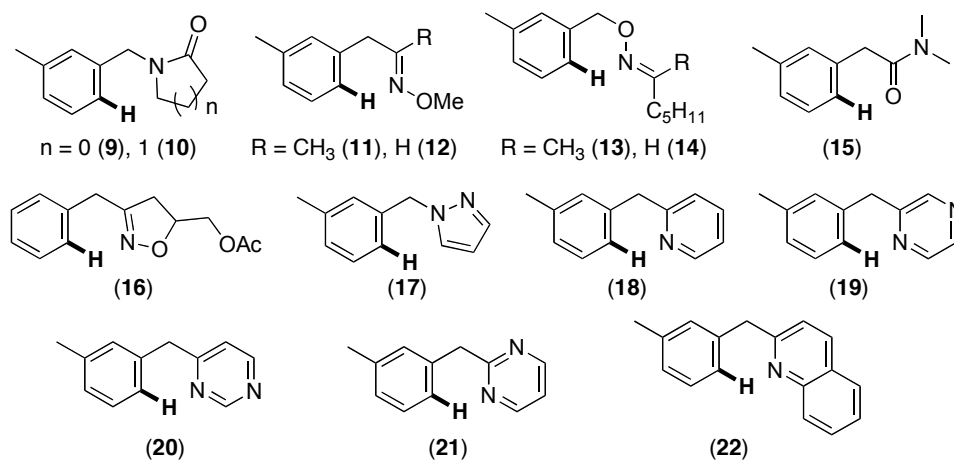
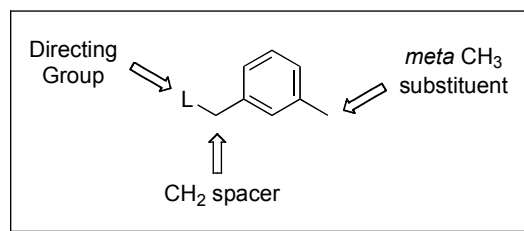


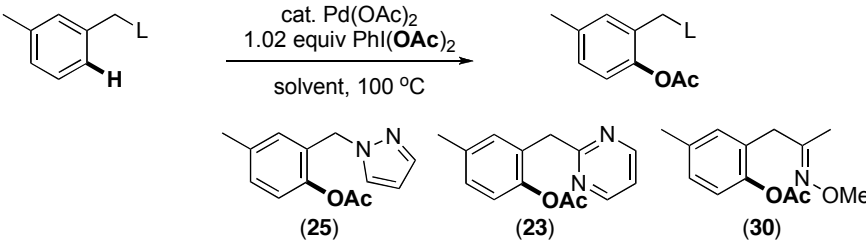
Figure 4.4. Elements for Substrate Design



Next, we conducted studies to obtain reaction conditions for the palladium-catalyzed C-H activation/acetoxylation of these substrates. A screen of different solvents, temperatures and catalyst loadings was performed. A representative set of data for the solvent and catalyst loading study is illustrated in Table 4.1. Interestingly, there is a significant solvent effect between different directing groups. While **21** lead to excellent yields of the acetoxyated product in all solvents, substrate **11** afforded the desired

product only in AcOH/Ac₂O. The catalyst loading could be reduced to 0.1 mol % for substrate **21** and still produce good (47%) yield of acetoxyated product (Table 4.1, entry 6). However, this low catalyst loading led to diminished reactivity for other substrates such as **17** and **11** (entry 6). Hence, we chose to conduct all our further studies with 1 mol % Pd(OAc)₂.

Table 4.1: Optimization Studies



Entry	% Pd(OAc) ₂	Solvent	% GC yield		
1	5	AcOH/Ac ₂ O	92%	96%	85%
2	5	Benzene	45%	89%	0%
3	5	DCE	39%	58%	0%
4	5	Nitromethane	14%	30%	0%
5	1	AcOH/Ac ₂ O	92%	96%	85%
6	0.1	AcOH/Ac ₂ O	39%	47%	29%

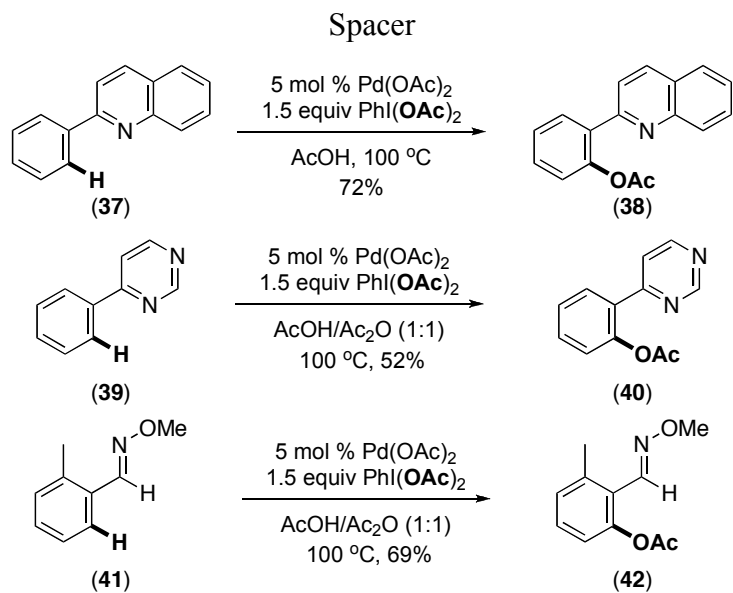
Substrates **11**, **13**, **15-19**, and **21** afforded the desired monoacetoxyated products **23-26** and **30-33** in good to excellent yields under our optimized reaction conditions (1 mol % Pd(OAc)₂, 1.02 – 1.8 equiv PhI(OAc)₂ in AcOH/Ac₂O at 100 °C) regardless of the nature of the directing group (Table 4.2, entries 1-4 and 8-11). The stronger oxidant PhI(OCOCF₃)₂ was required for substrates **9** and **10**, and even then only modest (49-55%) yields of products **34** and **35** were obtained (Table 4.2, entries 12 and 13). The low reactivity of **9** and **10** may be due to the larger seven-membered ring required for cyclopalladation with the amide carbonyl in these substrates, since amide substrate **15** affords the acetoxyated product **33** in good yield (entry 11).

Table 4.2: Scope of Substrates Bearing Different Directing Groups

Entry	Product	Yield	Entry	Product	Yield
1	 (23)	90%	8	 (30)	79%
2	 (24)	69%	9	 (31)	70%
3	 (25)	88%	10	 (32)	74%
4	 (26)	75%	11	 (33)	77%
5	 (27)	20%	12	 (34)	55%
6	 (28)	15%	13	 (35)	49%
7	 (29)	<5%	14	 (36)	<5%

Substrates **12** and **14** afforded no appreciable amount of the acetylated products **29** and **36** due to their faster relative rate of decomposition under our reaction conditions. Additionally, compounds **20** and **22** afforded the desired acetylated products **27** and **28** in low yields due to competing uncatalyzed acetylation at other positions in the molecule. This was surprising to us because substrates bearing the same directing group, but lacking a methylene spacer, afforded good yields of the *ortho*-acetylated products along with only trace amounts of the undesired products (Scheme 4.3).^{1,2}

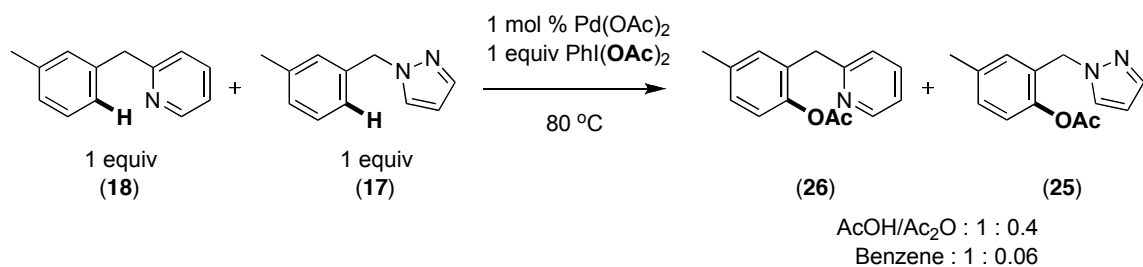
Scheme 4.3: Pyrimidine, Quinoline and Aldehyde Substrates Lacking a Methylene Spacer



4.3 Competition Studies

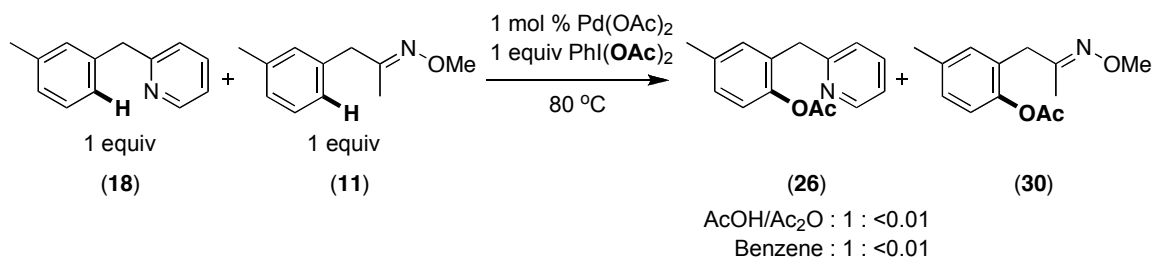
The competition experiments depicted in Scheme 4.4 above were conducted in two different solvents – an acidic medium (AcOH/Ac₂O) and a non-acidic medium (benzene). We examined both solvents in order to determine whether the trend of dominance observed was not affected by competitive protonation of the basic directing groups in AcOH. These studies were performed by subjecting a 1:1 molar ratio of two different substrates in either AcOH/Ac₂O (1:1) or benzene with 1 equivalent of PhI(OAc)₂ and 1 mol % Pd(OAc)₂. Upon completion of the reaction, the yields and ratios of the acetoxyated products were determined by gas chromatography. The ratio of the products reflected the relative rates of reaction of the two substrates towards C–H activation/acetoxylation. In a representative experiment, the reaction of an equimolar quantity of **18** and **17** in the same vessel afforded the acetoxyated products **26** and **25** in a ratio of 1:0.4 ($k_{\text{pyrazole}}/k_{\text{pyridine}} = 2/5$). The same experiment when conducted in benzene also led to **26** as the major product (**26:25** = 1:0.06), albeit with greater selectivity than in AcOH/Ac₂O (Scheme 4.4).

Scheme 4.4: Representative Competition Experiment



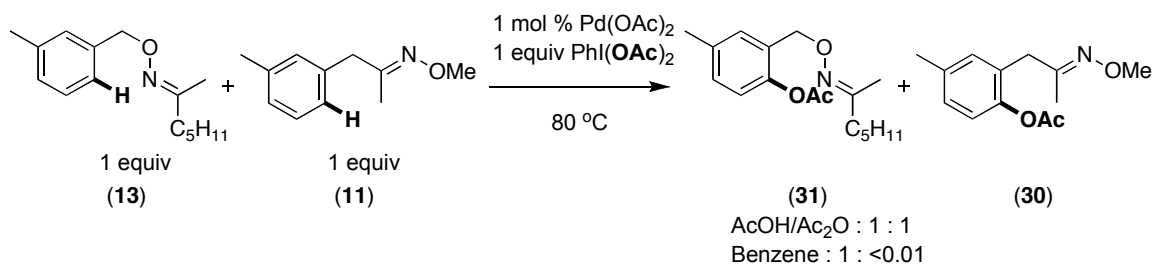
Interestingly, competition experiments between pyridine **18** and substrates bearing significantly less basic directing groups such as isoxazoline (**16**), oxime ethers (**11** and **13**), and amide (**15**) did not afford an appreciable amount of the acetoxyated products **24**, **30-31**, and **33** in either AcOH/Ac₂O or benzene. Instead, **26** was formed with a selectivity of > 50:1 (Scheme 4.5).

Scheme 4.5: Competition Between Benzylpyridine **18** and Oxime Ether **11**



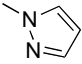
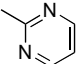
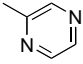
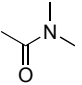
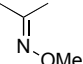
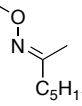
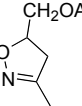
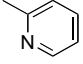
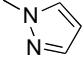
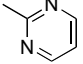
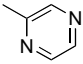
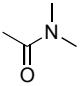
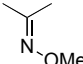
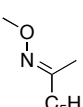
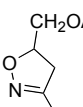
Analogous competition experiments were also conducted between substrates **11**, **13**, **15** and **16**. Interestingly, the two similar oxime ether derivatives **11** and **13** exhibited different reactivity when the solvent was changed from AcOH/Ac₂O to benzene (Scheme 4.6). Methyl oxime ether **11** did not afford any of the acetoxyated product **30** in benzene, whilst benzyl oxime ether **13** yielded 28% of product **31**.

Scheme 4.6: Competition between Oxime Ethers **13** and **11**



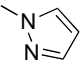
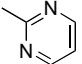
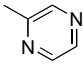
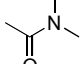
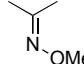
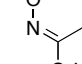
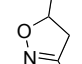
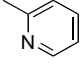
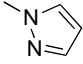
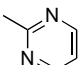
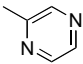
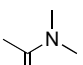
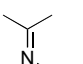
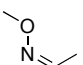
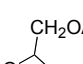
The ratios obtained from all of these competition experiments are compiled in Tables 4.3 and 4.4. Based on this data, the reactivity trend depicted in Figure 4.5 was obtained for AcOH/Ac₂O and benzene, respectively. In general, substrate **18**, bearing the most basic directing group (pyridine), afforded the predominant acetoxylated product in the presence of all other chelating ligands in both AcOH/Ac₂O and benzene.

Table 4.3: Competition Ratios in AcOH/Ac₂O

							
	1 : 0.4	1 : 0.3	1 : 0.04	1 : 0.01	1 : 0.01	1 : 0.01	1 : 0.01
	-	1 : 3.3	1 : 1.5	1 : 0.01	1 : 0.01	1 : 0.01	1 : 0.01
	1 : 0.3	-	n/a ^a	1 : 0.01	1 : 0.01	1 : 0.01	1 : 0.01
	0.7 : 1	n/a ^a	-	1 : 0.01	1 : 0.01	1 : 0.01	1 : 0.01
	0.01 : 1	0.01 : 1	0.01 : 1	-	0.01 : 1	0.01 : 1	0.01 : 1
	0.01 : 1	0.01 : 1	0.01 : 1	1 : 0.01	-	0.01 : 1	0.01 : 1
	0.01 : 1	0.01 : 1	0.01 : 1	1 : 0.01	1 : 0.01	-	1 : 1
	0.01 : 1	0.01 : 1	0.01 : 1	1 : 0.01	1 : 0.01	1 : 1	-

^a Ratio not obtained because starting materials and products have identical retention times by GC
 In the ratios depicted above the first number refers to the substrate in the column and the second number to the substrate in the row

Table 4.4: Competition Ratios in Benzene

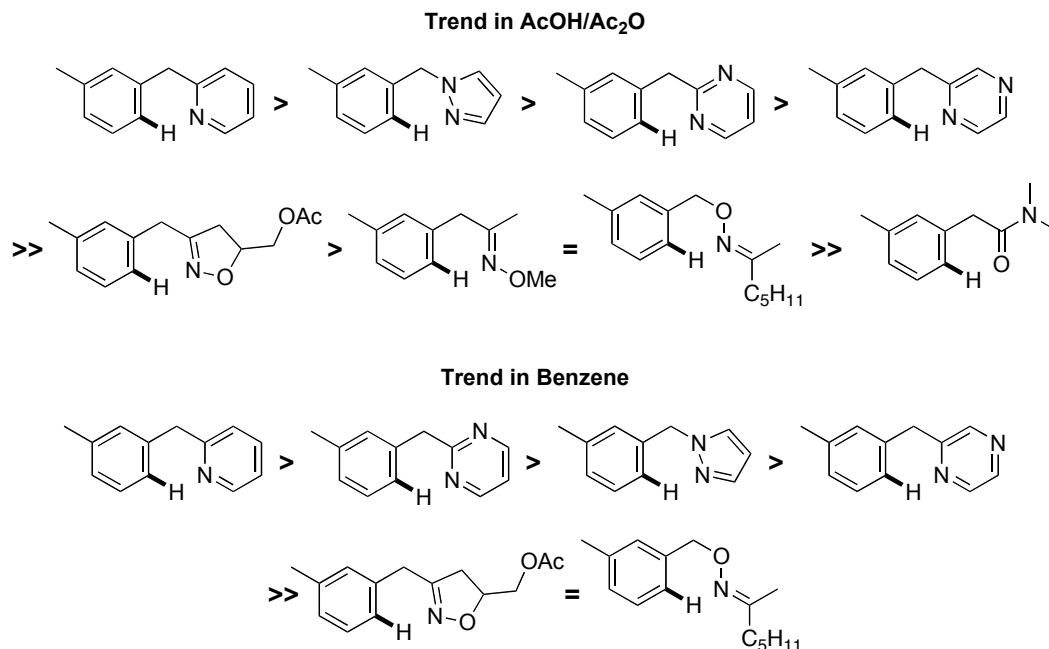
							
	1 : 0.06	1 : 0.2	1 : 0.05	1 : 0.01	1 : 0.01	1 : 0.01	1 : 0.01
	-	1 : 4	1 : 2	1 : 0.01	1 : 0.01	1 : 0.01	1 : 0.01
	1 : 0.25	-	n/a ^a	1 : 0.01	1 : 0.01	1 : 0.01	1 : 0.01
	0.5 : 1	n/a ^a	-	1 : 0.01	1 : 0.01	1 : 0.01	1 : 0.01
	0.01 : 1	0 : 1	0 : 1	-	n/a ^b	0.01 : 1	0.01 : 1
	0.01 : 1	0 : 1	0 : 1	n/a ^b	-	0.01 : 1	0.01 : 1
	0.01 : 1	0.01 : 1	0.01 : 1	1 : 0.01	1 : 0.01	-	1 : 1
	0.01 : 1	0.01 : 1	0.01 : 1	1 : 0.01	1 : 0.01	1 : 1	-

^a Ratio not obtained because starting materials and products have identical retention times by GC

^b Ratio not obtained because starting materials afford trace amounts of products in benzene

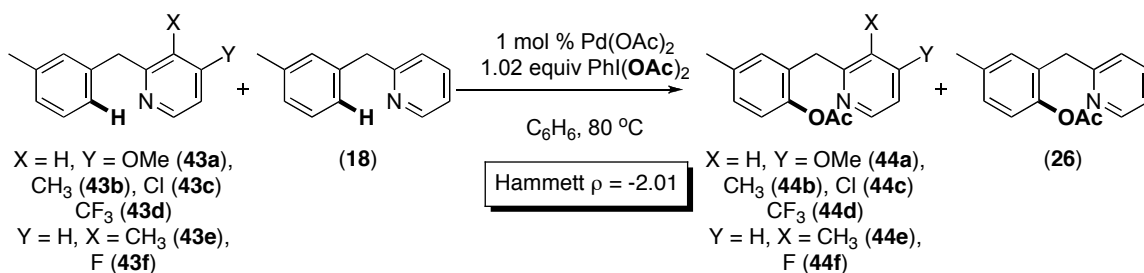
In the ratios depicted above the first number refers to the substrate in the column and the second number to the substrate in the row

Figure 4.5: Relative Reactivity of Directing Groups from Competition Studies in AcOH/Ac₂O and Benzene



While the trends in the two solvents varied slightly, in general the results were consistent with studies of substituted benzylpyridine derivatives **43a-43f** (Scheme 4.7), which were conducted by my colleague Kara Stowers. Kara obtained a Hammett ρ value of -2.01 when she carried out similar competition experiments with these substrates (Scheme 4.7). This ρ value implies that electron rich substrates are dominant in the competition studies.

Scheme 4.7: Electronic Effects with Substituted Benzylpyridine Derivatives



4.4 Individual Rate Studies

We next sought to investigate the reasons for predominant product formation by substrates bearing an electron rich ligand when substrates containing different directing groups were present in the same reaction vessel. In particular, we wondered if benzylpyridine substrate **18**, which afforded the major product in the presence of other directing groups, would also exhibit the fastest rate of acetoxylation. In order to probe this, we studied the kinetics of acetoxylation for each substrate individually in separate reaction vessels. The initial rate constant for each substrate was obtained under optimal conditions (1 mol % Pd(OAc)₂, 1.02 equiv PhI(OAc)₂, at 80 °C) in both AcOH/Ac₂O and in benzene, by monitoring the reaction progress by GC (Table 4.5). The initial rates for acetoxylation of substrates **11**, **13**, **15-19**, and **21** ranged from 0.01 to 0.64 mol/(L)(min) in AcOH/Ac₂O and 0.02 to 0.5 mol/(L)(min) in benzene.

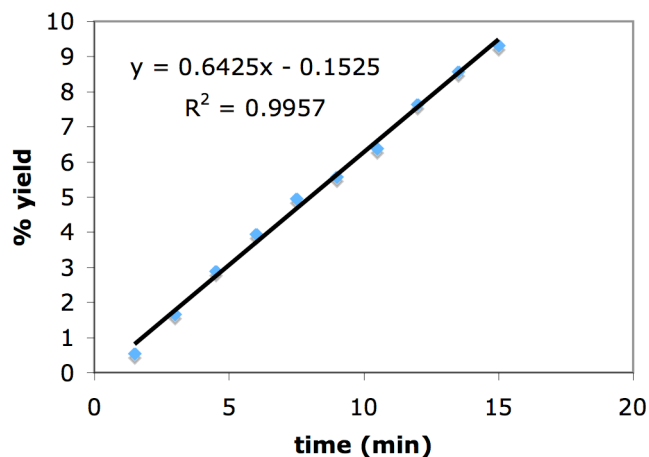
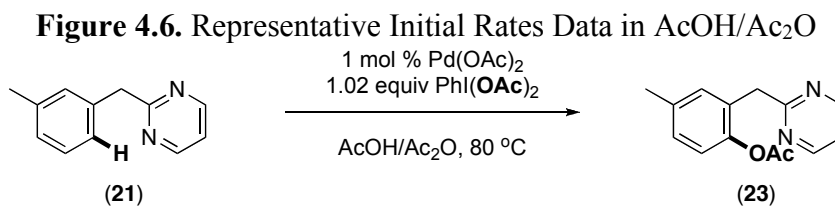
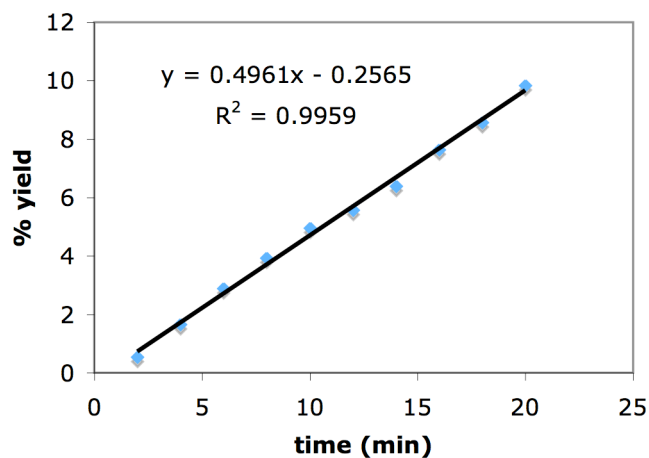
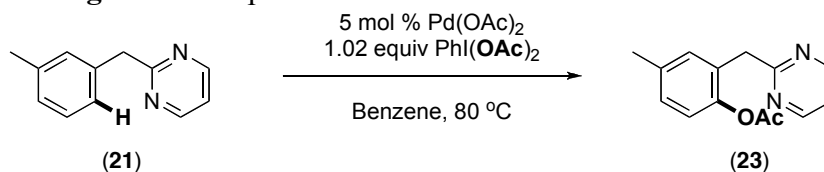


Figure 4.7. Representative Initial Rates Data in Benzene

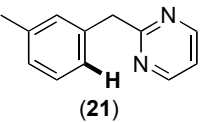
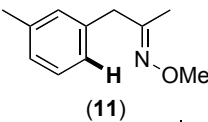
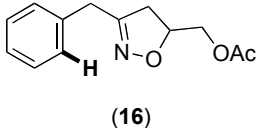
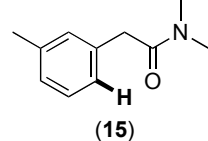
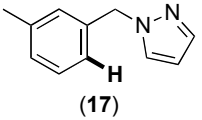
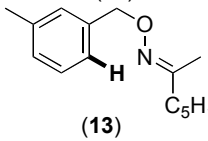
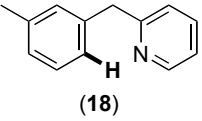
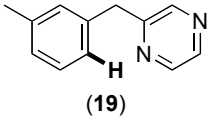


Notably, in AcOH/Ac₂O, the three substrates bearing very similar heterocyclic nitrogen-containing directing groups – pyridine **18**, pyrimidine **21**, and pyrazine **19** – exhibited very different initial rates. The pyrimidine reacted 60 times faster than the pyrazine and 4 times faster than the pyridine (Table 4.5, entries 1, 4, and 8). In contrast, substrates bearing two very different directing groups, methyl oxime ether (**11**) and pyridine (**18**), showed very similar initial rate constants (entries 4-5).

The solvent had a significant effect on the efficiency of the acetoxylation reactions by certain chelating ligands. For example, the isoxazoline and the pyrazole underwent reaction at similar rate constants in AcOH/Ac₂O, while in benzene the isoxazoline substrate **16** was twice as fast as the pyrazole. Notably, methyl oxime ether **11** and amide **15**, which showed good reactivity in AcOH/Ac₂O, led to only trace amounts of the corresponding acetoxyated products in benzene. Additionally, contrary to the competition studies, substrate **18**, bearing the most basic directing group – pyridine – did not exhibit the fastest rate of acetoxylation. However, these results were consistent with the data obtained by Kara Stowers with the substituted benzyl pyridines **43a-43f**. She obtained a Hammett ρ value of 1.40 when examining the initial rate constants of substituted benzyl pyridine derivatives. This implies that, in contrast to the competition

studies, electron deficient directing groups accelerate the rate of the reaction in individual experiments.

Table 4.5: Initial Rate Constants for Substrates **11**, **13**, **15-19**, and **21** in AcOH/Ac₂O and Benzene

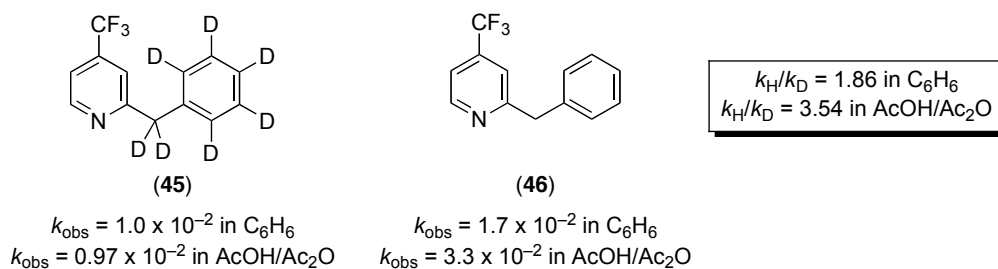
Entry	Substrate	k_{obs} ($\times 10^{-1}$)		Entry	Substrate	k_{obs} ($\times 10^{-1}$)	
		AcOH/Ac ₂ O ^a	Benzene ^b			AcOH/Ac ₂ O ^a	Benzene ^b
1	 (21)	6.4	5.0	5	 (11)	2.1	-
2	 (16)	2.2	1.0	6	 (15)	1.6	-
3	 (17)	2.2	0.5	7	 (13)	1.5	0.4
4	 (18)	2.0	0.6	8	 (19)	0.1	0.2

Conditions a: 1 mol % Pd(OAc)₂, 1.02 equiv PhI(OAc)₂, (1:1) 0.12M AcOH/Ac₂O at 80 °C
 Conditions b: 5 mol % Pd(OAc)₂, 1.02 equiv PhI(OAc)₂, 0.12M Benzene at 80 °C

4.5 Kinetic Isotope Effect Studies

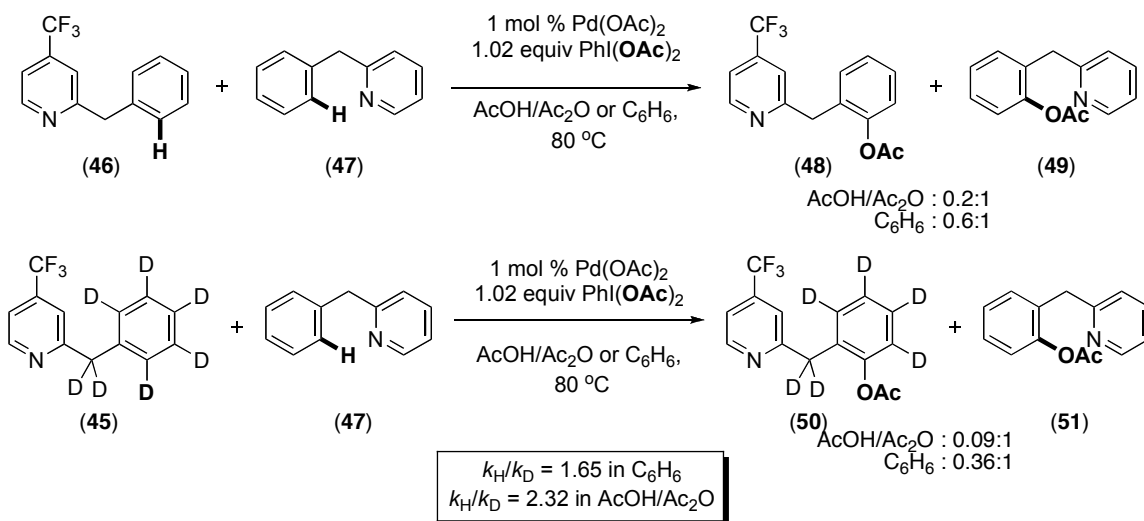
We next desired to determine the kinetic isotope effect (KIE) in the individual reactions and competition experiments. In order to elucidate the KIE in the individual reactions, the value of k_{obs} with substrate **46** was compared to that of its deuterated analogue **45** in both AcOH/Ac₂O and benzene (Scheme 4.8). From the initial rates, $k_{\text{H}}/k_{\text{D}}$ was calculated to be 3.54 in AcOH/Ac₂O and 1.86 in benzene.

Scheme 4.8: Kinetic Isotope Effect in Individual Rate Studies



We next determined the KIE in the competition experiments. The ratio of products at completion was determined when benzylpyridine **47** was subjected to the reaction conditions in the presence of either **46** or its deuterated analogue **45** (Scheme 4.9). The isotope effects obtained from this experiment were 2.32 and 1.65 in AcOH/Ac₂O and benzene, respectively.

Scheme 4.9: Kinetic Isotope Effect in Competition Studies



4.6 Order of PhI(OAc)₂

In order to gain insight into the relative position of the turnover limiting step in the catalytic cycle, we next investigated the order of the reaction in PhI(OAc)₂ in both the competition studies and the individual reactions. Under our optimal conditions for

acetoxylation with the benzylpyridine substrate **18** (Scheme 4.10), the reaction was found to be zero order in $\text{PhI}(\text{OAc})_2$ in both $\text{AcOH}/\text{Ac}_2\text{O}$ and benzene (Figure 4.8 and 4.9).

Scheme 4.10: Reaction Studied for Determining the Order in $\text{PhI}(\text{OAc})_2$

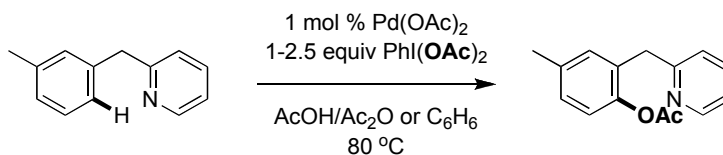


Figure 4.8. Initial Rate Constant as a Function of Oxidant Concentration in $\text{AcOH}/\text{Ac}_2\text{O}$

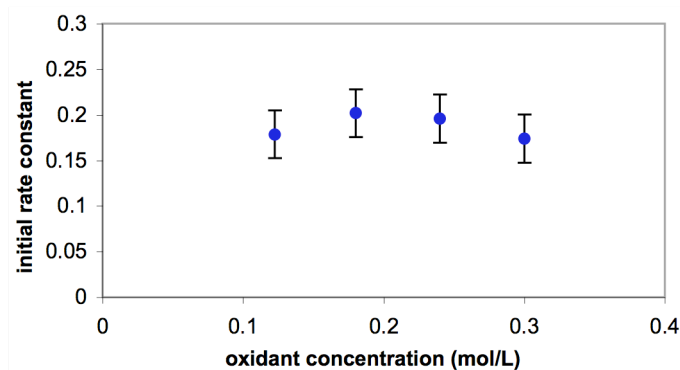
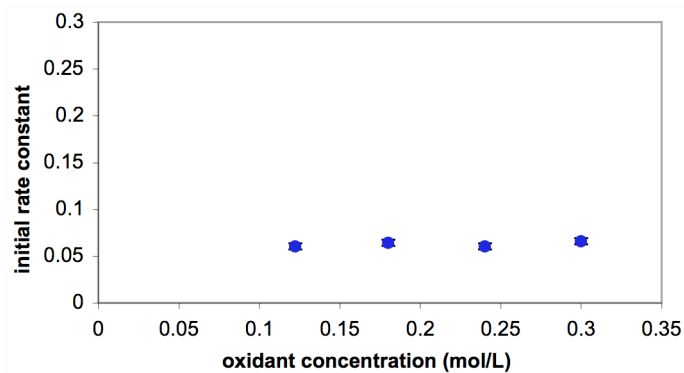


Figure 4.9. Initial Rate Constant as a Function of Oxidant Concentration in Benzene



Next, the order of the reaction in $\text{PhI}(\text{OAc})_2$ was obtained under the competition conditions. Similar to the experiment above, the order of $\text{PhI}(\text{OAc})_2$ in the competition study between **52** and **18** (Scheme 4.11) was also determined to be zero (Figure 4.10 and 4.11). Both the order studies were done in collaboration with Kara Stowers.

Scheme 4.11: Reaction Studied for Determining the Order in $\text{PhI}(\text{OAc})_2$ (Competition)

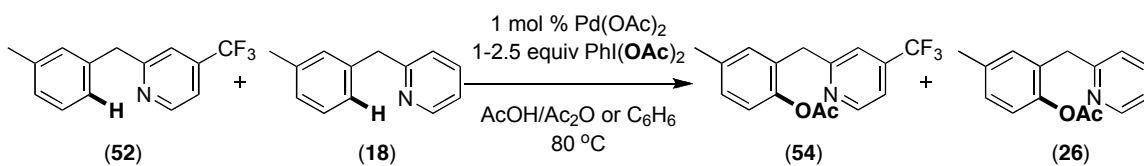


Figure 4.10. Initial Rate Constant of **18** in Presence of **52** as a Function of Oxidant Concentration in $\text{AcOH}/\text{Ac}_2\text{O}$

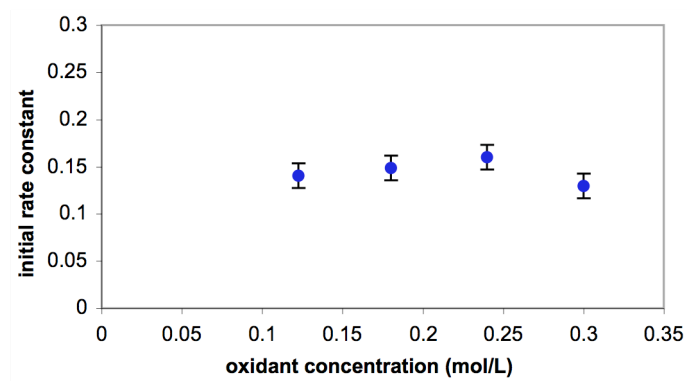
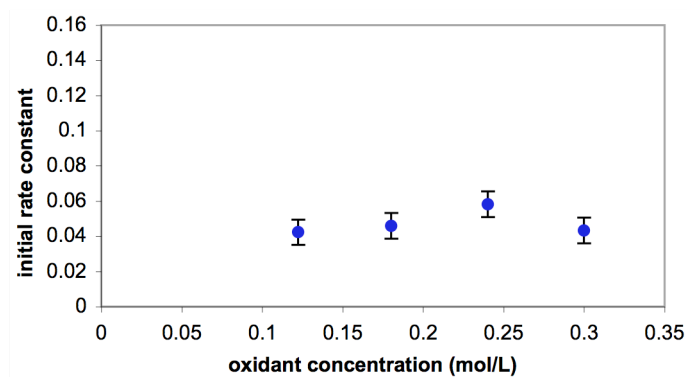


Figure 4.11. Initial Rate Constant of **18** in Presence of **52** as a Function of Oxidant Concentration in Benzene

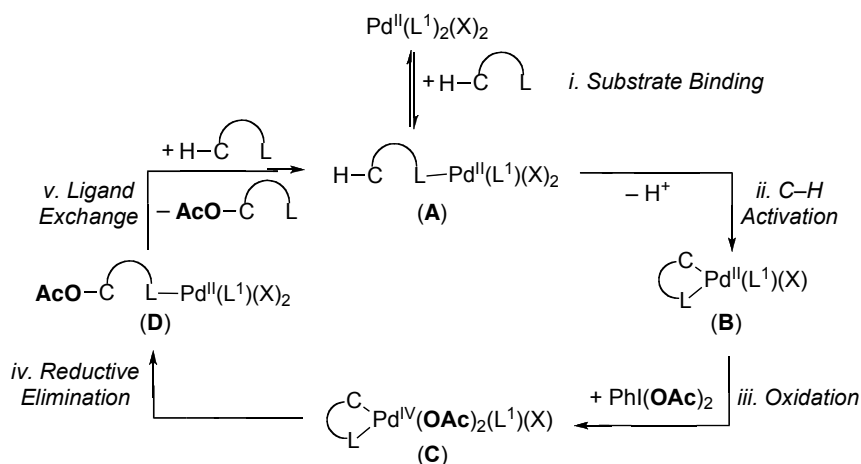


4.7 Discussion

With all these results in hand we sought to address the key mechanistic steps dictating the efficiency of a directing group in palladium-catalyzed ligand directed C–H activation/acetoxylation reactions both in the presence and absence of multiple chelating

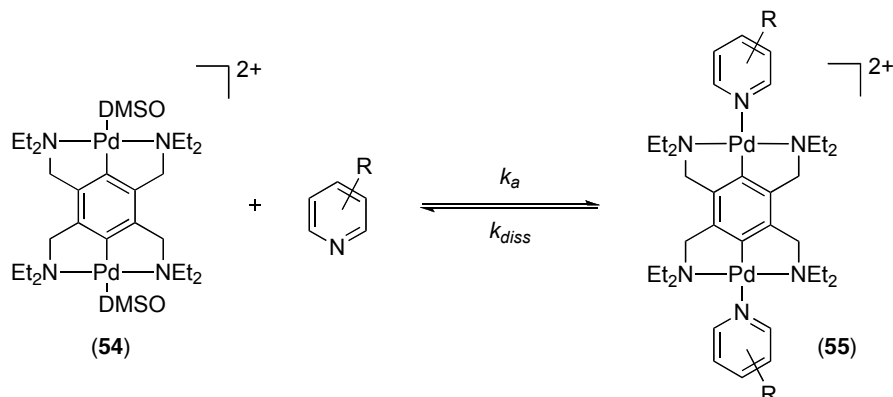
functionalities. The proposed mechanism for these acetoxylation reactions, (Figure 4.12) is believed to involve the following steps: (i) ligand coordination to palladium, (ii) C–H activation to form palladacycle **B**, (iii) oxidation of **B** by $\text{PhI}(\text{OAc})_2$ to afford the Pd^{IV} intermediate **C**, (iv) C–O bond forming reductive elimination from **C** to afford complex **D**, and (v) finally ligand exchange whereby a new substrate molecule displaces the product from the metal. The mechanistic features/requirements for each of the fundamental steps of this catalytic cycle are discussed in detail below.

Figure 4.12. Proposed Catalytic Cycle for Pd-Catalyzed C–H Bond Acetoxylation



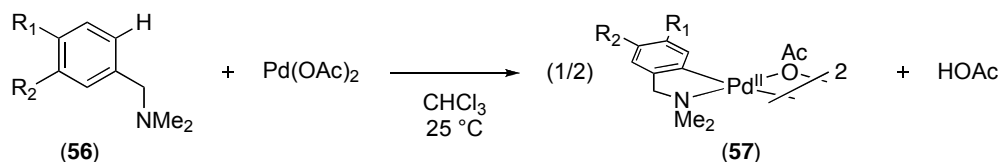
Ligand Binding (step i): The equilibrium constant for ligand binding to Pd^{II} centers is known to be highly dependent on the electronic nature of the coordinating group. For example, Craig has studied K_{eq} for the coordination of substituted pyridines to Pd^{II} pincer complexes (Scheme 4.12).¹⁶ The log of K_{eq} obtained for binding of differentially substituted pyridines was plotted against the sigma values. These studies demonstrated that the Hammett ρ value for this equilibrium is -1.90 in DMSO. The negative ρ value indicates that, in general, electron rich ligands form stronger bonds to palladium.

Scheme 4.12: Coordination Studies of Substituted Pyridines with Bimetallic Palladium Complexes



C–H activation (step ii): Ryabov reported the earliest studies on the mechanism of electrophilic arene C–H activation by palladium. His group investigated the kinetics of stoichiometric cyclopalladation of *meta*- and *para*-substituted dimethylbenzylamine derivatives with Pd(OAc)₂ (Scheme 4.13).¹⁷ A Hammett ρ value of -1.6 and a kinetic isotope effect of 2.02 were obtained for the reaction in CHCl₃. Based on this negative ρ value, the authors proposed that cyclopalladation proceeded by a Wheland intermediate that transfers a proton to an acetate ligand on the metal via a highly ordered six-membered transition state (Figure 4.13).

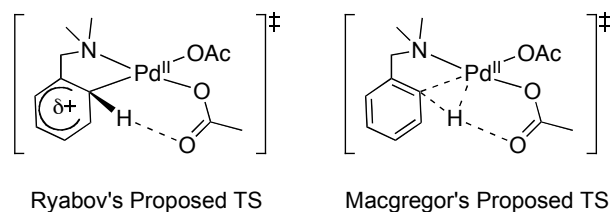
Scheme 4.13: Hammett Studies for Cyclopalladation of Substituted 3° Benzylamines



More recently, computational studies by Macgregor and co-workers provided further insights into the transition state for directed C–H activation at Pd^{II}.¹⁸ They obtained theoretical values of 13 kcal/mol for the activation barrier and 1.2 for the kinetic isotope effect. Based on this data, along with calculations of the transition state, they proposed that the C–H activation reaction proceeds via an agostic C–H complex, rather than a Wheland intermediate (Figure 4.13). This would account for the relatively small

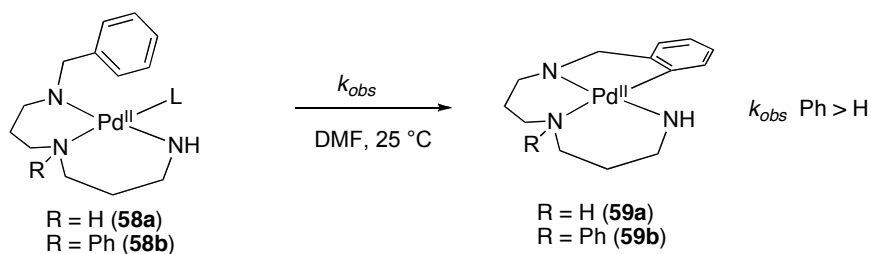
magnitude of ρ observed experimentally. For comparison, ρ for a typical electrophilic aromatic substitution reaction ranges from -6 to -12 .¹⁹ The agostic complexation is followed by an intramolecular hydrogen transfer via a six-membered transition state to a coordinated acetate. The authors propose that formation of the agostic complex is rate determining in this system; therefore, the small KIE is due to C–H bond elongation, as opposed to cleavage, in the transition state. Importantly, a similar mechanism has also been proposed by Fagnou²⁰ and by Echavarren²¹ for other arene activation reactions at Pd^{II}.

Figure 4.13: Proposed Transition States for Cyclopalladation



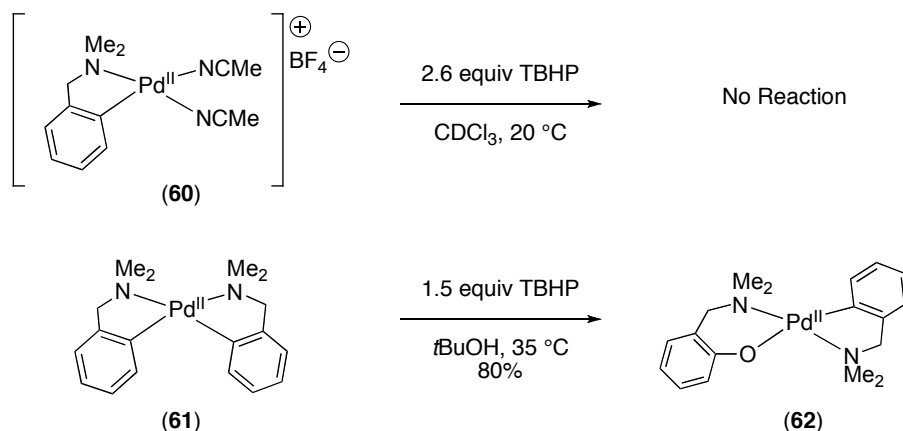
Based on the aforementioned computational and theoretical studies, it is now generally accepted that palladium mediated C–H activation proceeds via interaction of electrophilic Pd center with nucleophilic C–H bond. Hence, more electron deficient directing groups are expected to accelerate the C–H activation step. For example, Funahashi and co-workers have shown that the cyclopalladation of *N*-benzyltriamines is accelerated when the amine nitrogen bears less electron donating substituents.²² As shown in Scheme 4.14, the rate of cyclopalladation to form complex **59** increased significantly when R was changed from H to Ph in complex **58**.

Scheme 4.14: Directing Group Electronic Effects in the Cyclopalladation of *N*-Benzyl Triamines



Oxidation (step iii): Literature precedent suggests that more electron donating ligands on palladium will increase the rate of oxidation of Pd^{II} complex **A** to Pd^{IV} complex **B** by making the palladium more nucleophilic. For example, van Koten and co-workers have reported that the reactivity of cyclometalated *N,N*-dimethylbenzylamine complexes towards *t*-butylhydroperoxide (TBHP) increases as the electron density at the metal center increases.²³ Cationic complex **60** did not react with TBHP, whilst the more electron rich complex **61** reacted to form **62** in 80% yield (Scheme 4.15). These reactions were proposed to proceed via rate-limiting oxidation of Pd^{II} to a Pd^{IV}-oxo species.

Scheme 4.15: TBHP Oxidation of *N,N*-Dimethylbenzylamine Complexes



Reductive elimination (step iv): Reports in literature suggest that electron withdrawing ligands accelerate C-O bond forming reductive elimination from Pd^{II}.²⁴ Based on these reports and the principal of microscopic reversibility with the oxidation step, we propose that reductive elimination from Pd^{IV} will be similarly accelerated by electron deficient ancillary ligands.

Having this information about the expected trends for the different steps in the proposed catalytic cycle, we next sought to speculate on the factors controlling the dominance of a directing group based on our experimental results.

Individual Rate Studies. The kinetic studies of substrates in separate reaction vessels showed that, in general, substrates bearing electron deficient or less basic ligands react faster in the chelate-directed acetoxylation reaction. This is supported by the

positive ρ value (1.4) of the Hammett plot obtained for the acetoxylation of electronically differentiated benzylpyridine derivatives. This is further corroborated by the fact that the pyridine substrate (which bears the most basic chelating group) did not exhibit the fastest initial rate.

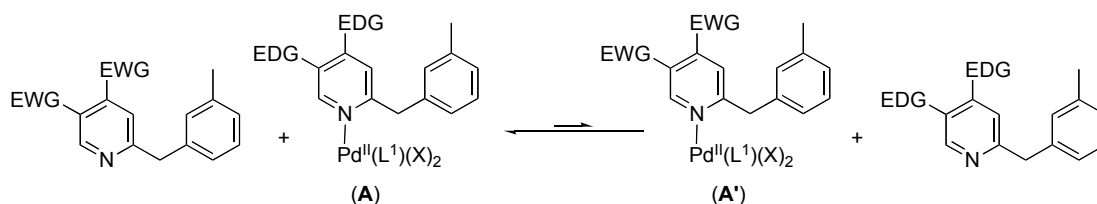
As described above, we would expect that both the C–H activation step and the reductive elimination step of the catalytic cycle to be accelerated by electron deficient directing groups. Hence, electronic effects alone cannot distinguish between either one of these steps being turnover limiting. However, the observed kinetic isotope effects of 1.86 and 3.45 in benzene and AcOH/Ac₂O, respectively, suggests a significant contribution of C–H bond breaking to the transition state of this reaction. Importantly, these KIE values are similar to those observed by Ryabov (2.02) and Daugulis (4.4)²⁵ for related stoichiometric and catalytic reactions, respectively. It is also important to note that literature reports have shown that Pd^{IV} intermediates analogous to those proposed in our reaction are highly unstable, suggesting that rate-limiting reductive elimination is highly unlikely. In all, this data suggests that C–H activation is the step controlling the rate of these individual reactions.

However, we note that in contrast to the results with the benzylpyridine derivatives, the individual rate studies with substrates **11**, **13**, **15** and **16** did not show a linear correlation between k_{obs} and the basicity of the directing group. For example, oxime **11** ($\text{pK}_{\text{a}} \sim -2.90$)²⁶ reacted at a similar rate to pyrazole **17** ($\text{pK}_{\text{a}} \sim 2.18$)²⁷ in benzene, despite a difference of 5 pK_{a} units between the two functional groups. This lack of direct correlation likely has both steric and electronic origins. First, unlike benzylpyridines **43a-43f**, which provide essentially sterically identical coordination environments at the Pd center, compounds **11**, **13**, **15-19** and **21** differ substantially in terms of both their steric parameters and their conformational flexibility. Literature reports have shown that even relatively subtle steric effects can have a significant influence on the relative and absolute rates of cyclopalladation reactions.²⁸ In addition, the pK_{a} of the directing group is not an ideal parameter for predicting the subtle electronic influence of these ancillary ligands on the C–H activation reaction, as it does not take into account the interplay of σ -donor and π -acceptor/donor properties of these directing groups.

Competition Studies. The competition studies show that when multiple potential chelating functionalities are present in solution, more electron rich/more basic directing groups react at faster relative rates. This can be concluded based on three key results: (i) the large negative ρ value from Hammett plots with substituted benzylpyridine derivatives, (ii) the observation that the most basic directing group (pyridine in substrate **18**) out-competes all of the other directing groups among substrates **11**, **13**, **15-19** and **21** (Figure 4.5) and (iii) the fact that heterocyclic ligands with pK_a values greater than zero (pyridine, pyrimidine, pyrazine, pyrazole) outcompete all substrates with pK_a values less than zero (oxime ethers, amides and isoxazolines). Based on the considerations above, this suggests that either ligand binding/exchange (steps *i* and *v*) or oxidation (step *iii*) controls the relative reactivity of the two substrates under these conditions. We were able to rule out the latter based the study of the order of the reaction in $\text{PhI}(\text{OAc})_2$. Under our optimal conditions for acetoxylation with substrate **18**, the reaction was found to be zero order in $\text{PhI}(\text{OAc})_2$, both in the presence and absence of another substrate (**52**), (Figures 4.8-4.11).

This result led us to propose that selectivity under these competition conditions is dictated by K_{eq} for binding of the two substrates to Pd. More specifically, we propose that the relative concentrations of the two coordination complexes (**A** and **A'** in Scheme 4.16) dictate the observed relative rates of reaction, and that this equilibrium favors binding of more electron rich directing group. Literature studies of K_{eq} for coordination of substituted pyridines to Pd, discussed above, show Hammett ρ values ranging from -1.7 to -2.1 in DMSO. These are similar to our results in benzene, where $\rho = -2.01$.

Scheme 4.16. Equilibrium for Substrate Binding Under Competition Conditions



Although ligand binding is the influential step when multiple ligands are present, C-H activation is still rate-limiting. This is supported by the significant KIE observed in

solvent systems, benzene and AcOH/Ac₂O. Relative binding abilities of the competing ligands in the reaction mixture will influence the concentration of the palladium bound substrate, complex **A** (Figure 4.12). The concentration of **A** will in turn affect the rate of C-H activation. Since substrates bearing electron rich ligands will bind to the metal preferentially over electron deficient ligands, increasing the concentration of coordinated complex **A**, they will exhibit a faster relative rate of reaction.

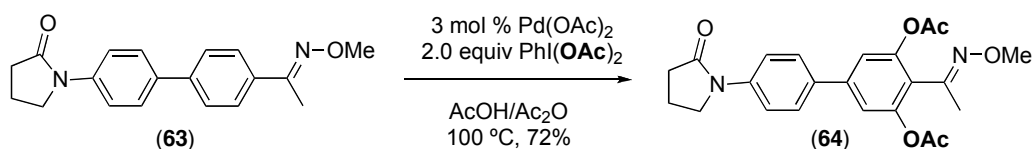
The observed effects in the competition studies have important implications for future applications of this chemistry. First, the solvent can clearly have a significant influence on the selectivity of functionalization in the presence of multiple directing groups. Trends for competition studies and rate of reactions were different depending on whether the reaction was carried out in a non-acidic solvent such as benzene or an acidic solvent such as acetic acid. This suggests that solvent selection could be used to obtain, alter, or improve selectivity. Second, these studies can be used to predict relative reactivity, even with substrates like **63** (illustrated later in section 4.8) that do not contain a methylene spacer between the directing group and the arene ring. Future studies will continue to explore how these effects (and the effects of other solvents and additives) translate into predicting and controlling the dominant directing group in other more complex systems.

4.8 Application

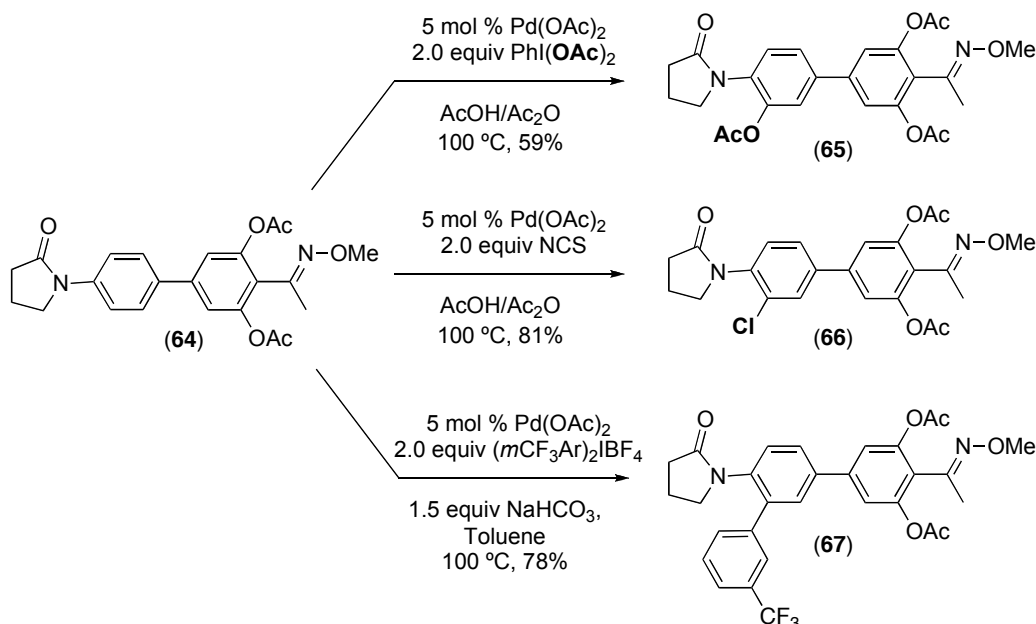
Having explored the factors controlling the dominant directing group in the presence of several chelating functionalities, our efforts focused towards applying the insights gained from our study towards selective palladium-catalyzed ligand mediated acetoxylation adjacent to one ligand in a substrate bearing multiple directing groups. In order to do this, substrate **63** containing an amide and a methyl oxime ether was synthesized. Based on the competition studies between substrates **11** and **15**, we expected the oxime ether to outcompete the amide, resulting in products of acetoxylation *ortho* to the oxime ether. We were pleased to find that, consistent with our hypothesis, the reaction of substrate **63** in the presence of 3 mol % Pd(OAc)₂ and 2.0 equiv PhI(OAc)₂ in AcOH/Ac₂O afforded the di-acetoxyated product **64** in 72% isolated yield (Scheme

4.17). Importantly, none of the product derived from acetoxylation of the C–H bond *ortho* to the amide directing group was observed. The acetoxyated product **64** was further elaborated to diverse compounds **65**, **66** and **67** employing Pd-catalyzed chelate-directed, chlorination,²⁹ phenylation,³ and acetoxylation methodologies, respectively (Scheme 4.18).

Scheme 4.17. Highly Selective Oxime Ether-Directed C–H Acetoxylation of Substrate **63**



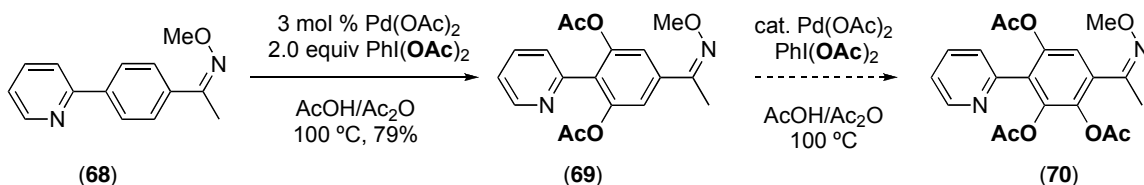
Scheme 4.18. Amide Directed C–H Functionalization of Product **64**



The results in Scheme 4.18 show that even though the oxime ether is dominant, if the *ortho* sites are blocked then the amide can direct functionalization. Hence, we next wondered if we could employ a similar strategy towards functionalizing the C–H bond adjacent to the oxime ether in a substrate like **68**, which contains both a pyridine and an oxime ether, by blocking the sites *ortho* to the pyridine moiety. Subjection of substrate **68** to standard reaction conditions with 2.0 equivalents of PhI(OAc)₂ afforded the

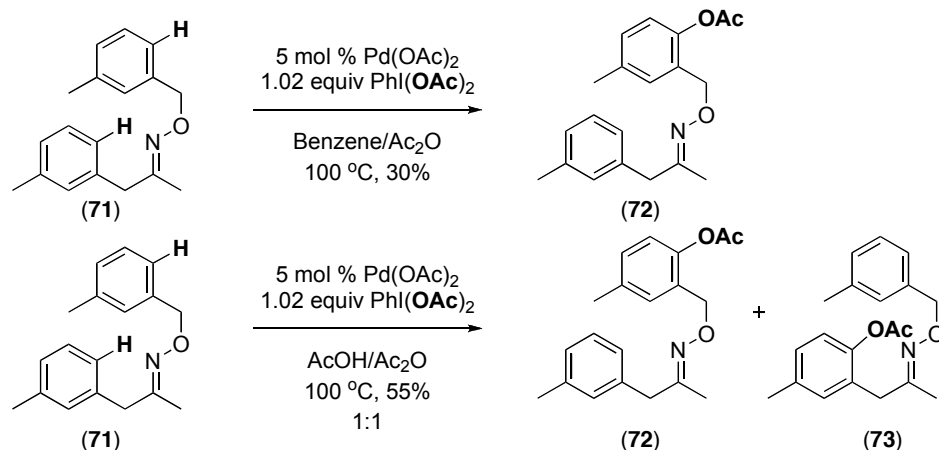
diacetylated product **69** in 79% (Scheme 4.19). However, disappointingly, subjecting of **69** to catalytic Pd and $\text{PhI}(\text{OAc})_2$ did not afford an appreciable amount of acetylated product **70**. This may be due to the fact that the C–H bonds at the site ortho to the oxime ether are very sterically hindered.

Scheme 4.19: Intramolecular Competition Between a Pyridine and an Oxime Ether



Next, substrate **71** was synthesized bearing an oxime ether directing group with the ability to direct C–H activation at two different aryl rings (Scheme 4.20). Based on the competition studies conducted with substrates **11** and **13** in benzene and $\text{AcOH}/\text{Ac}_2\text{O}$, we predicted a greater selectivity in benzene than AcOH . Excitingly, subjecting of substrate **71** under the optimized conditions of 5 mol % $\text{Pd}(\text{OAc})_2$, 1.02 equiv $\text{PhI}(\text{OAc})_2$ in benzene/ Ac_2O afforded a single acetylated product **72**. In contrast, subjecting of the same molecule in $\text{AcOH}/\text{Ac}_2\text{O}$ afforded a 1:1 ratio of products **72** and **73** (Scheme 4.20).

Scheme 4.20: Controlling Direction of C–H Activation/Functionalization



4.9 Conclusions

In summary, we have conducted detailed studies on elucidating the electronic requirements of a directing group in Pd-catalyzed directed C–H functionalization reactions. Through mechanistic studies we have determined that the rate-limiting step is C–H activation. However, when multiple ligands are present, the equilibrium of ligand coordination appears to control the relative rate of reaction. Interestingly, there is not a direct correlation between the intrinsic rate and the dominance of a directing group. These important findings allow for the further development of selective and effective transformations.

4.10 Experimental Procedure

General Procedures: NMR spectra were obtained on a Varian Inova 400 (399.96 MHz for ^1H ; 100.57 MHz for ^{13}C ; 376.34 MHz for ^{19}F) unless otherwise noted. ^1H NMR chemical shifts are reported in parts per million (ppm) relative to TMS, with the residual solvent peak used as an internal reference. Multiplicities are reported as follows: singlet (s), doublet (d), doublet of doublets (dd), doublet of doublets of doublets (ddd), doublet of triplets (dt), triplet (t), quartet (q), quintet (quin), multiplet (m), and broad resonance (br). IR spectra were obtained on a Perkin-Elmer spectrum BX FT-IR spectrometer

Materials and Methods: $\text{Pd}(\text{OAc})_2$ was obtained from Pressure Chemical and used as received, and $\text{PhI}(\text{OAc})_2$ was obtained from Merck Research Laboratories and used as received. Solvents were obtained from Fisher Chemical and used without further purification unless otherwise noted. THF was purified using an Innovative Technology (IT) solvent purification system composed of activated alumina, copper catalyst, and molecular sieves. Flash chromatography was performed on EM Science silica gel 60 (0.040–0.063 mm particle size, 230–400 mesh) and thin layer chromatography was performed on Merck TLC plates pre-coated with silica gel 60 F254. Melting points were determined with a Mel-Temp 3.0, a Laboratory Devices Inc, USA instrument and are uncorrected. HRMS data were obtained on a Micromass AutoSpec Ultima Magnetic

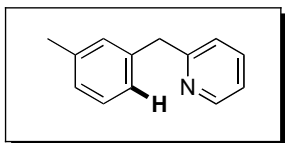
Sector mass spectrometer. Gas chromatography was carried out on a Shimadzu 17A using a Restek Rtx®-5 (Crossbond 5% diphenyl – 95 % dimethyl polysiloxane; 15 m, 0.25 mm ID, 0.25 μ m df) column.

Synthesis of Substrates 18, 19, 21, 45-47 and 52

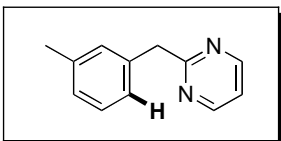
Substrates **18**, **19**, **21**, **45-47** and **52** were prepared via Pd-catalyzed Negishi coupling of (3-methylbenzyl)zinc(II) bromide with the corresponding halopyridine derivative using a modification of a literature procedure.³⁰

Synthesis of Zn reagent: A three-necked flask was charged with purified zinc dust (1.2 equiv) and anhydrous THF. The mixture was heated to reflux, and 1,2-dibromoethane (0.04 equiv) was added. After heating at reflux for 15 min, the reaction was cooled to room temperature and TMSCl (0.05 equiv) was added. The resulting mixture was stirred at room temperature for 30 min, and then a solution of *m*-bromoxylenes (1 equiv) in anhydrous THF was added dropwise over a period of 2 h.

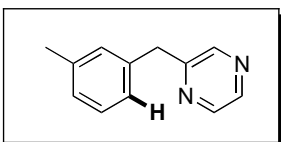
Negishi coupling. In a Schlenk flask, Pd(OAc)₂ (0.05 equiv) and P(*o*-tolyl)₃ (0.1 equiv) were dissolved in anhydrous THF, and this mixture was stirred for 10 min. The halopyridine (1.0 equiv) was then added, and the resulting mixture was cooled to 0 °C. The aryl zinc reagent (2.0 equiv) was added dropwise to this solution over the course of 15 min, and the reaction was allowed to warm to room temperature and stirred overnight. Importantly, **18**, **19**, **21**, **45-47** and **52** were purified by distillation to remove all residual palladium.



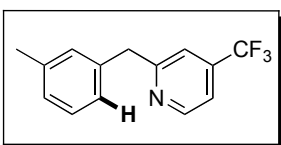
Substrate **18** was obtained as a clear oil (R_f = 0.28 in 70% hexanes/30% ethyl acetate). ¹H NMR (CDCl₃): δ 8.56 (dd, J = 4.4, 1.2 Hz, 1H), 7.56 (dt, J = 7.6 Hz, 2.0 Hz, 1H), 7.20 (t, J = 7.6 Hz, 1H), 7.13-7.03 (multiple peaks, 5H), 4.13 (s, 2H), 2.33 (s, 3H). ¹³C{¹H} NMR (CDCl₃): δ 161.02, 149.23, 139.30, 138.06, 136.40, 129.78, 128.34, 127.03, 126.02, 122.99, 121.08, 44.59, 21.30. HRMS electrospray (m/z): [M-H]⁺ calcd for C₁₃H₁₃N, 182.0970; found, 182.0970.



Substrate **21** was obtained as a pale yellow oil ($R_f = 0.28$ in 70% hexanes/30% ethyl acetate). ^1H NMR (CDCl_3): δ 8.66 (d, $J = 4.8$ Hz, 1H), 7.21-7.15 (multiple peaks, 3H), 7.08 (t, $J = 4.8$ Hz, 1H), 7.02 (d, $J = 6.8$ Hz, 1H), 4.26 (s, 2H), 2.31 (s, 3H). $^{13}\text{C}\{^1\text{H}\}$ NMR (CDCl_3): δ 170.02, 157.17, 138.00, 129.76, 128.32, 127.26, 126.02, 118.48, 45.92, 21.28. HRMS (ESI, m/z): $[\text{M}-\text{H}]^+$ calcd for $\text{C}_{12}\text{H}_{12}\text{N}_2$, 183.0922; found, 183.0920.

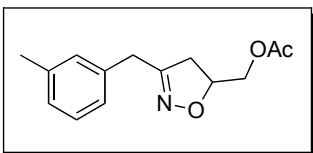


Substrate **19** was obtained as a clear oil ($R_f = 0.28$ in 75% hexanes/25% ethyl acetate). ^1H NMR (CDCl_3): δ 8.50- 8.47 (multiple peaks, 2H), 8.40 (d, $J = 2.8$ Hz, 1H), 7.21 (t, $J = 7.6$ Hz, 1H), 7.08-7.04 (multiple peaks, 3H), 4.13 (s, 2H), 2.32 (s, 3H). $^{13}\text{C}\{^1\text{H}\}$ NMR (CDCl_3): δ 156.53, 144.70, 144.00, 142.24, 138.34, 137.93, 129.67, 128.57, 127.44, 125.94, 41.84, 21.28. HRMS (ESI, m/z): $[\text{M}-\text{H}]^+$ calcd for $\text{C}_{12}\text{H}_{12}\text{N}_2$, 183.0922; found, 183.0920.

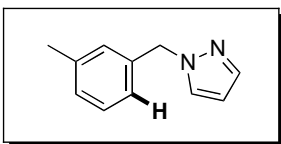


Substrate **52** was obtained as a colorless oil ($R_f = 0.26$ in 90% hexanes/10% ethyl acetate). ^1H NMR (CDCl_3): δ 8.74 (d, $J = 4.4$ Hz, 1H), 7.36-7.34 (multiple peaks, 2H), 7.23 (t, $J = 1.9$ Hz, 1H), 7.11-7.07 (multiple peaks, 3H), 4.21 (s, 2H), 2.35 (s, 3H). $^{13}\text{C}\{^1\text{H}\}$ NMR (CDCl_3): δ 162.68, 150.29, 138.71 (q, $^2J_{\text{CF}} = 33.7$ Hz), 138.40, 138.28, 129.80, 128.63, 127.50, 126.04, 122.80 (q, $^1J_{\text{CF}} = 271$ Hz), 118.56 (q, $^3J_{\text{CF}} = 3.6$ Hz), 116.84 (q, $^3J_{\text{CF}} = 2.9$ Hz), 44.58, 21.32. $^{19}\text{F}\{^1\text{H}\}$ NMR (CDCl_3): δ -64.78. HRMS (ESI, m/z): $[\text{M}-\text{H}]^+$ Calcd for $\text{C}_{14}\text{H}_{12}\text{F}_3\text{N}$, 250.0843; Found, 250.0842.

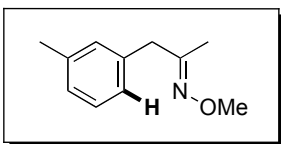
Synthesis of Substrates 11, 13, 15-16



Substrate **16** was prepared from 2-*m*-tolylacetaldehyde according to a literature procedure.³¹ Substrate **16** was obtained as a yellow oil ($R_f = 0.28$ in 70% hexanes/30% ethyl acetate). ^1H NMR (CDCl_3): δ 7.21 (t, $J = 7.4$ Hz, 1H), 7.09-7.01 (multiple peaks, 3H), 4.76 (m, 1H), 4.08 (qd, $J = 12.0, 4.8$ Hz, 2H), 3.64 (q, $J = 14.8$ Hz, 2H), 2.93 (dd, $J = 17.2, 11.2$ Hz, 1H), 2.60 (dd, $J = 17.2, 6.8$ Hz, 1H), 2.33 (s, 3H), 2.02 (s, 3H). $^{13}\text{C}\{^1\text{H}\}$ NMR (CDCl_3): δ 170.77, 157.56, 138.57, 135.36, 129.49, 128.72, 127.91, 125.72, 77.36, 65.04, 38.56, 33.85, 21.32, 20.07. IR (thin film): 1742 (br) cm^{-1} . HRMS (ESI, m/z): $[\text{M}]^+$ calcd for $\text{C}_{14}\text{H}_{17}\text{NO}_3$, 247.1208; found, 247.1201.

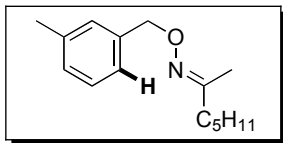


Substrate **17** was prepared from pyrazole and α -bromoxylenes according to a literature procedure.³² Substrate **17** was obtained as a red oil ($R_f = 0.24$ in 90% hexanes/10% ethyl acetate). ^1H NMR (CDCl_3): δ 7.56 (d, $J = 1.6$ Hz, 1H), 7.38 (d, $J = 2.4$ Hz, 1H), 7.24 (t, $J = 7.6$ Hz, 1H), 7.12 (d, $J = 7.6$ Hz, 1H), 7.04-7.01 (multiple peaks, 2H), 6.28 (t, $J = 2.0$ Hz, 1H), 5.28 (s, 2H), 2.33 (s, 3H). $^{13}\text{C}\{^1\text{H}\}$ NMR (CDCl_3): δ 139.41, 138.45, 136.47, 129.11, 128.69, 128.62, 128.34, 124.67, 105.82, 55.85, 21.31. HRMS (ESI, m/z): $[\text{M-H}]^+$ calcd for $\text{C}_{11}\text{H}_{12}\text{N}_2$, 171.0922; found, 171.0925.

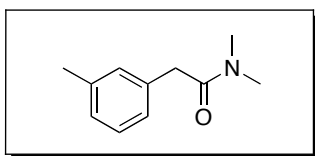


Substrate **11** was prepared from 3-methylphenylacetone and methoxyamine hydrochloride according to a literature procedure.³³ Substrate **11** was obtained as a clear oil as a 1 : 0.4 mixture of oxime isomers. Major oxime isomer: ^1H NMR (CDCl_3): δ 7.20 (m, 1H), 7.07-6.99 (multiple peaks, 3H), 3.91 (s, 3H), 3.44 (s, 2H), 2.35 (s, 3H), 1.75 (s, 3H). $^{13}\text{C}\{^1\text{H}\}$ NMR (CDCl_3): δ 156.62, 138.16, 136.78, 129.73, 128.39, 127.44, 126.04,

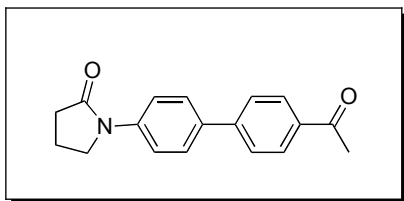
61.23, 41.97, 21.34, 13.52 . HRMS (ESI, m/z): $[M]^+$ calcd for $C_{11}H_{15}NO_3$, 177.1153; found, 177.1156.



Substrate **12** was prepared from 2-heptanone, hydroxylamine hydrochloride, and α -bromoxylenes according to a literature procedure.³⁴ Substrate **12** was obtained as a clear oil as a 1 : 0.9 mixture of oxime isomers ($R_f = 0.26$ in 97% hexanes/3% ethyl acetate). Major oxime isomer: 1H NMR ($CDCl_3$): δ 7.27 (t, $J = 7.6$ Hz, 1H), 7.20-7.17 (multiple peaks, 2H), 7.12 (d, $J = 7.2$ Hz, 1H), 5.07 (s, 2H), 2.40-2.38 (s, 3H), 2.19 (dd, $J = 8.0, 7.6$ Hz, 2H), 1.89 (s, 3H), 1.56-1.48 (multiple peaks, 2H), 1.37-1.27 (multiple peaks, 4H), 0.91 (m, 3H). $^{13}C\{^1H\}$ NMR ($CDCl_3$): δ 158.92, 138.18, 137.77, 128.61, 128.25, 128.12, 124.83, 75.15, 35.75, 31.30, 26.15, 22.38, 21.36, 14.07, 13.92. HRMS (ESI, m/z): $[M]^+$ calcd for $C_{15}H_{23}NO$, 233.1780; found, 233.1777.

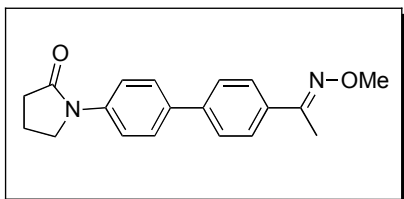


Substrate **13** was prepared from *m*-tolylacetic acid and dimethylamine according to a literature procedure. The 1H NMR and ^{13}C NMR data for **13** were identical to those reported in the literature.³⁵



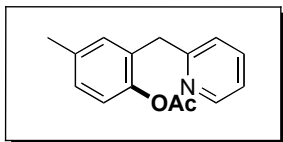
This compound was prepared via the Cu-catalyzed reaction of pyrrolidinone with 1-(4'-bromobiphenyl-4-yl) ethanone according to a literature procedure.³⁶ The product was obtained as a yellow solid. 1H NMR ($CDCl_3$): δ 8.02 (d, $J = 8.0$ Hz, 2H), 7.73 (d, $J = 8.8$ Hz, 2H), 7.69-7.63 (multiple peaks, 4H), 3.92 (t, $J = 6.8$ Hz, 2H), 2.67-2.63 (multiple peaks, 5H), 2.20 (quin, $J = 7.6$ Hz, 2H). $^{13}C\{^1H\}$ NMR ($CDCl_3$): δ 197.70, 174.37, 144.97, 139.52, 135.64, 135.60, 128.95, 127.58, 126.84, 120.07, 48.65, 32.76, 26.66,

17.97. IR (thin film): 1694, 1682 cm^{-1} . HRMS (ESI, m/z): $[M]^+$ calcd for $\text{C}_{18}\text{H}_{17}\text{NO}_2$, 279.1259; found, 279.1264.



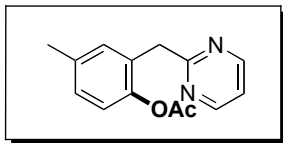
Substrate **63** was prepared from the corresponding ketone (above) and methoxyamine hydrochloride according to a literature procedure.³³ Substrate **63** was obtained as a yellow solid. ^1H NMR (CDCl_3): δ 7.73-7.69 (multiple peaks, 4H), 7.63-7.57 (multiple peaks, 4H), 4.02 (s, 3H), 3.90 (t, $J = 6.8$ Hz, 2H), 2.64 (t, $J = 8.0$ Hz, 2H), 2.24 (s, 3H), 2.19 (m, 2H). $^{13}\text{C}\{^1\text{H}\}$ NMR (CDCl_3): δ 174.25, 154.21, 140.94, 138.86, 136.37, 135.33, 127.27, 126.73, 126.41, 120.09, 61.93, 48.68, 32.72, 17.97, 12.51. IR (thin film): 1685 cm^{-1} . HRMS (ESI, m/z): $[M]^+$ calcd for $\text{C}_{19}\text{H}_{20}\text{N}_2\text{O}_2$, 308.1525; found, 308.1518.

General Procedure for Directed C-H Bond Acetoxylation: In a 20 mL vial, $\text{PhI}(\text{OAc})_2$ (0.49-0.86 mmol, 1.02-1.80 equiv) and $\text{Pd}(\text{OAc})_2$ (1.08 mg, 0.0048 mmol, 0.01 equiv) were combined in a mixture of AcOH (2.0 mL) and Ac_2O (2.0 mL). Substrate (0.48 mmol, 1.0 equiv) was added, the vial was sealed with a Teflon-lined cap, and the resulting solution was heated at 100 $^\circ\text{C}$ for 3-24 h. The reaction was cooled to room temperature, and the solvent was removed under vacuum. The resulting brown oil was purified by chromatography on silica gel. Each substrate was optimized for reaction time and equiv of the oxidant, as indicated below

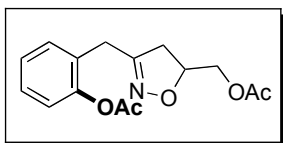


The reaction was run for 6 h with 1.02 equiv of $\text{PhI}(\text{OAc})_2$. The product **26** was obtained as a yellow oil (86.9 mg, 75% yield, $R_f = 0.27$ in 70% hexanes/30% ethyl acetate). ^1H NMR (CDCl_3): δ 8.52 (dd, $J = 4.8, 1.6$ Hz, 1H), 7.54 (dt, $J = 7.6, 1.6$ Hz, 1H), 7.11-7.02 (multiple peaks, 3H), 6.94 (d, $J = 8.0$ Hz, 1H), 4.06 (s, 2H), 2.30 (s, 3H), 2.16 (s, 3H), 2.58 (m, 1H), 0.88 (d, $J = 7.0$ Hz, 3H). $^{13}\text{C}\{^1\text{H}\}$ NMR (CDCl_3): δ 169.37, 159.88, 149.03, 146.79, 136.44, 135.78, 131.72, 130.83, 128.38, 122.85, 122.24, 121.24, 39.21, 20.78,

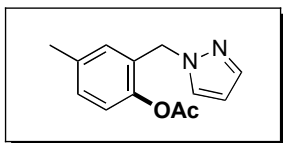
20.69. IR (thin film): 1759 cm^{-1} . HRMS (ESI, m/z): $[\text{M}+\text{H}]^+$ calcd for $\text{C}_{15}\text{H}_{15}\text{NO}_2$, 242.1181; found, 242.1177.



The reaction was run for 3 h with 1.02 equiv of $\text{PhI}(\text{OAc})_2$. The product **23** was obtained as a yellow oil (104.7 mg, 90% yield, $R_f = 0.28$ in 55% hexanes/45% ethyl acetate). ^1H NMR (CDCl_3): δ 8.62 (d, $J = 1.6$ Hz, 2H), 7.20 (s, 1H), 7.08-7.04 (multiple peaks, 2H), 6.92 (d, $J = 8.4$ Hz, 1H), 4.19 (s, 2H), 2.31 (s, 3H), 2.18 (s, 3H). $^{13}\text{C}\{^1\text{H}\}$ NMR (CDCl_3): δ 169.28, 169.14, 157.01, 146.73, 135.60, 131.84, 129.86, 128.47, 122.12, 118.51, 40.88, 20.72. IR (thin film): 1757 cm^{-1} . HRMS (ESI, m/z): $[\text{M}+\text{H}]^+$ calcd for $\text{C}_{14}\text{H}_{14}\text{N}_2\text{O}_2$, 243.1134; found, 243.1135.

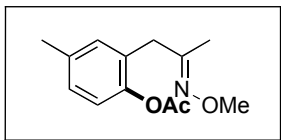


The reaction was run for 6 h with 1.1 equiv of $\text{PhI}(\text{OAc})_2$. The product **24** was obtained as a yellow oil (96.5 mg, 69% yield, $R_f = 0.28$ in 70% hexanes/30% ethyl acetate). ^1H NMR (CDCl_3): δ 7.09 (dd, $J = 8.0, 2.0$ Hz, 1H), 7.06 (s, 1H), 6.91 (d, $J = 8.0$ Hz, 1H), 4.71 (m, 1H), 4.10-4.01 (multiple peaks, 2H), 3.56 (s, 2H), 2.84 (dd, $J = 17.2, 10.8$ Hz, 1H), 2.51 (dd, $J = 17.2, 7.6$ Hz, 1H), 2.31 (s, 3H), 2.28 (s, 3H), 2.02 (s, 3H). $^{13}\text{C}\{^1\text{H}\}$ NMR (CDCl_3): δ 170.61, 169.68, 156.63, 146.98, 136.14, 131.18, 129.21, 127.10, 122.57, 77.48, 64.86, 38.38, 29.01, 20.69, 20.57. IR (thin film): 1746 (br) cm^{-1} . HRMS (ESI, m/z): $[\text{M}+\text{Na}]^+$ calcd for $\text{C}_{16}\text{H}_{19}\text{NO}_5$, 328.1161; found, 328.1150.

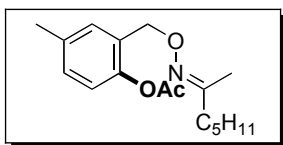


The reaction was run for 10 h with 1.02 equiv of $\text{PhI}(\text{OAc})_2$. The product **25** was obtained as a yellow oil (97.3 mg, 88% yield, $R_f = 0.28$ in 75% hexanes/25% ethyl acetate). ^1H NMR (CDCl_3): δ 7.53 (d, $J = 1.6$ Hz, 1H), 7.32 (d, $J = 2.4$ Hz, 1H), 7.14 (dd, $J = 8.4, 1.6$ Hz, 1H), 6.98 (d, $J = 8.4$ Hz, 1H), 6.95 (d, $J = 1.6$ Hz, 1H), 6.26 (t, $J = 2.0$ Hz, 1H), 5.23 (s, 2H), 2.30 (s, 3H), 2.26 (s, 3H). $^{13}\text{C}\{^1\text{H}\}$ NMR (CDCl_3): δ 169.07,

146.32, 139.18, 136.04, 130.11, 129.85, 129.14, 128.08, 122.34, 105.90, 50.73, 20.57, 20.50. IR (thin film): 1760 cm^{-1} . HRMS (ESI, m/z): $[\text{M}+\text{Na}]^+$ calcd for $\text{C}_{13}\text{H}_{14}\text{N}_2\text{O}_2$, 253.0953; found, 253.0953.

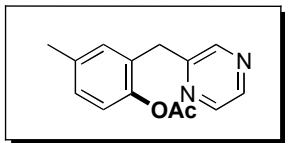


The reaction was run for 4.5 h with 1.1 equiv of $\text{PhI}(\text{OAc})_2$. The product **30** was obtained as a yellow oil as a 1 : 0.42 mixture of oxime isomers (89.2 mg, 79% yield, $R_f = 0.28$ in 89% hexanes/11% ethyl acetate). Major oxime isomer: ^1H NMR (CDCl_3): δ 7.06 (d, $J = 8.4$ Hz, 1H), 7.01 (s, 1H), 6.92 (d, $J = 8.4$ Hz, 1H), 3.88 (s, 3H), 3.57 (s, 2H), 2.32 (s, 3H), 2.28 (s, 3H), 1.71 (s, 3H). $^{13}\text{C}\{^1\text{H}\}$ NMR (CDCl_3): δ 169.45, 155.09, 146.92, 135.95, 131.52, 128.53, 128.42, 122.12, 61.21, 29.85, 20.86, 20.73, 19.37. IR (thin film): 1763 cm^{-1} . HRMS (ESI, m/z): $[\text{M}+\text{Na}]^+$ calcd for $\text{C}_{13}\text{H}_{17}\text{NO}_3$, 258.1106; found, 258.1100. Minor oxime isomer: ^1H NMR (CDCl_3): δ 7.08-7.05 (multiple peaks, 2H), 6.92 (d, $J = 8.0$ Hz, 1H), 3.87 (s, 3H), 3.37 (s, 2H), 2.32 (s, 3H), 2.30 (s, 3H), 1.70 (s, 3H). $^{13}\text{C}\{^1\text{H}\}$ NMR (CDCl_3): δ 169.60, 155.70, 147.18, 135.90, 131.52, 128.74, 128.47, 122.40, 61.24, 36.91, 20.90, 20.83, 13.33.

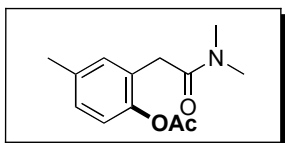


The reaction was run for 8 h with 1.1 equiv of $\text{PhI}(\text{OAc})_2$. The product **31** was obtained as a yellow oil as a 1 : 0.39 mixture of oxime isomers (97.9 mg, 70% yield, $R_f = 0.28$ in 90% hexanes/10% ethyl acetate). Major oxime isomer: ^1H NMR (CDCl_3): δ 7.23 (d, $J = 1.6$ Hz, 1H), 7.11 (dd, $J = 8.0, 1.6$ Hz, 1H), 6.94 (d, $J = 8.0$ Hz, 1H), 4.99 (s, 2H), 2.34 (s, 3H), 2.28 (s, 3H), 2.14 (t, $J = 7.6$ Hz, 2H), 1.83 (s, 3H), 1.48 (m, 2H), 1.34-1.24 (multiple peaks, 4H), 0.88 (t, $J = 7.2$ Hz, 3H). $^{13}\text{C}\{^1\text{H}\}$ NMR (CDCl_3): δ 169.33, 158.35, 146.63, 135.40, 130.40, 129.70, 129.24, 121.97, 70.47, 35.63, 31.23, 26.05, 22.29, 20.80, 20.73, 13.85. IR (thin film): 1757 cm^{-1} . HRMS (ESI, m/z): $[\text{M}+\text{Na}]^+$ calcd for $\text{C}_{17}\text{H}_{25}\text{NO}_3$, 314.1732; found, 314.1729. Minor oxime isomer: ^1H NMR (CDCl_3): δ 7.23 (d, $J = 1.6$ Hz, 1H), 7.11 (dd, $J = 8.0, 1.6$ Hz, 1H), 6.94 (d, $J = 8.0$ Hz, 1H), 4.96 (s, 2H), 2.34-2.28 (multiple peaks, 8H), 1.84 (s, 3H), 1.47 (m, 2H), 1.34-1.26 (multiple peaks, 4H), 0.88 (t,

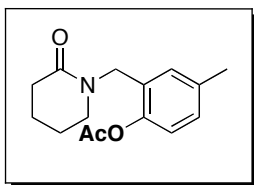
$J = 7.2$ Hz, 3H). $^{13}\text{C}\{^1\text{H}\}$ NMR (CDCl_3): δ 169.54, 159.15, 146.54, 135.55, 130.50, 130.36, 129.37, 121.04, 70.54, 35.74, 31.78, 29.29, 25.29, 22.41, 20.88, 20.86, 19.88.



The reaction was run for 24 h with 1.8 equiv of $\text{PhI}(\text{OAc})_2$. The product **32** was obtained as a yellow oil (86.1 mg, 74% yield, $R_f = 0.28$ in 60% hexanes/40% ethyl acetate). ^1H NMR (CDCl_3): δ 8.38 (s, 2H), 8.30 (s, 1H), 7.05 (s, 1H), 7.00 (d, $J = 8.0$ Hz, 1H), 6.89 (d, $J = 9.5, 8.0$ Hz, 1H), 3.99 (s, 2H), 2.23 (s, 3H), 2.13 (s, 3H). $^{13}\text{C}\{^1\text{H}\}$ NMR (CDCl_3): δ 168.79, 155.19, 146.43, 144.30, 143.59, 142.01, 135.54, 131.24, 129.44, 128.42, 122.06, 36.39, 20.41, 20.38. IR (thin film): 1760 cm^{-1} . HRMS (ESI, m/z): $[\text{M}+\text{H}]^+$ calcd for $\text{C}_{14}\text{H}_{14}\text{N}_2\text{O}_2$, 243.1134; found, 243.1132.

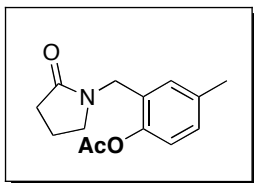


The reaction was run for 10 h with 1.1 equiv of $\text{PhI}(\text{OAc})_2$. The product **33** was obtained as a yellow oil (87 mg, 77% yield, $R_f = 0.28$ in 30% hexanes/60% ethyl acetate). ^1H NMR (CDCl_3): δ 7.07-7.06 (multiple peaks, 2H), 6.93 (d, $J = 8.8$ Hz, 1H), 3.52 (s, 2H), 2.96 (s, 3H), 2.93 (s, 3H), 2.30 (s, 3H), 2.29 (s, 3H). $^{13}\text{C}\{^1\text{H}\}$ NMR (CDCl_3): δ 170.16, 169.45, 146.49, 135.98, 130.63, 128.64, 127.00, 122.09, 37.55, 35.82, 35.57, 20.84. IR (thin film): $1759, 1645\text{ cm}^{-1}$. HRMS (ESI, m/z): $[\text{M}+\text{Na}]^+$ calcd for $\text{C}_{13}\text{H}_{17}\text{NO}_3$, 258.1106; found, 258.1101.

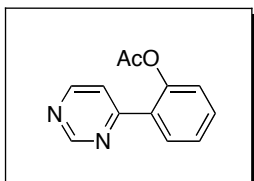


The reaction was run for 5 h with 0.10 equiv of $\text{Pd}(\text{OAc})_2$ and 2.02 equiv of $\text{PhI}(\text{OCOCF}_3)_2$ in AcOH (4 mL). The product **34** was obtained as a yellow oil (69 mg, 55% yield, $R_f = 0.24$ in 15% hexanes/85% ethyl acetate). ^1H NMR (CDCl_3): δ 7.09 (dd, $J = 8.0, 2.0$ Hz, 1H), 7.07 (br s, 1H), 6.91 (d, $J = 8.0$ Hz, 1H), 4.55 (s, 2H), 3.08 (t, $J = 5.6$ Hz, 2H), 2.42 (t, $J = 6.4$ Hz, 2H), 2.32 (s, 3H), 2.30 (s, 3H), 1.77-1.71 (multiple peaks,

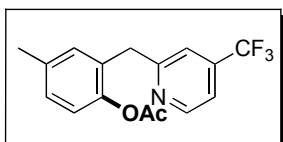
2H). $^{13}\text{C}\{^1\text{H}\}$ NMR (CDCl_3): δ 169.93, 169.51, 147.14, 135.88, 131.07, 129.42, 128.54, 122.43, 46.88, 44.87, 32.49, 23.03, 21.25, 21.00, 20.90. IR (thin film): 1759, 1639 cm^{-1} . HRMS (ESI, m/z): $[\text{M}+\text{Na}]^+$ calcd for $\text{C}_{15}\text{H}_{19}\text{NO}_3$, 284.1263; found, 284.1269.



The reaction was run for 5 h with 0.10 equiv of $\text{Pd}(\text{OAc})_2$ and 2.02 equiv of $\text{PhI}(\text{OCOCF}_3)_2$ in AcOH (4 mL). The product **35** was obtained as a yellow oil (58 mg, 49% yield, $R_f = 0.24$ in 15% hexanes/85% ethyl acetate). ^1H NMR (CDCl_3): δ 7.09 (dd, $J = 8.0, 2.0$ Hz, 1H), 7.06 (br s, 1H), 6.89 (d, $J = 8.0$ Hz, 1H), 4.34 (s, 2H), 3.13 (t, $J = 7.2$ Hz, 2H), 2.35 (t, $J = 8.0$ Hz, 2H), 2.30 (s, 3H), 2.27 (s, 3H), 1.91 (t, $J = 8.0$ Hz, 2H). $^{13}\text{C}\{^1\text{H}\}$ NMR (CDCl_3): δ 174.42, 169.91, 146.99, 135.83, 131.19, 129.60, 127.76, 122.45, 46.23, 41.73, 30.74, 20.87, 20.71, 17.57, 17.44. IR (thin film): broad strong peak at 1684 cm^{-1} . HRMS (ESI, m/z): $[\text{M}]^+$ calcd for $\text{C}_{15}\text{H}_{19}\text{NO}_3$, 189.1154; found, 189.1154.

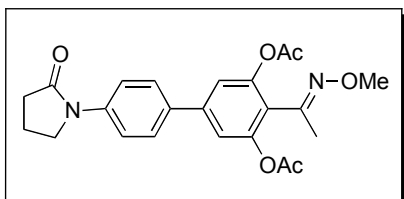


The reaction was run for 12 h with 2.0 equiv $\text{PhI}(\text{OAc})_2$. The product **40** was obtained as a yellow oil (140 mg, 52% yield, $R_f = 0.24$ in 75% hexanes/25% ethyl acetate). ^1H NMR (CDCl_3): δ 9.29 (d, $J = 1.2$ Hz, 1H), 8.77 (d, $J = 5.6$ Hz, 1H), 7.80 (dd, $J = 8.0, 1.6$ Hz, 1H), 7.60 (dd, $J = 6.4, 1.6$ Hz, 1H), 7.51 (td, $J = 8.0, 1.6$ Hz, 1H), 7.40 (td, $J = 8.0, 1.6$ Hz, 1H), 7.21 (d, $J = 8.0$ Hz, 1H), 2.24 (s, 3H). $^{13}\text{C}\{^1\text{H}\}$ NMR (CDCl_3): δ 169.18, 162.92, 158.91, 157.07, 148.44, 131.42, 130.64, 126.64, 123.65, 120.45, 21.02.

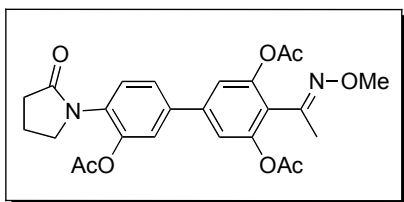


The reaction was run for 4.5 h with 1.02 equiv of $\text{PhI}(\text{OAc})_2$. The product **53** was obtained as a colorless oil (135.1 mg, 91% yield, $R_f = 0.27$ in 79% hexanes/21% ethyl acetate). ^1H NMR (500 MHz, CDCl_3): δ 8.71 (d, $J = 5.5$ Hz, 1H), 7.34 (d, $J = 5.0$ Hz, 1H), 7.29 (s, 1H), 7.11-7.09 (multiple peaks, 2H), 6.96 (d, $J = 8.5$ Hz, 1H), 4.12 (s, 2H),

2.33 (s, 3H), 2.19 (s, 3H). $^{13}\text{C}\{^1\text{H}\}$ NMR (CDCl_3): δ 169.26, 161.59, 150.22, 146.82, 138.66 (q, $^2J_{\text{C-F}} = 33.7$ Hz), 136.06, 131.71, 129.95, 128.88, 122.76 (q, $^1J_{\text{C-F}} = 271.7$ Hz), 122.43, 118.47 (q, $^3J_{\text{C-F}} = 3.7$ Hz), 116.96 (q, $^3J_{\text{C-F}} = 3.7$ Hz), 39.47, 20.82, 20.71. $^{19}\text{F}\{^1\text{H}\}$ NMR (CDCl_3): δ -64.85. IR (thin film): 1753 cm^{-1} . HRMS (ESI, m/z): $[\text{M}+\text{Na}^+]$ Calcd for $\text{C}_{16}\text{H}_{14}\text{F}_3\text{NO}_2$, 332.0874; Found, 332.0868.

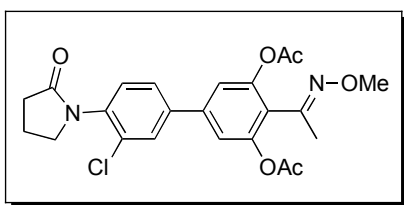


Substrate **63** (308 mg, 1.0 mmol, 1.0 equiv), $\text{Pd}(\text{OAc})_2$ (6.7 mg, 0.03 mmol, 0.03 equiv), and $\text{PhI}(\text{OAc})_2$ (902 mg, 2.8 mmol, 2.8 equiv) were combined in a 20 mL vial and were dissolved in a 1 : 1 mixture of AcOH and Ac_2O (8 mL). The vial was sealed with a Teflon-lined cap, and the mixture was heated at 100 °C for 12 h. The reaction was cooled to room temperature, the solvent was removed under vacuum, and the resulting brown oil was purified by column chromatography. The product **64** was obtained as a yellow solid (318 mg, 75% yield, $R_f = 0.30$ in 20% hexanes/80% ethyl acetate, mp = 234-237 °C). ^1H NMR (CDCl_3): δ 7.72 (d, $J = 8.8$ Hz, 2H), 7.57 (d, $J = 8.8$ Hz, 2H), 7.28 (s, 2H), 3.95 (s, 3H), 3.92 (t, $J = 7.6$ Hz, 2H), 2.66 (t, $J = 8.0$ Hz, 2H), 2.31 (s, 6H), 2.21 (quin, $J = 7.6$ Hz, 2H), 2.07 (s, 3H). $^{13}\text{C}\{^1\text{H}\}$ NMR (CDCl_3): δ 174.30, 168.74, 149.90, 149.23, 142.09, 139.48, 134.50, 127.33, 122.82, 119.88, 118.58, 62.03, 48.57, 32.72, 20.87, 17.88, 15.50. IR (thin film): 1769, 1686 cm^{-1} . HRMS (ESI, m/z): $[\text{M}+\text{H}]^+$ calcd for $\text{C}_{23}\text{H}_{24}\text{N}_2\text{O}_6$, 425.1713; found, 425.1705.

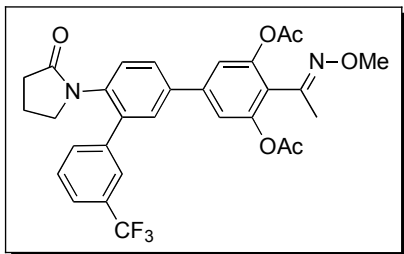


Substrate **64** (51 mg, 0.12 mmol, 1.0 equiv), $\text{Pd}(\text{OAc})_2$ (1.3 mg, 0.006 mmol, 0.03 equiv) and $\text{PhI}(\text{OAc})_2$ (121 mg, 0.24 mmol, 2.0 equiv) were combined in a 20 mL vial and were dissolved in a 1:1 mixture of AcOH and Ac_2O (1 mL). The vial was sealed with a Teflon-lined cap, and the mixture was heated at 100 °C for 12 h. The reaction was cooled to room temperature, the solvent was removed under vacuum, and the resulting brown oil

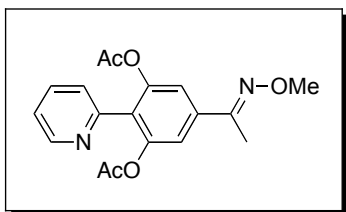
was purified by column chromatography. The product **65** was obtained as a yellow solid as a 1 : 0.2 mixture of oxime isomers (34 mg, 59% yield, $R_f = 0.25$ in 10% hexanes/90% ethyl acetate, mp = 64.5-70.1 °C). Major oxime isomer: ^1H NMR (CDCl_3): δ 7.43 (dd, $J = 8.0, 2.0$ Hz, 1H), 7.36-7.34 (multiple peaks, 2H), 7.21 (s, 2H), 3.95 (s, 3H), 3.76 (t, $J = 6.8$ Hz, 2H), 2.54 (t, $J = 8.0$ Hz, 2H), 2.28-2.22 (multiple peaks, 9H), 2.18 (m, 2H), 2.06 (s, 3H). $^{13}\text{C}\{^1\text{H}\}$ NMR (CDCl_3): δ 174.12, 168.64, 149.76, 149.27, 147.68, 145.93, 141.03, 138.87, 130.92, 128.25, 127.31, 125.04, 123.55, 122.51, 122.40, 118.95, 118.80, 62.05, 49.91, 31.10, 20.91, 20.83, 19.93, 19.24, 15.46. IR (thin film): 1770, 1700 cm^{-1} . HRMS (ESI, m/z): $[\text{M}+\text{Na}]^+$ calcd for $\text{C}_{25}\text{H}_{26}\text{N}_2\text{O}_8$, 505.1587; found, 505.1577.



Substrate **64** (51 mg, 0.12 mmol, 1.0 equiv), $\text{Pd}(\text{OAc})_2$ (1.3 mg, 0.006 mmol, 0.05 equiv) and *N*-chlorosuccinimide (32 mg, 0.24 mmol, 2.0 equiv) were combined in a 20 mL vial and were dissolved in AcOH (1 mL). The vial was sealed with a Teflon-lined cap, and the mixture was heated at 100 °C for 12 h. The reaction was cooled to room temperature, the solvent was removed under vacuum, and the resulting brown oil was purified by column chromatography. The product **66** was obtained as a yellow solid as a 1 : 0.5 mixture of oxime isomers (47 mg, 81% yield, $R_f = 0.28$ in 15% hexanes/85% ethyl acetate, mp = 66.8–73.2 °C). Major oxime isomer: ^1H NMR (CDCl_3): δ 7.64 (dd, $J = 5.2, 1.6$ Hz, 1H), 7.47 (m, 1H), 7.34 (s, 1H), 7.25 (s, 1H), 7.2 (s, 1H), 3.94 (s, 3H), 3.79 (t, $J = 6.8$ Hz, 2H), 2.58 (t, $J = 8.0$ Hz, 2H), 2.28-2.22 (multiple peaks, 8H), 2.06 (s, 3H). $^{13}\text{C}\{^1\text{H}\}$ NMR (CDCl_3): δ 175.00, 168.57, 149.79, 149.29, 147.59, 141.21, 139.84, 136.19, 132.51, 129.65, 128.98, 128.20, 126.44, 123.80, 118.94, 62.89, 49.84, 32.71, 36.34, 30.91, 20.93, 19.06, 15.41. IR (thin film): 1773, 1694 cm^{-1} . HRMS (ESI, m/z): $[\text{M}+\text{Na}]^+$ calcd for $\text{C}_{23}\text{H}_{23}\text{ClN}_2\text{O}_6$, 481.1142; found, 481.1144.

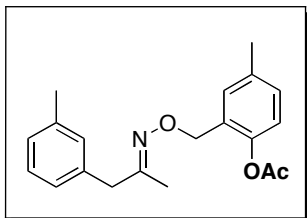


Substrate **64** (51 mg, 0.12 mmol, 1.0 equiv), Pd(OAc)₂ (1.3 mg, 0.006 mmol, 0.03 equiv) and [(*m*-CF₃C₆H₄)₂I]BF₄ (32 mg, 0.24 mmol, 2.0 equiv), NaHCO₃ (15 mg, 0.18 mmol, 1.5 equiv) were combined in a 20 mL vial and were dissolved in a toluene (1 mL). The vial was sealed with a Teflon-lined cap, and the mixture was heated at 100 °C for 12 h. The reaction was cooled to room temperature, the solvent was removed under vacuum, and the resulting brown oil was purified by column chromatography. The product **67** was obtained as a yellow solid as a 1:0.3 mixture of oxime isomers (53 mg, 78% yield, R_f = 0.28 in 25% hexanes/75% ethyl acetate, mp = 62.2-65.8 °C). Major oxime isomer: ¹H NMR (CDCl₃): δ 7.66-7.57 (multiple peaks, 4H), 7.53-7.49 (multiple peaks, 2H), 7.30 (s, 1H), 7.22 (s, 1H), 7.19 (s, 1H), 3.91 (s, 3H), 3.83 (t, *J* = 6.8 Hz, 1H), 3.25 (t, *J* = 6.8 Hz, 1H), 2.57 (t, *J* = 8.0 Hz, 1H), 2.36 (t, *J* = 8.0 Hz, 1H), 2.23 (s, 6H), 2.12 (t, *J* = 7.4 Hz, 1H), 2.03 (s, 3H), 1.88 (t, *J* = 7.4 Hz, 1H). ¹³C{¹H} NMR (CDCl₃): δ 175.46, 168.54, 168.48, 149.87, 149.31, 149.21, 141.45, 139.47, 138.62, 136.37, 131.81, 130.75 (q, ²*J*_{C-F} = 32.2 Hz), 129.25, 129.10, 128.82, 128.23, 127.31, 124.93 (q, ³*J*_{C-F} = 3.7 Hz), 124.45 (q, ³*J*_{C-F} = 3.8 Hz), 123.90 (q, ¹*J*_{C-F} = 271 Hz), 119.86, 118.98, 118.55, 61.99, 48.54, 32.69, 20.81, 18.85, 17.85, 15.46. ¹⁹F{¹H} NMR (CDCl₃): δ -62.57. IR (thin film): 1771, 1694 cm⁻¹. HRMS (ESI, *m/z*): [M+Na]⁺ calcd for C₃₀H₂₇F₃N₂O₆, 591.1719; found, 591.1719.

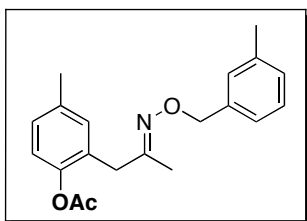


Pyridyl oxime ether substrate (250 mg, 1.11 mmol, 1.0 equiv), Pd(OAc)₂ (7.5 mg, 0.03 mmol, 0.03 equiv) and PhI(OAc)₂ (715 mg, 2.22 mmol, 2.0 equiv) were combined in a 20 mL vial and were dissolved in a 1 : 1 mixture of AcOH and Ac₂O (9.25 mL). The vial was sealed with a Teflon-lined cap, and the mixture was heated at 100 °C for 12 h. The reaction was cooled to room temperature, the solvent was removed under vacuum, and

the resulting brown oil was purified by column chromatography. The product **68** was obtained as a pale yellow solid (299 mg, 79% yield, $R_f = 0.26$ in 55% hexanes/45% ethyl acetate). $^1\text{H NMR}$ (CDCl_3): δ 8.73 (m, 1H), 7.74 (m, 1H), 7.42 (m, 2H), 7.35 (m, 1H), 7.27 (m, 1H), 4.01 (s, 3H), 2.21 (s, 3H), 2.04 (s, 6H).



Substrate **70** (200 mg, 0.75 mmol, 1.0 equiv), $\text{Pd}(\text{OAc})_2$ (8 mg, 0.04 mmol, 0.05 equiv) and $\text{PhI}(\text{OAc})_2$ (247 mg, 0.766 mmol, 1.02 equiv) were combined in a 20 mL vial and were dissolved in Benzene (6.3 mL). The vial was sealed with a Teflon-lined cap, and the mixture was heated at 100 °C for 12 h. The reaction was cooled to room temperature, the solvent was removed under vacuum, and the resulting brown oil was purified by column chromatography. The product **71** was obtained as a yellow oil as a 1 : 0.6 mixture of oxime isomers (73 mg, 30% yield, $R_f = 0.22$ in 91% hexanes/9% ethyl acetate). **Major oxime isomer:** $^1\text{H NMR}$ (CDCl_3): δ 7.25 (m, 1H) 7.18 (t, $J = 7.0$ Hz, 1H), 7.13 (dd, $J = 8.0, 2.0$ Hz, 1H), 7.04 (d, $J = 7.0$ Hz, 1H), 7.00 (br s, 1H), 6.97 (d, $J = 7.5$ Hz, 1H), 5.07 (s, 2H), 3.42 (s, 2H), 2.35 (s, 3H), 2.32 (s, 3H), 2.28 (s, 3H), 1.75 (s, 3H). **Minor oxime isomer:** $^1\text{H NMR}$ (CDCl_3): δ 7.24 (br s, 1H), 7.18-7.12 (multiple peaks, 2H), 7.04-6.96 (multiple peaks, 3H), 5.05 (s, 2H), 3.66 (s, 2H), 2.33 (s, 3H), 2.31 (s, 3H), 2.28 (s, 3H), 1.77 (s, 3H).



Substrate **70** (200 mg, 0.75 mmol, 1.0 equiv), $\text{Pd}(\text{OAc})_2$ (8 mg, 0.04 mmol, 0.05 equiv) and $\text{PhI}(\text{OAc})_2$ (247 mg, 0.766 mmol, 1.02 equiv) were combined in a 20 mL vial and were dissolved in a 1:1 mixture of AcOH and A_2O (6.3 mL). The vial was sealed with a Teflon-lined cap, and the mixture was heated at 100 °C for 12 h. The reaction was cooled to room temperature, the solvent was removed under vacuum, and the resulting brown oil

was purified by column chromatography. The product was obtained as a yellow oil as a 1:1 mixture of regio isomers **71** and **72**. Characterization for the oxime isomers for regioisomer **71** is shown above. Regioisomer **72** was obtained in a 1:0.4 mixture of oxime isomers (134 mg, 55% yield, $R_f = 0.22$ in 91% hexanes/9% ethyl acetate). **Major oxime isomer:** $^1\text{H NMR}$ (CDCl_3): δ 7.24 (d, $J = 7.0$ Hz, 1H) 7.18-7.17 (multiple peaks, 2H), 7.11 (d, $J = 7.0$ Hz, 1H), 7.06 (d, $J = 7.5$ Hz, 1H), 7.01 (br s, 1H), 6.91 (d, $J = 8.0$ Hz, 1H), 5.08 (s, 2H), 3.37 (s, 2H), 2.36 (s, 3H), 2.31 (s, 3H), 2.21 (s, 3H), 1.75 (s, 3H). **Minor oxime isomer:** $^1\text{H NMR}$ (CDCl_3): δ 7.23 (d, $J = 7.5$ Hz, 1H), 7.18-7.16 (multiple peaks, 2H), 7.11 (d, $J = 7.0$ Hz, 1H), 7.05 (d, $J = 8.0$ Hz, 1H), 7.00 (br s, 1H), 6.92 (d, $J = 8.5$ Hz, 1H), 5.08 (s, 2H), 3.62 (s, 2H), 2.36 (s, 3H), 2.29 (s, 3H), 2.22 (s, 3H), 1.73 (s, 3H).

General Procedure for Kinetics Experiments. Kinetics experiments were run in two dram vials sealed with Teflon-lined caps. Each data point represents a reaction in an individual vial, with each vial containing an identical concentration of oxidant, catalyst, and substrate. The vials were charged with $\text{PhI}(\text{OAc})_2$ (0.0158 g, 0.049 mmol, 1.02 equiv, added as a solid), substrate (0.048 mmol, 1.0 equiv, added as a 0.96 M stock solution in AcOH), and $\text{Pd}(\text{OAc})_2$ (0.11 mg, 0.00048 mmol, 0.01 equiv, added as a 0.0096 M stock solution in AcOH), and the resulting mixtures were diluted to a total volume of 400 mL of a 1 : 1 mixture of AcOH and Ac_2O . The vials were then heated at 80 °C for various amounts of time. Reactions were quenched by cooling the vial at 0 °C for 5 min, followed by the addition of a 2% solution of pyridine in CH_2Cl_2 (2 mL). An internal standard (pyrene) was then added, and the reactions were analyzed by gas chromatography. Each reaction was monitored to ~10% (8.6-11.0%) conversion, and rate constants were calculated for each reaction using the initial rates method. Each kinetics experiment was run in triplicate, and the data shown in the Hammett plots represent an average of these three runs.

General Procedure for Competition Experiments. A two dram vial was sequentially charged with $\text{PhI}(\text{OAc})_2$ (0.0158 g, 0.049 mmol, 1.02 equiv, added as a solid), substrate A (0.048 mmol, 1.0 equiv, added as a 0.96 M stock solution in AcOH),

substrate B (0.048 mmol, 1.0 equiv, added as a 0.96 M stock solution in AcOH), and Pd(OAc)₂ (0.11 mg, 0.00048 mmol, 0.01 equiv, added as a 0.0096 M stock solution in AcOH), and the resulting mixtures were diluted to a total volume of 400 mL of a 1 : 1 mixture of AcOH and Ac₂O. The reaction was heated at 80 °C for 12 h, and then cooled to room temperature. A GC standard (pyrene) was added, and the reaction was analyzed by gas chromatography.

4.11 References

- (1) Desai, L. V.; Malik, H. A.; Sanford, M. S. *Org. Lett.* **2006**, *8*, 1141-1144.
- (2) Dick, A. R.; Hull, K. L.; Sanford, M. S. *J. Am. Chem. Soc.* **2004**, *126*, 2300-2301.
- (3) Kalyani, D.; Deprez, N. R.; Desai, L. V.; Sanford, M. S. *J. Am. Chem. Soc.* **2005**, *127*, 7330-7331.
- (4) Kalyani, D.; Sanford, M. S. *Org. Lett.* **2005**, *7*, 4149-4152.
- (5) Hull, K. L.; Lanni, E. L.; Sanford, M. S. *J. Am. Chem. Soc.* **2006**, *128*, 14047-14049.
- (6) Giri, R.; Chen, X.; Hao, X. S.; Li, J. J.; Liang, J.; Fan, Z. P.; Yu, J. Q. *Tetrahedron-Asymmetr.* **2005**, *16*, 3502-3505.
- (7) Shabashov, D.; Daugulis, O. *Org. Lett.* **2005**, *7*, 3657-3659.
- (8) Zaitsev, V. G.; Shabashov, D.; Daugulis, O. *J. Am. Chem. Soc.* **2005**, *127*, 13154-13155.
- (9) Thu, H. -.; Yu, W. -.; Che, C. -. *J. Am. Chem. Soc.* **2006**, *128*, 9048-9049.
- (10) Daugulis, O.; Zaitsev, V. G. *Angew. Chem., Int. Ed.* **2005**, *44*, 4046-4048.
- (11) Natarajan, A.; Guo, Y.; Harbinski, F.; Fan, Y. -.; Chen, H.; Luus, L.; Diercks, J.; Aktas, H.; Chorev, M.; Halperin, J. A. *J. Med. Chem.* **2004**, *47*, 4979-4982.
- (12) Chen, J.; Deady, L. W.; Kaye, A. J.; Finlay, G. J.; Baguley, B. C.; Denny, W. A. *Bioorg. Med. Chem.* **2002**, *10*, 2381-2386.
- (13) deSouza, N. J.; Gupte, S. V.; Deshpande, P. K.; Desai, V. N.; Bhawsar, S. B.; Yeole, R. D.; Shukla, M. C.; Strahilevitz, J.; Hooper, D. C.; Bozdogan, B.; Appelbaum, P. C.; Jacobs, M. R.; Shetty, N.; Patel, M. V.; Jha, R.; Khorakiwala, H. F. *J. Med. Chem.* **2005**, *48*, 5232-5242.
- (14) Oh, L. M. *Tetrahedron Lett.* **2006**, *47*, 7943-7946.
- (15) Romine, J. L.; Martin, S. W.; Gribkoff, V. K.; Boissard, C. G.; Dworetzky, S. I.; Natale, J.; Li, Y.; Gao, Q.; Meanwell, N. A.; Starrett, J. E. *J. Med. Chem.* **2002**, *45*, 2942-2952.
- (16) Jeon, S. L.; Loveless, D. M.; Yount, W. C.; Craig, S. L. *Inorg. Chem.* **2006**, *45*, 11060-11068.
- (17) Ryabov, A. D. *Chem. Rev.* **1990**, *90*, 403-424.

- (18) Davies, D. L.; Donald, S. M. A.; Macgregor, S. A. *J. Am. Chem. Soc.* **2005**, *127*, 13754-13755.
- (19) Coombes, R. G. *In Electrophilic Aromatic Substitution; Organic Reaction Mechanisms*, 2002; **2006**, 209-221.
- (20) Lafrance, M.; Fagnou, K. *J. Am. Chem. Soc.* **2006**, *128*, 16496-16497.
- (21) Martín-Matute, B.; Mateo, C.; Cárdenas, D. J.; Echavarren, A. M. *Chemistry* **2001**, *7*, 2341-2348.
- (22) Yagyu, T.; Iwatsuki, S.; Aizawa, S.; Funahashi, S. *Bull. Chem. Soc. Jpn.* **1998**, *71*, 1857-1862.
- (23) Alsters, P. L.; Teunissen, H. T.; Boersma, J.; Spek, A. L.; van Koten, G. *Organometallics* **1993**, *12*, 4691-4696.
- (24) Viciu, M. S.; Nolan, S. P. *Palladium in Organic Synthesis* **2005**, 241-278.
- (25) Chiong, H. A.; Pham, Q.; Daugulis, O. *J. Am. Chem. Soc.* **2007**, *129*, 9879-9884.
- (26) Sokolov, S. D.; Tikhomirova, G. B.; Turchin, K. F. *Chem. Heterocycl. Compd.* **1985**, *21*, 507-509.
- (27) Catalan, J.; Claramunt, R. M.; Elguero, J.; Laynez, J.; Menendez, M.; Anvia, F.; Quian, J. H.; Taagepera, M.; Taft, R. W. *J. Am. Chem. Soc.* **1988**, *110*, 4105-4111.
- (28) Mossi, W.; Klaus, A. J.; Rys, P. *Helv. Chim. Acta* **1992**, *75*, 2531-2537.
- (29) Kalyani, D.; Dick, A. R.; Anani, W. Q.; Sanford, M. S. *Org. Lett.* **2006**, *8*, 2523-2526.
- (30) Utas, J.; Olofsson, B.; Åkermark, B. *Synlett* **2006**, 1965-1967.
- (31) Minter, A. R.; Fuller, A. A.; Mapp, A. K. *J. Am. Chem. Soc.* **2003**, *125*, 6846-6847.
- (32) Bogdal, D.; Pielichowski, J.; Jaskot, K. *Heterocycles* **1997**, *45*, 715-722.
- (33) Booth, S. E.; Jenkins, P. R.; Swain, C. J.; Sweeney, J. B. *J. Chem. Soc., Perkin Trans. 1* **1994**, 3499-3508.
- (34) Li, C. B.; Zhang, H.; Cui, Y.; Zhang, S. M.; Zhao, Z. Y.; Choi, M. C. K.; Chan, A. S. C. *Syn. Commun.* **2003**, *33*, 543-546.
- (35) Lu, T.; Xue, C.; Luo, F. *Tetrahedron Lett.* **2003**, *44*, 1587-1590.
- (36) Deng, W.; Zhang, C.; Liu, M.; Zou, Y.; Liu, L.; Guo, Q. *Chin. J. Chem.* **2005**, *23*, 1241-1246.

Chapter 5

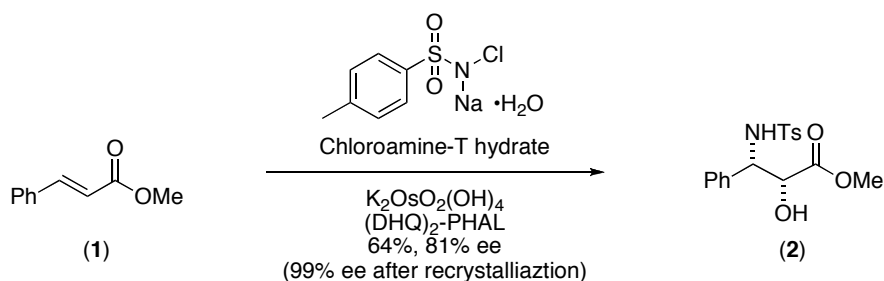
Palladium-Catalyzed 1,2-Difunctionalization of Alkenes

5.1 Background and Significance

Oxidative amination reactions have been an important area of research in organic chemistry.¹⁻⁴ In particular, aminooxygenation reactions of alkenes, leading to vicinally difunctionalized products, with two distinct carbon-heteroatom bonds, provide an attractive route towards the synthesis of small molecules of synthetic and pharmaceutical interest.

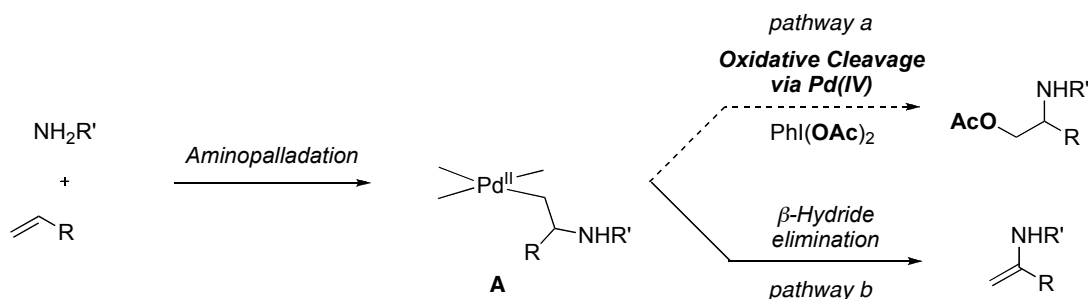
The development of a Pd^{II/IV} catalyzed method to form aminooxygenated products could allow access to β -amino alcohols (via intermolecular reactions) and nitrogen containing heterocycles (via intramolecular reactions).^{5, 6} Some of the most common alternative approaches to vicinal amino alcohols involve: (i) functional group manipulations of imine or carbonyl groups via reduction or nucleophilic addition,⁵ (ii) ring opening reactions of epoxides and aziridines,⁵ (iii) aminohydroxylation of olefins,⁵ and (iv) aldol or pinacol-type coupling reactions.⁵ Hydroxyamination of alkenes is the most straightforward route for vicinal amino alcohol synthesis, and the Sharpless Os-catalyzed asymmetric aminohydroxylation reaction (Scheme 5.1) is probably the most widely used of these reactions.⁷

Scheme 5.1: Osmium-Catalyzed Aminohydroxylation of Alkenes



We hope to access vicinal aminoxygenated compounds by developing a $\text{Pd}^{\text{II/IV}}$ catalyzed route. The two key steps of the proposed reaction involve (i) aminopalladation followed by (ii) oxidative cleavage of the resultant carbon-palladium bond (Scheme 5.2, pathway a).

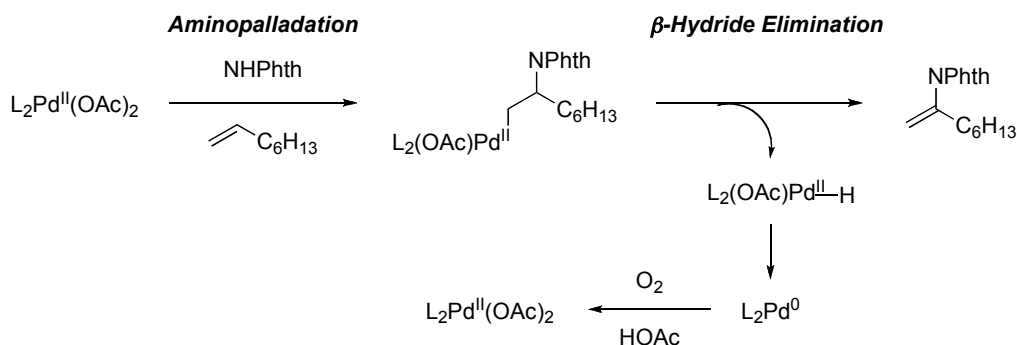
Scheme 5.2. Oxidative Cleavage of Pd-Alkyl Intermediates Formed via Aminopalladation



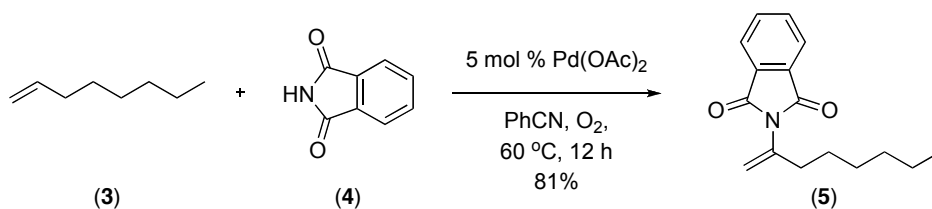
In order to achieve the desired aminoxygenation transformation, the key challenge that needs to be addressed is competing β -hydride elimination from the Pd-alkyl intermediate **A** (Scheme 5.2, pathway b). Importantly, several research groups have recently demonstrated that the undesired aminopalladation/ β -hydride elimination sequence can be a useful and efficient synthetic transformation.² Stahl and co-workers have developed the most effective of these systems.⁸ They have demonstrated the oxidative amination of activated and unactivated olefins with nitrogen nucleophiles including carboxamides, carbamates and sulfoamides via a $\text{Pd}^{\text{II/0}}$ reaction manifold (Scheme 5.3). A representative example is illustrated in Scheme 5.4, and involves the

synthesis of enamide **5** from octene and phthalimide in the presence of 5 mol % Pd(OAc)₂ and O₂ as the oxidant.

Scheme 5.3: Proposed Mechanism for Formation of Enamide **5** Formation



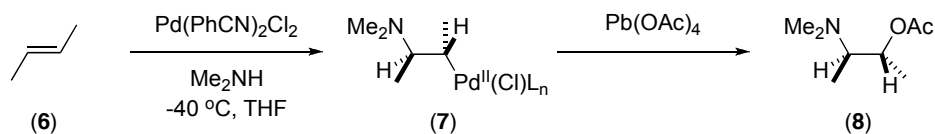
Scheme 5.4. Synthesis of Enamide **5** via Aminopalladation/ β -Hydride Elimination



In 1980, Backvall demonstrated that Pd-alkyl intermediates generated upon aminopalladation can be intercepted by strong oxidants at -40 °C without competing β -hydride elimination.⁹ For example, the reaction of *trans*-butene with stoichiometric Pd(PhCN)₂Cl₂ and dimethylamine afforded the Pd-alkyl intermediate **7**, and subsequent addition of Pb(OAc)₄ led to the formation of aminoxygenated product **8**. As shown in Scheme 5.5, this reaction was proposed to proceed via *trans*-aminopalladation followed by oxidative cleavage of the palladium-carbon bond with inversion of stereochemistry at the carbon. The mechanism of aminopalladation was elucidated by trapping the Pd^{II} intermediate **7** with LiAlD₄ at -70 °C to form deuterated amino butane. Cope elimination of the amine then allowed stereochemical analysis of the deuterated butene. Although this reaction illustrates the feasibility of aminoxygenation, it is limited by the need for a stoichiometric amount of palladium. The electron rich amines used in this reaction (for

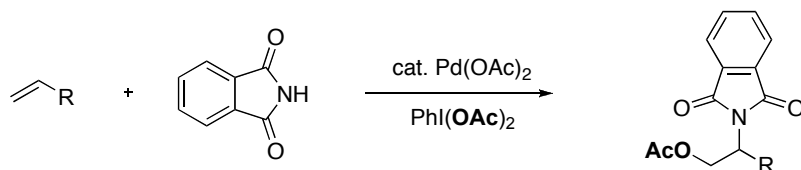
example, dimethylamine) coordinate more strongly to palladium than alkenes and therefore inhibit catalytic turnover.

Scheme 5.5. Stoichiometric Aminoacetoxylation Reaction Reported by Backvall



As described in Chapter 1, we have been able to successfully out-compete β -hydride elimination and intercept cyclopalladated Pd-alkyl intermediates with $\text{PhI}(\text{OAc})_2$ via a $\text{Pd}^{\text{II/IV}}$ catalytic cycle. Based on this and on Backvall's precedent,⁹ we envisioned the development of a Pd-catalyzed aminoxygenation reaction using a Pd^{II} catalyst and $\text{PhI}(\text{OAc})_2$ as a strong oxidant. As shown in Scheme 5.6, we speculated that the use of $\text{PhI}(\text{OAc})_2$ might allow us to oxidatively intercept the intermediate **A** (illustrated in Scheme 2). Additionally, the use of moderately nucleophilic phthalimide might attenuate its binding to Pd, hence allowing for catalytic turnover.

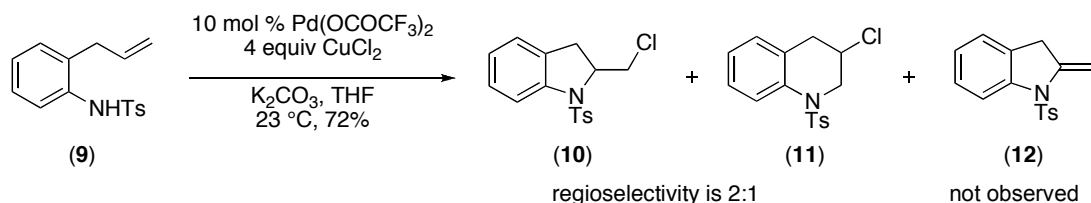
Scheme 5.6. Proposed $\text{Pd}^{\text{II/IV}}$ Catalyzed Aminoxygenation of Olefins



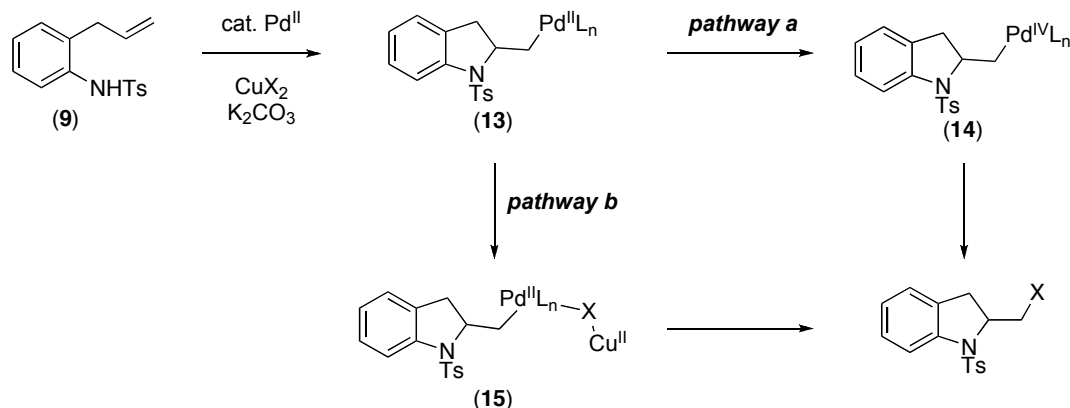
Palladium alkyl intermediates generated upon aminopalladation, such as **A**, have been previously shown to undergo a number of reactions, including olefin insertion,⁸ carbonylation,^{10, 11} and oxidative cleavage with CuCl_2 or CuBr_2 to form C–C, C–Cl and C–Br bonds, respectively. For example, Chemler has demonstrated the intramolecular aminochlorination of substrate **9** using 5 mol % $\text{Pd}(\text{OAc})_2$ and 4 equiv of CuCl_2 (Scheme 5.7).¹² Interestingly, competing β -hydride elimination products such as **12** were not observed in this reaction. Two possible mechanisms have been proposed, and both initiate with an intramolecular aminopalladation to afford intermediate **13** (Scheme 5.8) The first (Scheme 5.8, path a) involves oxidative cleavage of the Pd–C bond in **13** with

CuCl₂ via a Pd^{IV} intermediate. The second (Scheme 5.8, path b) proposes a copper assisted ligand transfer to form the C–Cl bond, without a change in oxidation state at Pd^{II}.

Scheme 5.7. Palladium-Catalyzed Intramolecular Aminochlorination with CuCl₂



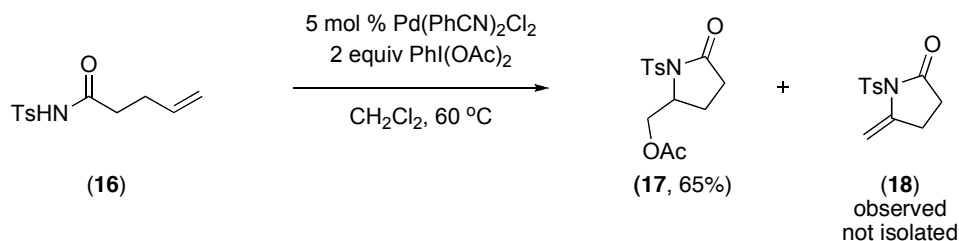
Scheme 5.8: Proposed Mechanism for Pd-Catalyzed Intramolecular Aminochlorination



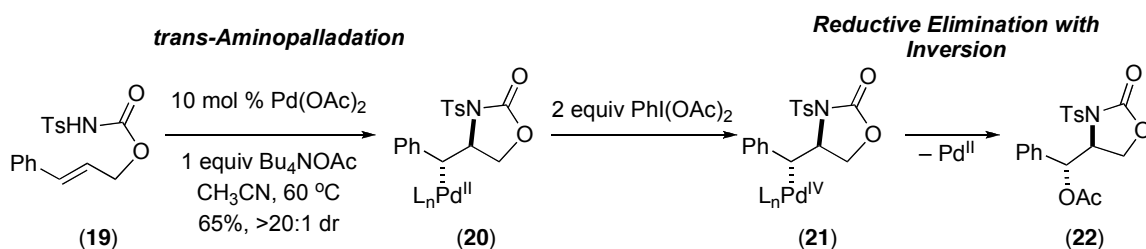
As we began this project, several groups reported Pd-catalyzed intramolecular olefin aminoacetoxylation and diamination reactions similar to the transformation that we proposed. For example, Sorensen demonstrated intramolecular aminopalladation with substrates such as *N*-tosylamide **16** to form oxazolidinone **17**.¹³ The use of Pd(OAc)₂ as a catalyst resulted in significant quantities of β-hydride product **18**. However, this pathway could be suppressed by employing a chloride-based catalyst. Hence, using 10 mol % Pd(PhCN)₂Cl₂ and 2 equiv PhI(OAc)₂ led to the formation of **17** in 65% yield (Scheme 5.9). Reaction of cinnamyl alcohol-derived *N*-tosyl carbamate **19** proceeded stereospecifically to afford product **22**, which led to speculation that the mechanism involved *trans*-aminopalladation followed by C–O bond-forming reductive elimination with inversion of stereochemistry at the carbon (Scheme 5.10). However, no other mechanistic experiments were conducted to support this claim. Later reports by Muniz

suggest that *cis*-aminopalladation followed by reductive elimination with inversion of stereochemistry is more likely.

Scheme 5.9. Palladium-Catalyzed Intramolecular Aminoacetoxylation with $\text{PhI}(\text{OAc})_2$

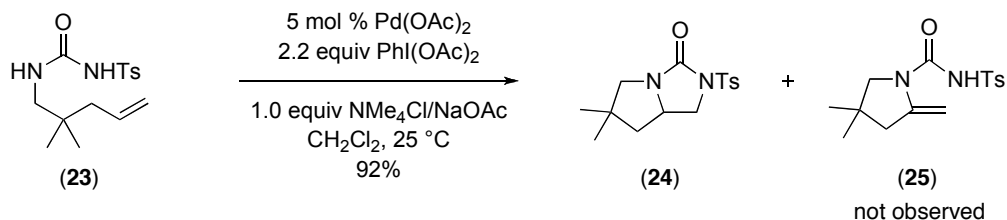


Scheme 5.10. Proposed Mechanism for Pd-Catalyzed Intramolecular Aminoacetoxylation

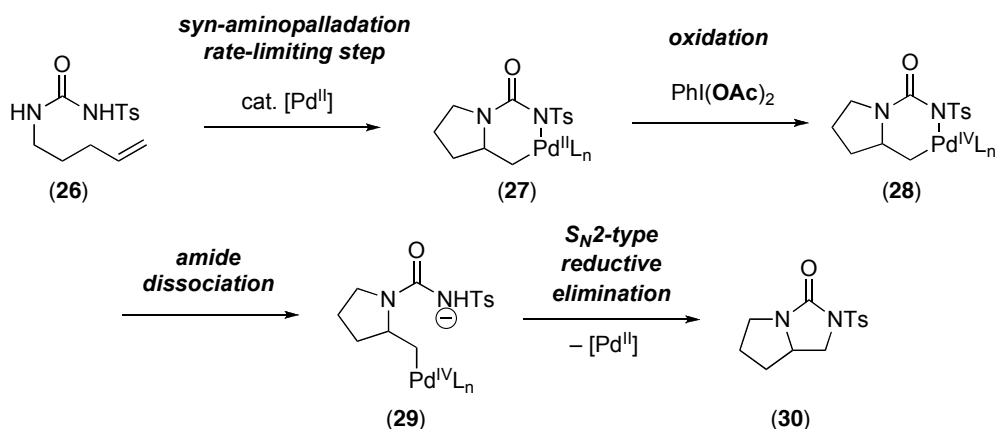


A later report by Muniz and co-workers demonstrated the Pd-catalyzed oxidative intramolecular diamination of olefins.^{14, 15} They were able to efficiently generate bicyclic and tricyclic substituted urea derivatives through diamination of substrates such as **23**, using 5 mol % $\text{Pd}(\text{OAc})_2$ and 2.2 equiv $\text{PhI}(\text{OAc})_2$ (Scheme 5.11). The authors did not observe products such as **25**, resulting from competing β -hydride elimination. A mechanism involving: (i) rate-limiting *cis*-aminopalladation to form **27**, (ii) oxidation to Pd^{IV} complex **28**, (iii) amide dissociation, and (iv) $\text{S}_{\text{N}}2$ -type reductive elimination with inversion of stereochemistry at carbon was proposed (Scheme 5.12). Experiments including deuterium labeling, kinetics, solvent effects, electronic substitution effects, and *in situ* NMR investigation were used to elucidate this mechanism.

Scheme 5.11. Palladium-Catalyzed Intramolecular Diamination Reactions

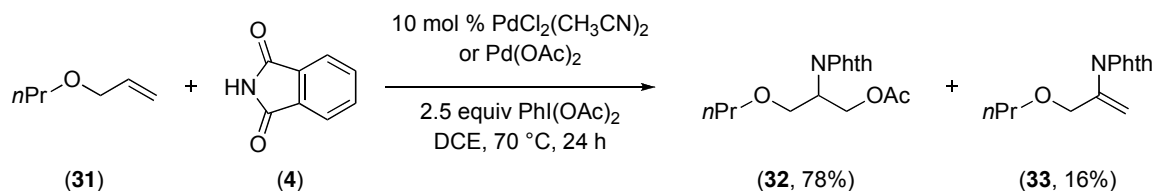


Scheme 5.12: Proposed Mechanism for Diamination Reactions



As discussed above, we desired to develop an intermolecular aminoacetoxylation reaction. Concurrent to our work, Stahl and co-workers published the intermolecular variant of oxidative aminoacetoxylation of olefins.¹⁶ Using phthalimide as the nitrogen nucleophile, they showed high yielding aminoacetoxylation of allyl ether substrates such as **31**. They also observed the formation of β -hydride elimination products such as **33**, albeit in low yield. They proposed that coordination of the metal with the oxygen in the ether linkage suppressed β -hydride elimination. Through detailed mechanistic experiments, they proposed a mechanism involving *cis*-aminopalladation followed by S_N2-type C–O bond-forming reductive elimination at Pd^{IV} with inversion of stereochemistry at carbon.

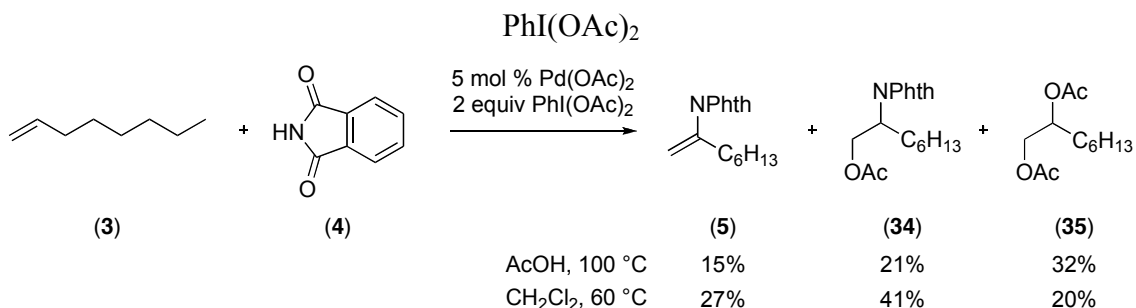
Scheme 5.13. Palladium-Catalyzed Intermolecular Aminoacetoxylation



5.2 Initial Investigation

Our initial studies focused on the reaction between 1-octene and phthalimide. These substrates were chosen because Stahl had demonstrated their ability to undergo efficient aminopalladation (Scheme 5.4).⁸ Gratifyingly, subjection of 1-octene and phthalimide to 5 mol% $\text{Pd}(\text{OAc})_2$ and 1.5 equiv $\text{PhI}(\text{OAc})_2$ in AcOH at 100 °C afforded the 1,2-aminoacetoxylation product **34** in 21% isolated yield. This low yield was due to competitive formation of two side products: (i) olefin **5** (generated via termination of the reaction by β -hydride elimination) and (ii) diacetoxylation product **35**. Notably, Stahl obtained similar results with substrate **3**.

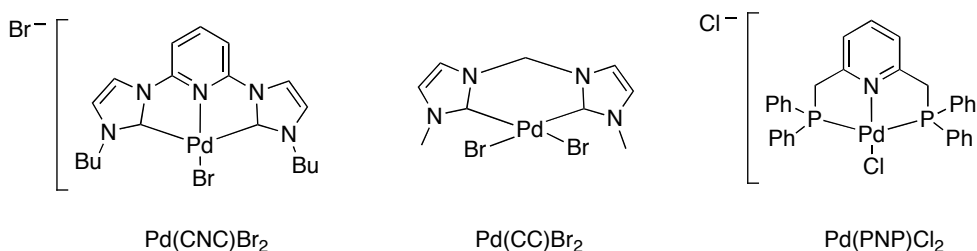
Scheme 5.14. Palladium-Catalyzed Reaction of 1-Octene with Phthalimide and



Optimization Studies. Several reaction parameters such as solvent, catalyst, and temperature were screened in order to increase the yield of the desired product **34**. Solvents such as AcOH led to increased yields of the undesired diacetoxylation product **35**, while dichloroethane, CH_3CN , and CH_2Cl_2 were most effective in affording **34**. Interestingly, reactions in THF only afforded the β -hydride elimination product **5**.

A survey of various catalysts revealed that $\text{Pd}(\text{PhCN})_2\text{Cl}_2$ and $\text{Pd}(\text{CH}_3\text{CN})_2\text{Cl}_2$ (which were found to decrease β -hydride elimination in Sorensen's system) led to similar yields of products **34** and **5** as $\text{Pd}(\text{OAc})_2$. In an attempt to suppress β -hydride elimination, we investigated palladium catalysts containing bidentate and tridentate ligands (Figure 5.1). We thought that having a multicoordinated ligand on the metal would limit vacant *cis* coordination sites, which are required for β -hydride elimination. Consistent with this hypothesis, $\text{Pd}(\text{CC})\text{Br}_2$, $\text{Pd}(\text{CNC})\text{Br}_2$, and $\text{Pd}(\text{PNP})\text{Cl}_2$ (Figure 5.1) afforded only trace amounts of the β -hydride products; however, the desired product **34** was also obtained in low yield with these catalysts. We next attempted to increase catalyst reactivity by moving to $\text{Pd}(\text{O}_2\text{CCF}_3)_2$, which contains a more electrophilic Pd center. However, with this catalyst we observed an increase in the relative rate of decomposition of the olefins. Lowering the temperature of the reaction from 100 °C to 60 °C did slow down the rate of Pd-catalyzed olefin decomposition.

Figure 5.1: Palladium Catalysts Containing Bi- and Tridentate Ligands

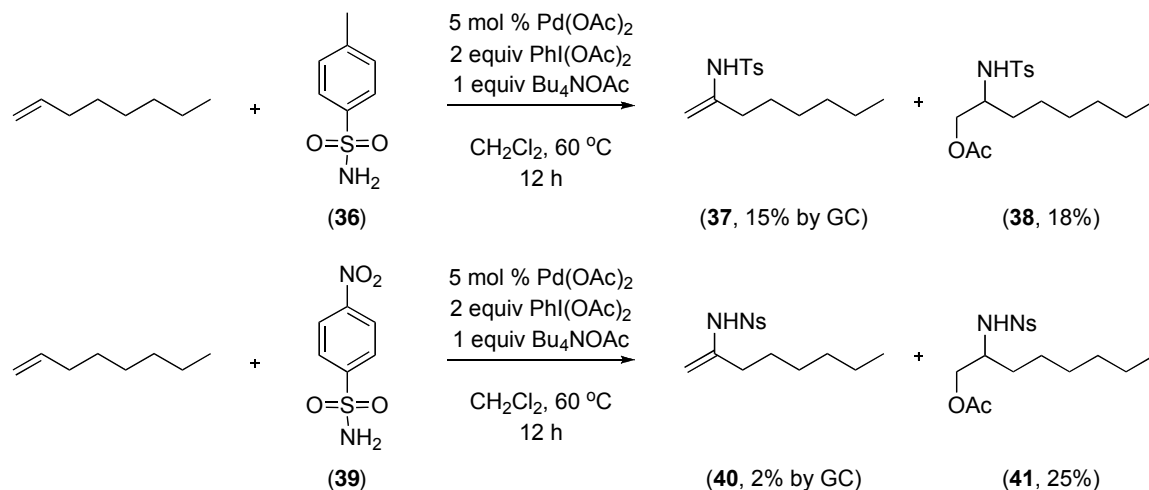


Based on all of these studies, the final optimized conditions for this reaction were 5 mol % $\text{Pd}(\text{OAc})_2$ and 2 equiv $\text{PhI}(\text{OAc})_2$ in CH_2Cl_2 at 60 °C, which afforded 41% yield of the desired product **34**. Despite these optimization studies, the relative rate of β -hydride elimination versus oxidation was still competitive, and 41% yield of 1,2-difunctionalized product **34** was obtained under these conditions.

Exploration of Different Olefin and Nucleophile Partners. We wondered if a different nucleophile partner would provide higher yields in this reaction. As such, a series of carboxamides, carbamates and sulfonamides were investigated; however, only *p*-toluenesulfonamide (TsNH_2) and *p*-nitrobenzenesulfonamide (NsNH_2) afforded the desired aminoacetoxylated product in greater than 5% yield under the optimized reaction

conditions from above (5 mol % Pd(OAc)₂, 2 equiv PhI(OAc)₂ in CH₂Cl₂ at 60 °C). We next attempted to increase the yield of the desired product with these nucleophiles through the addition of bases. Strong bases such as NaOtBu and Cs₂CO₃ either led to decomposition of 1-octene or resulted in greater quantities of the β-hydride elimination product (**37**). Weak bases such as Na₂SO₄ and MgO did not hamper the reaction, but also did not improve the yield of **38**. However, interestingly, the addition of acetate sources such as NaOAc and LiOAc increased the yield of the desired product **38** to 10%. We believed that solubility was a limitation with using these bases. Hence, tetrabutylammonium acetate was examined as a soluble acetate source, and was found to be optimal for reactions with TsNH₂ and NsNH₂. With optimal conditions of 5 mol % Pd(OAc)₂, 2 equiv PhI(OAc)₂, 1 equiv Bu₄NOAc, in CH₂Cl₂ at 60 °C, 1-octene reacted with TsNH₂ and NsNH₂ to provide **38** and **41** in 18% and 25% yield, respectively, (Scheme 5.15).

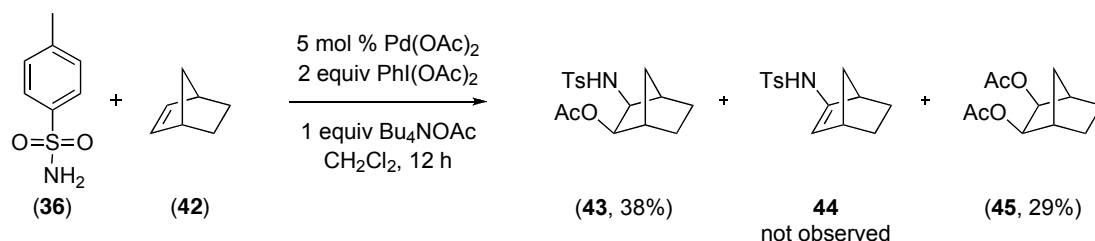
Scheme 5.15. Palladium-Catalyzed Reaction of 1-Octene with Tosylamine or Nosylamine and PhI(OAc)₂



Mechanistic studies by Stahl have shown that aminopalladation of norbornene with TsNH₂ occurs in a syn fashion.⁸ Hence, we decided to screen the reactions with norbornylene as the olefin partner, since we expected β-hydride elimination to be attenuated in this system due to conformational constraints. Consistent with this hypothesis, reaction of norbornene and TsNH₂ (with 5 mol % Pd(OAc)₂, 2 equiv

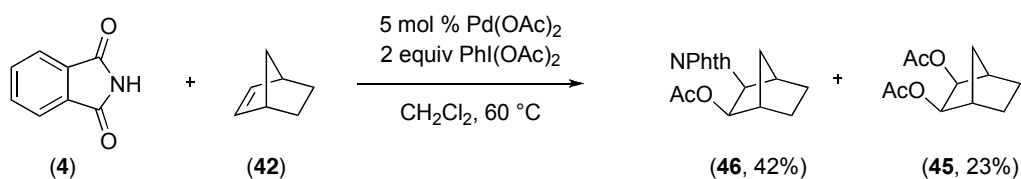
PhI(OAc)₂, 1 equiv Bu₄NOAc, in CH₂Cl₂ at 60 °C) did not afford any of the β-hydride elimination product **44**. However, due to low reactivity of the aminoacetoxylation reaction and formation of the undesired diacetoxylation product **45**, we obtained the desired product **43** in only 38% yield (Scheme 5.16).

Scheme 5.16. Palladium-Catalyzed Reaction of Norbornylene with *p*-Toluenesulfonamide and PhI(OAc)₂



We next explored the reactivity of norbornene with phthalimide as the nucleophile. Reaction of norbornene and phthalimide in CH₂Cl₂ with 5 mol % Pd(OAc)₂, 2.0 equiv PhI(OAc)₂ at 60 °C afforded the aminoacetoxyated product **46** and diacetoxylation product **45** in 41% and 23% yield respectively. Optimization reactions screening various solvents, temperatures, bases and catalysts did not improve the yield of **46**.

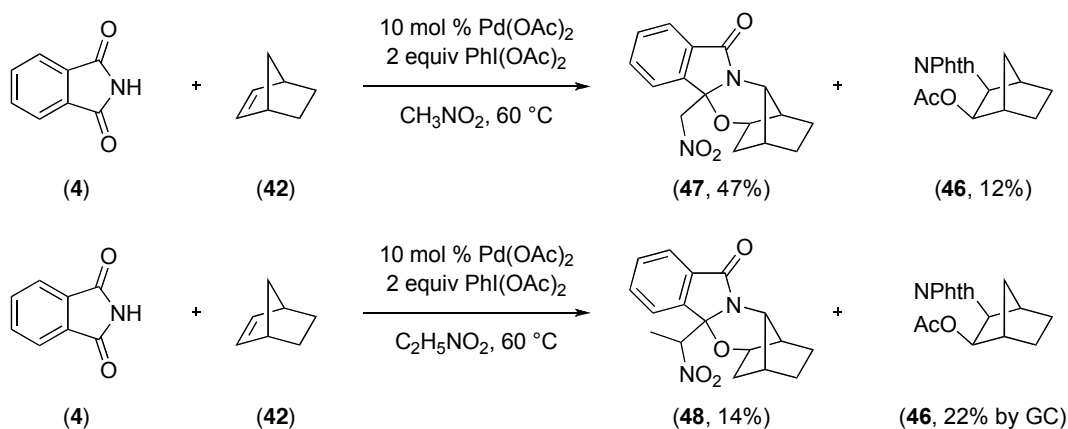
Scheme 5.17: Palladium-Catalyzed Reaction of Norbornene with Phthalimide and PhI(OAc)₂ in CH₂Cl₂



Interestingly, when the reaction of norbornylene and phthalimide with 5 mol % Pd(OAc)₂ and 2 equiv PhI(OAc)₂ was conducted in nitromethane, a new compound (**47**) was obtained along with the expected 1,2-aminoacetoxyated product **46**. Characterization of **47** by NMR spectroscopy and X-ray crystallography revealed that a molecule of nitromethane and a molecule of phthalimide had been incorporated to afford

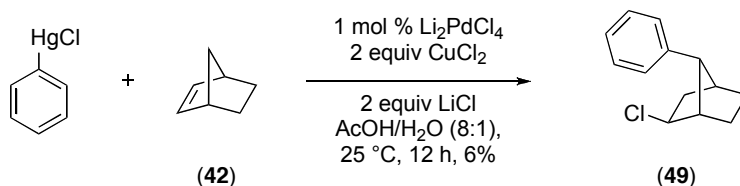
an unexpected 2,7-disubstituted norbornene derivative. When the solvent was changed from nitromethane to nitroethane, similar reactivity was observed to afford compound **48**, albeit in lower yield. In this case, the balance of the material was unreacted starting material (~41%) and the aminoacetoxylated product **46** (22%).

Scheme 5.18. Palladium-Catalyzed Reaction of Norbornene with Phthalimide and $\text{PhI}(\text{OAc})_2$ in Nitroalkane Solvents



Similar connectivity as product **47** and **48** has been observed by Heck in the Pd-catalyzed reaction of phenylmercuric chloride with norbornene.¹⁷ Reaction of PhHgCl and norbornene with catalytic Li_2PdCl_4 and stoichiometric CuCl_2 afforded exo-2-chloro-7-phenylnorbornene (**49**) (Scheme 5.19). The authors did not speculate on a possible mechanism for the formation of **49**.

Scheme 5.19: Halophenylation of Norbornene

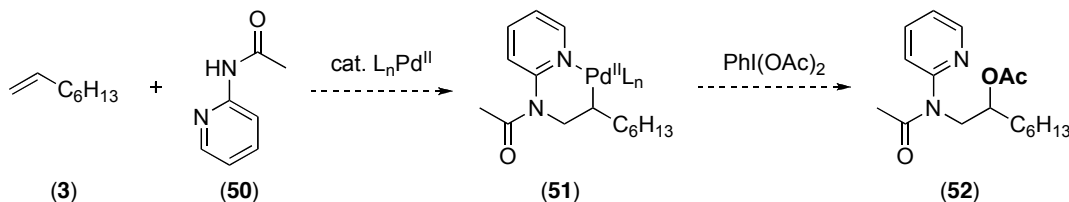


Substrates with Directing Groups. A substrate design strategy was next employed in an attempt to avoid competitive formation of β -hydride elimination products. In Chapter 2, we proposed that β -hydride elimination in the sp^3 C–H functionalization

reactions was attenuated by the formation of a cyclopalladated intermediate. In such an intermediate, coordination of the chelating functionality to the metal provides a cyclic structure, which renders β -hydride elimination conformationally unfavorable. Based on these systems, we reasoned that tethering a chelating group to the nucleophile of the alkene could have a similar effect.

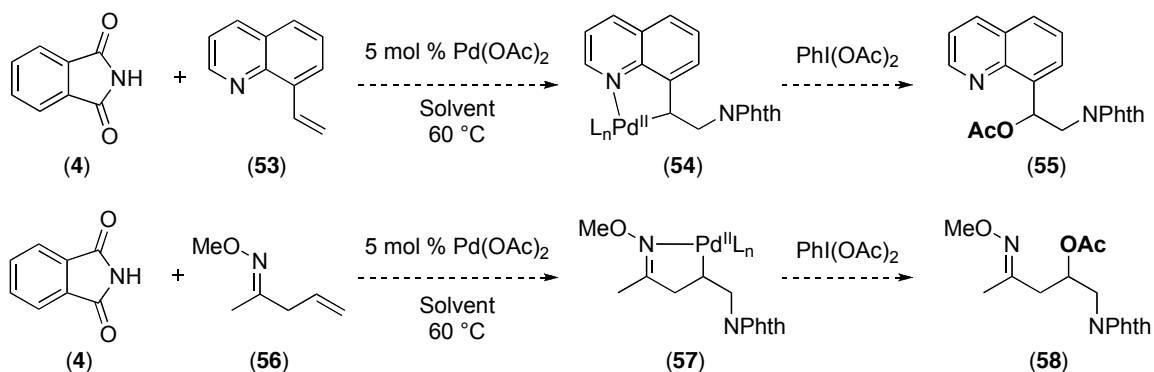
We first explored nucleophile **50**, which contains two basic functional groups, an amide and a pyridine. We anticipated that the former could undergo aminopalladation while the latter could subsequently bind to the metal to generate chelated intermediate **51** (Scheme 5.20). However, when reactions of **50** with 1-octene were explored under our optimized conditions (5 mol % Pd(OAc)₂, 2 equiv PhI(OAc)₂ and 1 equiv Bu₄NOAc in CH₂Cl₂ at 60 °C), **50** and the starting olefin were recovered quantitatively. Despite screening various solvents, temperatures, and bases, we did not observe any reactivity. We believe that the nucleophile may coordinate tightly with the metal and thereby prevent further reaction.

Scheme 5.20: Use of Directing Group-Containing Nucleophile **50**



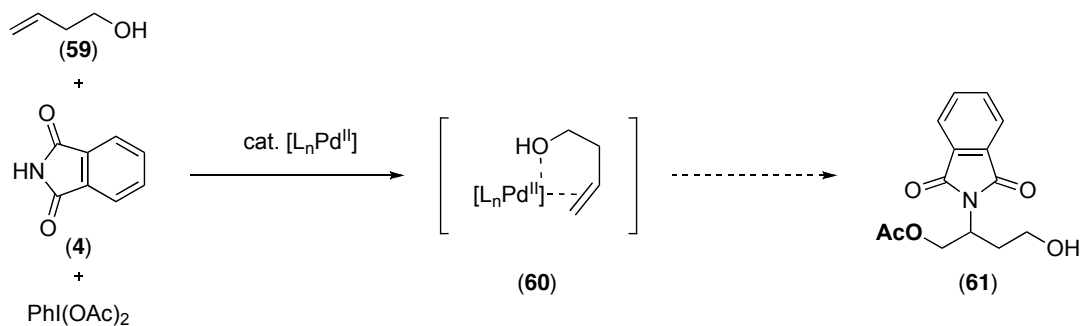
We next explored alkene substrates that contain either a quinoline or an oxime ether functionality, as these are both known to bind readily to Pd^{II}. We envisioned that interaction between the quinoline or oxime ether and palladium would bring the metal in the proximity of the olefin. Subsequent aminopalladation would then result in a cyclic Pd-alkyl intermediate like **54** or **57** (Scheme 5.21), which would be less susceptible to β -hydride elimination than their acyclic analogues. However, subjecting of substrates **53** and **56** to phthalimide with 5 mol % Pd(OAc)₂ and 2 equiv PhI(OAc)₂ in different solvents at 60 °C, with and without Bu₄NOAc, afforded unreacted starting material (with **53**) or undesired side reactions of the olefin (with **56**).

Scheme 5.21: Use of Directing Group-Containing Substrates 53-56



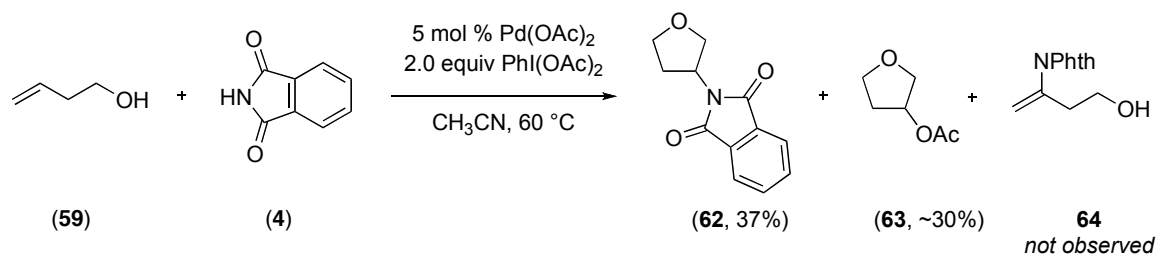
We hypothesized that **50**, **53** and **56** did not exhibit any reactivity towards oxidative amination because the directing group bound tightly to the Pd^{II} catalyst and thereby prevented coordination of the olefin and/or nucleophile. Hence, our next approach was to examine tethering a weaker ligand such as an alcohol to the olefin. In this system, the alcohol could chelate to the palladium and aminopalladation could occur followed by oxidation to produce the desired product (Scheme 5.22).

Scheme 5.22: Alcohol Tether Strategy



Initial studies focused on the Pd-catalyzed reaction of 3-buten-1-ol (**59**) and phthalimide with PhI(OAc)₂ (Scheme 5.22). Consistent with our hypothesis, when **59** was subjected to the optimized reaction conditions with 1-octene (Scheme 5.23), none of the β-hydride elimination product **64** was observed, which was confirmed by synthesizing an authentic sample. However, surprisingly, none of desired product **61** was observed either. Instead, the reaction afforded two tetrahydrofuran products - one incorporating the phthalimide (**62**) and the second incorporating an acetate (**63**).

Scheme 5.23: Palladium-Catalyzed Reaction of 3-Butene-1-ol with Phthalimide and $\text{PhI}(\text{OAc})_2$ to form Tetrahydrofurans

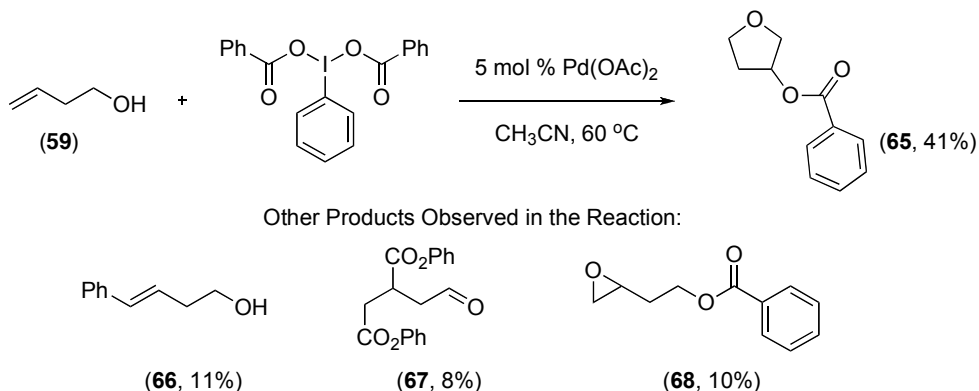


In order to explore the origin of products **62** and **63**, we next probed the scope and mechanism of this transformation. These studies are discussed below and divided into four sections. The first two sections describe the scope and mechanism for the formation of product **63**. The last two sections focus on efforts towards understanding the generality and mechanistic details of formation of product **62**.

5.3 Cyclization of Alcohols

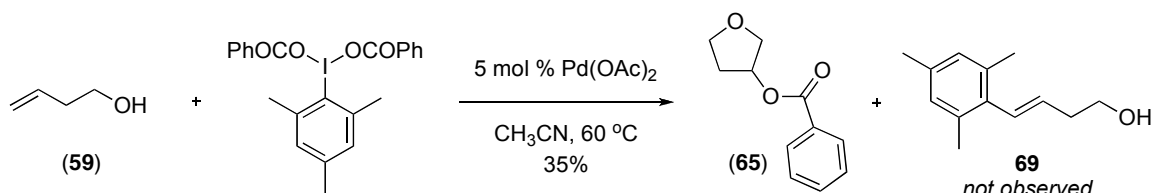
We believed that $\text{PhI}(\text{OAc})_2$ was the source of acetate in product **63** (Scheme 5.23). Hence, benzoate derivatives of $\text{PhI}(\text{OAc})_2$ were screened in order to add molecular weight to the products and facilitate isolation. Subjection of 3-buten-1-ol to 5 mol % $\text{Pd}(\text{OAc})_2$ and 2 equiv $\text{PhI}(\text{OCOPh})_2$ in CH_3CN at 60°C afforded the cyclized product **65** in 41% yield (Scheme 5.24).

Scheme 5.24. Palladium-Catalyzed Cyclization of 3-Buten-1-ol



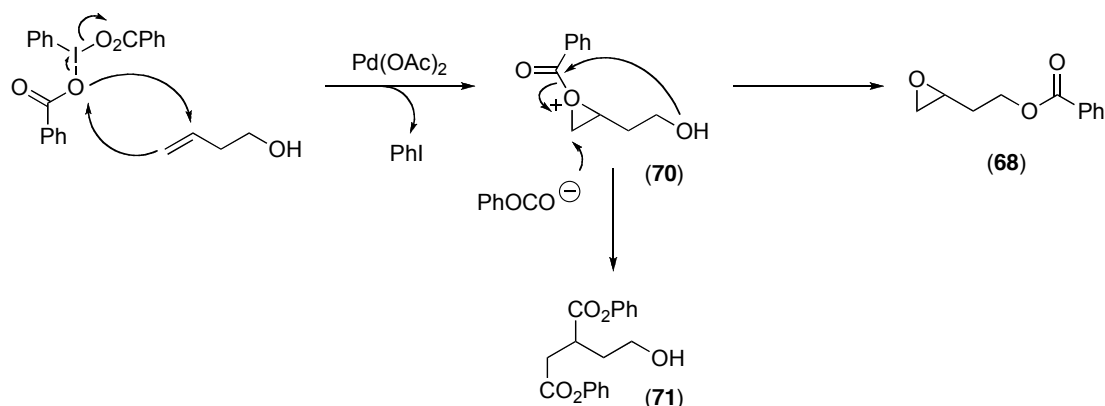
The modest yield of this cyclization reaction is believed to be due to side reactions of the 3-butene-1-ol starting material under the reaction conditions. Consistent with this hypothesis, traces of diacetylated aldehyde **67**, epoxide containing product **68**, and Heck side product **66** were isolated from the reaction. Notably, approximately 5% of product **65** and <5% of products **66** and **68** were observed when the reactions were run in the absence of Pd(OAc)₂. The formation of Heck product **66** could be suppressed through the use of (Mesityl)I(CO₂Ph)₂ in place of PhI(CO₂Ph)₂. However, this oxidant exhibited lower reactivity for the desired transformation (Scheme 5.25).

Scheme 5.25: Use of (Mesityl)I(CO₂Ph)₂ as the Oxidant



We speculated that the formation of the diacetylated aldehyde product **67** and epoxide product **68** would be increased by employing more reactive oxidants. Consistent with our hypothesis, when various electronically different iodosobenzoate derivatives were explored, the electron deficient oxidants (*para*-NO₂, CF₃, and Br substituted benzoates) led to greater quantities of products **67** and **68**. However, the yields obtained with the electron rich benzoate oxidants (*para*-OMe and CH₃ substituted benzoates) were similar to those obtained with PhI(CO₂Ph)₂. We believe Pd(OAc)₂ acts as a Lewis acid to catalyze the formation of the epoxide product **68** and diacetylated product **67** via a mechanism similar to epoxide formation with *m*-CPBA (Scheme 5.26). Subsequent reaction of product **71** with Pd, through β-hydride elimination, would form aldehyde **67**.

Scheme 5.26: Proposed Lewis Acid Catalyzed Mechanism for Formation of **67** and **68**



The scope of this reaction with respect to the alcohol substrate was next examined. In a representative example, 2-phenyl-1-butenol reacted under the optimal conditions (5 mol % $\text{Pd}(\text{OAc})_2$ and 2 equiv of $\text{PhI}(\text{OAc})_2$ in CH_3CN at 60 °C) to afford 35% of the desired substituted THF ring **73**, along with significant amounts of epoxide **74** (Scheme 5.27). Similar yields of THF products were obtained with a variety of other alcohol substrates **75-85** (Table 5.1), and in all cases, analogous epoxide side products were observed. Notably, the THF rings were formed with modest levels of diastereoselectivity, with dr ranging from 1:1 to 2:1.

Scheme 5.27: Alcohol Cyclization Reactions

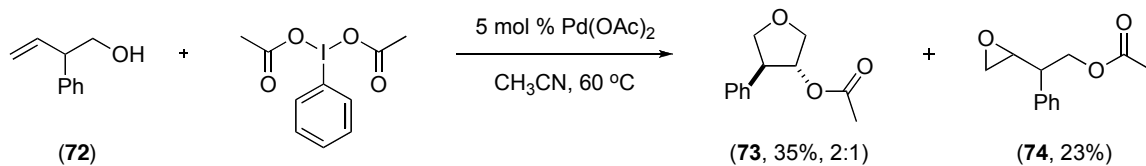
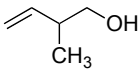
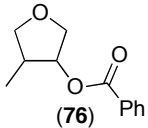
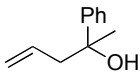
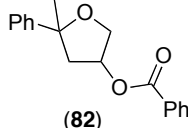
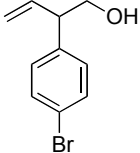
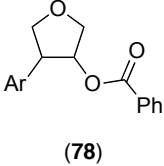
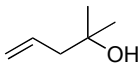
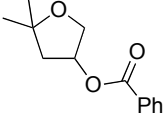
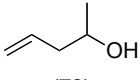
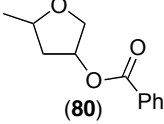
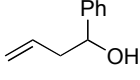
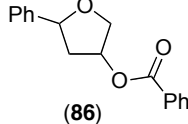


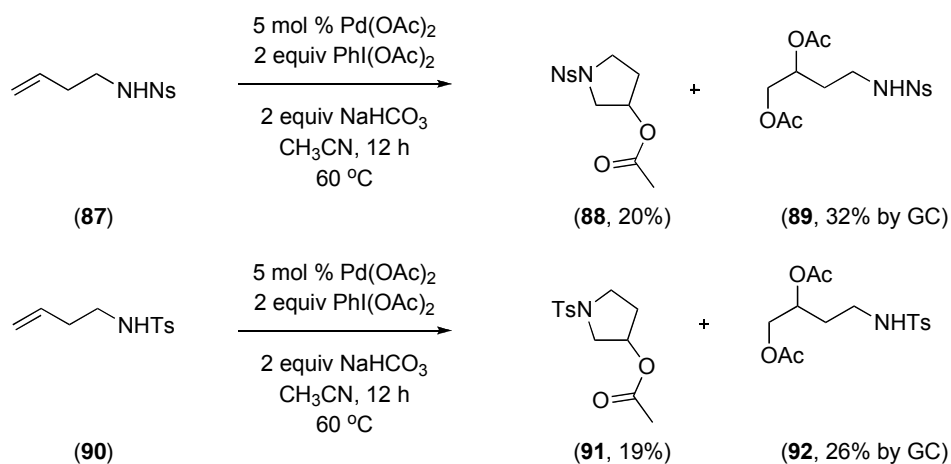
Table 5.1: Substrate Scope for Alcohol Cyclization Reactions

Entry	Substrate	Product	Yield (dr)	Entry	Substrate	Product	Yield (dr)
1	 (75)	 (76)	22% (1.4:1)	4	 (81)	 (82)	37%(2:1)
2	 (77)	 (78)	30%(1:1)	5	 (83)	 (84)	40%
3	 (79)	 (80)	25%(1.8:1)	6	 (85)	 (86)	29%(2:1)

5.4 Cyclization of Amines

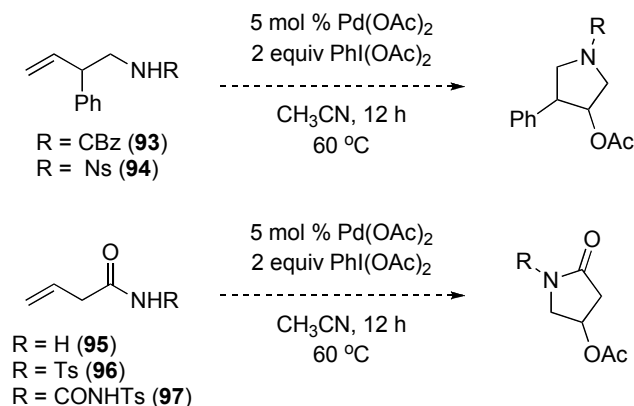
Analogous cyclization reactions of amino olefins were next examined. Amino olefin substrates containing various protecting groups (Cbz, Ts, Ns, Boc, and urea) were subjected to our optimal reaction conditions (5 mol % Pd(OAc)₂ and 2 equiv of PhI(OAc)₂ in CH₃CN at 60 °C). Only amines with Ns and Ts protecting groups exhibited trace reactivity towards the cyclization reaction (Scheme 5.28). Upon screening bases with substrates **87** and **90**, we determined that NaHCO₃ allowed us to access the pyrrolidine products **88** and **91** in about 20% yield. Diacetoxylation of the starting olefin, similar to that observed with 1-octene (Scheme 5.14), was again a competitive pathway in these reactions. The balance of material was accounted for by unreacted starting material.

Scheme 5.28: Amine Cyclization Reactions



We next synthesized protected amines **93** and **94**, which contain a phenyl substituent in the backbone (Figure 5.2). We anticipated that this group would facilitate cyclization via a Thorpe-like effect. In addition, we synthesized amides **95-97**, which we expected to be conformationally biased to undergo cyclization. However, in the reaction of substrates **93-94** and **96-97** under our optimal conditions (5 mol % Pd(OAc)₂ and 2 equiv of PhI(OAc)₂ in CH₃CN at 60 °C with and without NBu₄OAc or NaHCO₃) we either observed unreacted starting material (with **93-97**), diacetoxylation of the olefin (with **93** and **94**), Heck products (with **96** and **97**) or decomposition (with **95**).

Figure 5.2: Additional Amine and Amide Substrates



5.5 Cyclization of Acids

In order to further explore the scope of these cyclization reactions, we studied substrates containing carboxylic acids as the intramolecular nucleophile. Gratifyingly, subjecting 3-butenoic acid to our reaction conditions (5 mol % Pd(OAc)₂, 2 equiv of PhI(OCOPh)₂ and 2 equiv NaHCO₃ in CH₂Cl₂ at 60 °C) afforded the cyclized lactone product **100** in 56% yield (Scheme 5.29). As shown in Table 5.2, the scope of this cyclization was general for various different substituted acids. Substrates **101-111** cyclized to form lactones in better yields than the alcohols and amines. However, we still obtained low diastereoselectivity with substrates such as **101**. The diastereoselectivity did not improve upon addition of Pd catalysts containing various bidentate and tridentate ligands.

Scheme 5.29. Carboxylic Acid Cyclization Reactions

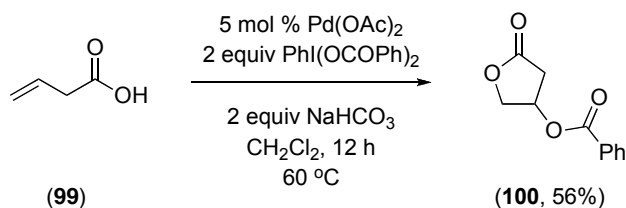


Table 5.2: Substrate Scope of Carboxylic Acid Cyclization Reactions

Entry	Substrate	Product	Yield (dr)
1			65% (2:1)
2			60%
3			66%
4			65% (13:1)
5			56% (1:9)
6			48% (all trans)

Conditions: 5 mol % Pd(OAc)₂, 2 equiv PhI(OCOPh)₂, 2 equiv NaHCO₃, CH₂Cl₂, 60 °C

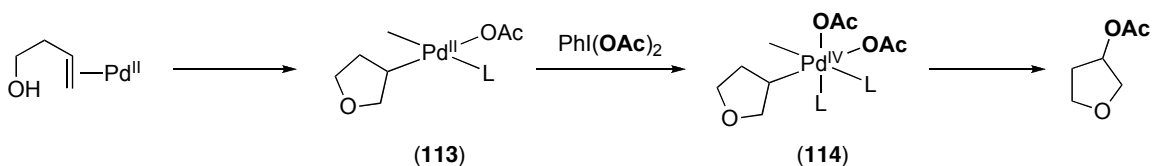
Reaction of substituted internal olefins did occur with high levels of stereospecificity. For instance, *trans*-4-ethylbutenoic acid **107** preferentially formed the *trans*-4,5-substituted lactone **108** with 13:1 selectivity (Table 5.2, entry 4), while *cis*-4-ethylbutenoic acid **109** preferentially afforded the *cis*-4,5-substituted lactone **110** with 9:1 selectivity (entry 5).

5.6 Mechanistic Investigations of the Cyclization Reactions

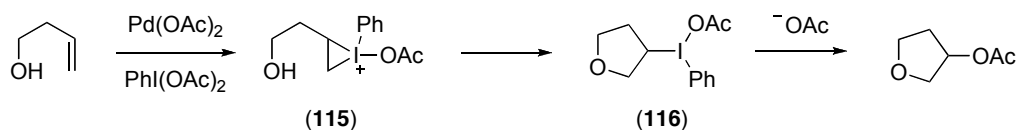
We next explored the role of palladium in these alcohol, amine and acid cyclization reactions. We speculated that there were at least two possible mechanisms: (i)

a Pd^{II/IV}-catalyzed pathway involving 5-endo-trig cyclization followed by oxidation (Scheme 5.30) or (ii) a mechanism involving Pd^{II} acting as a Lewis acid to promote the formation of iodonium ring **115**, that subsequently undergoes cyclization (Scheme 5.31).

Scheme 5.30. 5-Endo-trig Cyclization at Pd^{II}

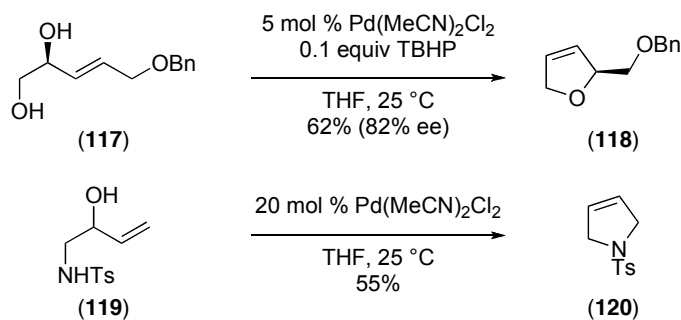


Scheme 5.31. Lewis Acid Catalyzed Cyclization

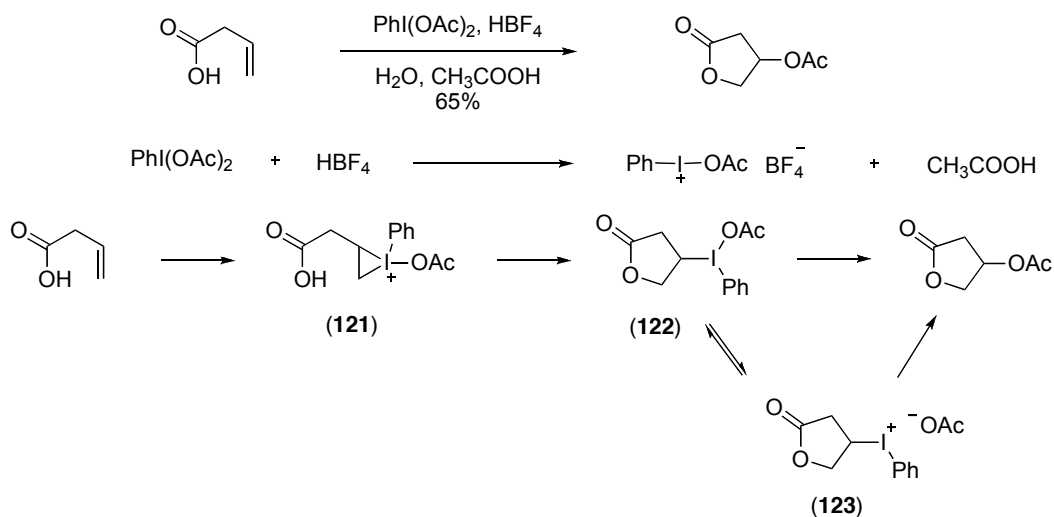


Importantly, there is limited literature precedent for Pd^{II}-promoted 5-endo trig cyclization reactions. As shown in Scheme 5.32, one example involved an alcohol and one involved an amine nucleophile.^{18, 19} In both cases, the final fate of the palladium alkyl intermediate, generated upon cyclization, was β -hydroxy elimination. There is literature precedent for Bronsted acid promoted cyclization of acids with hypervalent iodine oxidants. Butenoic acid was cyclized with PhI(OAc)₂ in AcOH in the presence of a strong acid, HBF₄ (Scheme 5.33).²⁰ Notably, Pd^{II} complexes have been used as Lewis acid catalysts in Baeyer Villiger oxidations, Diels Alder reactions, and the acetalization of aldehydes and ketones.²¹ Hence, we wondered if the role of palladium in these cyclization reactions was that of a Lewis acid.

Scheme 5.32. Literature Precedent for 5-Endo-trig Cyclization at Pd^{II}

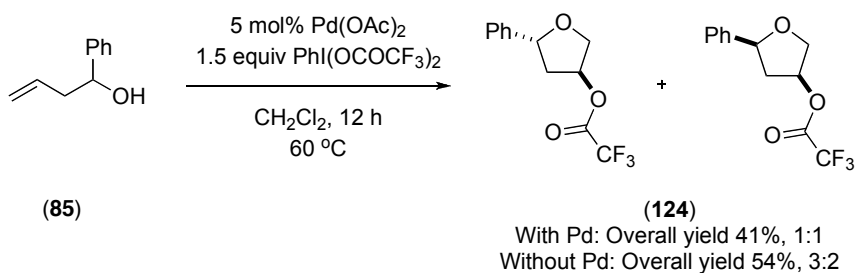


Scheme 5.33. Literature Precedent for Bronsted Acid-Catalyzed Cyclization



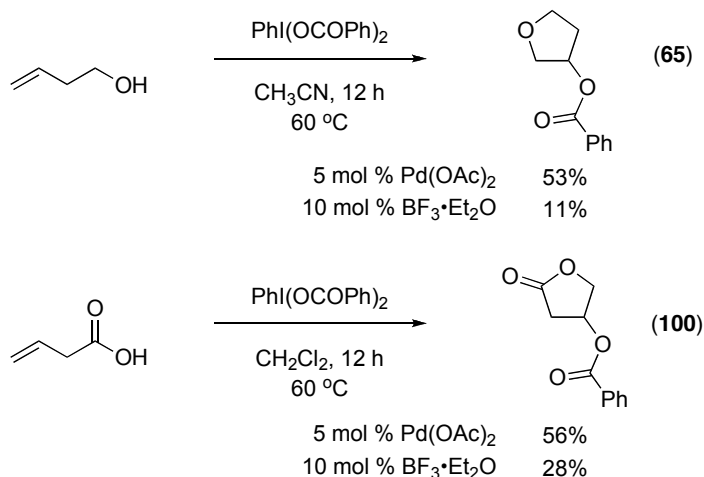
In order to distinguish between the two mechanisms, a number of control experiments were executed. First, the reactions were conducted with as $\text{PhI}(\text{O}_2\text{CCF}_3)_2$, which is a stronger oxidant and more electrophilic reagent than $\text{PhI}(\text{O}_2\text{CPh})_2$. As shown in Scheme 5.34, similar reactivity was observed with $\text{PhI}(\text{O}_2\text{CCF}_3)_2$ in the presence and absence of the Pd catalyst. In both cases, the THF product **124** was obtained in 41-54% yield as an approximately 1:1 ratio of diastereomers.

Scheme 5.34. Cyclization Reactions with $\text{PhI}(\text{OCOCF}_3)_2$



Secondly, Lewis acids such as $\text{BF}_3 \cdot \text{Et}_2\text{O}$ were screened in the reactions in place of the Pd^{II} catalyst. The desired cyclized products were again observed in the presence of $\text{BF}_3 \cdot \text{Et}_2\text{O}$, albeit in lower yield (Scheme 5.35). Our results and literature precedent led us to hypothesize that the cyclized products are likely forming through a Lewis acid mechanism and not a $\text{Pd}^{\text{II/IV}}$ cycle.

Scheme 5.35. Reactions with $\text{BF}_3 \cdot \text{Et}_2\text{O}$

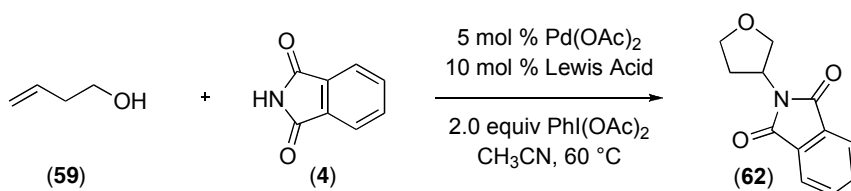


5.7 Aminooygenation Cyclization Reactions with 3-Alken1-ols

Initial Results. We sought to optimize for the THF ring **62** that had incorporated the nucleophile. Subjection of 3-buten-1-ol and phthalimide to 5 mol % $\text{Pd}(\text{OAc})_2$ and 2 equiv $\text{PhI}(\text{OAc})_2$ in CH_3CN at 60 °C afforded the aminooygenated THF product **62** in 27% isolated yield. This low yield was due to two major side reactions: (i) the

concomitant formation of tetrahydrofuran **63** discussed above (Scheme 5.23) and (ii) competitive undesired side reactions of the alcohol substrate **59** (Scheme 5.24). Notably, no products resulting from β -hydride elimination were observed, presumably due to the formation of a cyclic intermediate. We thought that using additives that can promote formation of free sites at the metal, might facilitate coordination of the nucleophile and the alcohol to the catalyst. Hence we studied the effect of the addition of 10 mol % of various additives to our reaction. Interestingly, additives containing potentially coordinating counterions such as AgI, ZnCl₂, and AuCl₃ led to decreased reactivity, whilst additives with non-coordinating counterions, such as AgBF₄, AgOTf and SbF₅ significantly improved the yield (Table 5.3). Further optimizations showed that two sequential additions of catalyst, silver salt, oxidant and alcohol further increased the yield of this reaction to 45%.

Table 5.3: Addition of Additives to the Palladium-Catalyzed Reaction of 3-Butene-1-ol with Phthalimide and PhI(OAc)₂



Entry	Lewis Acid	G.C. Yield (Isolated yield)
1	none	26% (31%)
2	AgBF ₄	42% (50%)
3	Ag(OTf)	40%
4	Ag ₂ SO ₄	9%
5	AgF	32%
6	Ag(OCOCF ₃)	25%
7	Ag ₂ CO ₃	0%
8	AgOAc	5%
9	AgI	3%
10	Cu(OTf) ₃	21%
11	ZnCl ₂	6%
12	SbF ₅	40%
13	Sc(OTf) ₃	12%
14	AuCl ₃	12%

Scope of Aminooxygenation Reactions. With optimal conditions in hand, the scope of this transformation was next studied. We reasoned that a substituent at the allylic position might accelerate the cyclization due to a Thorpe-like effect. We were delighted to find that substrate **72**, bearing a phenyl group in the allylic position, afforded the desired product in 77% yield and 10:1 diastereoselectivity. The stereochemistry was confirmed via NMR analysis and an x-ray crystal structure. Electron donating (Table 5.4, entries 2-4 and 8-9) and electron withdrawing (entries 5-7) substituents as well as halogens were tolerated on the phenyl ring.²² Tertiary alcohols also afforded the desired products in modest yield (entry 13).

Table 5.4: Substrate Scope of Aminooxygenation Reactions

Entry	Alcohol	Substituents	Major Product	Product #	Yield (dr)
1		Ph (72)		126	77% (10:1)
2		<i>p</i> -MeOC ₆ H ₄ (72a)		127	62% (15:1)
3		<i>m</i> -MeOC ₆ H ₄ (72b)		128	55% (5.4:1)
4		<i>o</i> -MeOC ₆ H ₄ (72c)		129	63% (7.8:1)
5		<i>p</i> -CF ₃ C ₆ H ₄ (72d)		130	54% (>20:1)
6		<i>m</i> -CF ₃ C ₆ H ₄ (72e)		131	60% (16:1)
7		<i>p</i> -BrC ₆ H ₄ (72f)		132	56% (>20:1)
8		2-naphthyl (72g)		133	80% (12:1)
9		mesityl (72h)		134	72% (1.4:1)
10		(75)			135
11		R = benzyl (125a)		136	27% (1.5:1)
12		R = <i>i</i> -propyl (125b)		137	< 5%
13		(83)		138	47%

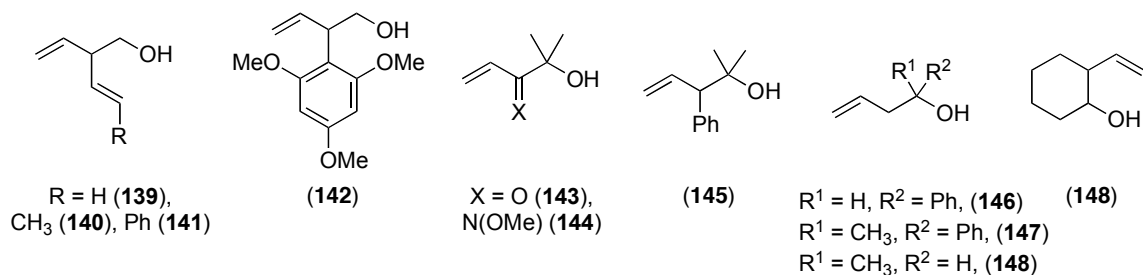
Conditions: 10 mol % Pd(OAc)₂, 20 mol % AgBF₄, 2.0 equiv PhI(OAc)₂, CH₃CN, 60 °C

While similar yields of products were obtained with different electronically and sterically substituted aryl rings at the allylic position, the diastereoselectivities were affected by the nature of the allylic substituent. In general, the diastereoselectivities were higher for electron withdrawing substituents in the *para*-position of the aryl ring and for

less sterically hindered aryl substituents. Interestingly, reduced yields and diastereoselectivities were obtained with substrates bearing non-aromatic substituents such as benzyl, methyl or isopropyl groups at the allylic position (Table 5.4, entries 10-12).

In contrast to the reactivity of substrate **83**, the reaction of substituted tertiary alcohols such as **143-145**, and **147** resulted in either unreacted starting material, decomposition, or the formation of Heck products. Similar reactivity was observed with substrates **139-141** and **143-144** that contained functionalities with the ability to coordinate to the metal, such as another olefin, a carbonyl, or an oxime ether, creating the possibility of dual chelation. Conformationally constrained substrate **148** also afforded only trace amounts of products under our standard conditions.

Scheme 5.36. Alkenol Substrates that Exhibited Low Reactivity



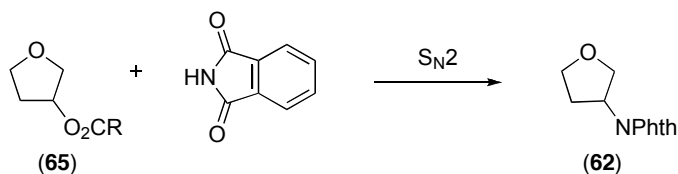
Other nitrogen nucleophiles were also examined in this reaction. However, we were surprised to find that *p*-toluenesulfonamide, *p*-nitrophenylsulfonamide, oxazolidinone, pyrrolidinone, and succinimide did not react to form even traces of cyclized products under our optimal reaction conditions.

5.8 Mechanistic Investigations of Aminoxygenation Cyclization

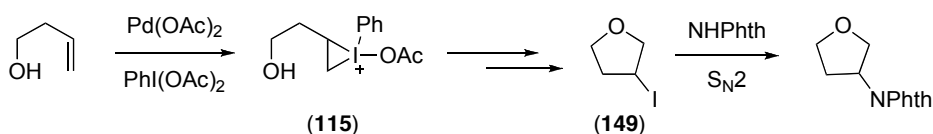
With the aforementioned results in hand, we were interested in investigating the mechanism of the aminoxygenation transformation. There are at least six distinct mechanistic possibilities for the Pd-catalyzed formation of the phthalimide substituted tetrahydrofuran rings: (i) S_N2 reaction of phthalimide with THF **65** (Scheme 5.37), (ii) iodocyclization to form product **149** followed by subsequent intermolecular S_N2 reaction

with phthalimide (Scheme 5.38), (iii) Lewis acid catalyzed cyclization (Scheme 5.39), (iv) Pd-catalyzed 1,2-aminoacetoxylation of the olefin to form product **150** followed by a subsequent intramolecular S_N2 reaction (Scheme 5.40), (v) 5-endo-trig oxypalladation to form intermediate **151** followed by oxidatively induced C–N bond forming reductive elimination (Scheme 5.41), and (vi) aminopalladation of the olefin followed by oxidative cyclization and C–O bond formation (Scheme 5.42).

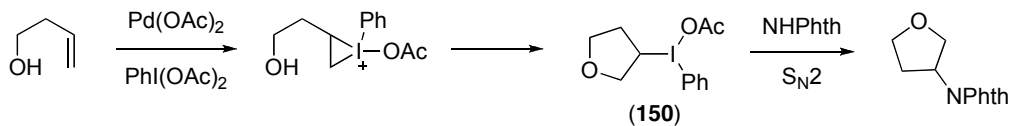
Scheme 5.37: Mechanistic Pathway (i)



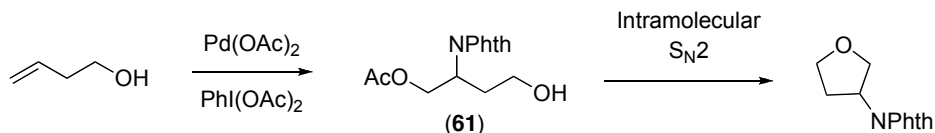
Scheme 5.38: Mechanistic Pathway (ii)



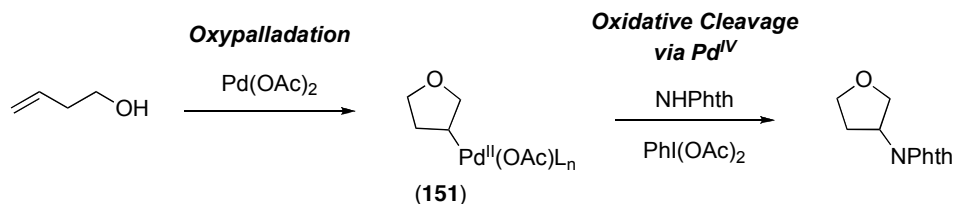
Scheme 5.39: Mechanistic Pathway (iii)



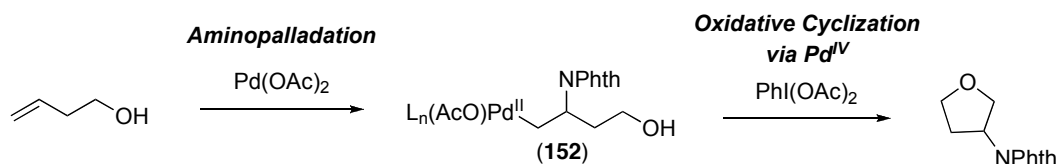
Scheme 5.40: Mechanistic Pathway (iv)



Scheme 5.41: Mechanistic Pathway (v)

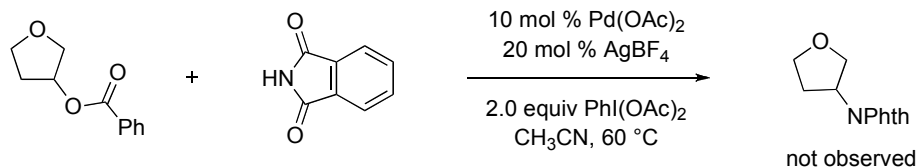


Scheme 5.42: Mechanistic Pathway (vi)



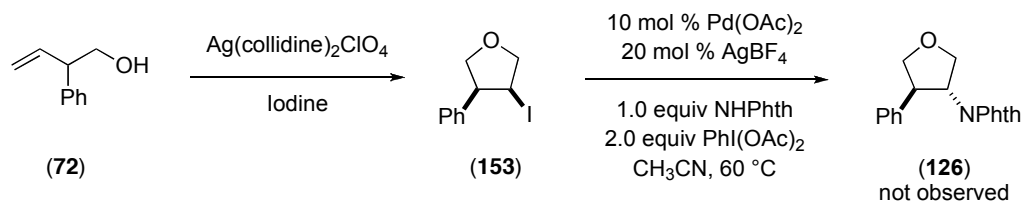
In order to examine the viability of the first mechanism, compound **65** was synthesized via the previously discussed cyclization reaction (Scheme 5.24). Subjection of product **65** and phthalimide to the standard reaction conditions (10 mol % Pd(OAc)₂, 20 mol % AgBF₄, 2 equiv PhI(OAc)₂ in CH₃CN at 60 °C) did not afford any of the aminoxygenated product **62** (Scheme 5.43). This result suggested strongly that product **62** was not formed by mechanism i.

Scheme 5.43. Possible S_N2 Reaction between Phthalimide and THF **65**



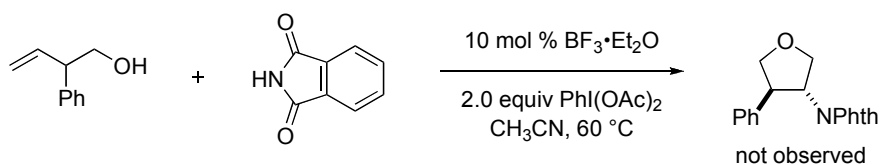
The viability of mechanism ii was examined by preparing an authentic sample of the iodo-substituted THF **149** (Scheme 5.38). Substrate **72** was chosen instead of **59** due to ease of isolation. Compound **153** was treated under the standard reaction conditions with phthalimide (10 mol % Pd(OAc)₂, 20 mol % AgBF₄, 2 equiv PhI(OAc)₂ in CH₃CN at 60 °C), and again, we did not observe the formation of product **126**. Based on this result, we conclude that mechanism ii is also not a viable route to **126** under our reaction conditions.

Scheme 5.44. Possible S_N2 Reaction between Phthalimide and Iodide Product **153**



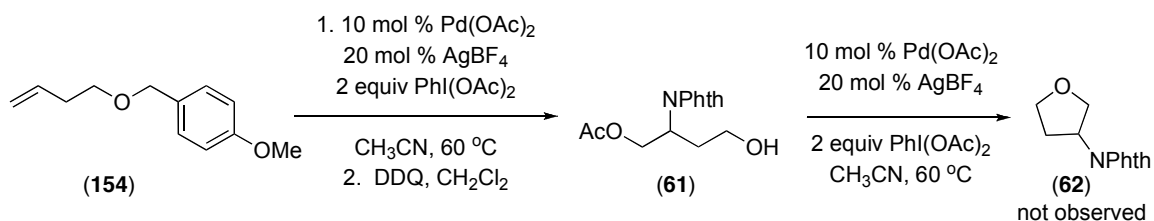
The third possible route to **126** would involve Pd acting as a Lewis acid to promote cyclization. In order to probe for this, we examined the reaction in the absence of palladium catalyst and in the presence of $\text{BF}_3 \cdot \text{Et}_2\text{O}$. Substrate **72** was subjected to 10 mol % $\text{BF}_3 \cdot \text{Et}_2\text{O}$ with 2 equiv PhI(OAc)_2 in CH_3CN at 60°C , and as shown in Scheme 5.45, product **126** was again not observed in this control reaction.

Scheme 5.45: Attempt to Obtain Aminooxygenation Product **126** with Catalytic $\text{BF}_3 \cdot \text{Et}_2\text{O}$



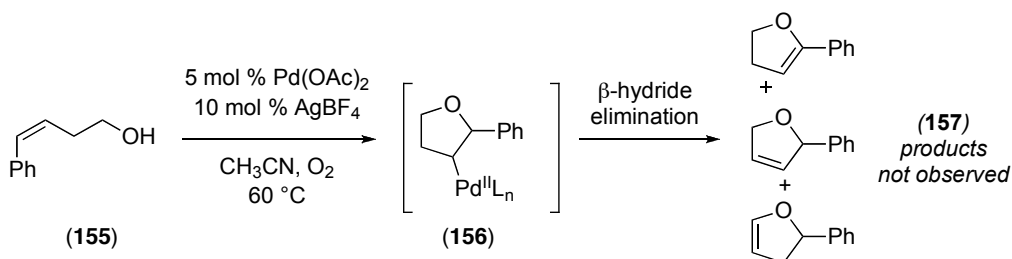
In order to determine if mechanism iv was occurring, we synthesized **154** by subjecting benzyl-protected 3-butenol and phthalimide to our reaction conditions followed by DDQ deprotection (Scheme 5.46). Subjection of **61** to the reaction conditions (10 mol % Pd(OAc)_2 , 20 mol % AgBF_4 , 2 equiv PhI(OAc)_2 in CH_3CN at 60°C) did not afford even traces of product **62**. This result suggested that mechanism iv was not operational.

Scheme 5.46. S_N2 Reaction of Aminoacetoxyated Intermediate **61**



If the reaction were proceeding via 5-endo trig cyclization (mechanism v), then we would expect that conducting the reaction of 4-phenyl-1-butenol and phthalimide in the presence of oxygen instead of PhI(OAc)₂ would form product **157** or its isomers, resulting from β-hydride elimination from intermediate **156** (Scheme 5.47). As seen earlier in examples by Stahl and co-workers (Scheme 5.4) in the absence of a strong oxidant that can intercept the Pd^{II} intermediate, β-hydride elimination is the most favorable pathway. Hence, substrate **155** and phthalimide were subjected to 5 mol % Pd(OAc)₂, 10 mol % AgBF₄ in CH₃CN at 60 °C under 1 atm of O₂. However, this reaction did not provide even traces of **157** or its isomers, suggesting against mechanism v.

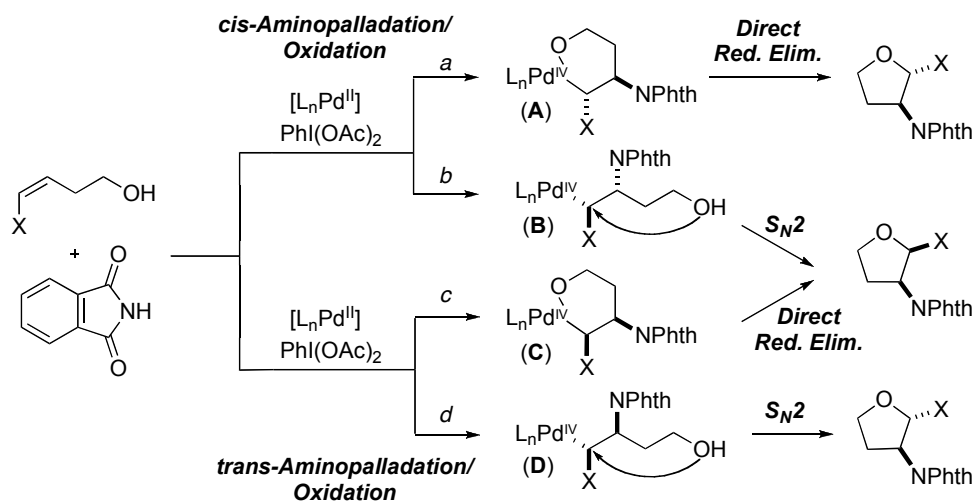
Scheme 5.47. Subjection of 4-Phenyl-3-buten-1-ol to Reaction Conditions with O₂ as the Terminal Oxidant



With these results in hand, we surmised that the formation of product **62** was catalyzed by palladium through the Pd^{II/IV} amination/oxidation pathway vi.²² As shown in Scheme 5.48, we envisioned four different pathways for the desired aminoxygenation reactions. The first step of the reaction might involve *cis*- or *trans*-aminopalladation. Upon aminopalladation, the reaction could then proceed via two different routes: (i) oxidation to Pd^{IV} followed by reductive elimination via an S_N2 pathway leading to

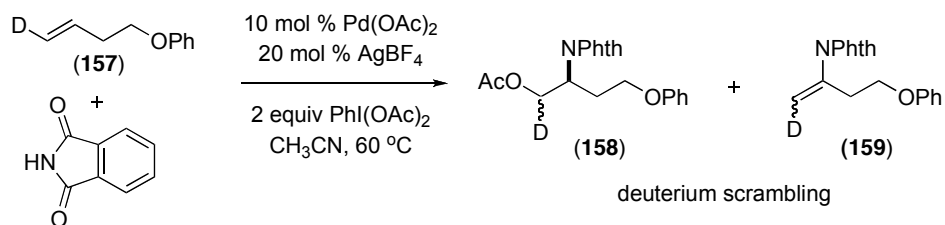
inversion of configuration at carbon or (ii) chelation of the tethered alcohol to the palladium followed by oxidation to Pd^{IV} and then direct reductive elimination with retention of stereochemistry. Importantly, in the latter case, chelation/oxidation could occur in the opposite order. As mentioned in the background section, both *cis* and *trans* aminopalladation have been observed previously.^{9, 13, 15, 16, 23} Additionally, reductive elimination at Pd^{IV} has been shown to occur with either retention or inversion of stereochemistry at carbon, depending on the substrate and the reaction conditions.

Scheme 5.48. Mechanism vi: Aminopalladation Followed by Oxidatively Induced Cyclization



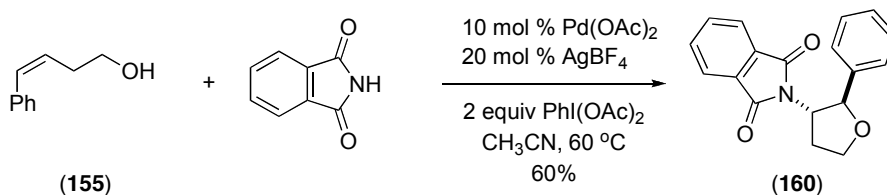
In order to distinguish between these four mechanistic possibilities, the deuterium labelled substrate **157** was synthesized (Scheme 5.49). Subjection of substrate **157** and phthalimide to our reaction conditions afforded the aminoacetoxylated product **158** along with product **159**, resulting from β -hydride elimination. The deuterium had scrambled in products **158** and **159**. We speculated that the deuterium scrambling in the products might be due to the isomerization of the olefin in the starting material, rather than an inherent lack of stereospecificity of the reaction. Indeed, this hypothesis was confirmed when **157** was subjected to our reaction in the absence of phthalimide and $PhI(OAc)_2$. This reaction provided a 1:1 mixture of the *cis* and *trans* isomers of **157**.

Scheme 5.49. Studies with Deuterium Labelled Substrate **157**



Because the deuterium-labelled substrate **157** did not provide the desired mechanistic information, we next explored the reactivity of *trans*- and *cis*-4-phenylbutenol, **155**, with phthalimide, 10 mol % Pd(OAc)₂, 20 mol % AgBF₄, and 2 equiv PhI(OAc)₂ in CH₃CN at 60 °C. In this case, the *cis* substrate **155** afforded a single diastereomeric product (**160**) that had a *trans* relationship between the phenyl ring and the phthalimide (Scheme 5.50). The stereochemistry was confirmed via NMR analysis and an x-ray crystal structure. In contrast, the *trans* substrate did not afford any of the desired aminooxygenated product under our reaction conditions. This result shows that even if isomerization between *cis* and *trans* phenyl butenols occurred under our reaction conditions, only the *cis*-isomer reacts to form the product. The *trans* relationship between the phenyl ring and the phthalimide in product **160** led us to believe that either mechanistic pathway a or d (Scheme 5.48) was operational in these reactions.

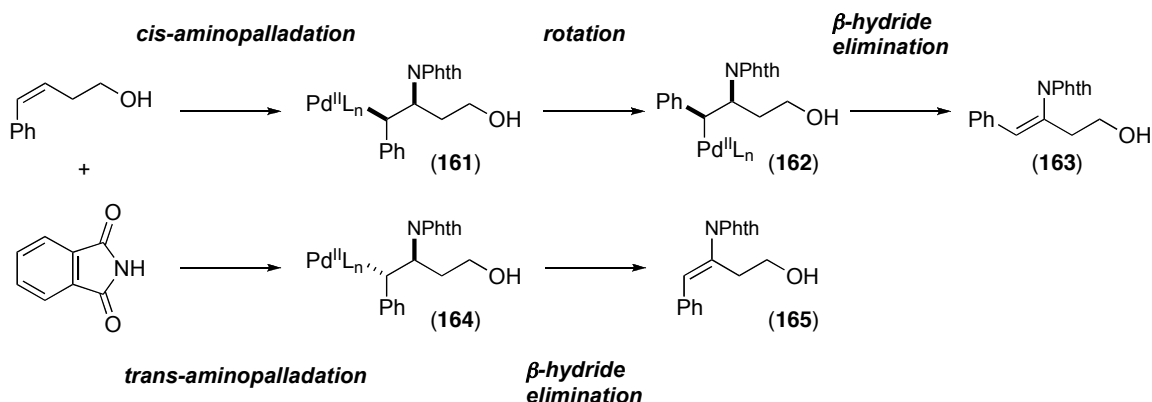
Scheme 5.50. Aminooxygenation with 4-Phenyl-3-buten-1-ol



In order to distinguish between mechanisms a and d, we needed to determine the mechanism of aminopalladation. A prior study by Stahl suggested that the geometry of β -hydride elimination products from Pd^{II} intermediate **A** or **D** would provide this information.¹⁶ As shown in Scheme 5.51, if *cis*-aminopalladation were operational, then Pd^{II} intermediate **151** would have to undergo σ -bond rotation to achieve the required *syn* relationship between the Pd and the β -hydrogen to achieve β -hydride elimination. As

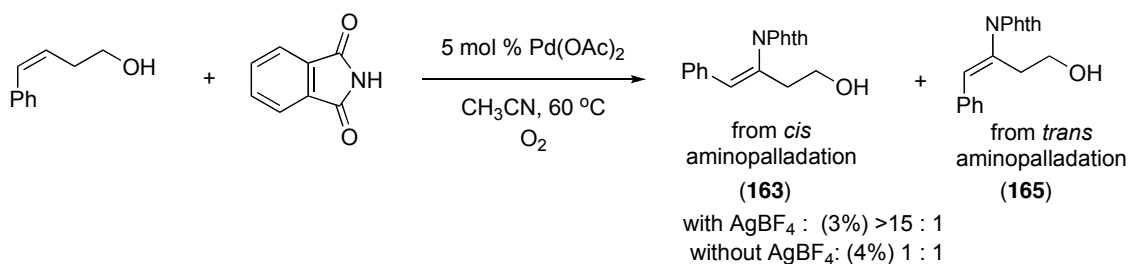
such, this reaction would afford the *Z*-substituted olefin **163** (Scheme 5.51). In contrast, the Pd^{II} product of *trans*-aminopalladation can undergo direct β-hydride elimination, leading to the *E*-substituted olefin **165**.

Scheme 5.51: Rationale for Outcome from β-Hydride Elimination



Subjection of substrate **155** to our optimized reaction conditions in the presence of O₂ instead of PhI(OAc)₂ (to promote termination of the reaction via β-hydride elimination) afforded the β-hydride elimination product **163**, albeit in low 3% yield (Scheme 5.52). This result suggests that our reaction goes through a *cis*-aminopalladation pathway. The low yield in this reaction is due to competitive olefin isomerization of the starting material, which yields the unreactive *trans* isomer. Interestingly, when the reaction shown in Scheme 5.52, was conducted in the absence of AgBF₄, we obtained 4% yield of a 1:1 ratio of *Z* and *E* substituted β-hydride elimination products (Scheme 5.52), suggesting that *cis* and *trans* aminopalladation are competitive under these conditions. Importantly, control experiments showed that neither product **163** nor product **165** isomerized under either set of reaction conditions.

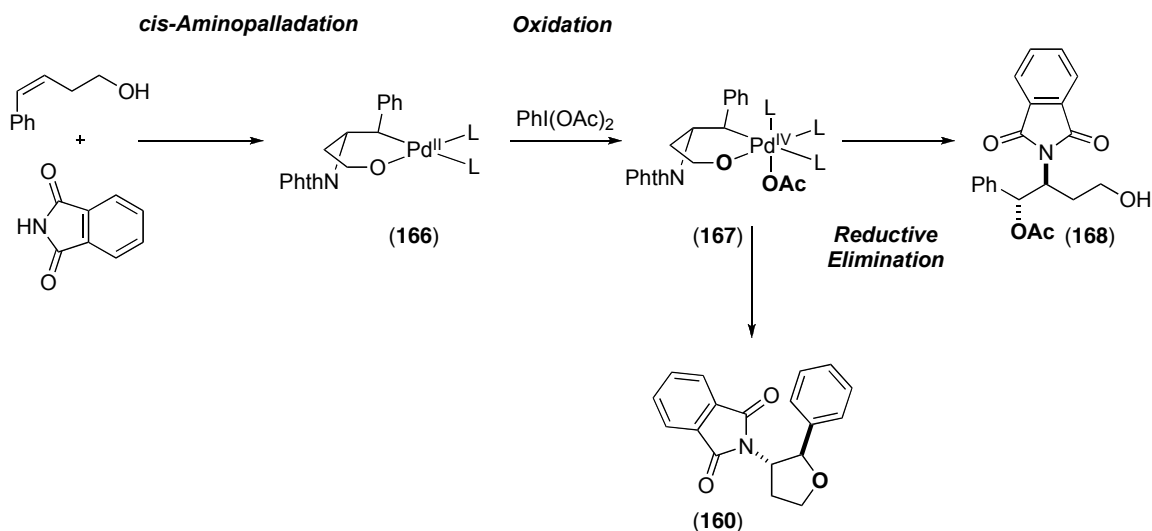
Scheme 5.52. Geometry of Amination Product Under Pd^{II/0} Reaction Conditions



Analyzing all the mechanistic data allowed us to conclude that mechanistic pathway a is governing the reaction (Scheme 5.48). It is notable that during reductive elimination from Pd^{IV}, there exists a choice for either reductive elimination of the acetate, to form aminoacetoxylated product **168**, or the alkoxide to form the THF ring **160** (Scheme 5.53). As discussed above, we obtain the THF ring product exclusively. Notably, C–OAc reductive elimination at Pd^{IV} is certainly possible, as it was observed in the C–H activation/acetoxylation reactions. We believe the preference for reductive elimination of the alkoxide over the acetate in the current systems can be attributed to the greater nucleophilicity of the alkoxide as discussed in chapter 2.²⁴

As discussed above, we observe reductive elimination with retention at the carbon. This is in sharp contrast to what was reported by Muniz (Scheme 5.12)¹⁵ and Stahl (Scheme 5.13)¹⁶ for related aminopalladation/oxidation reactions. However, other reports have suggested that reductive elimination from high oxidation state Pd complexes can occur with retention at carbon.^{25, 26} We believe that pre-coordination of the alkoxide is a likely reason for reductive elimination occurring with retention in our system.

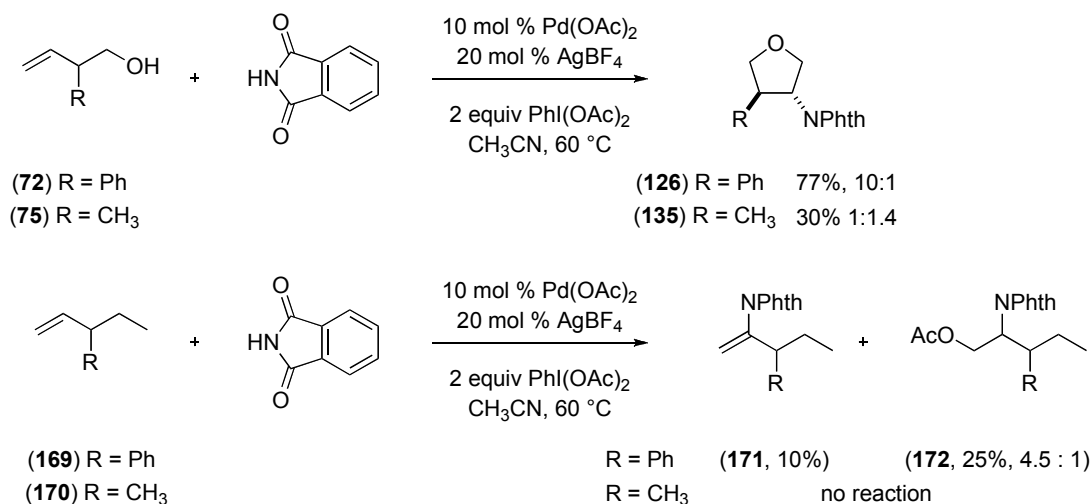
Scheme 5.53. Summary of Proposed Mechanism



Origin of Diastereoselectivity. We next sought to rationalize the observed diastereoselectivity and the role of silver in the aminooxygenation reaction. Silver is known to facilitate the dissociation of acetate from group 10 metal centers through coordination.²⁷ Based on the results from Scheme 5.52 and Table 5.3, we propose that silver reacts to produce a vacant coordination site on the palladium by promoting dissociation of an acetate ligand. This vacant coordination site allows the palladium to bind to the phthalimide nucleophile, facilitating *cis*-aminopalladation.

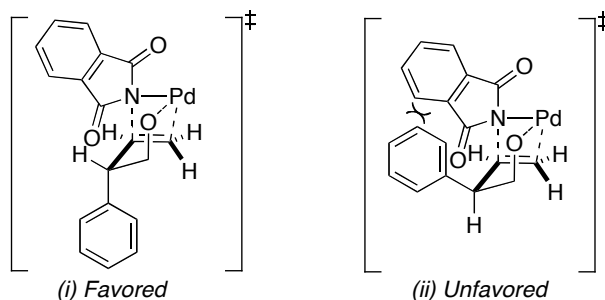
Substrates **169** and **170**, where the alcohol had been replaced with a carbon, were chosen to elucidate the origin of diastereoselectivity. Subjection of substrate **170** to our reaction conditions did not lead to any observable reactivity (Scheme 5.54). This was in contrast to substrate **75**, which yielded 30% of product **135**. Substrate **169** underwent aminoacetoxylation to afford product **172** in 4 : 1 diastereoselectivity along with the β -hydride elimination product **171** (Scheme 5.54). The diastereoselectivity observed with substrate **72** is significantly greater than the dr observed with substrate **169**. This implies that there exists some interaction between the palladium and the alcohol in the transition state for aminopalladation.

Scheme 5.54. Probing the Role of the Tethered Alcohol



These results can be rationalized based on the proposed transition state in Figure 5.3. Here the palladium is interacting with the nitrogen of the nucleophile, the tethered alcohol, and the olefin in a cyclic transition state. In order to avoid unfavorable steric interactions with the coordinated phthalimide, the allylic substituent assumes a pseudo-equatorial position, resulting in a *trans* delivery of the phthalimide. However, this transition state does not completely explain the observed steric and electronic effects on the diastereoselectivity, particularly with the methyl, benzyl, and mesityl substituted substrates **75**, **125a**, and **72h**. It is possible that alternative and/or competing transition states are accessed in these systems.

Figure 5.3. Possible Transition States



5.9 Conclusion

In summary, palladium alkyl intermediates generated via nucleopalladation were intercepted to form carbon-oxygen bonds. Aminopalladation reactions, using nucleophiles such as phthalimide, *p*-toluenesulfonamide, and *p*-nitrophenylsulfonamide and olefins such as octene and norbornene were explored to form 1,2-aminoacetoxylated products. These products were obtained in low yields due to competitive undesired β -hydride elimination. This undesired pathway was attenuated by tethering chelating functionalities, such as alcohols, amines and acids, to the olefin. Reaction of the tethered olefin in the absence of amine nucleophiles led to formation of acetate substituted cyclic compounds. We propose that these cyclization reactions occur via a Lewis acid catalyzed mechanism to form the tetrahydrofuran, pyrrolidinone, or lactone products, respectively. Reaction of the alkenols in the presence nucleophiles such as phthalimide afforded phthalimide-substituted THF rings. Mechanistic experiments have shown that this aminoxygenated compound is formed by *cis*-aminopalladation followed by oxidative cleavage with $\text{PhI}(\text{OAc})_2$ to afford the final product with retention of stereochemistry at the carbon.

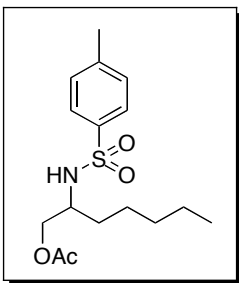
5.10 Experimental Procedure

General Procedures: NMR spectra were obtained on a Varian Inova 500 (499.90 MHz for ^1H ; 125.70 MHz for ^{13}C) unless otherwise noted ^{19}F NMR spectra were obtained on Varian Inova 300 (282 MHz for ^{19}F). ^1H NMR chemical shifts are reported in parts per million (ppm) relative to TMS, with the residual solvent peak used as an internal reference. Multiplicities are reported as follows: singlet (s), broad singlet (br, s), doublet (d), doublet of doublets (dd), doublet of doublets of doublets (ddd), doublet of triplets (dt), triplet (t), quartet (q), quintet (quin), multiplet (m), and broad resonance (br). IR spectra were obtained on a Perkin-Elmer Spectrum BX FT-IR spectrometer.

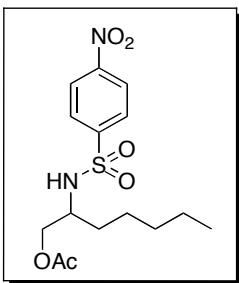
Materials and Methods: Alcohol substrates **77**, **72**, **72a-72h**, and **155** were prepared according to literature procedures. Substrate **125a** was synthesized by alkylation

of 3-butenic acid with benzyl bromide followed by LiAlH₄ reduction of the acid to afford the alcohol. PhI(O₂CPh)₂ was prepared according to a literature procedure. Pd(OAc)₂ was obtained from Pressure Chemical and used as received, and PhI(OAc)₂ was obtained from Merck Research Laboratories and used as received. Solvents were obtained from Fisher Chemical. Acetonitrile was freshly distilled from calcium hydride under a nitrogen atmosphere. Dichloromethane, tetrahydrofuran, and diethyl ether were purified using an Innovative Technology (IT) solvent purification system composed of activated alumina, copper catalysts and molecular sieves. Flash chromatography was performed on EM Science silica gel 60 (0.040–0.063 mm particle size, 230–400 mesh), and thin layer chromatography was performed on Merck TLC plates pre-coated with silica gel 60 F254. HPLC was performed on a Varian Prostar 210 HPLC using Waters μ Porasil® 10 μ m silica (19 x 300 mm) columns. Melting points were determined with a Mel-Temp 3.0, a Laboratory Devices Inc, USA instrument and are uncorrected. HRMS data were obtained on a Micromass AutoSpec Ultima Magnetic Sector mass spectrometer. The geometries of the diastereomeric tetrahydrofuran products were determined based on ¹H NMR nOe studies (substrates **5a-14a**) and by X-ray crystallography (**3a** and **4a**).

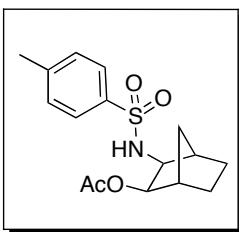
Typical Procedure for Olefin reaction with Nucleophile: Phthalimide (100 mg, 0.68 mmol, 1 equiv), PhI(OAc)₂ (0.440 g, 1.36 mmol, 2 equiv), and Pd(OAc)₂ (8 mg, 0.034 mmol, 0.05 equiv) were combined in CH₂Cl₂ (1.4 mL) in a 20 mL vial. Octene (98 mg, 1.36 mmol, 2.0 equiv) was added to the reaction, the vial was sealed with a Teflon-lined cap, and the reaction was heated at 60 °C for 12 h. The reaction mixture was evaporated to dryness and then taken up in diethyl ether (10 mL). The ether layer was washed with 10% aqueous Et₃N (10 mL), H₂O (2 x 20 mL), saturated aqueous NaHCO₃ (20 mL), and saturated aqueous NaCl (20 mL). The ether extracts were dried over MgSO₄, filtered, and concentrated to afford a red oil, which was purified by chromatography on silica gel.



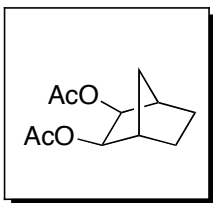
Product **38** was obtained as a yellow oil (18%). $^1\text{H NMR}$ (CDCl_3): δ 7.75 (d, $J = 8.0$ Hz, 2H), 7.29 (d, $J = 8.5$ Hz, 2H), 4.77 (m, 1H), 3.97 (dd, $J = 10.8, 5.2$ Hz, 1H), 3.89 (dd, $J = 10.8, 3.6$ Hz, 1H), 2.42 (s, 3H), 1.94 (s, 3H), 1.47-1.13 (multiple peaks, 8H), 0.84 (t, $J = 6.8$ Hz, 3H).



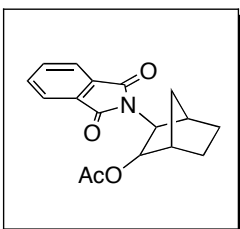
Product **41** was obtained as a yellow oil (25%). $^1\text{H NMR}$ (CDCl_3): δ 8.34 (d, $J = 7.2$ Hz, 2H), 8.07 (d, $J = 7.2$ Hz, 2H), 3.99 (dd, $J = 9.2, 4.0$ Hz, 1H), 3.95 (dd, $J = 9.2, 4.0$ Hz, 1H), 3.56 (m, 1H), 1.94 (s, 3H), 1.47-1.13 (multiple peaks, 8H), 0.84 (t, $J = 5.6$ Hz, 3H).



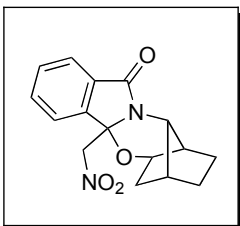
Product **43** was obtained as a yellow oil (38%). $^1\text{H NMR}$ (CDCl_3): δ 7.74 (d, $J = 8.0$ Hz, 2H), 7.29 (d, $J = 8.5$ Hz, 2H), 5.11 (d, $J = 9.0$ Hz, 1H), 4.68 (d, $J = 7.5$ Hz, 1H), 3.37 (d, $J = 8.5$ Hz, 1H), 2.42 (s, 3H), 2.10 (m, 1H), 2.04 (s, 3H), 1.98 (d, $J = 4.5$ Hz, 1H), 1.84 (dd, $J = 14.5, 8.0$ Hz, 1H), 1.65 (m, 1H), 1.58-1.46 (multiple peaks, 2H), 1.04 (m, 1H).



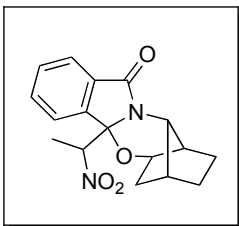
Product **45** was obtained as a yellow oil (29%). ^1H NMR (CDCl_3): δ 4.72, (br s, 1H), 4.62 (br s, 1H), 2.48 (m, 1H), 2.42 (m, 1H), 2.29 (m, 1H), 2.04 (s, 3H), 1.94 (s, 3H), 1.94 (m, 1H), 1.70 (m, 1H), 1.59 (m, 1H), 1.21 (m, 1H), 1.13 (m, 1H).



Product **46** was obtained as a yellow oil (42%). ^1H NMR (CDCl_3): δ 7.81 (m, 2H), 7.69 (m, 2H), 4.73 (d, $J = 8.0$ Hz, 1H), 3.59-3.57 (multiple peaks, 2H), 3.47 (d, $J = 4.5$ Hz, 1H), 1.92 (dd, $J = 14.0, 7.0$, 1H), 1.81 (m, 1H), 1.74 (m, 1H), 1.64 (m, 1H), 1.54 (s, 3H), 1.24 (m, 2H).

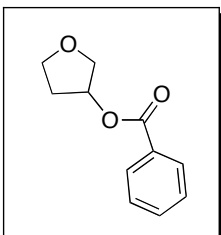


Product **47** was obtained as a yellow oil (47%). ^1H NMR (CDCl_3): δ 7.67 (d, $J = 8.0$ Hz, 1H), 7.54-7.51 (multiple peaks, 2H), 7.43 (m, 1H), 4.88 (d, $J = 11.0$ Hz, 1H), 4.75 (d, $J = 11.0$ Hz, 1H), 4.15 (d, $J = 6.4$ Hz, 1H), 4.09 (br s, 1H), 2.95 (br s, 1H), 2.87 (d, $J = 5.2$ Hz, 1H), 1.79 (m, 1H), 1.53 (m, 1H), 1.45 (m, 1H), 1.18-1.10 (multiple peaks, 2H). ^{13}C $\{^1\text{H}\}$ NMR (CDCl_3): δ 169.28, 145.79, 132.98, 130.24, 129.77, 128.29, 123.72, 122.38, 85.46, 82.50, 78.97, 59.35, 38.58, 38.08, 37.40, 25.24, 21.36. IR (thin film): 1711, 1552, 1377 cm^{-1} . HRMS electrospray (m/z): $[\text{M} + \text{H}]^+$ calcd for $\text{C}_{16}\text{H}_{16}\text{N}_2\text{O}_4$, 301.1188; found, 301.1188.



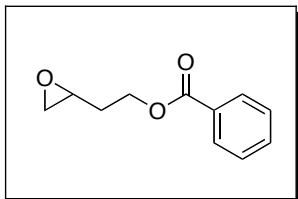
Product **48** was obtained as a yellow oil (14%). ^1H NMR (CDCl_3): δ 7.79-7.76 (multiple peaks, 2H), 7.61 (t, $J = 7.0$ Hz, 1H), 7.53 (t, $J = 7.5$ Hz, 1H), 5.23 (q, $J = 6.5$ Hz, 1H), 4.22 (d, $J = 6.5$ Hz, 1H), 4.13 (br s, 1H), 3.11 (d, $J = 4.5$ Hz, 1H), 3.00 (br s, 1H), 1.84 (m, 1H), 1.61 (m, 1H), 1.51 (dd, $J = 14.0, 6.5$ Hz, 1H), 1.32-1.20 (multiple peaks, 2H), 1.04 (d, $J = 6.5$ Hz, 3H). ^{13}C $\{^1\text{H}\}$ NMR (CDCl_3): δ 169.77, 144.15, 133.69, 132.67, 130.33, 129.98, 124.11, 123.45, 122.85, 89.00, 87.91, 78.52, 59.50, 38.69, 37.83, 37.48, 25.19, 21.36, 15.12. IR (thin film): 1711, 1552, 1377 cm^{-1} . HRMS (ESI, m/z): $[\text{M} + \text{H}]^+$ calcd for $\text{C}_{16}\text{H}_{16}\text{N}_2\text{O}_4$, 301.1188; found, 301.1188.

Typical Procedure for Alcohol cyclization: $\text{PhI}(\text{O}_2\text{CPh})_2$ (90 mg, 2.77 mmol, 2.0 equiv) and $\text{Pd}(\text{OAc})_2$ (15 mg, 0.069 mmol, 0.05 equiv) were combined in CH_3CN (2.8 mL) in a 20 mL vial. 3-Buten-1-ol (100 g, 1.39 mmol, 1.0 equiv) was added, the vial was sealed with a Teflon-lined cap, and the reaction was stirred at 60 $^\circ\text{C}$ for 18 h. The resulting mixture was evaporated to dryness and then taken up in diethyl ether (10 mL). The ether layer was washed with H_2O (2 x 20 mL), saturated aqueous NaHCO_3 (10 mL), and saturated aqueous NaCl (10 mL). The ether layer was then dried over MgSO_4 , filtered, and concentrated to afford a red oil, which was purified by chromatography on silica gel ($R_f = 0.28$ in 70% hexanes/30% ethyl acetate).

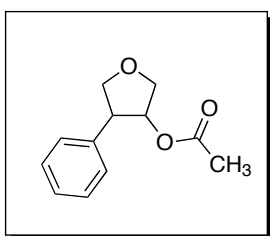


The product **65** was obtained as a clear oil (113 mg, 42% yield). ^1H NMR (CDCl_3): δ 8.03 (d, $J = 8.4$ Hz, 2H), 7.56 (m, 1H), 7.43 (t, $J = 7.9$ Hz, 2H), 5.54 (m, 1H), 4.00-3.88 (multiple peaks, 4H), 2.26 (m, 1H), 2.15 (m, 1H). ^{13}C $\{^1\text{H}\}$ NMR (CDCl_3): δ 166.24,

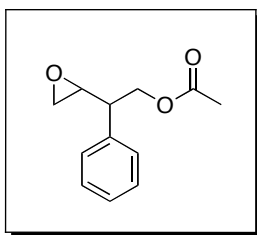
133.07, 129.92, 129.56, 128.32, 75.34, 73.15, 67.09, 32.89. IR (thin film): 1717 cm^{-1} . HRMS (ESI, m/z): $[M + H]^+$ calcd for $\text{C}_{11}\text{H}_{12}\text{O}_3$, 193.0865; found, 193.0865.



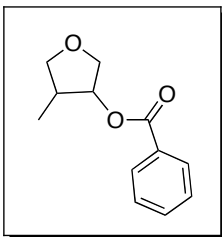
The product **68** was obtained as a clear oil (10% yield). ^1H NMR (CDCl_3): δ 8.06-8.03 (multiple peaks, 2H), 7.58 (m, 1H), 7.46-7.42 (multiple peaks, 2H), 4.36 (t, $J = 6.8$ Hz, 2H), 4.05-3.86 (multiple peaks, 3H), 1.92 (m, 2H).



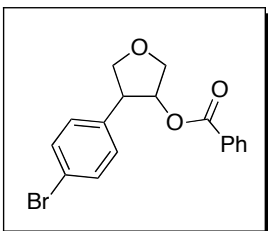
The product **73** was obtained as a clear oil (35%, 2:1 dr). ^1H NMR (CDCl_3): δ 7.35-7.28 (multiple peaks, 5H), 5.19 (quin, $J = 2.5$ Hz, 1H), 4.28 (dd, $J = 9.0, 7.0$ Hz, 1H), 4.17 (dd, $J = 10.5, 5.0$ Hz, 1H), 3.96 (dd, $J = 9.0, 5.0$ Hz, 1H), 3.89 (dd, 10.5, 2.0 Hz, 1H), 3.47 (m, 1H), 2.10 (s, 3H). ^{13}C $\{^1\text{H}\}$ NMR (CDCl_3): δ 170.73, 168.30, 128.82, 127.40, 127.11, 81.37, 73.08, 72.76, 51.18, 29.60. HRMS (ESI, m/z): $[M + \text{Na}]^+$ calcd for $\text{C}_{17}\text{H}_{16}\text{O}_3$, 229.0841; found, 229.0839.



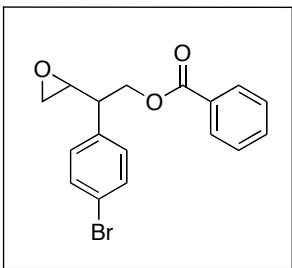
The product **74** was obtained as a clear oil (23%). ^1H NMR (CDCl_3): δ 7.37-7.25 (multiple peaks, 5H), 4.45 (m, 2H), 3.21 (m, 1H), 2.76 (m, 2H), 2.56 (dd, $J = 4.5, 3.0$ Hz, 1H), 2.04 (s, 3H). ^{13}C $\{^1\text{H}\}$ NMR (CDCl_3): δ 170.90, 137.89, 128.72, 127.94, 127.45, 65.46, 53.31, 47.64, 46.03, 20.85. IR (thin film): 1740 cm^{-1} . HRMS (ESI, m/z): $[M + \text{Na}]^+$ calcd for $\text{C}_{17}\text{H}_{16}\text{O}_3$, 229.0841; found, 229.0838.



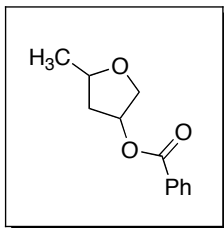
The product **76** was obtained as a clear oil (22%, 1.4:1 dr). $^1\text{H NMR}$ (CDCl_3): δ 8.05 (m, 2H), 7.57 (m, 1H), 7.44(m, 2H), 5.15 (m, 1H), 4.19-4.15 (multiple peaks, 2H), 3.98 (d, $J = 13.0$ Hz, 1H), 3.55 (dd, $J = 8.5, 4.5$ Hz, 1H), 1.18 (d, $J = 6.5$ Hz, 3H).



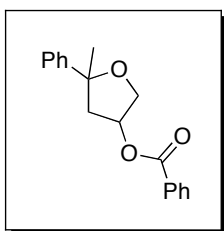
The product **78** was obtained as a clear oil (30%, 1:1 dr). $^1\text{H NMR}$ (CDCl_3): δ 7.99 (d, $J = 8.5$ Hz, 2H), 7.86 (d, $J = 8.5$ Hz, 2H), 7.55-7.42 (multiple peaks, 5H), 5.41 (m, 1H), 4.35 (dd, $J = 9.5, 6.0$ Hz, 1H), 4.29 (dd, $J = 11.0, 5.0$ Hz, 1H), 4.08-4.05 (multiple peaks, 2H), 3.60 (m, 1H).



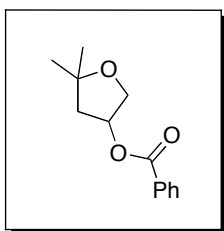
The product **78'** was obtained as a viscous oil (10%). $^1\text{H NMR}$ (CDCl_3): δ 8.13 (d, $J = 7.0$ Hz, 2H), 7.99 (d, $J = 8.0$ Hz, 2H), 7.50-7.41 (multiple peaks, 3H), 7.22 (d, $J = 8.0$ Hz, 2H), 4.66 (d, $J = 6.5$ Hz, 2H), 3.28 (m, 1H), 2.93 (q, $J = 7.0$ Hz, 1H), 2.81 (t, $J = 4.5$ Hz, 1H), 2.61 (dd, $J = 4.5, 3.0$ Hz, 1H).



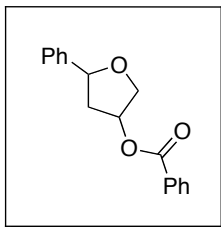
Mixture of cis and trans Isomers in a 1.0:1.8 ratio. ^1H NMR (CDCl_3): δ 8.08-8.04 (multiple peaks, 4H), 7.68-7.27 (multiple peaks, 2H), 7.48-7.43 (multiple peaks, 4H), 5.50 (m, 1H), 5.37 (m, 1H), 4.42-4.39 (multiple peaks, 2H), 4.10-4.04 (multiple peaks, 4H), 1.78-1.71 (multiple peaks, 2H), 1.66-1.62 (multiple peaks, 2H), 1.39 (d, $J = 86.5$ Hz, 3H), 1.23 (d, $J = 6.0$ Hz, 3H).



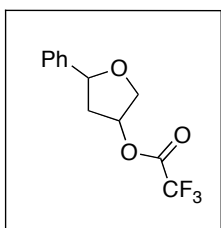
Product **82** was obtained as a yellow oil (37%, 2:1 dr). **Isomer 1**: ^1H NMR (CDCl_3): δ 7.49-7.43 (multiple peaks, 5H), 7.45-7.38 (multiple peaks, 2H), 7.29-7.25 (multiple peaks, 3H), 5.64 (m, 1H), 4.43 (dd, $J = 10.5, 5.5$ Hz, 1H), 4.08 (dd, $J = 10.5, 0.5$ Hz, 1H), 2.68 (d, $J = 14.0$, 1H), 2.41 (dd, $J = 14.0, 5.5$ Hz, 1H), 1.63 (s, 3H). ^{13}C $\{^1\text{H}\}$ NMR (CDCl_3): δ 165.96, 147.25, 132.84, 129.75, 129.45, 128.04, 126.29, 124.69, 84.74, 75.92, 72.77, 45.83, 30.23, 29.68. **Isomer 2**: ^1H NMR (CDCl_3): δ 8.10 (dd, $J = 8.0, 1.0$ Hz, 2H), 7.61 (t, $J = 7.5$ Hz, 1H), 7.49 (t, $J = 8.0$ Hz, 2H), 7.44 (dd, $J = 8.5, 1.0$ Hz, 2H), 7.38 (t, $J = 8.0$ Hz, 2H), 7.27 (t, $J = 7.5$ Hz, 1H), 5.51 (m, 1H), 4.22 (d, $J = 11.0$ Hz, 1H), 4.15 (dd, $J = 11.0, 5.0$ Hz, 1H), 2.75 (dd, $J = 14.0, 7.0$ Hz, 1H), 2.45 (dd, $J = 14.0, 2.5$ Hz, 1H), 1.71 (s, 3H). ^{13}C $\{^1\text{H}\}$ NMR (CDCl_3): δ 166.25, 147.25, 133.16, 129.99, 129.63, 128.43, 128.39, 126.76, 124.45, 84.52, 72.29, 45.69, 30.63, 29.70.



Product **83** was obtained as a yellow oil (40%). $^1\text{H NMR}$ (CDCl_3): δ 7.97 (d, $J = 8.0$ Hz, 2H), 7.52 (t, $J = 7.5$ Hz, 1H), 7.40 (t, $J = 8.0$ Hz, 2H), 5.54 (m, 1H), 4.19 (dd, $J = 11.0$, 5.0 Hz, 1H), 4.03 (d, $J = 11$ Hz, 1H), 2.18 (dd, $J = 14.0$, 7.0, 1H), 2.04 (d, $J = 14.0$ Hz, 1H), 1.72 (s, 3H), 1.42 (s, 3H), 1.31 (s, 3H).



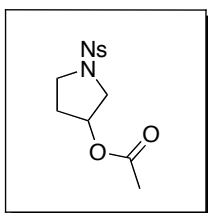
Product **86** was obtained as a yellow oil (29%, 2:1 dr). **Cis Isomer:** $^1\text{H NMR}$ (CDCl_3): δ 7.90 (dd, $J = 7.5$, 1.6 Hz, 2H), 7.55 (t, $J = 7.5$ Hz, 1H), 7.44-7.30 (multiple peaks, 7H), 5.63 (m, 1H), 5.02 (t, $J = 8.0$ Hz, 1H), 4.30 (d, $J = 11.0$ Hz, 1H), 4.11 (dd, $J = 11.0$, 5.0 Hz, 1H), 2.84 (m, 1H), 2.18 (m, 1H). **Trans Isomer:** $^1\text{H NMR}$ (CDCl_3): δ 7.39-7.29 (multiple peaks, 10H), 5.62 (t, $J = 6.0$ Hz, 1H), 5.11 (dd, $J = 10.5$, 5.0 Hz, 1H), 4.44 (dd, $J = 11.0$, 5.0 Hz, 1H), 4.04 (dd, $J = 11.0$, 2.0 Hz, 1H), 2.54 (dd, $J = 14.5$, 6.0 Hz, 1H), 2.17 (m, 1H).



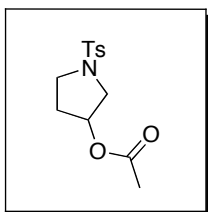
Product **124** was obtained as a yellow oil (29%, 2:1 dr). **Trans Isomer:** $^1\text{H NMR}$ (CDCl_3): δ 7.39-7.29 (multiple peaks, 5H), 5.62 (t, $J = 5.0$ Hz, 1H), 5.11 (dd, $J = 10.0$, 5.0 Hz, 1H), 4.44 (dd, $J = 11.5$, 5.0 Hz, 1H), 4.05 (dd, $J = 11.5$, 3.0 Hz, 1H), 2.54 (dd, $J = 14.0$, 5.5 Hz, 1H), 2.17 (ddd, $J = 14.0$, 10.0, 5.5 Hz, 1H). **Cis Isomer:** $^1\text{H NMR}$ (CDCl_3): δ 7.38-7.31 (multiple peaks, 5H), 5.56 (m, 1H), 4.93 (t, $J = 9.0$ Hz, 1H), 4.29 (d, $J = 14.0$ Hz, 1H), 4.01 (dd, $J = 14.0$, 6.0 Hz, 1H), 2.86 (quin, $J = 9.0$ Hz, 1H), 2.08 (m, 1H).

Typical Procedure for Amine cyclization: $\text{PhI}(\text{O}_2\text{CH}_3)_2$ (90 mg, 2.77 mmol, 2.0 equiv), NaHCO_3 (90 mg, 2.77 mmol, 2.0 equiv) and $\text{Pd}(\text{OAc})_2$ (15 mg, 0.069 mmol, 0.05 equiv) were combined in CH_3CN (2.8 mL) in a 20 mL vial. Amine (1.0 equiv) was

added, the vial was sealed with a Teflon-lined cap, and the reaction was stirred at 60 °C for 18 h. The resulting mixture was evaporated to dryness and then taken up in diethyl ether (10 mL). The ether layer was washed with H₂O (2 x 20 mL), saturated aqueous NaHCO₃ (10 mL), and saturated aqueous NaCl (10 mL). The ether layer was then dried over MgSO₄, filtered, and concentrated to afford a red oil, which was purified by chromatography on silica gel ($R_f = 0.28$ in 70% hexanes/30% ethyl acetate).



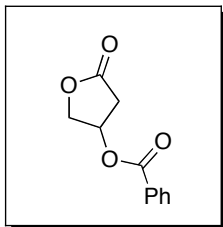
Product **88** was obtained as a yellow oil (20%). ¹H NMR (CDCl₃): δ 8.40 (d, $J = 8.8$ Hz, 2H), 8.03 (d, $J = 8.8$ Hz, 2H), 5.17 (m, 1H), 3.57 (q, $J = 4.8$ Hz, 1H), 3.52 (d, $J = 4.8$ Hz, 1H), 3.43-3.32 (multiple peaks, 2H), 2.04 (m, 2H), 1.83 (s, 3H).



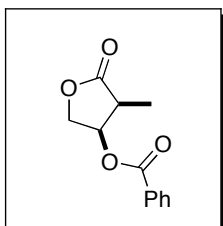
Product **91** was obtained as a yellow oil (19%). ¹H NMR (CDCl₃): δ 7.72 (d, $J = 8.0$ Hz, 2H), 7.33 (d, $J = 8.0$ Hz, 2H), 5.10 (m, 1H), 3.53 (dd, $J = 8.8, 5.0$ Hz, 1H), 3.46 (dd, $J = 12.0, 5.0$ Hz, 1H), 3.42 (m, 1H), 4.31 (m, 1H), 2.42 (s, 3H), 1.95-1.93 (multiple peaks, 2H), 1.80 (s, 3H).

Typical Procedure for Acid cyclization: PhI(O₂CPh)₂ (90 mg, 2.77 mmol, 2.0 equiv), NaHCO₃ (90 mg, 2.77 mmol, 2.0 equiv) and Pd(OAc)₂ (15 mg, 0.069 mmol, 0.05 equiv) were combined in CH₂Cl₂ (2.8 mL) in a 20 mL vial. 3-Butenoic Acid (100 g, 1.39 mmol, 1.0 equiv) was added, the vial was sealed with a Teflon-lined cap, and the reaction was stirred at 60 °C for 18 h. The resulting mixture was evaporated to dryness and then taken up in diethyl ether (10 mL). The ether layer was washed with H₂O (2 x 20 mL), saturated aqueous NaHCO₃ (10 mL), and saturated aqueous NaCl (10 mL). The ether layer was then dried over MgSO₄, filtered, and concentrated to afford a red oil, which

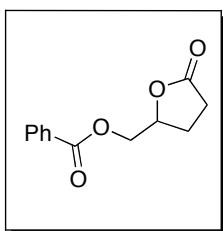
was purified by chromatography on silica gel ($R_f = 0.28$ in 70% hexanes/30% ethyl acetate).



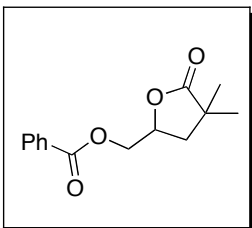
Product **100** was obtained as a yellow oil (56%). $^1\text{H NMR}$ (CDCl_3): δ 8.03 (d, $J = 8.0$ Hz, 2H), 7.61 (t, $J = 8.0$ Hz, 1H), 7.47 (t, $J = 7.5$ Hz, 2H), 4.63 (dd, $J = 11.1, 4.8$ Hz, 1H), 4.53 (d, $J = 11.1$ Hz, 1H), 3.00 (dd, $J = 18.5, 6.7$ Hz, 1H), 2.81 (d, $J = 18.5$ Hz, 1H).



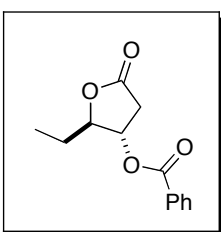
Product **102** was obtained as a yellow oil (65%, 1:1 dr). **Cis Isomer:** $^1\text{H NMR}$ (CDCl_3): δ 8.03 (d, $J = 7.5$ Hz, 2H), 7.61 (t, $J = 7.5$ Hz, 1H), 7.47 (t, $J = 7.5$ Hz, 2H), 5.76 (m, 1H), 4.51 (dd, $J = 11.0, 4.5$ Hz, 1H), 4.45 (d, $J = 11.0$ Hz, 1H), 2.91 (quin, $J = 7.5$ Hz, 1H), 1.34 (d, $J = 7.5$ Hz, 3H). **Trans Isomer:** $^1\text{H NMR}$ (CDCl_3): δ 8.04 (d, $J = 7.0$ Hz, 2H), 7.61 (t, $J = 7.0$ Hz, 1H), 7.46 (t, $J = 7.5$ Hz, 2H), 5.32 (m, 1H), 4.70 (dd, $J = 11.0, 5.5$ Hz, 1H), 4.35 (dd, $J = 11.0, 3.5$ Hz, 1H), 2.91 (m, 1H), 1.44 (d, $J = 7.0$ Hz, 3H).



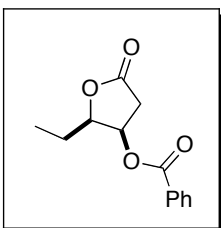
Product **104** was obtained as a yellow oil (60%). $^1\text{H NMR}$ (CDCl_3): δ 8.03 (dd, $J = 8.0, 1.5$ Hz, 2H), 7.59 (t, $J = 8.0$ Hz, 1H), 7.46 (t, $J = 8.0$ Hz, 2H), 4.88 (m, 1H), 4.54 (dd, $J = 12.0, 3.0$ Hz, 1H), 4.44 (dd, $J = 12.0, 5.0$ Hz, 1H), 2.69-2.56 (multiple peaks, 2H), 2.43 (m, 1H), 2.14 (m, 1H). IR (thin film): 1776, 1722 cm^{-1} .



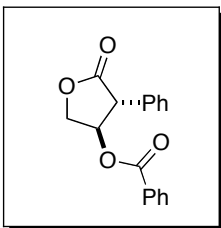
Product **106** was obtained as a yellow oil (66%). $^1\text{H NMR}$ (CDCl_3): δ 8.05 (dd, $J = 8.1$, 1.2 Hz, 2H), 7.59 (t, $J = 8.1$ Hz, 1H), 7.46 (t, $J = 8.1$ Hz, 2H), 4.79 (m, 1H), 4.57 (dd, $J = 12.0$, 3.3 Hz, 1H), 4.37 (dd, $J = 12.0$, 6.3 Hz, 1H), 2.22 (dd, $J = 12.9$, 6.3 Hz, 1H), 1.95 (dd, $J = 12.9$, 9.9 Hz, 1H), 1.33 (s, 3H), 1.31 (s, 3H).



Product **108** was obtained as a yellow oil (65%, 13:1 dr). $^1\text{H NMR}$ (CDCl_3): δ 8.03 (d, $J = 7.5$ Hz, 2H), 7.61 (t, $J = 8.0$ Hz, 1H), 7.47 (t, $J = 8.0$ Hz, 2H), 5.37 (dt, $J = 7.5$, 2.0 Hz, 1H), 4.58 (td, $J = 7.0$, 2.0 Hz, 1H), 3.04 (dd, $J = 20.0$, 7.5 Hz, 1H), 2.72 (dd, $J = 20.0$, 2.0 Hz, 1H), 1.88-1.71 (multiple peaks, 2H), 1.10 (t, $J = 7.0$ Hz, 3H).

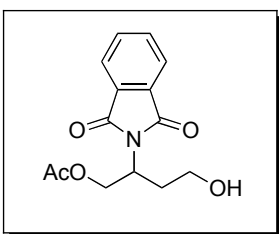


Product **110** was obtained as a yellow oil (56%, 9:1 dr). $^1\text{H NMR}$ (CDCl_3): δ 8.02 (dd, $J = 8.0$, 1.5 Hz, 2H), 7.61 (t, $J = 7.5$ Hz, 1H), 7.50-7.46 (multiple peaks, 2H), 5.74 (t, $J = 5.0$ Hz, 1H), 4.57 (m, 1H), 3.02 (dd, $J = 8.5$, 5.5 Hz, 1H), 2.73 (d, $J = 18.5$ Hz, 1H), 1.95 (septet, $J = 7.0$ Hz, 1H), 1.80 (m, 1H), 1.06 (t, $J = 7.0$ Hz, 3H).



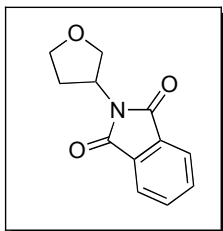
Product **112** was obtained as a yellow oil (48%, >50:1 dr). $^1\text{H NMR}$ (CDCl_3): δ 8.08 (dd, $J = 8.4, 1.6$ Hz, 2H), 7.64 (t, $J = 7.2$ Hz, 1H), 7.52-7.38 (multiple peaks, 8H), 5.75 (br s, 1H), 5.54 (dt, $J = 6.4, 1.5$ Hz, 1H), 3.01 (dd, $J = 18.4, 6.4$ Hz, 1H), 2.78 (dd, $J = 18.4, 1.5$, 1H).

Typical Procedure for Formation of Amino-Tetrahydrofurans: Phthalimide (100 mg, 0.68 mmol, 1 equiv), $\text{PhI}(\text{OAc})_2$ (0.440 g, 1.36 mmol, 2 equiv), AgBF_4 (13 mg, 0.068 mmol, 0.10 equiv), and $\text{Pd}(\text{OAc})_2$ (8 mg, 0.034 mmol, 0.05 equiv) were combined in CH_3CN (1.4 mL) in a 20 mL vial. 3-Buten-1-ol (98 mg, 1.36 mmol, 2.0 equiv) was added to the reaction, the vial was sealed with a Teflon-lined cap, and the reaction was heated at 60 °C for 1 h. The reaction was cooled to room temperature and additional $\text{PhI}(\text{OAc})_2$ (0.22 g, 0.68 mmol, 1.0 equiv) along with a solution of $\text{Pd}(\text{OAc})_2$ (8 mg, 0.034 mmol, 0.05 equiv) and AgBF_4 (13 mg, 0.068 mmol, 0.10 equiv) in CH_3CN (0.4 mL) was added to the reaction. Another equivalent of the alcohol (49 mg, 0.68 mmol) was also added, and the reaction was heated at 60 °C for an additional 8 h. The resulting mixture was evaporated to dryness and then taken up in diethyl ether (10 mL). The ether layer washed with 10% aqueous Et_3N (10 mL), H_2O (2 x 20 mL), saturated aqueous NaHCO_3 (20 mL), and saturated aqueous NaCl (20 mL). The ether extracts were dried over MgSO_4 , filtered, and concentrated to afford a red oil, which was purified by chromatography on silica gel.

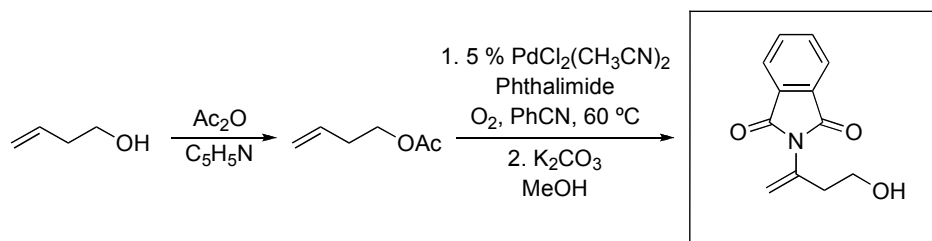


Product **61** was obtained as a yellow viscous oil ($R_f = 0.22$ in 50% hexanes/50% ethyl acetate). $^1\text{H NMR}$ (CDCl_3): δ 7.85 (dd, $J = 5.6, 3.1$ Hz, 2H), 7.74 (dd, $J = 5.3, 3.1$ Hz,

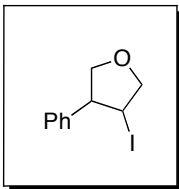
2H), 4.70 (m, 1H), 4.59 (dd, $J = 11.2, 9.3$ Hz, 1H), 4.46 (dd, $J = 11.2, 4.9$ Hz, 1H), 3.71 (m, 1H), 3.59 (m, 1H), 2.26 (m, 1H), 2.03 (m, 1H), 1.98 (s, 3H), 1.74 (br s, 1H). ^{13}C $\{^1\text{H}\}$ NMR (CDCl_3): δ 170.63, 168.61, 134.16, 131.67, 123.39, 63.51, 59.12, 47.77, 31.42, 20.74.



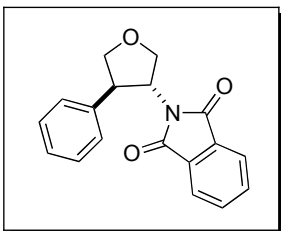
The second addition of catalyst, oxidant, and alcohol was after 1 h. Product **62** was isolated as a white solid (66 mg, 45% yield, $R_f = 0.10$ in 70% hexanes/30% ethyl acetate). mp = 81.4-84.6 °C. ^1H NMR (CDCl_3): δ 7.83 (dd, $J = 5.5, 3.1$ Hz, 2H), 7.71 (dd, $J = 5.4, 3.1$ Hz, 2H), 4.91 (m, 1H), 4.22 (q, $J = 8.4$ Hz, 1H), 4.04 (t, $J = 8.7$ Hz, 1H), 3.98 (td, $J = 8.4, 5.2$ Hz, 1H), 3.91 (dd, $J = 8.8, 6.9$ Hz, 1H), 2.39 (m, 1H), 2.25 (m, 1H). ^{13}C $\{^1\text{H}\}$ NMR (CDCl_3): δ 167.99, 134.05, 131.77, 123.21, 69.40, 68.34, 49.55, 29.72. IR (thin film): 1700 cm^{-1} . HRMS (ESI, m/z): $[\text{M} + \text{Na}]^+$ calcd for $\text{C}_{12}\text{H}_{11}\text{NO}_3$, 240.0637; found, 240.0634.



3-Buten-1-ol was treated with acetic anhydride in pyridine to protect the alcohol functionality. This alkene was then treated with phthalimide and $\text{Pd}(\text{OAc})_2$ in PhCN under an oxygen atmosphere at 60 °C for 24 h.⁸ The resulting product was deprotected with K_2CO_3 in MeOH to afford an authentic sample of **64**. Product **64** was obtained as a pale yellow viscous oil ($R_f = 0.15$ in 65% hexanes/35% ethyl acetate). ^1H NMR (CDCl_3): δ 7.89 (dd, $J = 5.2, 3.3$ Hz, 2H), 7.77 (dd, $J = 5.3, 3.1$ Hz, 2H), 5.58 (s, 1H), 5.30 (s, 1H), 3.66 (t, $J = 5.8$ Hz, 2H), 2.68 (t, $J = 5.8$ Hz, 2H), 2.22 (br s, 1H). ^{13}C $\{^1\text{H}\}$ NMR (CDCl_3): δ 167.65, 135.65, 134.41, 131.76, 123.76, 119.83, 59.26, 37.96.



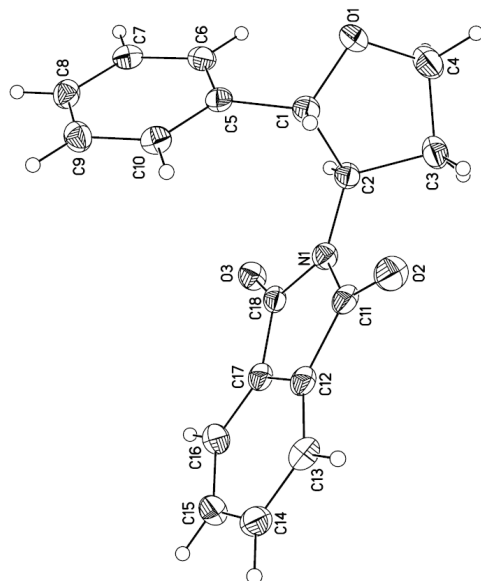
^1H NMR (CDCl_3): δ 7.37-7.34 (multiple peaks, 2H), 7.31-7.27 (multiple peaks, 3H), 4.42 (dd, $J = 9.0, 6.0$ Hz, 1H), 4.24 (t, $J = 8.0$ Hz, 1H), 4.17 (q, $J = 8.0$ Hz, 1H), 4.10 (dd, $J = 9.0, 8.0$ Hz, 1H), 3.92 (dd, $J = 9.0, 7.0$ Hz, 1H), 3.63 (q, $J = 8.0$ Hz, 1H). ^{13}C $\{^1\text{H}\}$ NMR (CDCl_3): δ 138.86, 128.90, 127.47, 127.24, 73.45, 56.57, 25.94.



The second addition of catalyst, oxidant, and alcohol was after 10 h. The product was obtained as a 10:1 ratio of diastereomers (154 mg, 77% yield, $R_f = 0.12$ in 70% hexanes/30% ethyl acetate). The diastereomers were separated by HPLC (90% hexanes/10% ethyl acetate, 20 mL/min, Waters μ -porasil 19.1 mm). **Major diastereomer (126)**: white solid, mp = 105.4-108.2 °C. ^1H NMR (CDCl_3): δ 7.82 (dd, $J = 5.4, 3.1$ Hz, 2H), 7.71 (dd, $J = 5.4, 3.1$ Hz, 2H), 7.32-7.27 (multiple peaks, 4H), 7.22 (m, 1H), 5.07 (q, $J = 8.3$ Hz, 1H), 4.51 (dd, $J = 8.6, 7.9$ Hz, 1H), 4.26-4.17 (multiple peaks, 3H), 3.96 (dd, $J = 8.7, 7.7$ Hz, 1H). ^{13}C $\{^1\text{H}\}$ NMR (CDCl_3): δ 167.94, 139.58, 134.15, 131.69, 128.88, 127.37, 127.19, 123.37, 75.04, 68.94, 56.95, 47.29. IR (thin film): 1713 cm^{-1} . HRMS (ESI, m/z): $[\text{M} + \text{Na}]^+$ calcd for $\text{C}_{18}\text{H}_{15}\text{NO}_3$, 316.0950; found, 316.0948. **Minor diastereomer**: ^1H NMR (CDCl_3): δ 7.66 (dd, $J = 5.4, 3.1$ Hz, 2H), 7.61 (dd, $J = 5.5, 3.2$ Hz, 2H), 7.14-7.08 (multiple peaks, 4H), 7.02 (m, 1H), 5.24 (td, $J = 8.8, 5.3$ Hz, 1H), 4.63 (dd, $J = 10.0, 8.3$ Hz, 1H), 4.57 (dd, $J = 9.5, 5.3$ Hz, 1H), 4.37-4.32 (multiple peaks, 2H), 3.80 (q, $J = 9.4$ Hz, 1H). ^{13}C $\{^1\text{H}\}$ NMR (CDCl_3): δ 168.22, 135.43, 133.88, 131.18, 128.33, 128.19, 126.96, 122.99, 71.37, 68.93, 54.00, 48.86.

Structure Determination of **126**.

Colorless, needle-like crystals of **126** were grown by diffusion of pentane into a chlorobenzene solution at 22 deg. C. A crystal of dimensions 0.48 x 0.13 x 0.12 mm was



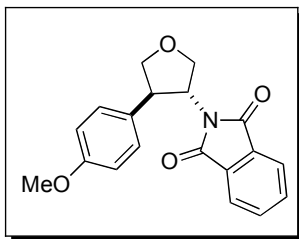
mounted on a standard Bruker SMART 1K CCD-based X-ray diffractometer equipped with a LT-2 low temperature device and normal focus Mo-target X-ray tube ($\lambda = 0.71073 \text{ \AA}$) operated at 2000 W power (50 kV, 40 mA). The X-ray intensities were measured at 108(2) K; the detector was placed at a distance 4.969 cm from the crystal. A total of 2450 frames were collected with a scan width of 0.5° in ω and 0.45° in ϕ with an exposure time of 30 s/frame. The integration of the data yielded a total of 28419 reflections to a maximum 2θ value of 56.60°

of which 2053 were independent and 1780 were greater than $2\sigma(I)$. The final cell constants (Table 1) were based on the xyz centroids of 7712 reflections above $10\sigma(I)$. Analysis of the data showed negligible decay during data collection; the data were processed with SADABS and corrected for absorption. The structure was solved and refined with the Bruker SHELXTL (version 6.12) software package, using the space group $P2(1)2(1)2(1)$ with $Z = 4$ for the formula $C_{18}H_{15}NO_3$. All non-hydrogen atoms were refined anisotropically with the hydrogen atoms placed in idealized positions. Full matrix least-squares refinement based on F^2 converged at $R1 = 0.0297$ and $wR2 = 0.0689$ [based on $I > 2\sigma(I)$], $R1 = 0.0402$ and $wR2 = 0.0742$ for all data.

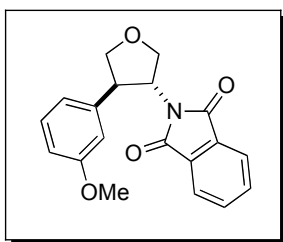
Sheldrick, G.M. SHELXTL, v. 6.12; Bruker Analytical X-ray, Madison, WI, 2001.

Sheldrick, G.M. SADABS, v. 2.10. Program for Empirical Absorption Correction of Area Detector Data, University of Gottingen: Gottingen, Germany, 2003.

Saint Plus, v. 7.01, Bruker Analytical X-ray, Madison, WI, 2003

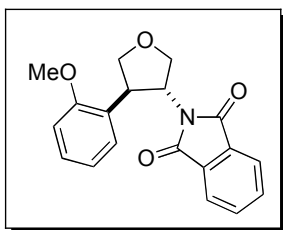


The second addition of catalyst, oxidant, and alcohol was after 30 min. The product was obtained as a 15:1 ratio of diastereomers (136 mg, 62% yield, $R_f = 0.08$ in 70% hexanes/30% ethyl acetate). The diastereomers were separated by HPLC (90% hexanes/10% ethyl acetate, 20 mL/min, Waters μ -porasil 19.1 mm). **Major diastereomer (127)**: white solid, mp = 129.2-130.8 °C. ^1H NMR (CDCl_3): δ 7.81 (dd, $J = 5.4, 3.1$ Hz, 2H), 7.70 (dd, $J = 5.5, 3.1$ Hz, 2H), 7.20 (d, $J = 8.8$ Hz, 2H), 6.82 (d, $J = 8.8$ Hz, 2H), 5.02 (q, $J = 8.4$ Hz, 1H), 4.46 (t, $J = 8.0$ Hz, 1H), 4.23-4.14 (multiple peaks, 3H), 3.90 (dd, $J = 8.7, 8.1$ Hz, 1H), 3.75 (s, 3H). ^{13}C $\{^1\text{H}\}$ NMR (CDCl_3): δ 167.91, 158.65, 134.08, 131.65, 131.11, 128.36, 123.30, 114.23, 74.98, 68.71, 56.97, 55.18, 46.42. IR (thin film): 1712 cm^{-1} . HRMS (ESI, m/z): $[\text{M} + \text{Na}]^+$ calcd for $\text{C}_{19}\text{H}_{17}\text{NO}_4$, 346.1055; found, 346.1051. **Minor diastereomer**: ^1H NMR (CDCl_3): δ 7.68 (dd, $J = 5.0, 3.3$ Hz, 2H), 7.62 (dd, $J = 5.1, 3.2$ Hz, 2H), 7.04 (d, $J = 8.8$ Hz, 2H), 6.64 (d, $J = 8.7$ Hz, 2H), 5.18 (td, $J = 8.7, 5.2$ Hz, 1H), 4.59-4.53 (multiple peaks, 2H), 4.36-4.29 (multiple peaks, 2H), 3.76 (m, 1H), 3.63 (s, 3H). ^{13}C $\{^1\text{H}\}$ NMR (CDCl_3): δ 168.31, 158.31, 133.91, 131.26, 129.37, 127.27, 123.05, 113.62, 71.63, 69.01, 55.09, 54.01, 48.24.



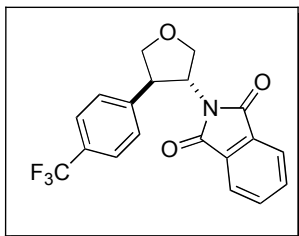
The second addition of catalyst, oxidant, and alcohol was after 3.5 h. The product was obtained as a 5.4:1 ratio of diastereomers (121 mg, 55% yield, $R_f = 0.07$ in 70% hexanes/30% ethyl acetate). The diastereomers were separated by HPLC (90% hexanes/10% ethyl acetate, 20 mL/min, Waters μ -porasil 19.1 mm). **Major diastereomer (128)**: white solid, mp = 95.8-100.8 °C. ^1H NMR (CDCl_3): δ 7.81 (dd, $J = 5.4, 3.1$ Hz, 2H), 7.70 (dd, $J = 5.6, 3.1$ Hz, 2H), 7.21 (t, $J = 7.8$ Hz, 1H), 6.87 (d, $J = 7.7$ Hz, 1H),

6.82 (t, $J = 2.2$ Hz, 1H), 6.76 (dd, $J = 8.2, 2.6$ Hz, 1H), 5.07 (q, $J = 8.3$ Hz, 1H), 4.49 (t, $J = 8.2$ Hz, 1H), 4.25-4.14 (multiple peaks, 3H), 3.95 (dd, $J = 8.6, 7.7$ Hz, 1H), 3.77 (s, 3H). ^{13}C $\{^1\text{H}\}$ NMR (CDCl_3): δ 167.88, 159.86, 141.25, 134.11, 131.66, 129.85, 123.32, 119.56, 113.08, 112.43, 74.91, 68.88, 56.76, 55.14, 47.26. IR (thin film): 1712 cm^{-1} . HRMS (ESI, m/z): $[\text{M} + \text{Na}]^+$ calcd for $\text{C}_{19}\text{H}_{17}\text{NO}_4$, 346.1055; found, 346.1056. **Minor diastereomer**: ^1H NMR (CDCl_3): δ 7.81 (dd, $J = 5.4, 3.1$ Hz, 2H), 7.70 (dd, $J = 5.6, 3.1$ Hz, 2H), 7.22-7.19 (multiple peaks, 2H), 6.84-6.82 (multiple peaks, 2H), 5.02 (q, $J = 8.4$ Hz, 1H), 4.46 (t, $J = 8.3$ Hz, 1H), 4.18-4.13 (multiple peaks, 3H), 3.90 (t, $J = 8.4$ Hz, 1H), 3.75 (s, 3H). ^{13}C $\{^1\text{H}\}$ NMR (CDCl_3): δ 167.93, 158.65, 141.25, 134.13, 131.11, 128.37, 123.31, 119.57, 114.23, 74.99, 68.72, 56.97, 55.19, 46.43. The minor diastereomer was isolated in a mixture with the major diastereomer (**128**); one ^{13}C resonance of this compound appears to overlap with a resonance associated with **128**.

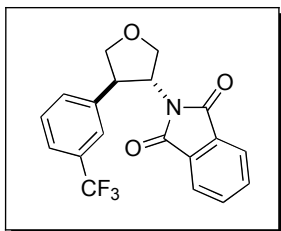


The second addition of catalyst, oxidant, and alcohol was after 3 h. The product was obtained as a 7.8:1 ratio of diastereomers (139 mg, 63% yield, $R_f = 0.09$ in 70% hexanes/30% ethyl acetate). The diastereomers were separated by HPLC (90% hexanes/10% ethyl acetate, 20 mL/min, Waters μ -porasil 19.1 mm). **Major diastereomer (129)**: white solid, mp = $115.8\text{-}120.7\text{ }^\circ\text{C}$. ^1H NMR (CDCl_3): δ 7.82 (dd, $J = 5.6, 3.0$ Hz, 2H), 7.70 (dd, $J = 5.4, 3.0$ Hz, 2H), 7.31 (d, $J = 7.6$ Hz, 1H), 7.19 (t, $J = 8.1$ Hz, 1H), 6.91 (t, $J = 8.3$ Hz, 1H), 6.80 (d, $J = 8.2$ Hz, 1H), 5.14 (q, $J = 8.1$ Hz, 1H), 4.51 (t, $J = 8.2$ Hz, 1H), 4.44 (q, $J = 7.6$ Hz, 1H), 4.21 (d, $J = 8.3$ Hz, 2H), 4.01 (t, $J = 8.4$ Hz, 1H), 3.67 (s, 3H). ^{13}C $\{^1\text{H}\}$ NMR (CDCl_3): δ 167.99, 157.56, 133.97, 131.80, 128.03, 127.66, 127.18, 123.19, 120.75, 110.42, 72.94, 68.93, 55.18, 55.17, 41.97. IR (thin film): 1712 cm^{-1} . HRMS (ESI, m/z): $[\text{M} + \text{Na}]^+$ calcd for $\text{C}_{19}\text{H}_{17}\text{NO}_4$, 346.1055; found, 346.1054. **Minor diastereomer**: ^1H NMR (CDCl_3): δ 7.64 (dd, $J = 5.3, 3.1$ Hz, 2H), 7.59 (dd, $J = 5.6, 3.1$ Hz, 2H), 7.12 (d, $J = 8.5$ Hz, 1H), 7.02 (t, $J = 8.1$ Hz, 1H), 6.73 (t, $J = 7.8$ Hz, 1H), 6.62 (d, $J = 8.2$ Hz, 1H), 5.41 (q, $J = 8.1$ Hz, 1H), 4.75 (dd, $J = 10.6, 8.0$ Hz, 1H),

4.36-4.35 (multiple peaks, 2H), 4.29 (t, $J = 7.3$ Hz, 1H), 3.96 (q, $J = 9.3$ Hz, 1H), 3.70 (s, 3H). ^{13}C $\{^1\text{H}\}$ NMR (CDCl_3): δ 167.78, 157.06, 133.61, 131.24, 127.91, 127.86, 123.68, 122.67, 119.83, 109.32, 70.53, 69.20, 54.97, 52.34, 42.86.

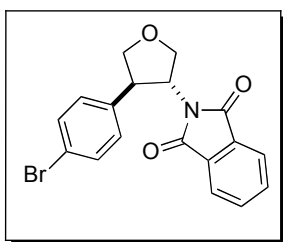


The second addition of catalyst, oxidant, and alcohol was after 4.5 h. The product **130** was obtained as white solid as a single diastereomer (133 mg, 54% yield, $R_f = 0.18$ in 70% hexanes/30% ethyl acetate). mp = 87.1-89.4 °C. ^1H NMR (CDCl_3): δ 7.83 (dd, $J = 5.6, 3.3$ Hz, 2H), 7.73 (dd, $J = 5.5, 3.3$ Hz, 2H), 7.56 (d, $J = 8.1$ Hz, 2H), 7.41 (d, $J = 8.5$ Hz, 2H), 5.04 (q, $J = 8.2$ Hz, 1H), 4.53 (dd, $J = 8.6, 8.0$ Hz, 1H), 4.28-4.17 (multiple peaks, 3H), 3.97 (dd, $J = 8.8, 6.9$ Hz, 1H). ^{13}C $\{^1\text{H}\}$ NMR (CDCl_3): δ 167.83, 144.29, 134.30, 131.57, 129.47 (q, $^2J_{\text{C-F}} = 32.3$ Hz), 127.70, 125.86 (q, $^3J_{\text{C-F}} = 3.9$ Hz), 124.01 (q, $^1J_{\text{C-F}} = 271$ Hz), 123.46, 74.85, 68.97, 56.98, 47.37. ^{19}F NMR (CDCl_3): δ -62.59. IR (thin film): 1715 cm^{-1} . HRMS (ESI, m/z): $[\text{M} + \text{Na}]^+$ calcd for $\text{C}_{19}\text{H}_{14}\text{NO}_3\text{F}_3$, 384.0823; found, 384.0823.

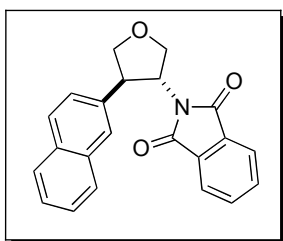


The second addition of catalyst, oxidant and alcohol was after 12 h. The product was obtained as a 16:1 ratio of diastereomers (147 mg, 60% yield, $R_f = 0.17$ in 70% hexanes/20% ethyl acetate). The diastereomers were separated by HPLC (90% hexanes/10% ethyl acetate, 20 mL/min, Waters μ -porasil 19.1 mm). **Major diastereomer (131)**: white solid, mp = 117.9-120.7 °C. ^1H NMR (CDCl_3): δ 7.83 (dd, $J = 5.3, 3.0$ Hz, 2H), 7.72 (dd, $J = 5.3, 3.0$ Hz, 2H), 7.51-7.41 (multiple peaks, 4H), 5.03 (q, $J = 8.2$ Hz, 1H), 4.54 (q, $J = 8.4$ Hz, 1H), 4.27 (t, $J = 8.4$ Hz, 1H), 4.22-4.16 (multiple peaks, 2H), 3.97 (dd, $J = 8.8, 6.7$ Hz, 1H). ^{13}C $\{^1\text{H}\}$ NMR (CDCl_3): δ 167.83, 141.45, 134.27, 131.59, 131.14 (q, $^2J_{\text{C-F}} = 32.2$ Hz), 130.55 (q, $^4J_{\text{C-F}} = 1.3$ Hz), 129.46, 123.92 (q, $^1J_{\text{C-F}} =$

272.6 Hz), 124.30 (q, $^1J_{C-F} = 3.7$ Hz), 124.10 (q, $^1J_{C-F} = 3.7$ Hz), 123.45, 75.00, 69.05, 57.11, 47.46. ^{19}F NMR (CDCl_3): δ -62.64. IR (thin film): 1713 cm^{-1} . HRMS (ESI, m/z): $[\text{M} + \text{Na}]^+$ calcd for $\text{C}_{19}\text{H}_{14}\text{NO}_3\text{F}_3$, 384.0823; found, 384.0824. **Minor diastereomer**: ^1H NMR (CDCl_3): δ 7.67 (dd, $J = 5.6, 3.1$ Hz, 2H), 7.63 (dd, $J = 5.5, 3.3$ Hz, 2H), 7.37-7.35 (multiple peaks, 2H), 7.30-7.24 (multiple peaks, 2H), 5.26 (m, 1H), 4.64-4.60 (multiple peaks, 2H), 4.38-4.33 (multiple peaks, 2H), 3.84 (q, $J = 9.6$ Hz, 1H). ^{13}C $\{^1\text{H}\}$ NMR (CDCl_3): δ 168.14, 147.00, 136.86, 134.08, 131.91, 131.01, 128.72, 125.13 (q, $^3J_{C-F} = 3.8$ Hz), 123.79 (q, $^3J_{C-F} = 4.0$ Hz), 123.06, 71.27, 68.68, 53.96, 48.64. ^{19}F NMR (CDCl_3): δ -63.01.

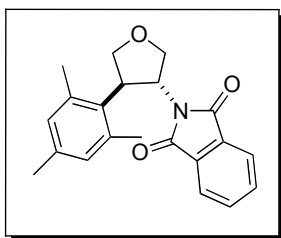


The second addition of catalyst, oxidant, and alcohol was after 12 h. The product **132** was obtained as a white solid as a single diastereomer (142 mg, 56% yield, $R_f = 0.19$ in 70% hexanes/30% ethyl acetate). mp = 40.7-45.3 $^\circ\text{C}$. ^1H NMR (CDCl_3): δ 7.82 (dd, $J = 5.3, 3.1$ Hz, 2H), 7.71 (dd, $J = 5.5, 3.1$ Hz, 2H), 7.41 (d, $J = 8.3$ Hz, 2H), 7.15 (d, $J = 8.3$ Hz, 2H), 4.99 (q, $J = 8.2$ Hz, 1H), 4.48 (t, $J = 8.35$ Hz, 1H), 4.24-4.10 (multiple peaks, 3H), 3.92 (dd, $J = 8.7, 7.4$ Hz, 1H). ^{13}C $\{^1\text{H}\}$ NMR (CDCl_3): δ 167.84, 138.85, 134.21, 131.86, 131.58, 129.06, 123.40, 121.02, 74.78, 68.81, 56.96, 46.89. IR (thin film): 1713 cm^{-1} . HRMS (ESI, m/z): $[\text{M} + \text{Na}]^+$ calcd for $\text{C}_{18}\text{H}_{14}\text{BrNO}_3$, 394.0055; found, 394.0055.



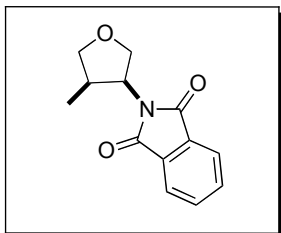
The second addition of catalyst, oxidant, and alcohol was after 3 h. The product was obtained as a 12:1 ratio of diastereomers (187 mg, 80% yield, $R_f = 0.20$ in 70% hexanes/30% ethyl acetate). The diastereomers were separated by HPLC (90% hexanes/10% ethyl acetate, 20 mL/min, Waters μ -porasil 19.1 mm). **Major diastereomer (133)**: white solid, mp = 105.6-108.6 $^\circ\text{C}$. ^1H NMR (CDCl_3): δ 7.83-7.75 (multiple peaks,

5H), 7.71-7.68 (multiple peaks, 3H), 7.46-7.42 (multiple peaks, 3H), 5.18 (q, $J = 8.3$ Hz, 1H), 4.58 (dd, $J = 8.6, 8.0$ Hz, 1H), 4.37 (q, $J = 7.8$ Hz, 1H), 4.32-4.23 (multiple peaks, 2H), 4.07 (dd, $J = 8.7, 7.4$ Hz, 1H). ^{13}C $\{^1\text{H}\}$ NMR (CDCl_3): δ 167.92, 137.02, 134.12, 133.38, 132.55, 131.66, 128.83, 127.62, 127.60, 126.33, 126.21, 125.77, 125.16, 123.35, 75.01, 68.97, 57.01, 47.50. IR (thin film): 1711 cm^{-1} . HRMS (ESI, m/z): $[\text{M} + \text{Na}]^+$ calcd for $\text{C}_{22}\text{H}_{17}\text{NO}_3$, 366.1106; found, 366.1103. **Minor diastereomer**: ^1H NMR (CDCl_3): δ 8.05 (d, $J = 9.3$ Hz, 1H), 7.80 (dd, $J = 5.5, 3.1$ Hz, 2H), 7.74 (d, $J = 8.2$ Hz, 1H), 7.69 (dd, $J = 5.5, 3.1$ Hz, 2H), 7.65 (d, $J = 6.8$ Hz, 1H), 7.49-7.44 (multiple peaks, 4H), 5.38 (q, $J = 8.4$ Hz, 1H), 5.09 (q, $J = 8.0$ Hz, 1H), 4.73 (dd, $J = 8.7, 8.1$, 1H), 4.33 (d, $J = 8.3$ Hz, 2H), 4.00 (dd, $J = 8.8, 7.4$ Hz, 1H). ^{13}C $\{^1\text{H}\}$ NMR (CDCl_3): δ 168.05, 135.37, 134.15, 133.91, 132.16, 131.64, 128.92, 127.65, 126.34, 125.75, 125.70, 123.37, 123.20, 122.98, 74.81, 68.71, 55.28, 42.46.

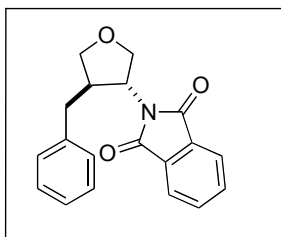


The second addition of catalyst, oxidant, and alcohol was after 2.5 h. The product was obtained as a 1.4:1 mixture of diastereomers (164 mg, 72% yield, $R_f = 0.24$ in 70% hexanes/30% ethyl acetate). The diastereomers were separated by HPLC (90% hexanes/10% ethyl acetate, 20 mL/min, Waters μ -porasil 19.1 mm). **Major diastereomer (134)**: white solid, mp = 111.3-115.3 $^\circ\text{C}$. ^1H NMR (CDCl_3): δ 7.81 (dd, $J = 5.3, 3.1$ Hz, 2H), 7.70 (dd, $J = 5.4, 3.1$ Hz, 2H), 6.79 (s, 2H), 5.37 (q, $J = 9.5$ Hz, 1H), 4.83 (q, $J = 9.5$ Hz, 1H), 4.42 (t, $J = 9.8$ Hz, 1H), 4.25 (d, $J = 7.6$ Hz, 2H), 4.11 (t, $J = 8.6$ Hz, 1H), 2.36 (s, 6H), 2.19 (s, 3H). ^{13}C $\{^1\text{H}\}$ NMR (CDCl_3): δ 168.06, 137.02, 136.02, 134.09, 131.95, 131.61, 130.28, 123.30, 72.12, 68.68, 54.89, 41.08, 20.91, 20.61. IR (thin film): 1714 cm^{-1} . HRMS (ESI, m/z): $[\text{M} + \text{Na}]^+$ calcd for $\text{C}_{21}\text{H}_{21}\text{NO}_3$, 358.1419; found, 358.1414. **Minor diastereomer**: white solid, mp = 130.6-134.2 $^\circ\text{C}$. ^1H NMR (CDCl_3): δ 7.68 (dd, $J = 5.4, 3.0$ Hz, 2H), 7.62 (dd, $J = 5.5, 3.0$ Hz, 2H), 6.64 (s, 2H), 5.33 (td, $J = 8.4, 4.6$ Hz, 1H), 4.89 (dd, $J = 9.7, 8.3$ Hz, 1H), 4.61 (dd, $J = 9.6, 4.5$ Hz, 1H), 4.29-4.20 (multiple peaks, 2H), 3.99 (q, $J = 9.2$ Hz, 1H), 2.35 (s, 3H), 2.07 (s, 6H). ^{13}C $\{^1\text{H}\}$ NMR (CDCl_3): δ

168.06, 137.85, 135.95, 133.83, 131.30, 130.18, 129.03, 122.99, 70.86, 67.93, 53.06, 48.13, 21.91, 20.41. IR (thin film): 1710 cm^{-1} . HRMS (ESI, m/z): $[\text{M} + \text{Na}]^+$ calcd for $\text{C}_{21}\text{H}_{21}\text{NO}_3$, 358.1419; found, 358.1419.

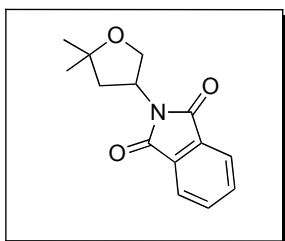


Five reactions, each carried out on a 20 mg scale with respect to phthalimide, were combined for this substrate. The product was obtained as 1.4:1 mixture of diastereomers (47 mg, 30% yield, $R_f = 0.28$ in 70% hexanes/30% ethyl acetate). The diastereomers were separated by HPLC (90% hexanes/10% ethyl acetate, 20 mL/min, Waters μ -porasil 19.1 mm). **Major diastereomer (135)**: viscous oil. ^1H NMR (CDCl_3): δ 7.84 (dd, $J = 5.6, 3.1$ Hz, 2H), 7.73 (dd, $J = 5.6, 3.1$ Hz, 2H), 4.92 (td, $J = 8.6, 5.2$ Hz, 1H), 4.32 (dd, $J = 9.5, 5.1$ Hz, 1H), 4.21 (dd, $J = 9.5, 8.4$ Hz, 1H), 4.08 (t, $J = 7.8$ Hz, 1H), 3.80 (dd, $J = 10.1, 8.1$ Hz, 1H), 2.58 (m, 1H), 0.88 (d, $J = 7.0$ Hz, 3H). ^{13}C $\{^1\text{H}\}$ NMR (CDCl_3): δ 168.64, 134.12, 131.55, 123.29, 74.56, 69.15, 53.19, 37.56, 10.53. IR (thin film): 1713 cm^{-1} . **Minor diastereomer**: white solid, mp = 85.9-87.9 $^\circ\text{C}$. ^1H NMR (CDCl_3): δ 7.84 (dd, $J = 5.4, 3.1$ Hz, 2H), 7.72 (dd, $J = 5.6, 3.0$ Hz, 2H), 4.47 (q, $J = 7.6$ Hz, 1H), 4.28 (t, $J = 8.1$ Hz, 1H), 4.10-4.02 (multiple peaks, 2H), 3.51 (t, $J = 7.4$ Hz, 1H), 2.92 (m, 1H), 1.09 (d, $J = 6.8$ Hz, 3H). ^{13}C $\{^1\text{H}\}$ NMR (CDCl_3): δ 168.08, 134.08, 131.75, 123.26, 74.85, 68.57, 57.22, 36.83, 16.32. IR (thin film): 1713 cm^{-1} . HRMS (ESI, m/z): $[\text{M} + \text{Na}]^+$ calcd for $\text{C}_{13}\text{H}_{13}\text{NO}_3$, 254.0793; found, 254.0798.

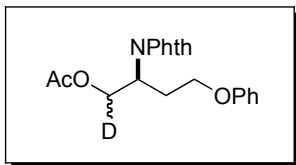


The second addition of catalyst, oxidant, and alcohol was after 5 h. The product was obtained as 1.5:1 mixture of diastereomers (56 mg, 27% yield, $R_f = 0.25$ in 70% hexanes/30% ethyl acetate). The diastereomers were separated by HPLC (90% hexanes/10% ethyl acetate, 20 mL/min, Waters μ -porasil 19.1 mm). **Major diastereomer**

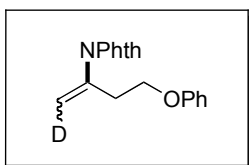
(**136**): off-white viscous oil. ^1H NMR (CDCl_3): δ 7.74 (dd, $J = 5.5, 3.1$ Hz, 2H), 7.68 (dd, $J = 5.4, 3.1$ Hz, 2H), 7.12-7.08 (multiple peaks, 4H), 6.95 (m, 1H), 4.62 (q, $J = 8.3$ Hz, 1H), 4.25 (dd, $J = 8.6, 7.6$ Hz, 1H), 4.08-4.00 (multiple peaks, 2H), 3.68 (dd, $J = 8.76, 7.35$ Hz, 1H), 3.34 (m, 1H), 2.84 (dd, $J = 13.8, 7.6$ Hz, 1H), 2.72 (dd, $J = 13.79, 7.9$, 1H). ^{13}C $\{^1\text{H}\}$ NMR (CDCl_3): δ 167.84, 138.89, 133.91, 131.61, 128.53, 128.32, 126.05, 123.06, 72.98, 68.74, 55.26, 42.28, 37.98. IR (thin film): 1712 cm^{-1} . HRMS (ESI, m/z): $[\text{M} + \text{Na}]^+$ calcd for $\text{C}_{19}\text{H}_{17}\text{NO}_3$, 330.1106; found, 330.1100. **Minor diastereomer**: white solid, mp = $81.1\text{-}84.8\text{ }^\circ\text{C}$. ^1H NMR (CDCl_3): δ 7.84 (dd, $J = 5.4, 3.1$ Hz, 2H), 7.74 (dd, $J = 5.5, 3.1$ Hz, 2H), 7.19-7.10 (multiple peaks, 3H), 7.05-7.03 (multiple peaks, 2H), 5.01 (td, $J = 8.8, 5.5$ Hz, 1H), 4.33 (dd, $J = 9.4, 5.5$ Hz, 1H), 4.23 (dd, $J = 9.4, 8.5$ Hz, 1H), 4.05-3.98 (multiple peaks, 2H), 2.86 (m, 1H), 2.67 (dd, $J = 13.9, 6.2$ Hz, 1H), 2.56 (dd, $J = 13.8, 9.7$ Hz, 1H). ^{13}C $\{^1\text{H}\}$ NMR (CDCl_3): δ 168.53, 139.40, 134.18, 131.58, 128.47, 128.22, 126.21, 123.34, 73.36, 69.50, 52.00, 44.16, 32.99. IR (thin film): 1712 cm^{-1} . HRMS (ESI, m/z): $[\text{M} + \text{Na}]^+$ calcd for $\text{C}_{19}\text{H}_{17}\text{NO}_3$, 330.1106; found, 330.1098.



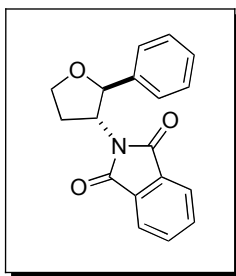
The second addition of catalyst, oxidant, and alcohol was after 1 h. The product **138** was obtained as a white solid (78 mg, 47% yield, $R_f = 0.20$ in 70% hexanes/30% ethyl acetate). mp = $93.8\text{-}94.6\text{ }^\circ\text{C}$. ^1H NMR (CDCl_3): δ 7.82 (dd, $J = 5.4, 3.1$ Hz, 2H), 7.71 (dd, $J = 5.4, 3.1$ Hz, 2H), 4.99 (m, 1H), 4.20 (t, $J = 9.2$ Hz, 1H), 4.04 (t, $J = 8.3$ Hz, 1H), 2.45 (dd, $J = 12.1, 9.6$ Hz, 1H), 2.06 (dd, $J = 12.1, 9.4$ Hz, 1H), 1.48 (s, 3H), 1.31 (s, 3H). ^{13}C $\{^1\text{H}\}$ NMR (CDCl_3): δ 168.06, 134.06, 131.79, 123.21, 81.14, 66.86, 50.15, 40.40, 28.26, 28.15. IR (thin film): 1710 cm^{-1} . HRMS (ESI, m/z): $[\text{M} + \text{Na}]^+$ calcd for $\text{C}_{14}\text{H}_{15}\text{NO}_3$, 268.0950; found, 268.0934.



The product **158** was obtained as a yellow oil. ^1H NMR (CDCl_3): δ 7.88-7.83 (multiple peaks, 4H), 7.73-7.72 (multiple peaks, 4H), 7.23 (t, $J = 7.5$ Hz, 2H), 7.18 (t, $J = 7.5$ Hz, 2H), 6.93-6.84 (multiple peaks, 4 H), 6.70 (d, $J = 8.5$ Hz, 2H), 4.81-4.78 (multiple peaks, 2H), 4.50 (dd, $J = 9.5, 4.5$ Hz, 1H), 4.22 (d, $J = 6.0$ Hz, 1H), 4.17-4.09 (multiple peaks, 2H), 3.99 (m, 1H), 3.95 (m, 1H), 2.61 (m, 1H), 2.52 (m, 1H), 2.25 (m, 2H), 1.98 (s, 3H), 1.92 (s, 3H).



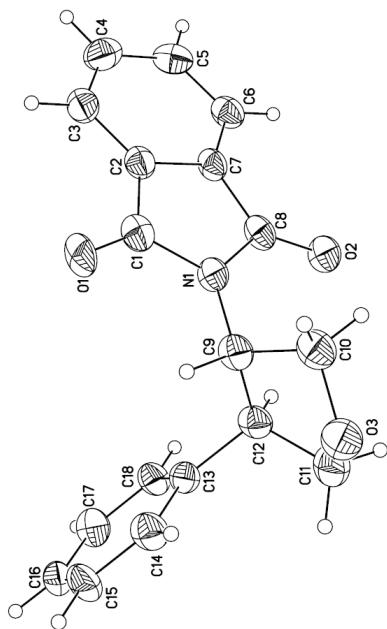
The product **159** was obtained as a white solid (78 mg, 47% yield, $R_f = 0.20$ in 70% hexanes/30% ethyl acetate). mp = 93.8-94.6 °C. ^1H NMR (CDCl_3): δ 7.88 (dd, $J = 5.0, 2.5$ Hz, 4H), 7.75 (dd, $J = 5.0, 3.0$ Hz, 4H), 7.19 (t, $J = 7.5$ Hz, 4H), 6.88 (t, $J = 7.5$ Hz, 2H), 6.72 (d, $J = 8.0$ Hz, 4H), 5.51 (s, 1H), 5.28 (s, 1H), 4.11 (t, $J = 6.0$ Hz, 4H), 2.98 (t, $J = 6.5$ Hz, 4H).



The second addition of catalyst, oxidant, and alcohol was after 7.5 h. The product **160** was obtained as a white solid as a single diastereomer (120 mg, 60% yield, $R_f = 0.12$ in 70% hexanes/30% ethyl acetate). mp = 125.6-128.4 °C. ^1H NMR (CDCl_3): δ 7.83 (dd, $J = 5.5, 3.0$ Hz, 2H), 7.72 (dd, $J = 5.5, 3.5$ Hz, 2H), 7.34-7.25 (multiple peaks, 5H), 5.23 (d, $J = 8.0$ Hz, 1H), 4.76 (m, 1H), 4.40 (q, $J = 8.5$ Hz, 1H), 4.29 (td, $J = 8.0, 5.0$ Hz, 1H), 2.59 (m, 1H), 2.41 (m, 1H). ^{13}C $\{^1\text{H}\}$ NMR (CDCl_3): δ 167.94, 139.31, 134.14, 131.71, 128.56, 128.09, 126.01, 123.36, 80.68, 67.82, 56.82, 29.58. IR (thin film): 1712 cm^{-1} . HRMS (ESI, m/z): $[\text{M} + \text{Na}]^+$ calcd for $\text{C}_{18}\text{H}_{15}\text{NO}_3$, 316.095; found, 316.0941.

Structure Determination of **160**.

Colorless, needle-like crystals of **160** were grown by diffusion of pentane into a dichloromethane solution at 22 deg. C. A crystal of dimensions 0.40 x 0.08 x 0.04 mm



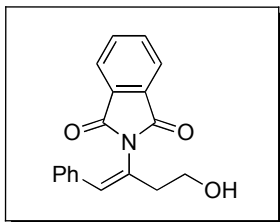
was mounted on a standard Bruker SMART 1K CCD-based X-ray diffractometer equipped with a LT-2 low temperature device and normal focus Mo-target X-ray tube ($\lambda = 0.71073 \text{ \AA}$) operated at 2000 W power (50 kV, 40 mA). The X-ray intensities were measured at 108(2) K; the detector was placed at a distance 4.969 cm from the crystal. A total of 2640 frames were collected with a scan width of 0.6° in ω and 0.45° in ϕ with an exposure time of 75 s/frame. The integration of the data yielded a total of 10058 reflections to a maximum 2θ value of 45.32° of which 1947 were independent and 1198 were greater than $2\sigma(I)$. The final cell constants (Table 1)

were based on the xyz centroids of 2032 reflections above $10\sigma(I)$. Analysis of the data showed negligible decay during data collection; the data were processed with SADABS and corrected for absorption. The structure was solved and refined with the Bruker SHELXTL (version 6.12) software package, using the space group $P1\bar{1}$ with $Z = 2$ for the formula $C_{15}H_{18}NO_3$. All non-hydrogen atoms were refined anisotropically with the hydrogen atoms placed in idealized positions. Full matrix least-squares refinement based on F^2 converged at $R1 = 0.0546$ and $wR2 = 0.1212$ [based on $I > 2\sigma(I)$], $R1 = 0.1094$ and $wR2 = 0.1415$ for all data.

Sheldrick, G.M. SHELXTL, v. 6.12; Bruker Analytical X-ray, Madison, WI, 2001.

Sheldrick, G.M. SADABS, v. 2.10. Program for Empirical Absorption Correction of Area Detector Data, University of Gottingen: Gottingen, Germany, 2003.

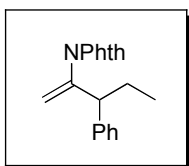
Saint Plus, v. 7.01, Bruker Analytical X-ray, Madison, WI, 2003.



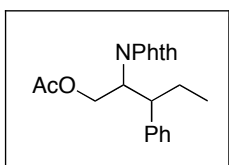
Phthalimide (100 mg, 0.68 mmol, 1 equiv), AgBF₄ (13 mg, 0.07 mmol, 0.10 equiv), and Pd(OAc)₂ (8 mg, 0.034 mmol, 0.05 equiv) were combined in CH₃CN (1.4 mL) in a 20 mL vial. *cis*-1-Phenyl-buten-4-ol (0.202 g, 1.36 mmol, 2.0 equiv) was added to the reaction. The vial was purged with O₂ and sealed with a Teflon-lined cap, and the reaction was heated at 60 °C for 12 h. The resulting mixture was cooled to room temperature and evaporated to dryness, then taken up in ether (10 mL). The ether layer washed with 10% aqueous Et₃N (10 mL), H₂O (2 x 20 mL), saturated aqueous NaHCO₃ (20 mL), and saturated aqueous NaCl (20 mL). The ether layer was then dried over MgSO₄, filtered, and concentrated to afford a red oil, which was purified by chromatography on silica gel. The product *Z*-**163** was obtained as a major isomer (>10:1 as determined by HPLC analysis of the crude reaction mixture), (6 mg, 3% yield, R_f = 0.21 in 55% hexanes/45% ethyl acetate). An authentic sample of the *E*-isomer (**165**) was obtained by repeating the reaction above in DCE without AgBF₄. These conditions led to a 2:1 mixture of the *Z* and *E*-isomers, which could be separated by HPLC (65% hexanes/35% ethyl acetate, 20 mL/min, Waters μ-porasil 19.1 mm). *Z*-isomer (**163**): viscous oil. ¹H NMR (CDCl₃): δ 7.85 (dd, *J* = 5.3, 3.6 Hz, 2H), 7.75 (dd, *J* = 5.3, 3.6 Hz, 2H), 7.20-7.15 (multiple peaks, 5H), 6.94 (s, 1H), 3.69 (t, *J* = 5.1 Hz, 2H), 2.73 (t, *J* = 5.5 Hz, 2H), 2.56 (br s, 1H). ¹³C {¹H} NMR (CDCl₃): δ 167.79, 134.45, 134.43, 134.32, 131.69, 128.55, 127.95, 127.50, 127.42, 123.86, 58.85, 39.62. IR (thin film): 3461, 1712 cm⁻¹. HRMS (ESI, m/z): [M + Na]⁺ calcd for C₁₈H₁₅NO₃, 316.0950; found, 317.0977. *E*-isomer (**165**): ¹H NMR (CDCl₃): δ 7.92 (dd, *J* = 5.6, 3.1 Hz, 2H), 7.79 (dd, *J* = 5.6, 3.1 Hz, 2H), 7.53 (d, *J* = 7.5 Hz, 2H), 7.39 (t, *J* = 7.3 Hz, 2H), 7.38 (d, *J* = 7.2 Hz, 1H), 6.78 (s, 1H), 3.71 (t, *J* = 5.4 Hz, 2H), 2.86 (t, *J* = 5.7 Hz, 2H), 2.55 (br s, 1H).

Discussion of low yield of 163. ¹H NMR studies (with 1,3,5-trimethoxybenzene as an internal standard) were carried out in order to determine the reasons for the low yield of **163** in these transformations. The low yield of **163** appears to be due to several factors.

First, in all of these reactions, the precipitation of Pd black was observed almost immediately (approximately 2 min) after heating was commenced, suggesting that catalyst decomposition is extremely fast (and/or reoxidation of Pd(0) to Pd(II) is very slow) under these conditions). Second, the *cis*-starting material **155** exhibited low reactivity under these conditions, and significant quantities of unreacted **155** are recovered. In addition, significant isomerization of **155** to the corresponding *trans* isomer (which is unreactive towards aminopalladation) was observed, particularly at higher catalyst loadings. Finally, ^1H NMR spectroscopy of the crude mixture showed the presence of a significant quantity of a resonance at 10.03 ppm, consistent with an aldehyde functionality. This suggests that one mode of catalyst decomposition under these conditions likely involves oxidation of the alcohol substrate with concomitant reduction of the Pd catalyst.



The product **171** was obtained as a yellow oil (10% yield). ^1H NMR (CDCl_3): δ 7.76 (m, 2H), 7.67 (m, 2H), 7.42-7.26 (multiple peaks, 5H), 5.53 (br s, 1H), 5.27 (br s, 1H), 3.83 (m, 1H), 1.33 (m, 2H), 0.85 (t, $J = 7.2$ Hz, 3H).



The product **172** was obtained as a viscous oil (25% yield, 4.5:1). **Major Isomer:** ^1H NMR (CDCl_3): δ 7.65 (dd, $J = 5.5, 3.0$ Hz, 2H), 7.59 (dd, $J = 5.5, 3.0$ Hz, 2H), 7.12-7.08 (m, 4H), 7.01 (m, 1H), 4.75 (dd, $J = 10.5, 2.5$ Hz, 1H), 4.66-4.59 (multiple peaks, 2H), 3.40 (td, $J = 10.5, 3.0$ Hz, 1H), 1.68 (m, 2H), 0.75 (t, $J = 7.0$ Hz, 3H).

5.11 References

- (1) Hegedus, L. S.; Akermark, B.; Zetterberg, K.; Olsson, L. F. *J. Am. Chem. Soc.* **1984**, *106*, 7122-7126.
- (2) Hegedus, L. S. *Tetrahedron* **1984**, *40*, 2415-2434.
- (3) Li, G. G.; Chang, H. T.; Sharpless, K. B. *Angew. Chem., Int. Ed.* **1996**, *35*, 451-454.
- (4) Tamaru, Y.; Kimura, M. *Synlett* **1997**, 749-&.
- (5) [Reference to Bergmeier], Stephen C. *Tetrahedron*, **2000**, *56*, 2561-2576.
- (6) Li, G. G.; Chang, H. T.; Sharpless, K. B. *Angew. Chem., Int. Ed.* **1996**, *35*, 451-454.
- (7) Bodkin, J. A.; McLeod, M. D. *J. Chem. Soc., Perkin Trans. I* **2002**, 2733-2746.
- (8) Brice, J. L.; Harang, J. E.; Timokhin, V. I.; Anastasi, N. R.; Stahl, S. S. *J. Am. Chem. Soc.* **2005**, *127*, 2868-2869.
- (9) Backvall, J. E.; Bjorkman, E. E. *J. Org. Chem.* **1980**, *45*, 2893-2898.
- (10) Hegedus, L. S.; Winton, P. M.; Varapath, S. *J. Org. Chem.* **1981**, *46*, 2215-2221.
- (11) Hegedus, L. S.; Siirala-Hansen, K. *J. Am. Chem. Soc.* **1975**, *97*, 1184-1188.
- (12) Manzoni, M. R.; Zabawa, T. P.; Kasi, D.; Chemler, S. R. *Organometallics* **2004**, *23*, 5618-5621.
- (13) Alexanian, E. J.; Lee, C.; Sorensen, E. J. *J. Am. Chem. Soc.* **2005**, *127*, 7690-7691.
- (14) Streuff, J.; Hovelmann, C. H.; Nieger, M.; Muniz, K. *J. Am. Chem. Soc.* **2005**, *127*, 14586-14587.
- (15) Muniz, K.; Hovelmann, C. H.; Streuff, J. *J. Am. Chem. Soc.* **2008**, *130*, 763-773.
- (16) Liu, G.; Stahl, S. S. *J. Am. Chem. Soc.* **2006**, *128*, 7179-7181.
- (17) Heck, R. F. *J. Am. Chem. Soc.* **1968**, *90*, 5538-5542.
- (18) Kimura, M.; Harayama, H.; Tanaka, S.; Tamaru, Y. *J. Chem. Soc., Chem. Commun.* **1994**, 2531-2533.
- (19) Saito, S.; Hara, T.; Takahashi, N.; Hirai, M.; Moriwake, T. *Synlett* **1992**, 237-238.

- (20) Tiecco, M.; Testaferri, L.; Tingoli, M.; Bartoli, D. *Tetrahedron*, **1990**, *46*, 7139-7150.
- (21) Strukul, G. *Top. Catal.* **2002**, *19*, 33-42.
- (22) Desai, L. V.; Sanford, M. S. *Angew. Chem., Int. Ed.* **2007**, *46*, 5737-5740.
- (23) Ney, J. E.; Wolfe, J. P. *Angew. Chem., Int. Ed.* **2004**, *43*, 3605-3608.
- (24) Dick, A. R.; Kampf, J. W.; Sanford, M. S. *J. Am. Chem. Soc.* **2005**, *127*, 12790-12791.
- (25) Zhu, G. X.; Ma, S. M.; Lu, X. Y.; Huang, Q. C. *J. Chem. Soc., Chem. Commun.* **1995**, 271-273.
- (26) Baeckvall, J. E. *Acc. Chem. Res.* **1983**, *16*, 335-342.
- (27) Williams, B. S.; Goldberg, K. I. *J. Am. Chem. Soc.* **2001**, *123*, 2576-2587.